

# **Systematic Selection and Application of Backfill in Underground Mines**

Der Fakultät für Geowissenschaften, Geotechnik und Bergbau  
der Technischen Universität Bergakademie Freiberg  
genehmigte

DISSERTATION

zur Erlangung des akademischen Grades

Doctor-Ingenieur

(Dr.-Ing.)

vorgelegt

von M.Eng. Manoon Masniyom

geboren am 11.12.1971 in Songkhla/Thailand

Gutachter: Prof.Dr. Carsten Drebenstedt, Freiberg  
Prof.Dr. -Ing. Thomas A. Bier, Freiberg  
Prof.Dr. Pitsanu Bunnaul, Songkhla

Tag der Verleihung: 17.04.2009

## **Abstract**

The use of backfill in underground mining is increasing due to need for systematic backfilling of mine openings and workings. Backfill is defined as the material or materials that are utilised in void openings of underground mines for mining technical or mining safety purposes. Backfill is applied in order to prevent fires and explosions, to improve mine ventilation, to improve the stability of the rock, to reduce subsidence effects at the surface, as well as for economical and environmental factors. Sources of materials were from the mining industries and mining related (e.g. fly ash, Flue Gas Desulfurization (FGD) –gypsum, slag, infertile overburden, tailings, filter dust, residues from mineral processing) or other industries (e.g. incineration ash, used building material, old bricks, used foundry sand, furnace blow-out). Mining with backfill technology helps mining companies achieve many of these goals. The technology of backfilling enables a wide range of engineering solutions for particular mine sites and their unique sets of problems and opportunities. Carefully engineered and efficiently run backfill systems can significantly enhance a mining operation. By contrast, badly engineered and poorly run backfill can be a serious impediment to the mine and, worst of all, compromise safety.

This study is to investigate backfill materials and techniques suited for systematic selection and application of backfill in underground mines. Laboratory tests were carried out on physical, chemical and mechanical properties of different backfill materials and mixtures thereof. Special attention was paid to materials generated as by-products and other cheaply available materials e.g. fly ash and FGD-gypsum from power plants, natural and synthetic anhydrite. The system selection, application and placement of backfill in mines are truly multi disciplinary processes. Backfill technologies investigated more in depth are paste, hydraulic and dump backfill as well as combinations thereof. There is a good chance that one of the different material mixtures investigated can be used as a technically and economically viable backfill for underground mines. The testwork may be required to confirm the suitability of available materials for a particular system. In summary, the systematic selection of backfill materials from by-products, mine waste and tailings from the mineral processing of mining industry and other industries were suited as a backfill material.

---

## Acknowledgements

I would like to express my deepest and heartily thanks and great indebtedness and gratitude to my supervisor Prof.Dr.Carsten Drebensted for his kind supervision, guidance, valuable advice, reviewing the manuscript and support during my study.

I am deeply grateful to Prof.Dr.Werner Klemm, Institute of Mineralogy and Dr.-Ing Hans-Dieter Voigt, Institute of Drilling Engineering and Fluid Mining for their supervision.

I express my sincere thanks to the staff of the Institute of Mining and Special Civil Engineering, Faculty of Geoscience, Geotechnology and Mining, TU Bergakademie Freiberg, especially Dipl.-Ing.Brigitte Wasowiecz for her laboratory help, Dipl.-Ing.Dorel Gusat for his both field and laboratory help.

I extend my heartily thanks to Mr.Douglas Walls for his help in the final draft of this thesis.

I would like to acknowledge all my colleagues for their continuous moral support.

I extend my special and heartily thanks and gratitude to my country (Thailand) for awarding me a Thai scholarship to do doctoral work in Mining Engineering, Institute of Mining and Special Civil Engineering, TU Bergakademie Freiberg, Germany.

Finally, I am indebted to my wife Ms.Phat Masniyom, my son and my parents for giving me the patience to complete this work.

## Table of Contents

Title Page.....	I
Abstract.....	II
Acknowledgements.....	III
Table of Contents.....	IV
List of Figures.....	IX
List of Tables.....	XIV
List of Abbreviations.....	XVII
<b>Chapters</b>	
<b>1. Actuality of backfill research.....</b>	<b>1</b>
1.1 Actuality and importance of backfill.....	1
1.2 Analysis of backfill research.....	4
1.3 New method of systematic selection of backfill.....	13
<b>2. Analysis of mining and backfill techniques.....</b>	<b>16</b>
2.1 Mining technique specification .....	16
2.2 Mining methods with backfill .....	18
2.2.1 Cut and fill methods.....	21
2.2.2 Delayed backfill methods.....	22
2.2.3 Room and pillar.....	23
2.2.4 Longwall mining.....	24
2.2.5 Block caving.....	25
2.3 Backfill technologies.....	26
2.3.1 Mechanical backfill.....	26
2.3.2 Pneumatic backfill.....	29

---

2.3.3 Hydraulic backfill.....	29
2.3.4 Paste backfill.....	32
2.3.5 Pumping paste.....	36
2.4 Financial and technical considerations.....	38
<b>3. Backfill material characteristics.....</b>	<b>40</b>
3.1 Importance material characteristics for Backfill.....	40
3.1.1 Geomechanics of backfill.....	40
3.1.1.1 Strength of materials.....	42
3.1.1.2 Component of backfill.....	43
3.1.1.3 Particle shape and friction angle.....	44
3.1.1.4 Particle size distribution.....	45
3.1.1.5 Bulk density, unit weight, and specific gravity.....	47
3.1.1.6 Friction angle and cohesion .....	48
3.1.1.7 Backfill failure.....	50
3.1.1.8 Consolidation and compaction.....	51
3.1.1.9 Stiffness .....	52
3.1.1.10 Permeability and percolation rate.....	53
3.1.2 Backfill materials specification.....	55
3.1.2.1 Backfill binders.....	56
3.1.2.2 Portland cement.....	57
3.1.2.3 Pozzolans.....	58
3.1.2.4 Mixture proportions.....	60

---

3.2 Instrumentation of determination.....	61
3.2.1 Setting time of backfill.....	61
3.2.2 Simultaneous Thermal Analysis (STA) of backfill materials.....	62
3.2.3 Permeability measurement .....	63
3.2.4 Specimen preparation and mechanical strength test.....	64
3.2.5 Ultrasonic test.....	65
3.2.6 Chemical characterization .....	66
3.3 Result for backfill materials investigation.....	65
3.3.1 Selection of materials.....	66
3.3.1.1 Synthetic anhydrite.....	66
3.3.1.2 Natural anhydrite.....	68
3.3.1.3 Fly ash.....	68
3.3.1.4 Filter dust.....	69
3.3.1.5 Cement.....	69
3.3.1.6 Flue gas desulfurization (FGD) gypsum.....	70
3.3.1.7 Tailing from potash mine.....	70
3.3.1.8 Salinity water.....	71
3.3.2 Results of materials characteristics.....	71
3.3.2.1 Physical characteristics.....	72
3.3.2.2 Optimal ratio of backfill.....	73
3.3.2.3 Scanning electron microscope investigations.....	75
3.3.2.4 Simultaneous Thermal Analysis (STA).....	77

---

3.3.2.5 Permeability measurement.....	81
3.3.2.6 Mineralogical characterization.....	81
3.3.2.7 Uniaxial compressive strength (UCS) tests and evolution of the dynamic elastic parameters.....	82
3.3.2.8 Effects of water salinity on backfill properties.....	90
3.3.2.9 Triaxial compression test of backfill specimens.....	91
3.3.3 Chemical composition.....	92
3.3.3.1 Chemical composition.....	92
<b>4. Discussion of the results.....</b>	<b>99</b>
4.1 Effect of different parameters on backfill behavior.....	99
4.1.1 Grain size analysis.....	99
4.1.2 Age of specimens.....	100
4.1.3 Binder factor and water to binder ratio.....	100
4.1.4 Fly ash and filter dust content.....	101
4.1.5 Fly ash and filter dust content on permeability.....	101
4.1.6 Backfill technology.....	102
4.1.7 Costs.....	102
4.1.8 Eluate and metals concentration in backfill.....	103
4.1.9 Thermal analysis.....	104
<b>5. Application of new method.....</b>	<b>106</b>
5.1 Application of backfill in underground potash mines in Thailand.....	106
5.1.1 Mining method of ASEAN potash project.....	107
5.1.2 Mining method of APPC potash project.....	108

---

5.1.3 Application of backfill in potash mine.....	108
5.2 Application of backfill in coalfield fires and underground coal mines in China.....	109
<b>6. Conclusions and recommendations for further research.....</b>	<b>114</b>
6.1 Conclusions.....	114
6.2 Recommendations for further research.....	115
6.2.1 Chemical effect in backfill.....	115
6.2.2 Backfill transportation.....	115
6.2.3 Environmental effect of acid generating tailings.....	115
6.2.4 Other backfill materials in underground mines.....	116
<b>References.....</b>	<b>118</b>
<b>Appendices.....</b>	<b>137</b>
<b>Appendix A.....</b>	<b>137</b>
<b>Appendix B.....</b>	<b>157</b>
<b>Appendix C.....</b>	<b>165</b>
<b>Appendix D.....</b>	<b>167</b>



## List of Figures

Figure 1.1: Children’s hospital affected by underground mine subsidence in Oppenheim, Germany.....	1
Figure 1.2: Cross-section of subsidence trough.....	2
Figure 1.3: Systematic selection and application of backfill flowsheet.....	15
Figure 2.1: Typical mining methods: cut and fill.....	18
Figure 2.2: Typical mining methods: open stope.....	19
Figure 2.3: Typical mining methods: room and pillar.....	19
Figure 2.4: Typical mining methods: Longwall mining .....	20
Figure 2.5: Typical mining methods: block caving mining.....	20
Figure 2.6: Representation of a mechanical backfill.....	27
Figure 2.7: Pneumatic pipe feeder system.....	29
Figure 2.8: Hydraulic backfill.....	30
Figure 2.9: Paste backfill.....	32
Figure 2.10: Comparison of the mining cycle between using paste backfill and slurry backfill in a VRM stope.....	34
Figure 2.11: Relationship between slump and solids density for Golden Giant Mine Paste Fill.....	35
Figure 2.12: Flow chart for conceptual design of paste backfill system.....	35
Figure 2.13 : GEHO positive displacement pump.....	37
Figure 3.1: Principal stresses acting upon a backfill cylinder and resultant stress conditions upon a potential shear plane surface.....	42
Figure 3.2: Phase diagram of backfill.....	43
Figure 3.3: Particle shape of distribution.....	44
Figure 3.4: Electron microscope images (from left to right: mica bearing base metal tailings, gold tailings, construction sand and a base metal tailings).....	46

Figure 3.5: Typical particle size distribution curves for poorly graded (A) and well graded (B) aggregate materials.....	47
Figure 3.6: Shear plane development within backfill under load.....	50
Figure 3.7: Mohr-Coulomb failure locus.....	51
Figure 3.8: Ternary diagram of binders.....	56
Figure 3.9: Schematic of Ferrous Blast Furnace.....	58
Figure 3.10: Coal ashes produced by thermal power plants.....	59
Figure 3.11: Vicat test setting time of backfill.....	62
Figure 3.12: STA 409 PC <i>Luxx</i> .....	63
Figure 3.13: Laboratory measurement of permeability.....	63
Figure 3.14: Permeability measurement.....	64
Figure 3.15: Size of specimen.....	65
Figure 3.16: Mechanical press (ZD 100).....	65
Figure 3.17: Computer-based ultrasonic wave velocity measuring device.....	66
Figure 3.18: Function diagram – Production of hydrogen fluoride (HF) and hydrofluoric acid (H <sub>2</sub> SO <sub>4</sub> ).....	67
Figure 3.19: Synthetic anhydrite.....	67
Figure 3.20: Natural anhydrite from Germany.....	68
Figure 3.21: Fly ash from Germany, Thailand and China.....	68
Figure 3.22: Filter dust from Germany.....	69
Figure 3.23: Cement from Germany, Thailand and China.....	69
Figure 3.24: FGD- gypsum from Thailand.....	70
Figure 3.25: Tailing from potash mine Thailand.....	70
Figure 3.26: Particle size distribution of backfill materials.....	71
Figure 3.27: Initial setting time of backfill materials.....	73
Figure 3.28: Setting time of dust filter by Vicat test.....	73

Figure 3.29: Slump test.....	74
Figure 3.30: SEM image showing synthetic anhydrite.....	75
Figure 3.31: SEM image showing fly ash from Germany.....	75
Figure 3.32: SEM image showing filter dust.....	76
Figure 3.33: SEM image showing FGD-Gypsum.....	76
Figure 3.34: SEM image showing mixture of synthetic anhydrite, fly ash and salt solution.....	76
Figure 3.35: SEM image showing mixture of natural anhydrite, fly ash and salt solution.....	77
Figure 3.36: SEM image showing mixture of tailing, fly ash and salt solution.....	77
Figure 3.37: P1 and P2 samples.....	78
Figure 3.38: Thermogravimetry (TG) and Differential Scanning Calorimetry (DSC) curves of mixture of cement, fly ash and filter dust.....	79
Figure 3.39: Thermogravimetry (TG) and Differential Scanning Calorimetry (DSC) curves of mixture of cement and fly ash.....	80
Figure 3.40: Compression test of mixture of cement (20 %) and filter dust (80 %) after 7 days ( $w/s = 0.4$ ).....	82
Figure 3.41: Compressive strength of synthetic anhydrite.....	83
Figure 3.42: Compressive strength of natural anhydrite.....	84
Figure 3.43: Compressive strength of FGD-gypsum (T).....	85
Figure 3.44: Compressive strength of cement and fly ash (G) mixtures.....	86
Figure 3.45: E and G modulus of cement and fly ash (G).....	87
Figure 3.46: Compressive strength of cement and fly ash (C).....	87
Figure 3.47: E and G modulus of cement and fly ash (C).....	87
Figure 3.48: Compressive strength of cement and fly ash (T).....	88
Figure 3.49: E and G modulus of cement and fly ash (T).....	88

Figure 3.50: Compressive strength of cement and filter dust (G).....	89
Figure 3.51: E and G modulus of cement and filter dust (G).....	89
Figure 3.52: Influence of water quality on backfill (anhydrite).....	90
Figure 3.53: Influence of water quality on backfill (cement and fly ash) properties...	91
Figure 5.1: Locations of ASEAN and APPC Potash mine project in Sakon Nakhon Basin and Khorat basin in the northeast of Thailand.....	106
Figure 5.2: Underground mine layout of the ASEAN project (Bamnet Narong Mine).....	107
Figure 5.3: Underground mine layout of the APPC project (Udon thani Potash Mine).....	108
Figure 5.4: Localization of coal fires in China.....	110
Figure 5.5: Localization of coal fires in Wuda Inner Mongolia.....	111
Figure 5.6: The borehole site.....	111
Figure 5.7: Paste backfill placement in fracture.....	113
Figure 5.8: Paste backfill placement in borehole.....	113
Figure B.1: SEM image showing synthetic anhydrite.....	157
Figure B.2: SEM image showing natural anhydrite from Ellrich.....	157
Figure B.3: SEM image showing natural anhydrite from Obrigheim.....	157
Figure B.4: SEM image showing fly ash from Germany.....	158
Figure B.5: SEM image showing fly ash from China.....	158
Figure B.6: SEM image showing fly ash from Thailand.....	158
Figure B.7: SEM image showing filter dust.....	159
Figure B.8: SEM image showing FGD-Gypsum.....	159
Figure B.9: SEM image showing mixture of synthetic anhydrite and fly ash.....	159
Figure B.10: SEM image showing mixture of synthetic anhydrite, fly ash and salt solution.....	160

---

Figure B.11: SEM image showing mixture of natural anhydrite and fly ash.....	160
Figure B.12: SEM image showing mixture of natural anhydrite, fly ash and salt solution.....	160
Figure B.13: SEM image showing mixture of cement (G).....	161
Figure B.14: SEM image showing mixture of cement(G) and fly ash.....	161
Figure B.15: SEM image showing mixture of cement (G), fly ash and salt solution..	161
Figure B.16: SEM image showing mixture of cement (C) and fly ash (C).....	162
Figure B.17: SEM image showing mixture of cement (C), fly ash (C) and salt solution.....	162
Figure B.18: SEM image showing mixture of cement and filter dust.....	162
Figure B.19: SEM image showing mixture of cement,filter dust and fly ash.....	163
Figure B.20: SEM image showing mixture of cement,filter dust, fly ash and salt solution.....	163
Figure B.21: SEM image showing mixture of FGD-Gypsum and fly ash.....	163
Figure B.22: SEM image showing mixture of FGD-Gypsum, flyash and salt solution	164
Figure B.23: SEM image showing mixture of tailing, fly ash and salt solution.....	164

## List of Tables

Table 3.1: Effect of particle shape and packing density on friction angle.....	45
Table 3.2: Details of backfill mix proportions.....	61
Table 3.2: Physical characteristics of backfill materials.....	72
Table 3.4: Time of setting with vicat test of backfill materials (5 % cement) at w/s 0.45).....	74
Table 3.5: Permeability measurement.....	81
Table 3.6: Mineralogical characterization of backfill materials.....	82
Table 3.7: Compressive strength of cement.....	86
Table 3.8: Triaxial test of backfill materials.....	92
Table 3.9: Chemical composition of backfill materials.....	93
Table 3.10: Trace elements in mixing water.....	94
Table 3.11: pH and conductivity of backfill materials.....	95
Table 3.12: Values for eluates.....	97
Table 3.13: Value concentrations of metals in backfill materials.....	98
Table 5.1: Borehole coordinates.....	112
Table 5.2: Results of temperature measurements in borehole.....	112
Table A.1: Mechanical properties of mixture of synthetic anhydrite (G) and fly ash at w/s 0.18.....	137
Table A.2: Mechanical properties of mixture of synthetic anhydrite (T) and fly ash (w/s 0.18).....	137
Table A.3: Mechanical properties of mixture of Ellich natural anhydrite and fly ash (w/s 0.18).....	138
Table A.4: Mechanical properties of mixture of Obrigheim natural anhydrite (< 4 mm) and fly ash (w/s 0.18).....	138
Table A.5: Mechanical properties of mixture of Obrigheim natural anhydrite	

( $< 8$ mm) and fly ash (w/s 0.18).....	139
Table A.6: Mechanical properties of mixture of cement (T) and fly ash (w/s 0.4).....	139
Table A.7: Mechanical properties of mixture of cement (T) and fly ash (w/s 0.45)....	140
Table A.8: Mechanical properties of mixture of cement (T) and fly ash (w/s 0.5).....	140
Table A.9: Mechanical properties of mixture of cement (G) and fly ash (w/s 0.4).....	141
Table A.10: Mechanical properties of mixture of cement (G) and fly ash (w/s 0.45)..	141
Table A.11: Mechanical properties of mixture of cement (G) and fly ash (w/s 0.5)....	142
Table A.12: Mechanical properties of mixture of cement (C) and fly ash (w/s 0.4).....	142
Table A.13: Mechanical properties of mixture of cement (C) and fly ash (w/s 0.45)..	143
Table A.14: Mechanical properties of mixture of cement (C) and fly ash (w/s 0.5)....	143
Table A.15: Mechanical properties of mixture of cement (G) and filter dust (w/s 0.4).....	144
Table A.16: Mechanical properties of mixture of cement (G) and filter dust (w/s 0.45).....	144
Table A.17: Mechanical properties of mixture of cement (G) and filter dust (w/s 0.5).....	145
Table A.18: Mechanical properties of mixture of cement (G), fly ash and filter dust (w/s 0.4).....	146
Table A.19: Mechanical properties of mixture of cement (G), fly ash and filter dust (w/s 0.45).....	147
Table A.20: Mechanical properties of mixture of cement (G), fly ash and filter dust (w/s 0.5).....	148
Table A.21: Mechanical properties of mixture of cement (C), fly ash and filter dust (w/s 0.4).....	149
Table A.22: Mechanical properties of mixture of cement (C), fly ash and filter dust (w/s 0.45).....	150

Table A.23: Mechanical properties of mixture of cement (C), fly ash and filter dust (w/s 0.5).....	151
Table A.24: Mechanical properties of mixture of FGD-gypsum (T) and fly ash (w/s 0.4).....	152
Table A.25: Mechanical properties of mixture of FGD-gypsum (T) and fly ash (w/s 0.45).....	152
Table A.26: Mechanical properties of mixture of FGD-gypsum (T) and fly ash (w/s 0.5).....	153
Table A.27: Mechanical properties of mixture of tailing (T), cement and fly ash (w/s 0.4).....	154
Table A.28: Mechanical properties of mixture of tailing (T), cement and fly ash (w/s 0.45).....	155
Table A.29: Mechanical properties of mixture of tailing (T), cement and fly ash (w/s 0.5).....	156
Table C.1: Limit value concentrations for metals in wastes.....	165
Table C.2: Limit value for solids.....	165
Table C.3: Correlation values for solids.....	166
Table C.4: Limit values for eluates.....	166
Table D.1: Methods of analysis – solids.....	167
Table D.2: Methods of analysis– eluates.....	168



## List of Abbreviations

AMD	Acid mine drainage
APPC	Asian Pacific Potash Corporation
ASEAN	Association of Southeast Asian Nations
BF	Blast furnace
BTEX	Aromatic compound
C	Cement
$C_c$	Coefficient of curvature
$C_u$	Uniformity coefficient
$D_{50}$	Diameter of particles for which 50 % of the particles are finer
DIN	Deutsches Institut für Normung
$D_s$	Effective particle diameter
DSC	Differential Scanning Calorimetry
DTA	Differential Thermal Analysis
E	Elastic modulus
EGAT	Electricity Generating Authority of Thailand
FA	Fly ash
FD	Filter dust
FGD-gypsum	Flue gas desulfurization gypsum
G	Shear modulus
GPS	Global Positioning System
ICP AES	Inductively Coupled Plasma - Atomic Emission Spectrometry
ICP MS	Inductively-Coupled-Plasma Mass-Spectrometry
LHD	Load-haul-dump
LHKW	Highly volatile halogenated hydrocarbons
LOI	Loss on ignition
MSL	Mean sea level
MSW	Municipal solid waste

NA	Natural anhydrite
NPC	Normal portland cement
PAHs	Polynuclear aromatic hydrocarbons
PCB	Polychlorinated biphenyls
PSD	Particle size distribution
SA	Synthetic anhydrite
SEM	Scanning electron microscope
STA	Simultaneous Thermal Analysis
T	Tailing
TDS	Total Dissolved Solids
TG	Thermal Gravimetric
TOC	Total Organic Carbon
TU BAF	Technische Universität Bergakademie Freiberg
UCS	Uniaxial compressive strength
US	United State
VRM	Vertical retreat mining
XRD	X-ray diffraction
(T)	Thailand
(G)	Germany
(C)	China
OB	Obrigheim
EL	Ellrich

### **Symbol**

$\rho$	Density of materials ( $\text{g/cm}^3$ )
$\rho_d$	Dry density ( $\text{g/cm}^3$ )
C	Cohesion (MPa)
E	Modulus of Elasticity (Young's Modulus) (MPa)
$k$	Permeability coefficient (m/s)

---

K	Permeability of a porous medium ( $m^2$ )
Q	Quantity rate of flow of fluid through a porous medium (N/s)
L	Length of porous medium, in direction of flow (m)
H	Static pressure differential across a porous medium (m)
$\eta$	Absolute viscosity of fluid flowing ( $Ns/m^2$ )
A	Cross-sectional area of sample ( $m^2$ )
$L$	Unit length (m)
$M_g$	Mass of gas (kg)
$M_s$	Mass of solids (kg)
$M_w$	Mass of water (kg)
n	Porosity (%)
P	Applied force (N)
$V_g$	Volume of gas ( $m^3$ )
$V_s$	Volume of solids ( $m^3$ )
$V_w$	Volume of water ( $m^3$ )
w	Water content (%)
$G_s$	Specific gravity of the soil particles, dimensionless
$\rho_w$	Density of water unit weight ( $kg/m^3$ )
w/s	Water to solid ratio
$\gamma$	Unit weight ( $kN/m^3$ )
$\Phi$	Friction Angle ( $^\circ$ )
$\Delta L$	Deformation (m)
$\Delta L$	Deformation induced by the applied force (m)
$\varepsilon$	Axial strain (%)
$\kappa$	Stiffness (N/m)
$\sigma_1$	Major principal stress (MPa)
$\sigma_2$	Intermediate principal stress (MPa)
$\sigma_3$	Minor principal stress (MPa)
$\sigma_n$	Resolved stress perpendicular to the failure plane (kPa)

$\tau_c$	Cohesive shear stress developed along a failure plane (kPa)
$\tau_f$	Frictional shear stress developed along a failure plane (kPa)

### **Elements/compound**

$Al_2O_3$	Aluminum oxide
$As$	Arsenic
$CaCO_3$	Calcium carbonate
$CaO$	Calcium oxide
$CaSO_4$	Calcium sulfate
$Cd$	Cadmium
$CN^- total$	Cyanide, total
$Cr total$	Chromium, total
$Cr$	Chromium
$Cu$	Copper
$Fe$	Iron
$Fe_2O_3$	Iron oxide
$H_2SO_4$	Hydrofluoric acid
$HF$	Hydrogen fluoride
$Hg$	Mercury
$K_2O$	Potassium oxide
$MgCl_2$	Magnesium chloride
$MgO$	Magnesium oxide
$MnO_2$	Manganese oxide
$Na_2O$	Sodium dioxide
$NaCl$	Sodium chloride
$Ni$	Nickel
$P_2O_5$	Phosphorus pentoxide

<i>Pb</i>	Lead
<i>SiO<sub>2</sub></i>	Silicon dioxide
<i>Sn</i>	Tin
<i>TiO<sub>2</sub></i>	Titanium oxide
<i>Zn</i>	Zinc

## Units

°C	Degree celsius
cm	Centimeter
cm <sup>3</sup>	Cubiccentimeter
d	Day
g/cm <sup>3</sup>	Gram per cubiccentimeter
Pa	Pascal
Mpa	Megapascal
GPa	Gigapascal
h	Hour
m	Meter
m/s	Meter per Second
m <sup>2</sup>	Square meter
m <sup>3</sup>	Cubic Meter
m <sup>3</sup> /s	Cubic Meter Per Second
mg/m <sup>3</sup>	Milligramm per cubicmeter
mg/kg	Milligramm per Kilogramm
mg/l	Milligramm per liter
mm	Millimeter
mm <sup>2</sup>	Square millimeter
ml	Millilite
mm/m	Millimeter per meter
mW/g	Milliwatt per gram
MPa/s	Megapascal per second
N/mm <sup>2</sup>	Newton per square millimeter
μS/cm	Microsiemens per centimeter

---

$\mu\text{g/l}$	Microgramm per liter
$\mu\text{m}$	Micrometer
s	Second
t	Tonne
t/a	Tonne per year

## Chapter 1

### Actuality and Importance of Backfill Use in Mines

#### 1.1 Actuality and importance of backfill

Underground mining activities lead to surface impacts caused by subsidence movements (Fig. 1.1 and 1.2). The mining method is the component of subsidence that influences its environmental impact. The following mining techniques produce associated surface subsidence (Whittaker and Reddish, 1989):

1. Longwall mining
2. Sub-level caving
3. Room-and-pillar mining
4. Block caving
5. Stope mining



Figure 1.1: Children's hospital affected by underground mine subsidence in Oppenheim, Germany (after Bell et al., 2005)

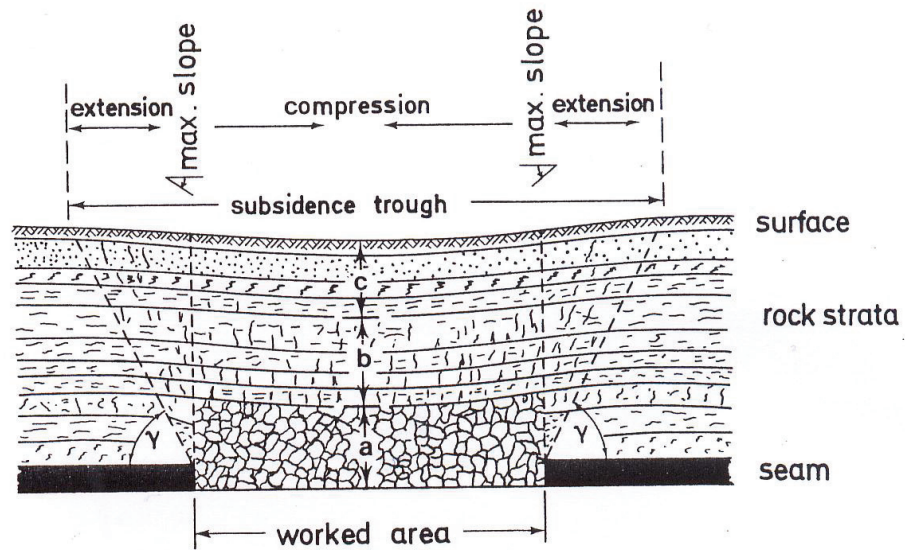


Figure 1.2: Cross-section of subsidence trough, a Zone of shattered roof beds over mine excavation; b fissured intermediate zone; c surface zone;  $\gamma$  limit angle from edge of working to trough margin (after Kratzsch, 1983).

The resultant surface impact is a large shallow depression or basin in the ground, which is usually circular or elliptical in shape, depending primarily on the geometry of the mine workings and the geological conditions.

Four types of measures may control subsidence damage: alteration in mining techniques; post-mining stabilization; architectural and structural design; and comprehensive planning (SME, 1986). None of these measures entirely prevents subsidence, and most of the measures address only impacts to man-made structures and facilities and not impacts to land use, including aquatic species, wildlife habitat and human recreation, or water quality and flow.

Alteration in mining techniques can be accomplished through a variety of methods including partial mining, backfilling, mine layout or configuration, and extraction rate. Partial mining involves leaving protective features such as pillars. It should be noted that in areas supported by protective zones, water might become perched at a higher level than the surrounding ground that has subsided. If a water table was high, the area intended for protection may become an island or experience a lowered water table (SME, 1986). This may be an important limitation with respect to establishment of protective zones to protect surface water such as lakes or wetlands.



Backfilling may be done by hydraulic or pneumatic techniques, using a variety of materials including run of mine waste rock, milled tailings, or other materials, and may include the use of cement or other modifiers to increase strength. It may also have a beneficial effect on the environment by addressing water quality impacts (such as from acid drainage), reducing waste rock disposal requirements, reducing ground fissuring, and increasing long-term strata stability and providing roof support. Backfilling does not eliminate subsidence entirely, but only reduces the amount of subsidence (SME, 1986).

Post-mining stabilization techniques include backfilling, grouting, excavation and fill placement, and blasting (SME, 1986). The extent to which post-mining stabilization techniques can be relied on to mitigate subsidence damage is uncertain, as they require assessment of long-term stability. But analytical methods to predict the long-term stability of overburden in room-and-pillar (Mine, 1986) and other mining methods need significant improvement.

The use of backfill in underground mine openings and workings is increasing due to need for systematic selection (Grice, 2001). Backfill is defined as the material or materials that are utilised in void openings of underground mines for mining technical or mining safety purposes. Backfill is applied in order to prevent fires and explosions, to improve mine ventilation, to improve the stability of the rock, to reduce subsidence effects at the surface, as well as for economical and environmental factors. Sources of materials are from the mining industries and mining related (e.g. fly ash, Flue Gas Desulfurization (FGD) –gypsum, slag, infertile overburden, tailings, filter dust, residues from mineral processing) or other industries (e.g. incineration ash, used building material, old bricks, used foundry sand, furnace blow-out). Mining with backfill technology helps mining companies achieve many of these goals. The technology of backfilling enables a wide range of engineering solutions for particular mine sites and their unique sets of problems and opportunities. Carefully engineered and efficiently run backfill systems can significantly enhance a mining operation. By contrast, badly engineered and poorly run backfill can be a serious impediment to the mine and, worst of all, compromise safety.

## 1.2 Analysis of backfill research

In the 1970s, the emphasis in industrialised countries was on mechanisation and high production rates, leading the way to bulk mining methods and large open stopes. This meant that backfill exposures were becoming larger and that pressure for producing structurally stable backfill masses at a low cost was increasing. Backfill research initiatives pursued at operations such as Kidd Creek mine in Ontario, Canada and Mount Isa Mines in Queensland, Australia led to the development of varieties of cemented backfills having relatively strong structural properties and low overall cement content (Potvin, 2005).

For example, the addition of waste rock, quarried rock or aggregate to cemented tailings at a 2 to 1 ratio allowed backfill walls exceeding 200 m in height by 40 m wide to be routinely exposed without significant dilution at Mount Isa Mines. This backfill effectively contained less than 10 % cement content (Cowling, 1998).

Sustained research led to further reductions in cemented backfill cost by substituting cement, an effective but often expensive binder, with cheaper substitutes such as ground furnace slag and fly ash. It was found that although such substitution can produce backfill with low early strength, in the long term, the backfill strength was adequate for most applications.

The North American mining industry in the 1980s and 90s faced new challenges, including the extraction of deep reserves and the recovery of highly stressed sill pillars. The trend towards mechanisation and high productivity was accelerating. Whilst stope dimensions gradually became smaller to accommodate high stress conditions, the requirement for the rapid turn around of stopes and high tonnage output called for mine backfills of different characteristics. Rapid curing time became an essential specification to achieve the compressed production cycles (Potvin, 2005).

The practice of mixing waste rock with thin cement slurry (with no tailings) eliminates the need for drainage and bulkheads. It produces a matrix of rocks bound at contact points with cement offering not only a fast curing and structurally strong backfill mass

but also a very simple, flexible and low capital cost backfilling system, with overall cost depending mainly on that of delivering the waste rock. Delivery of cemented slurry rock backfill to stopes is done with mobile equipment gathering rock backfill from passes or chutes, then driving through underground cement stations where cement slurry is poured over the rock. Mixing of the rock and cement slurry occurs as it is tipped from the edge of the stope.

Research into paste backfill technology undertaken in the 1980s, followed by its implementation in many North American mines in the 90s, was also driven by the elimination of drainage, fast curing and fast turn-around time to backfill stopes. The paste backfill was promising another strategic advantage over cemented slurry rock backfill in that it disposed of large volumes of mine tailings underground. This increasingly became the main driver for the development and implementation of paste backfill, as the mining industry wanted to improve its image towards impact on the environment, and realised the true cost of tailings surface disposal.

Not long after, the first North American paste backfill application followed at the Lucky Friday mine in Idaho in the US (Brackebusch, 1994). The plant was designed like a concrete batching plant. Although the paste was pumped to the shaft, the underground reticulation was gravity driven. The pipelines were not kept full and excessive wear issues had to be overcome.

Also in the early 1980s, Australia attempted to implement a paste backfill system at the Elura mine in New South Wales (Barrett, 2000). However, a number of technical issues were never overcome and the plant was later transformed to produce hydraulic backfill. This unsuccessful trial may have contributed to the relatively slow implementation of this technology in Australia, with the first fully producing plant commissioned in 1997 at Henty Gold mine (Henderson et al., 1998), followed by Cannington in 1998 (Skeeles, 1998) and Mount Isa mines (Kuganathan, 2001), and Junction mine.

Grice (1989) has described backfill research activities at Mount Isa Mines that cover a wide range of topics and include the design, production and placement of multiple

backfill types into the underground operation. A variety of backfill types and placement methods are used at Mount Isa to suit the different mining methods and performance requirements of the backfill. Where the backfill is required only to backfill the extracted void and to provide regional support, uncemented backfills are used. However, the majority of backfill is subsequently re-exposed and therefore must be cemented. Backfilling is an integral component of the mining operations and the research activities are targeted at the optimisation of ore extraction by improvements in backfill design and techniques. Research covers the major areas of backfill type and system design, production, placement and performance.

Inco Limited has led the paste backfill R&D effort in Canada, from the early 1980s to the commissioning of the first Canadian paste backfill plant at the Garson mine in 1994. Following the success at Garson, paste backfill was rapidly adopted by a number of other Canadian operations such as Chimo (Vallieres and Greiner, 1995), Lupin (Hinton, 1996), and Louvicourt (Lavoie, 1995).

Fall et al (2004) have described how the increasing use of paste backfill in underground mining makes it necessary to quantify the effect of sulphate on the strength development and economical performance of paste backfill. Therefore, the main objective of this study was to develop a methodological approach and a mathematical model to analyze and predict the strength development and cost of underground paste backfill containing different amounts of sulphate. This study demonstrates that the paste backfill can be defined as a “mixture system”. It was able to show that a material model based on quadratic functions can be a suitable basis for the prediction of both the mechanical (Uniaxial Compressible Strength : UCS) and economic (binder cost) properties of paste backfill. The developed models allowed to obtain valuable results about the relationship between the sulphate quantity and the mechanical performance of the backfill and the prediction of its strength at different curing times. This study has demonstrated that the sulphate significantly influences paste backfill strength. This influence is related to its concentration, the curing time and the amount and chemical composition of the cement.

Kesimal (2003) has studied one of the most important characteristics of a backfill material is the particle size distribution. This experiment has focused on the effect of deslimed mill tailings on paste backfill performance at a copper–zinc mine in northeast Turkey. The use of sedimentation methods to deslime has a widespread utilisation and is regarded as a true fractional size analysis practice. The common laboratory method of beaker decantation was used for desliming in order to determine the optimum particle size distribution. For studying the beaker decantation, two mine tailings, namely tailings samples A and B are used which have particles 52 and 54 wt % finer than 20  $\mu\text{m}$ , respectively. The fines content (20  $\mu\text{m}$ ) of each tailing were reduced to 15, 20, 25 and 30 wt % via desliming. Deslimed tailings then were tested to investigate the relationship between particle size and strength gain. It was found that strength ranges of the deslimed tailings were from 12 % to 52 % higher than as-received mill tailings.

Benzaazoua et al (2004) have studied the pollution potential of pyrite and arsenopyrite was examined through tailings from a European gold mine. The project was to study the geochemical behaviour of the tailings both before and after their inclusion into a cementitious matrix. Such a study requires extensive characterization of the tailings. The performance of Solidification and Stabilization Processes (SSP) was examined by studying the evolution of the leaching process in the tailings in alkaline media as well as the evolution of the microstructure and chemical composition of paste samples after enhanced leaching experiments done in a Soxhlet extractor. Both general and specific tendencies of weathering patterns were obtained from optical microscope observations coupled with a semi-quantitative EDS analysis in the weathering fronts. XRD SEM investigations and XPS were used to characterize the formation of secondary products. The main findings were that transfers inside paste samples are minimized due to the low permeability of the paste and the in situ precipitation of calcium sulphates and arsenates. These leaching tests show that lime enriched cement has high retention potential for arsenic, even though its porosity is increased by the dissolution of portlandite at the periphery of leached samples. In other samples, the carbonation of portlandite in the border front could be the factor which leads to arsenic release. As revealed by optical and SEM microscopies, the observed weathering fronts remain small, even in long duration experiments. These observations reinforce the interest in paste backfill using conventional hydraulic binders for the solidification and stabilization of sulphide tailings.

The first operational paste backfill system was built in the early 1980s at the Bad Grund mine in Germany (Potvin, 2005). Paste backfill reticulation was assisted with piston pumps to overcome the long horizontal distance from the shaft to the delivery points in the active stowing area. The pipelines were run full to minimise wear and the cement was added in the pipeline only near the delivery point.

Minkley et al. (2006) has described in the Merkers potash mine those working areas which have not been dimensioned in the past in a stable way are now stabilized by inserting rock salt as backfill material. The procedure concerns predominantly such working areas which have been mined in the carnallite of the Thuringia seam following the room-and-pillar technique. The purpose of this type of stowing is to provide a permanent stabilization of the mine layout and thus to prevent rock burst danger. The purpose is fulfilled by limiting the de-strengthening processes running in the pillars since several dozens of years.

Brennecke and Schrimpf (2004) have referred in Germany, abandoned and still operating mines have been used for hazardous waste disposal for many years. With respect to the disposal of chemotoxic waste and other residues more than 20 mines are presently in operation. One of the most well-known facilities is the Herfa-Neurode mine, part of a still-operating potash mine in the bedded salt of the Werra-Fulda district in central Germany. This mine particularly accomodates chemotoxic waste. Joint operations of ongoing mineral extraction and waste emplacement provides the advantage of a shared infrastructure, reducing operating costs.

Wendland and Himmelsbach (2002) have proposed the subsurface disposal of industrial residues in coal mine beneath densely populated urban areas is important in North-Rhine-Westphalia, Germany. The residues from electric power plants consist of filter ashes (fly ash) and desulphurization residues. These are being injected underground because suitable surface storage areas are no longer available. Furthermore, long-term enclosure of potentially toxic pollutants at the surface requires expensive technical measures and constant monitoring of the landfill area. On the other hand, existing geological barriers surrounding and underground repository can ensure some of these measures. Appropriate geological host rock condition are found in underground mines

in the Ruhr Region. The waste material is being used for construction and for backfilling cavities behind longwall facings. This process diminishes surface subsidence and renders the ventilation of the underground pits more effective. From the viewpoint of waste disposal as well as mining, underground deposition is thus economically reasonable. However, this procedure is only acceptable if the environmental compatibility is guaranteed; the materials should not endanger the biosphere or hydrosphere. Human, animal, and plant life must be unconditionally protected. The use of mines as repositories therefore requires a clear demonstration that contaminants that might reach the surface after thousand of year will not cause any harm.

Martens and Kaufmann (1997) studied surface subsidence and day falls in old underground mines caused two companies to order research studies on how to plan backfilling. One of the mining field is still operating and accessible, while the other is not accessible anymore and can only be reached by drilling from the surface. Both fields are situated within nature reserves so that noise and other emissions have to be kept at a low level. The planning of these backfill operations is based on the comparison and assessment of ways to deliver backfill material to minesites, on the backfill infrastructure (storing, mixing, transport) and the backfilling methods. Besides technical set-up of the equipment also the procedure of backfilling has to be planned. The backfill material is modified to guarantee sufficient flowability and the sufficient compressive strength. For backfilling in both mines variable and fixed costs are estimated. Tests proved the suitability of a rented concrete mixing plant to backfill the closed mine. The operating mine currently implements the results of this study into their operation.

Knissel and Helms (1983) have described laboratory tests of uniaxial compression strength of cement rockfill from washery refuse of coal mines in the Ruhr District of Germany and portland cement have shown, that the main factor of influence are cement content, age and water-cement ratio. For cement content up to 15 % strength will increase proportionally with increasing content of binding agents. Moisture content respectively water-cement ratio is the greatest influence to strength. For a definite aggregate type and cement content an optimum water-cement ratio can be calculated to achieve maximum possible strength. Density respectively porosity of cement aggregate

mixtures depends linearly on moisture content, if the rockfall is not compacted. Measuring the consistence of fresh mixtures is difficult. The vane shear test seems to be appropriate for in situ tests.

Palarski (1994) introduced tailings backfill into Polish coal mines in 1994. Over the past hundred years, considerable work has been done on the assessment of optimum mixtures, the development of flexible delivery system, and the adjustment of fill technology to a wide variety of mining and geological conditions. Sand or industrial waste material for the backfilling of underground workings is used as a support mechanism to control ground deformations and surface subsidence.

Mohrmann et al. (1995) have described to use of brown coal filter ash (BFA) in German mining. Every year, brown coal used in coal-fired power stations to produce electricity. A by-product from power station process is the BFA. The remaining voids in underground mine were completely backfilled by BFA mix with cement and mine waste. The backfilling with BFA was performed slurry via pipes and dumped into the mine voids.

Menninger et al. (2003) have described to the company GEOMIN-Erzgebirgische Kalkwerke GmbH, which has its main department in Lengefeld, also belong plants in Hermsdorf, Hammerunterwiesenthal and Oberscheibe, just south of the State Saxony. GEOMIN produces by underground mining calcitic and dolomitic marble which is processed to fillers, powder, fine sand, granules and decorative gravel. After century-long mining in up to 5 limestone-quarries, the underground room and pillar production began in the year of 1880 in the part of the quarry "Fiskalischer Bruch". The excavation of deep underground structures disturbs the initial stress field of the surrounding rock. The remaining underground mine voids between the pillars and host rock will be dumped backfill with low grade limestone and mine waste. The backfill material will compact sufficiently to support the rock around the pillars and drifts.

Li et al. (2002) have described the development and application of paste fill using dry tailings at St Ives Gold, Gold Fields. Three phases of extensive sampling and testing were conducted on dry tailings and examined various material properties, including



moisture content, sizing, mineralogy, residual cyanide, salinity and rheology. The success of these tests and of a large scale in situ trial led to a purpose built plant, with a capacity of 120 to 150 m<sup>3</sup>/hr, which was commissioned during October-December 2001. The behaviour of the paste was monitored using hydraulic pressure cells and showed very consistent results during the curing and exposing of the paste fill. Some numerical modelling has also been undertaken to analyse the paste behaviour. It has been demonstrated that paste fill made from dry tailings can reduce the capital cost and shorten the project start-up time significantly. The operating costs are comparable to that of the conventional paste fill using wet tailings. The other major benefit is the consistency of the dry tailings and dune sands, resulting in high paste fill quality.

As a relatively new underground mine backfill technique, the approach to backfill selection and application in practical mining operations is still development, although some rules and rationales have been established through recent research and company standards. The backfill selection procedure is very data-intensive, bringing a wide range of relevant data and knowledge together to support the necessary decision making and is very time consuming. As with most engineering problems, backfill selection requires substantial practical judgement based on a large amount of information and experience. The reasons for backfilling include ground control, economics, environmental considerations and the need for preparation of a working floor as in cut and fill operations for example. The environmental concern has grown in recent years and this trend is unlikely to end. Backfill operational concerns include backfill transportation, bulkheads, quality control, backfill material preparation, placement, maintenance, labour and stope preparation.

In underground mining with backfill, inter-chamber pillar recovery operations are closely related to stability of surrounding backfill, which is governed by stope size and mechanical properties of the host rock. Backfill of various solid compositions has been employed as an artificial support with considerable popularity in recent years. The most widely used cemented backfill consists of classified tailings, or mixtures of rock, sand and cement. Results of practical studies show that cement content in a backfill and its slurry density are essential factors affecting backfill stability and the economy of backfilling. The uncertainty in backfill selection, based solely on theoretical or

numerical modelling techniques, without experimental or practical input, may result in backfill block failure or excessive consumption of cementing material. In cyclic backfilling, the backfilled orebody is utilized mainly as a work platform and so the cement content required of this platform is generally higher than that necessary in delayed backfill, because of the short curing times available and need for rapid deployment of heavy mining equipment in the stopes. Hence, the backfill strength must be properly designed not only for pillar recovery in subsequent mining operations, but also for heavy equipment use.

The backfilling method used is often dependent on the mining system adopted and can be classified into two general groups; these are cyclic and delayed backfilling methods. With delayed backfill, the backfill must be capable of existing as a free standing wall after being exposed during pillar recovery. In-situ monitoring and observations have shown that stress and deformation conditions developed within backfill resulting from self-weight effects relate mainly to exposed backfill height, and so the stope size can be regarded as a key parameter in determining appropriate backfill strength requirements. In cyclic backfilling systems, backfill in each operation cycle acts as a platform for mining equipment or mining may occur below, beside or through the backfill and the engineer must design for these conditions and requirements (i.e. under cut & fill or undermining). The major factors determining traffic stresses are: loads transmitted by vehicle wheels, area of load influence, number of load repetitions, vehicle speed, contact area of tires, number of tires in the assembly, and spacing between axles.

To define appropriate backfilling methods, the following criteria are proposed:

1. Backfill technology should be reliable and guarantee safety and continuity in mining operations. The filled body should provide good support for the surrounding rock mass.
2. Backfill capacity should be optimized based on technical and economic analysis and backfilling operation time should not exceed 20 % to 25 % of the overall mining operation period.

### 1.3 New method of systematic selection of backfill

This study is for the selection process of backfill. Therefore, backfill performs many functions in underground mining operations, depending on the mining methods used, available materials and other factors. The backfill system selected must be capable of backfilling mined voids at a rate that will not interrupt the mining schedule. The systematic selection procedure of backfill consist of (Fig. 1.3):

- The primary source of backfill materials will be local to the mine. The material delivered must be strong enough to support mining equipment and/or subsequent backfill exposures with acceptable stability and minimal failures, to ensure complete extraction of ore reserves.
- Dilution of ore can come from slabbing of waste from the walls and/or back of a stope and from collapse of a backfill exposure from an adjacent stope. Ore loss will occur if dilution and/or local instability prevent the extraction of mineable ore reserves, or if dilution becomes excessive. Both can be minimised if the backfill material is strong enough to support all exposures and stiff enough to provide adequate confinement to stope walls to prevent or restrict local failures.
- The backfill must contribute to maintaining the overall stability of the mine, so that operations can proceed safely.
- Higher backfill strengths are achieved by adding more binder, so costs are higher. However, any required strength can usually be achieved using a number of different mixes, so testing is necessary to identify the optimum mix from the available materials. The relative prices of Portland cement and pozzolans, the cost-effectiveness of chemical additives and the potential savings from disposal of tailings or waste rock as backfill must all be incorporated into the determination of capital and operating costs.
- The choice of a system often depends on the cost and availability of the necessary constituents at a particular site. In practical terms, most materials are usually available and their application will be determined by their relative costs, performance characteristics and convenience of use. This system involves a cost/benefit analysis of those systems that meet the basic technical and operational requirements. Some systems can usually be eliminated because the materials required are not available locally, or because they are not applicable to the particular mining methods being considered. In

some instances, environmental considerations may significantly narrow the range of options.

- The use of commercial by-products, including mineral industry and other industry, binders such as portland cement, FGD-gypsum and pozzolans (e.g. fly ash or bottom ash) and chemical additives, may be advantageous where such products are locally available and where suitable natural materials cannot be found. Water is required for transport of hydraulic materials, hydration of binders and for dust control in dry systems. The suitability of these materials will depend upon the desirable characteristics of the backfill and the engineering characteristics of the products.
- Preliminary test work is required to confirm the suitability of available materials for a particular system. A particle size analysis of mill tailings is essential if hydraulic or paste fills are being considered. Tests that relate achievable strengths to the required rheological behaviour of the proposed distribution system are also valuable. Validation of assumptions and identification of local priorities (eg production flexibility, mullock disposal) and any constraints (eg impact on metallurgical recovery, environmental impact etc) are essential.
- It is important to accept that the optimum system is the one that contributes to achieving the maximum value for the entire operation, not necessarily the lowest capital cost or the lowest cost per tonne of backfill placed. Therefore the backfill system selection cannot be made in isolation, but must be integrated into the overall design and optimisation process.
- For backfilling an application of the following techniques is possible: gravity backfill, hydraulic backfill, pump backfill, pneumatic backfill, slinger backfill, dumped and slided backfill and stacking backfill
- In the case of wastes containing or contaminated with organic substance or heavy metal, limit of elution of backfill materials being considered. To reduce the elution from the backfill from mine waste or industrial waste in order to get high strength, binder had to be added.

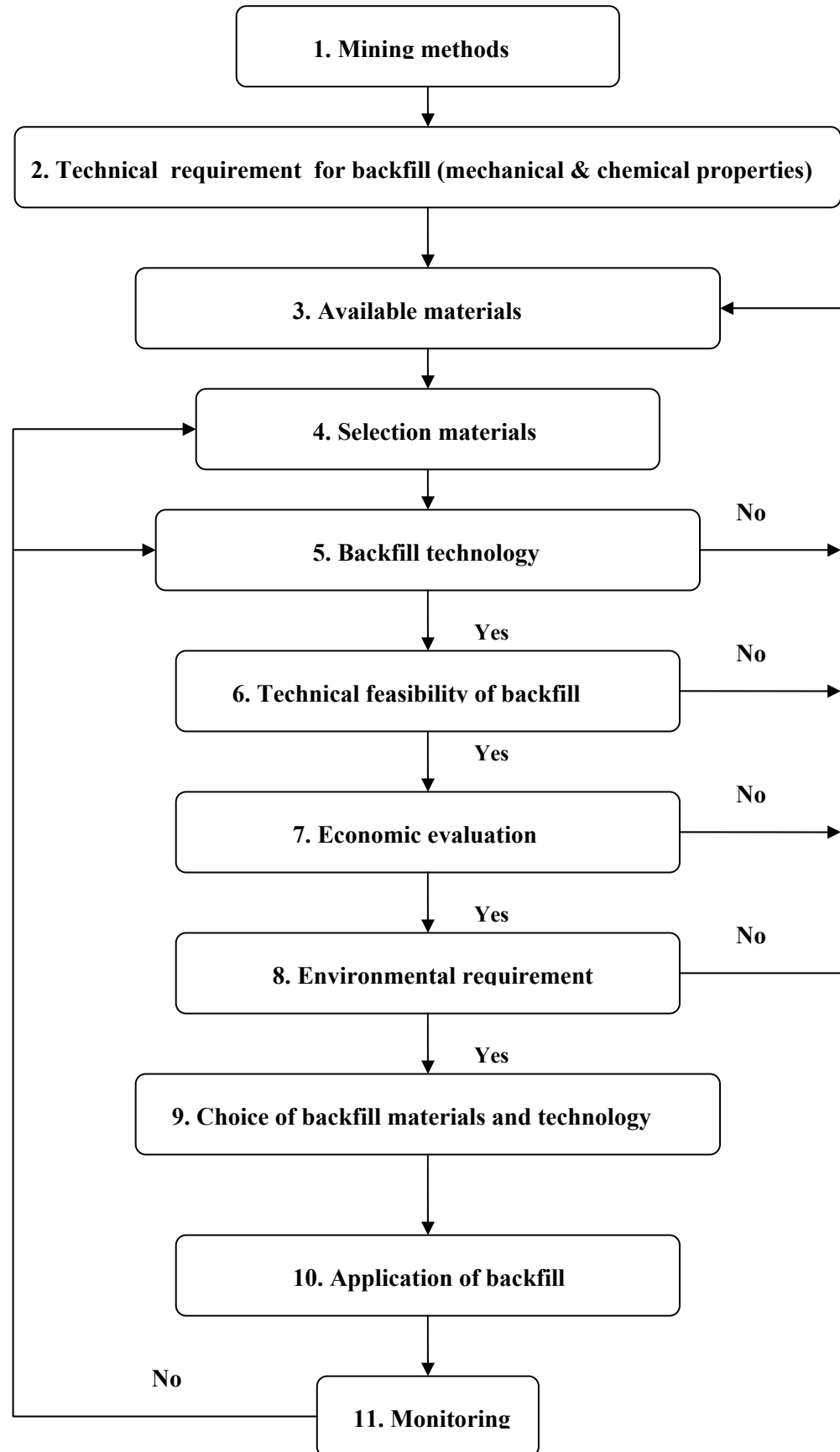


Figure 1.3: Systematic selection and application of backfill flowsheet

## Chapter 2

### Analysis of Mining and Backfill Techniques

#### 2.1 Mining technique specification

The selection of the mining technique relies on the mining conditions, equipment available, industrial regulation, financial situation etc. Mining techniques applied to the backfill operation can be classified as either "cyclic backfill" or "delayed backfill" with certain constraints for each classification. Before describing the backfill techniques, it is necessary to understand the following terms (Hassani, 1998):

(a) Mining object: Ore deposits are usually cut into smaller units - stopes or pillars. Each unit is a mining object.

(b) Mining life: A period of time starting from the beginning to the end of the certain mining operation. It could be the stope life, pillar life, etc.

(c) Backfill Purpose: The reason the backfill materials are employed in the mining operation. Backfill material is used in mining operations for at least one of the following reasons:

- 1) Pillar recovery
- 2) Sill pillar recovery
- 3) Working Platform
- 4) Ground support
- 5) Waste disposal
- 6) Mining on top, beside or under backfill

(d) Mining Geometry: The dimension of the mining objects which is described by three parameters: length, height and width, and location of stopes relative to surface operations and other workings.

Generally speaking, delayed backfill is applied for the situation where the rock mass conditions are relatively stable and efficient production is required. Stope recovery is normally fulfilled by delayed backfill except when the mining conditions are not

favourable. Cyclic backfilling is usually applied to situations where the rock conditions are relatively poor and a low dilution operation is required. Mining techniques related to delayed backfill are the following:

- 1) Vertical Crater Retreat
- 2) Shrinkage
- 3) Sublevel Stopping
- 4) Blasthole Stopping
- 5) Room and Pillar
- 6) Longwall
- 7) Block caving

The mining techniques related to cyclic backfill are the following:

- 1) Overhand Cut & Fill
- 2) Underhand Cut and Fill
- 3) Cut and Fill with Post Pillar

The specification of the mining techniques includes the following parameters:

- 1) Mining object: Stope or Pillar.
- 2) Rock condition (include the hanging wall, footwall, ore body).
- 3) Mining operation productivity.
- 4) Backfill Purpose.
- 5) Life of mining object: Operation period of certain mining object.
- 6) Mining method: Mining method and its classification.
- 7) Mining geometry: Height, Length, Width of mining object.
- 8) Primary Stress: Major principal stress, Intermediate principal stress, and Minor principal stress.

Various approaches have been investigated to predict the optimum dimensions of certain mining objects, among which are finite element, boundary element and other

empirical formulas for specific mining cases. Previous mining experience and personal expertise also play an important role in practical mining design.

## 2.2 Mining methods with backfill

Mining methods using backfill are very popular and a large variety exist (Fig. 2.1-2.5). Backfill methods are used when ground can not be left open for any length of time after ore has been mined out. Cut and fill methods are recommended if high recovery is important, for instance in high grade orebodies. On the other hand, backfill is placed in sub-level open stopes which remain open during the active mining phase, but cannot remain open for long periods of time without jeopardizing general mine stability. Backfill is also used in open stopes for later pillar recovery.

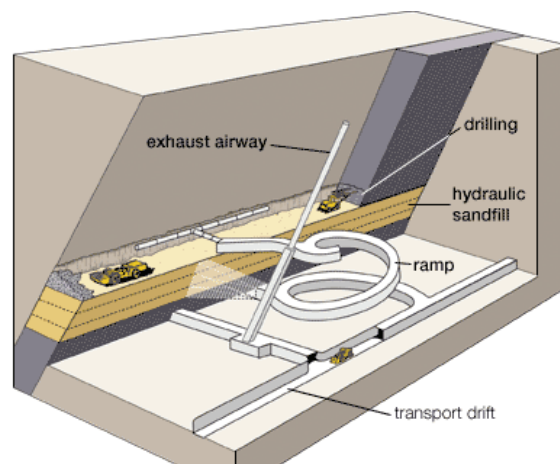


Figure 2.1: Typical mining methods: cut and fill (Hamrin, 1997)



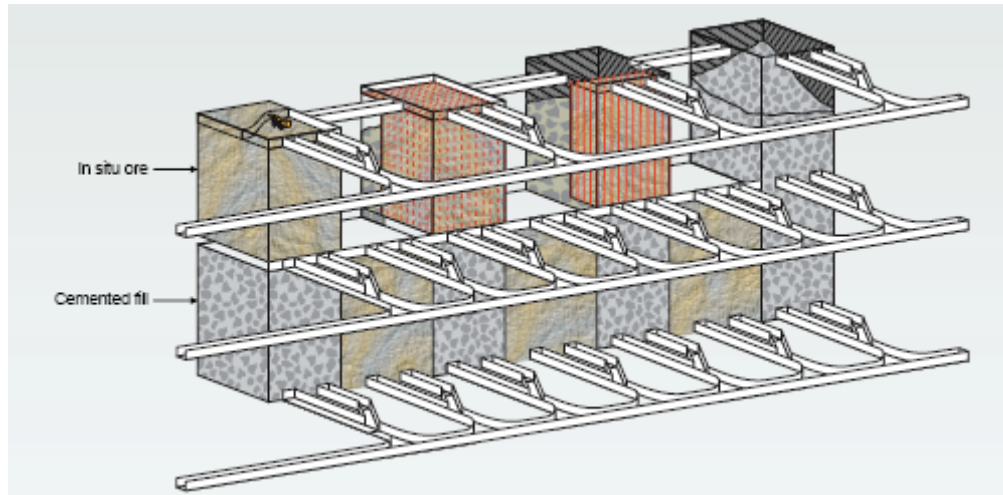


Figure 2.2: Typical mining methods: open stope (Potvin, 2005)

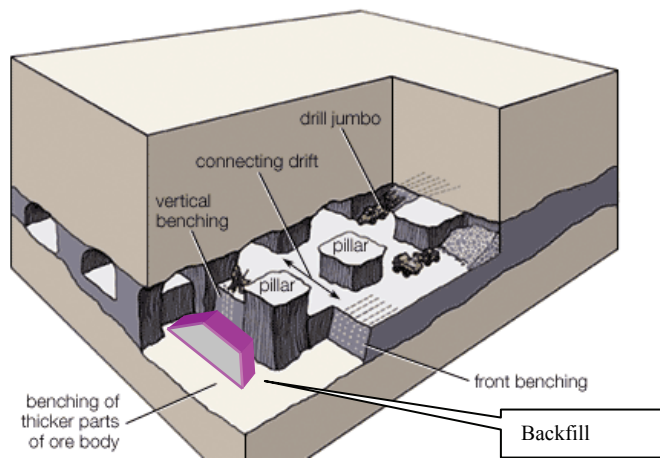


Figure 2.3: Typical mining methods: room and pillar (Hamrin, 1997)

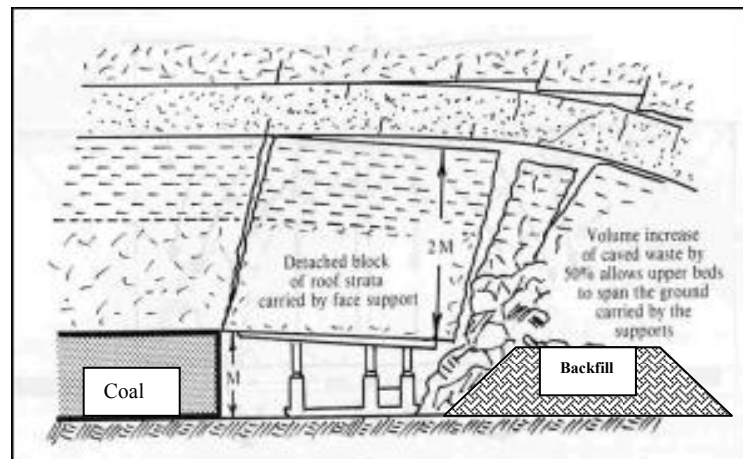


Figure 2.4: Typical mining methods: Longwall mining (Whittaker and Reddish, 1989)

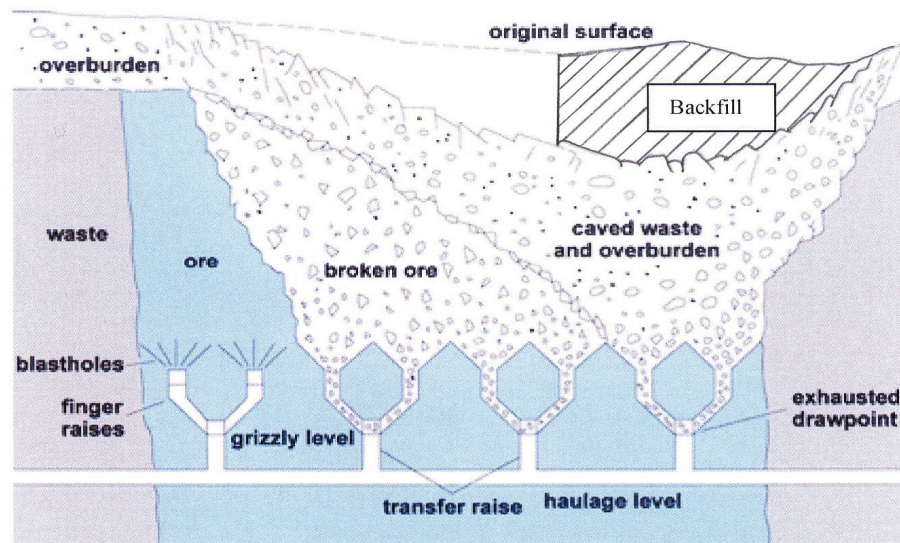


Figure 2.5: Typical mining methods: block caving mining (Brady and Brown, 1985)

The classification presented below is considered the most basic for mining methods using backfill.

**Cyclic fill methods;** overhand cut and fill and underhand cut and fill

**Delayed fill methods;** sub-level open stopes and pillars, shrinkage stopes, room and pillar and post-pillar and stope and pillar mining

### 2.2.1 Cut and fill methods

In both overhand and underhand methods, ore is mined in horizontal slices a few meters thick.

**Overhand methods.** The most popular cut and fill method is the overhand method. Ore is removed in a series of horizontal slices, and as each slice is removed, backfill is placed into the stope, leaving sufficient working headroom to drill ore for the next slice. Operations in the stope normally consist of: backfilling, drilling, blasting, scaling, rock bolting, and muck removal. Depending on the nature of the surrounding rock, the thickness of slices can vary from a couple of meters in weak ground to 3 to 4 m in good ground. With some cut and fill stope configurations, a high degree of mechanization is possible using drilling jumbos and scooptrams. The efficiency of the method is linked to how independently all the various mining operations can occur without interfering with one another. Dilution can occur when ore is blasted on the cemented backfill floor, as some of the backfill may be scooped up with the ore. Great care needs to be exercised during mucking in order to minimize dilution of ore with backfill. A typical cut and fill method is captive cut and fill. This method requires minimal development work, but has the disadvantage of the equipment being 'captive' within the stope until the upper level drifts are gained. A variation called drift and backfill makes use of the drifting approach. Ore is drifted with jumbo and scooptrams; after the ore is removed, the drift is backfilled and mining can resume alongside, parallel to, or above the original drift.

Another method, vertical cut and fill, can be used where the ore and walls are more competent and can be exposed over a height of 10 to 12 m. With this method, ore is drifted longitudinally with development equipment. After a slice has been mined out, it is backfilled tightly to the back. Mining can then proceed one or two lifts above the previously mined-out slice. When this last slice has been mined out, benching equipment is used to drill down holes to the first slice and the ore in between is benched out. Broken ore is removed and two cuts are then ready to be backfilled.

Sub-level cut and fill uses the principle described for the vertical cut and fill method, with the distance between the cuts being expanded. This method can be used where ground conditions are good and the wall can be left exposed over a greater distance. This method represents an improvement over normal cut and fill because drilling, blasting, mucking, and backfilling can be done independently of one another.

**Underhand cut and fill.** As the name implies, ore is mined from the top level towards the lower level. This is a very specialized method and is not widely used. Mining ore starts on the top elevation in a horizontal cut. After enough ground is opened, posts are installed underneath the previously constructed backfill materials. The materials is then built and backfilling can proceed. Once the backfill has cured, the slice below can be mined. The operation is repeated until the level below is reached.

### 2.2.2 Delayed backfill methods

#### **Sub-level open stopes and pillars**

The most widely used mining methods using backfill are in the broad category of sub-level open stope methods. Sub-level stoping is best adapted to steeply inclined ore bodies which have strong walls and where ground conditions permit large opening sizes without causing undue dilution. The methods are used in large tonnage orebodies of low to medium grade. If the ore body is large, it will be mined with transverse stopes and pillars or perpendicular to the strike of the ore body. If the ore body is narrow (up to 30 or 40 m), it is mined longitudinally. There is no limit to the size of ore bodies that can be mined with this method; it is one of the cheapest and most efficient when conditions are suitable. Used in combination with appropriate backfill material, 100 % ore recovery can be ensured.

The general approach is to divide the orebody into a series of primary stopes and pillars, whose size depends on ground conditions and the size of the orebody. Mining then proceeds with the primary stopes in a sequence often referred to as the 1-3-5 sequence. Once a good number of primary stopes have been mined, mining the pillars can proceed and this is referred to as the 2-4-6 sequence. A typical sub-level method is Blasthole Mining with Delayed Backfill employing transverse mining panels. Both hydraulic

backfill and rock can be used in sub-level open stopes. Hydraulic backfill is introduced over an extended period of time through pipes located strategically in the upper end of the stopes, in order to achieve the best backfilling results. Cemented backfill is normally used in the primary stopes and non-cemented backfill is used to backfill the secondaries as, due to future mining, the stope will not be exposed.

**Shrinkage stopes.** Ore is mined in a succession of horizontal layers and broken ore becomes the working floor. Only the exceeding swell is taken out of the stopes through a series of drawpoints or chutes. Once the upper level has been reached, the entire stope is emptied of its ore. At this stage the stope can be left open, or backfilled if the surrounding rock mass is not competent enough and poses a threat to the general stability of the mine. Shrinkage stopes are best suited for steep and narrow orebodies with competent walls.

### 2.2.3 Room and pillar

Room and pillar mining is well suited to horizontal or flat dipping orebodies extending over large areas. Ore is mined in rooms separated by rib or square pillars. Pillar design is guided by the depth of the mining zone, thickness of ore, stresses in the rock, and strength of the rock mass. Pillar design can in some cases ensure as much as 80 to 92 % ore recovery. For general mine stability and to limit surface subsidence, backfill is introduced between pillars after the ore has been mined.

Post-pillar mining evolved from cut and fill transverse mining. Pillars are designed to fail after backfill has been placed around them. One interesting feature of the method is that the pillars can be designed with safety factors of less than 1. The failed pillars are held together by the lateral earth pressure of the backfill and have load carrying capabilities. A number of cuts can then be made on top of each other. Post pillar mining offers advantages in variable shaped orebodies, too thick for regular room and pillar. The backfill introduced will be cemented for the working floors using a mixture of 1 to 10 backfill to cement over approximately 30 cm thicknesses.

Stope and pillar mining is one of a variety of open stope techniques and only differs from room and pillar in that it is less systematic, having excavations and pillars of irregular sizes and shapes. This method is used only in hard rock mining, whereas room and pillar is more common in soft rock formations. Both stope and pillar and room and pillar mining are usually methods of choice in tabular orebodies. Production mining consists of mining a top slice of the ore zone and leaving behind both waste and ore rock as pillars for back support. Production mining continues downward by benching or upward by slabbing, while maintaining the continuity and integrity of the pillars. In slabbing, slices of ore are removed from the back much like cut and fill stoping. In the production mucking cycle, not all of the ore is removed, as some must be retained to build a ramp so that the production drill equipment can reach the back to mine the next slice of ore. The main disadvantage of the slabbing technique is the extra roof support required after each lift. The remaining underground mine voids between the pillars and host rock will be dumped backfill with low grade limestone and mine waste in Lengefeld Mine. The backfill material will compact sufficiently to support the rock around the pillars and drifts.

#### **2.2.4 Longwall mining**

Longwall mining is a highly productive underground coal mining technique. Longwall mining machines consist of multiple coal shearers mounted on a series of self-advancing hydraulic ceiling supports (Palarski, 1994). The entire process is mechanized. Longwall mining machines are about 240 m in width and 1.5 to 3 m tall. Longwall miners extract "panels" - rectangular blocks of coal as wide as the mining machinery and as long as 3,650 m. Massive shearers cut coal from a wall face, which falls onto a conveyor belt for removal. As a longwall miner advances along a panel, the roof behind the miner's path is allowed to collapse. Longwall mining was first introduced in the 1950s and 1960s. Today it accounts for more than half of all coal production in the United States. On any given day, a typical longwall mining system is capable of extracting between 10,000 and 30,000 tons of coal from a panel. The primary downside to this very productive technique is a prohibitive initial investment - longwall mining machines usually run between 5 and 15 million dollars. Longwall mining replaces the historical "room-and-pillar method", whereby underground "rooms" of coal are manually extracted and pillars are left to support the roof so miners can work safely. In mining regions deeper than 300 m., the room-and-pillar method becomes highly

uneconomical because the size of pillars required to support the roof are much larger, meaning that valuable coal cannot be extracted from them. Longwall systems make deep mining feasible.

In Australia almost all backfill is placed into metalliferous mines which use stoping methods of ore extraction. Overseas, backfill is widely used in coal mines to minimise surface subsidence behind longwall mining operations. One longwall coal mine in Germany, Walsum Colliery, takes local municipal and industrial wastes and stows them permanently. The backfilling operation results in minimal subsidence and the cost of filling is largely offset by the fees charged to perform the disposal service (Grice, 1999). Extensive experience has been developed in Australia with specialised design and application of backfill technology to particular problems. One particular issue had been encountered in two American coal operations. In these examples, backfill was used to stabilise pre-driven roadways ahead of longwall mining.

### **2.2.5 Block caving**

Block cave mining is a mass mining method that allows for the bulk mining of large, relatively lower grade, orebodies. This method is increasingly being proposed for a number of deposits worldwide, thus the scope for a better understanding of block caving behaviour. Because many existing large open-pit mines are also planning to extend their operations underground by block caving, research is undergoing to investigate the rock deformation mechanisms associated with the transition from surface to underground mining operations. In general terms block cave mining is characterized by caving and extraction of a massive volume of rock which potentially translates into the formation of a surface depression whose morphology depends on the characteristics of the mining, the rock mass, and the topography of the ground surface (Figure 2.5). Block cave mining can be used on any orebody that is sufficiently massive and fractured; a major challenge at the mine design stage is to predict how specific orebodies will cave depending on the various geometry of the undercut.

Block caving has been applied to large scale extraction of various metals and minerals, sometimes in thick beds of ore but more usually in steep to vertical masses. Examples

of block caving operations include Northparkes (Australia), Palabora (South Africa), Questa Mine (New Mexico), Henderson Mine (Colorado) and Freeport (Indonesia).

Another way to understand what block caving is all about is to examine this figure:

It shows the essential aspects of block caving: an underground tunnel leading to draw points where the overlying rock, broken by gravity more or less flows to the draw point, to be gathered and taken away for processing (David Chambers, 2008).

Coal-mining subsidence badly destroys environment. Backfill in caving area refers to any mineral waste material or sand that is placed into roof fall rocks in order to reinforce the roof fall broken rock. Backfill is performed to resist to roof fall and reduce surface subsidence. The grouting backfill method of fall rocks has been used in Poland for many years. The method is based on longwall with caving, and surface deformation value decreased 30~40%. The configuration of the roof fall rocks and grouting materials mixture is call to backfill; The backfill will be compacted after strata cracks; so the compaction character is a key factor influencing coal-mining subsidence (Li et al, 2007).

## **2.3 Backfill technologies**

Backfilling technologies can be classified as gravity backfill, hand backfill, mechanical backfill, pneumatic backfill, hydraulic backfill and paste backfill. Hand backfill require the presence of personnel near the face for packing dirt, which is almost impossible due to very low quality. Gravity backfilling requires high dipping ore seams so that backfill material can roll into the void created by mining. Mechanical backfilling has been left out mainly due to its lack of effectiveness. In this method waste material is introduced using some kind of mechanical device like conveyor belts, slinger belt and load-haul-dump (LHD) into voids created by mining.

### **2.3.1 Mechanical backfill**

Mechanical backfilling techniques were developed with the introduction of conveyors into underground mining operations and have been used for backfilling of the waste rock and for the construction of packwalls (Bucek and others, 1980). Mechanical systems require less labour and permit more rapid placement of the packs compared to hand packing and so offer support to the roof in a shorter time. Numerous mechanical



methods now exist for constructing packwalls at advancing longwall faces. Backfill is used for underground mines, the major application being for the construction of roadside packs. With mechanical backfilling the waste is mechanically slung into voids created by mining. One of the first applications was the use of shaker conveyors, with scrapers, slushers and slinger-type machines being subsequently introduced. Actual placement of the backfill materials in the stope may be accomplished in the following ways:

- Slushing; the backfill may be slushed directly from a waste raise to the stope area to be filled. Usually, the waste raise leading to the stope is supplied by rail car, front-end loader, or LHD from a waste pass or transfer raise, which is the materials source for the entire mining area.
- Slinger belt placement; this system may use a high-speed belt and hopper supplied by truck or LHD (Fig. 2.6). The materials may also be placed by slinger belt mounted under a hopper. Slinger belt systems provide good compaction and relatively strong fill if gradation of the materials is proper.



Figure 2.6: Representation of a mechanical backfill (K+S, 2005)

The compacking system is a versatile mechanized system of modular construction that can form a part of many face-end systems. The system consists of a number of cylindrical quadrants pivoted vertically and mounted within protection boxes so that they can oscillate. Other components of the system include the cam box mounting, the power pack, and a hydraulic circuit. During operation the rippings are fed into the first

cam, called the feeder cam, and as the set of cams oscillates the waste is transferred from cam to cam and is ultimately placed into the pack, Cam oscillation is achieved by means of a hydraulic activator. Several installations at mines using the campacker system are outlined by the mining company.

For example in room-and-pillar mining where mobile scoops and ram cars can be used away from the site of coal extraction. Bucek and others (1980) provide a conceptual design of a backfilling system involving mechanical transport and mechanical emplacement for a room-and-pillar mine. The system uses battery powered scoop cars for placing the waste in mined out rooms. The volume of material that can be stowed would depend upon the degree of compaction of waste and the extent to which the goaf is filled. The outline a procedure for evaluating the proportion of the mined out capacity that is filled by mechanical stowing.

Gravity transport systems make use of gravity to move material down vertical or inclined chutes, boreholes or pipes. These techniques are currently used to move material to depths of up to 600 m, e.g. in the Doubrava Mine of Czechoslovakia (Zvacek, 1979). The most effective pipe diameter is reported as being 300 mm when the material is up to 80 mm diameter with some clay content. Gravity transport systems have the advantage of being able to be installed in ventilation shafts, thus easing congestion in roadways, etc. All methods of gravity transport generally require that the lowering of backfill via the vertical or declined pipe is accompanied by continuous unloading at the bottom via some discharge/feeder mechanism. This will avoid clogging of pipes or chutes (Bucek and others, 1980). It is also usual to incorporate a velocity damping chamber at the bottom end of the pipe, in which some of the waste is allowed to accumulate to form a cushion. Note that the gravity transport system is just one of a variety of transport modes both above and below the ground. A gravity feed transport mechanism has also been included in a conceptual design for mechanical backfilling outlined by Bucek and others (1980). For gravity stowing the most important features of the waste material are its free-fall characteristics which are determined by moisture content and size. The material should have a low moisture content, so that it is not sticky, and the maximum size should not exceed 300 mm in order to avoid impact damage to support structures. Bucek and others (1980) indicate that the waste preparation requirements for gravity stowing are dewatering of the fine fraction and blending of this with the coarse fraction. Kuhn (1979) considers that the particle size

should be up to 120 mm with a maximum of 20 % fines less than 1 mm, and with a water content of between 5 to 9 %. This is sufficient to suppress dust, but not enough to cause handling problems or to result in a large water content within the deposited fill.

### 2.3.2 Pneumatic backfill

Pneumatic backfilling is in a way transporting bulk material through a pipeline by applying either negative or positive pressure air stream and subsequently dumping the material in voids. It can also be described as harnessing of air movement to accomplish work. Material is feed into the system using a pipe feeder system shown in Figure 2.7 (Crandall, 1992). Air is supplied to the pneumatic pipe feeder at 0.69 MPa and expands to pipeline pressure of 27.58 kPa. The material should be dry and free flowing. It must be noted that pump connected to the compressor used for conveying may get unbalanced due to wear and tear which will reduce the efficiency of the system due to air leakage. The pump should not be allowed to operate for a sustained period of time without material or substantially under loaded. Hence material should always be available for conveying.

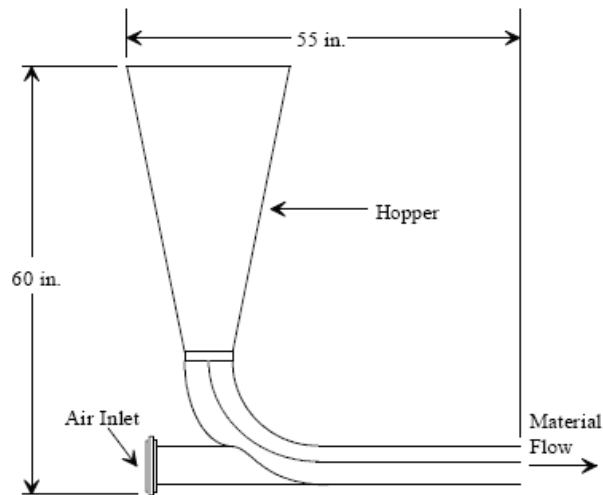


Figure 2.7: Pneumatic pipe feeder system (Burnett, 1995)

### 2.3.3 Hydraulic backfill

Hydraulic backfilling of voids involves the utilization of water as a transporting medium of solids (Fig. 2.8). The typical components of this system includes a mixing

installation for making the slurry, a slurry pump or pumps, and pipes for distributing the backfill material underground. The mixing installation includes a mixing tank into which prepared backfill is fed and mixed with water to form an evenly mixed slurry. Apart from mixer, slurry pumps are used for transporting the mixture.



Figure 2.8: Hydraulic backfill (K+S, 2005)

The material chosen to be used for hydraulic backfilling requires large quantities of cement (about 10 %). Hence before using hydraulic backfilling, the economic benefits derived from it should be stringently measured. Moreover, the backfill material has very low water content. Hence it must be flushed very quickly into the mined out area as soon as possible, otherwise there is a danger of the whole mixture setting in the pump and the pipes. Fly ash and very fine washery refuse show thixotropic properties which prevent the slurry from settling down and also help in reducing friction on pipeline wall. The chances of setting can be further reduced if cement is mixed at the end of the transportation phase just before introduction into the mined out stall. The use of high density backfill has been successfully implemented in Grund mine in West Germany. Highly consistent paste like backfill material has been successfully transported over a distance of 6,500 ft with discharge rate of 137 fpm (Crandell, 1992).

Major bottle neck of hydraulic backfilling over pneumatic backfilling is the availability of the transporting medium that is water. It may or may not be widely available in the mine and hence hydraulic backfilling cannot be applied universally. On the other hand a pneumatic system does not have any such bottleneck. But hydraulic backfill provides a much better backfill strength compared to pneumatic backfill. As a result where high

strength backfilling is required due to high strata pressure and/or weak pillar strength, hydraulic backfill will perform better compared to pneumatic backfill. Hence the choice of backfilling system is site specific and no general rule of thumb is available for selection.

There are two types of hydraulic transportation system namely 1) open hydraulic system, and 2) circulating hydraulic system. The open system requires only one length of pipe from the slurry preparation plant to the face. For this system, mine water is supplied from existing dewatering system within the mine. The pumped out water is used to transport the slurry down to the face for final injection into the stall. A circulating hydraulic system on the other hand works on a closed loop where water used for transporting the fill material is recycled and returned to the surface to be used again. Hence depending upon site condition, any one of the system can be used for transporting backfill material. Various different types of pumps are available in the industry for pumping slurry. There are listed below.

- Plunger pump
- Piston pump
- Double piston pumps
- Rotary ram pump
- Centrifugal pumps
- Hydraulic exchange pumps

All these pumps are capable of producing high flow rate and high heads, but only the hydraulic exchange pump is capable of handling high concentration slurries of the order of 60 % solids.

Pumps of such capacity are widely available. However, another major cost center associated with hydraulic backfilling are the pipes. For the purpose of backfilling, abrasion resistant steel pipes have to be used for transporting the slurries to the panels and epoxy coated fiberglass slurry lines for injecting the material into the stalls. These are substantially more expensive than PVC pipes which can be used in case of pneumatic backfilling.

### 2.3.4 Paste backfill

First used at the Grund Mine in Germany during the 1980's, paste backfill is a uniform, low permeability, generally consisting of high solids density mixture with about 15 % minus 45  $\mu\text{m}$  (325 mesh) fines content. Due to compaction, paste backfill's constituent particles do not settle out of suspension at zero flow rates with the fine particles of the matrix forming an annulus around a plug of coarser particles to act as a form of lubrication thereby greatly reducing pipeline frictional resistance (Fig. 2.9).

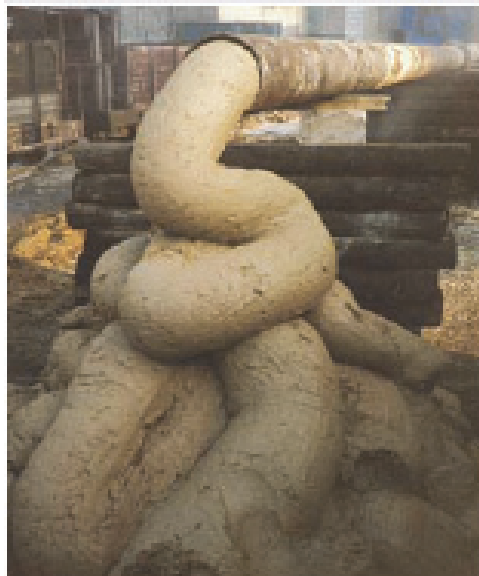


Figure 2.9: Paste backfill (Potvin, 2005)

Slurry backfill requires considerable transport water to flush it through the underground backfill distribution system and deliver the alluvial sand or tailing solids to a stope. Such excess transport water must be drained from the stope and hence, fine particles (i.e. slimes) are not desirable as they serve to reduce the overall permeability of the backfill. In contrast, paste backfill requires the presence of slimes to maximize solids content and to act as a lubricant for pipeline flow. This significantly reduces the need for high transport water volumes and the water that is used tends not to bleed out of the emplaced backfill as it is consumed by cement hydration or locked interstitially within the backfill mass. This greatly reduces or eliminates the need for backfill drainage and

hence the significance of backfill permeability. Other advantages of using paste backfill include:

- A shorter mining cycle due to the earlier development of higher compressive strength.
- Reduced binder consumption for equivalent or better slurry backfill strengths.
- High tailings usage thereby reducing surface disposal needs.
- A cleaner operation as slimes draining from the stope are eliminated.
- Potential reduction in backfill dilution of adjacent ore due to increased strengths for similar cement contents, relative to slurry backfill.

Disadvantages of paste backfill include:

- The need for superior dewatering facilities/technology and greater technical precision.
- The presence of increased pipeline pressures.
- That it is a relatively new technology in which many technical aspects are not yet fully understood.

The transportation of highly viscous substances has become common in the food processing and sewage industries, but the transportation of paste backfill owes more to the concrete industry for its technology. Concrete has a similar broad grain size distribution as some paste fills and the material flow regime associated with concrete transportation has become the most likely model for describing paste backfill.

When attempting to analyze the flow behaviour of paste material in comparison with concrete a few distinctions must be drawn (Hassani, 2005):

1. The abrasive characteristics of the paste backfill particles are likely to be far higher than with concrete.
2. The majority of the fines in paste backfill are made up of tailings rather than cement; this results in higher cohesion and hence a higher resistance to flow.
3. Paste backfill is often transported over greater distances.
4. Material preparation is far more complex.

These factors result in higher, and larger, ranges in estimates of pressure losses.

An example of a reduced mining cycle can be seen in Figure 2.10, where a hypothetical VRM (vertical retreat mining) stope is being backfilled first with a paste backfill and then, for comparison, with a slurry backfill. While the initial steps of the mining cycle, namely blasting and mucking, are independent of backfill type, the preparation time for barricade construction and plug preparation is significantly reduced for the paste backfill. Complete backfilling of the stope and the curing of such backfill can be achieved considerably faster for paste backfill due to higher solids concentrations and the reduced need for handling excess transport water.

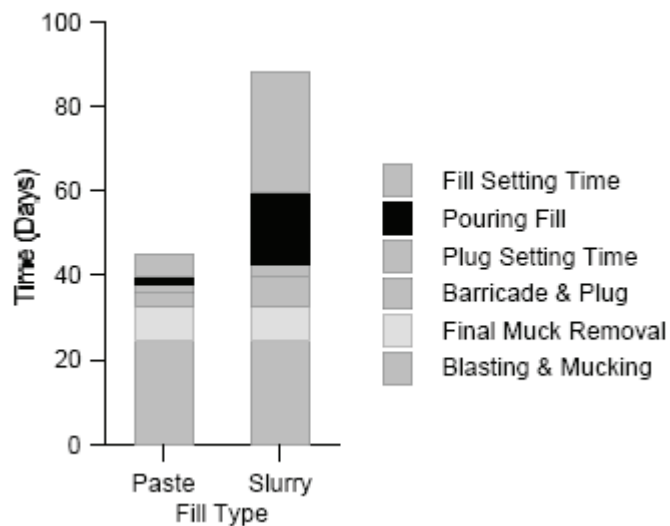


Figure 2.10: Comparison of the mining cycle between using paste backfill and slurry backfill in a VRM stope (Mark et al, 1990)

Paste backfill consistency is often described in terms of its slump character. Inherited from the concrete industry, slump is a measure of the subsidence, typically from 0 cm to 30 cm, of a paste material that has been molded by a standard truncated cone using standard method. Figure 2.11 shows an example of the characteristic slump and solids content of a mine paste backfill. It should be noted that slump will vary from material to material and is designed ideally for comparison between the same materials using different mixing properties, not between different materials.



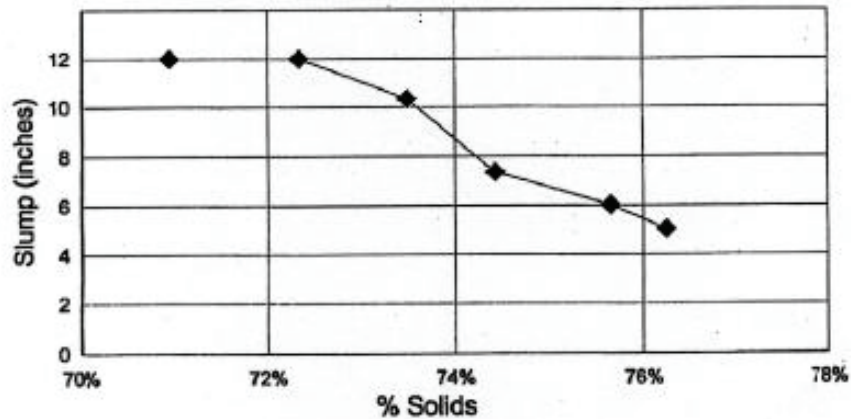


Figure 2.11: Relationship between slump and solids density for Golden Giant Mine Paste Fill (Paynter and Dodd, 1997)

A conceptual model developed by Aref et al (1992) outlines the main aspects to be considered when designing a high density paste backfill system. These aspects are important for determining backfill material sources, transportation and placement requirements and should be reconciled so as to satisfy backfill quality and schedule requirements as shown in figure 2.12.

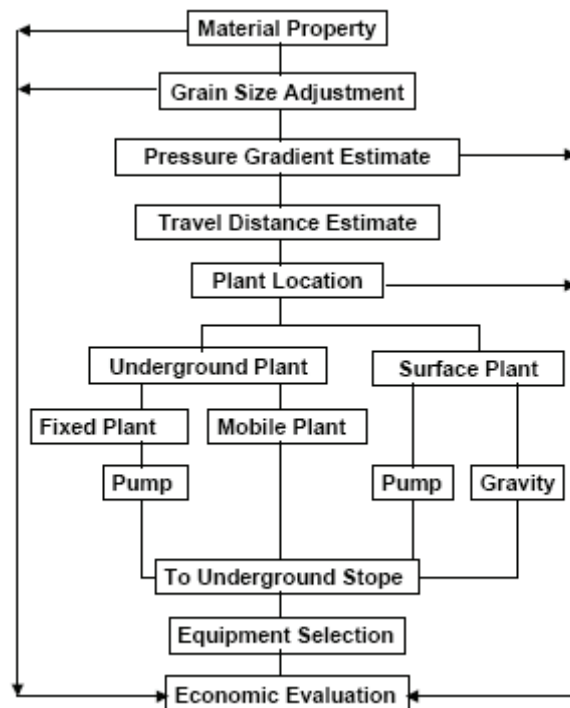


Figure 2.12: Flow chart for conceptual design of paste backfill system (Aref et al, 1992)

Material property characterization is necessary for determining the suitability of the available materials in producing a desirable backfill. Paste backfill requires a certain proportion of fine particles described by Brackebusch (1994) as 15 %, by weight, of minus 20  $\mu\text{m}$  (625 mesh) material and by Aref et al (1992) as 15 %, by weight, of minus 45  $\mu\text{m}$  (325 mesh) material. Due to a level of uncertainty in predicting paste flow, a full scale pumping loop test may be required in order to ensure accurate pressure gradient measurements. Practical horizontal pipeline pumping distances for paste backfill range up to 1 km with vertical dropping distances being unlimited (depending upon pipeline pressure ratings). Horizontal distances at the bottom of a vertical pipeline can range from one to several kilometres depending upon the height of the vertical column of paste (Brackebusch, 1994). Paste material preparation plants and cement mixing facilities have been located both on surface and underground.

Underground operations are often limited in production scale due to the confining nature of the mine workings but have a distinct advantage of adding backfill binder 'just in time' immediately before emplacement within the stope and thereby greatly reducing the risk of a plugged pipeline. Underground dewatering facilities generate excess waste water that must be pumped to the surface; such reject water may contain up to 40 % solids (by weight). As such, surface plants are far more appealing in most cases for paste fill preparation. Concrete is typically pumped in civil engineering applications and many early experiments with mine paste backfill employed positive displacement pumps to transport the backfill to the stope. While they may be required for surface transportation of paste, more recent experience has demonstrated that there is sufficient gravity head in most mines to distribute paste fill unassisted by pumping. As with all backfilling technology, all technical gains associated with paste fill must be subject to an economic consideration and everything must be balanced so as to produce high quality backfill when and where it is required.

### **2.3.5 Pumping paste**

Where the gravity head contributed by the vertical drop alone is insufficient to overcome the high pressure gradients within the horizontal section of the pipeline it is necessary to use a positive displacement pump to add additional energy to the backfill distribution system. As described by Hassani and Bois (1992), with the recent increased interest in paste backfill a few companies have emerged as experienced suppliers of

high pressure, high capacity positive displacement pumps. Putzmeister have developed their successful concrete pumps and now supply pumps for transporting high density backfill in Germany, the USA, South Africa and Canada. GEHO is a company from Holland with a long history of pump manufacture (Figure 2.13), some of which will transport highly viscous abrasive materials at pressures of up to 165 Bar. Schwing is one among many other companies who has been able to apply their experience in pumping large volumes of heavy sludge to solve problems associated with paste backfill.

### DHT

The GEHO piston-type slurry pump with transfer tube

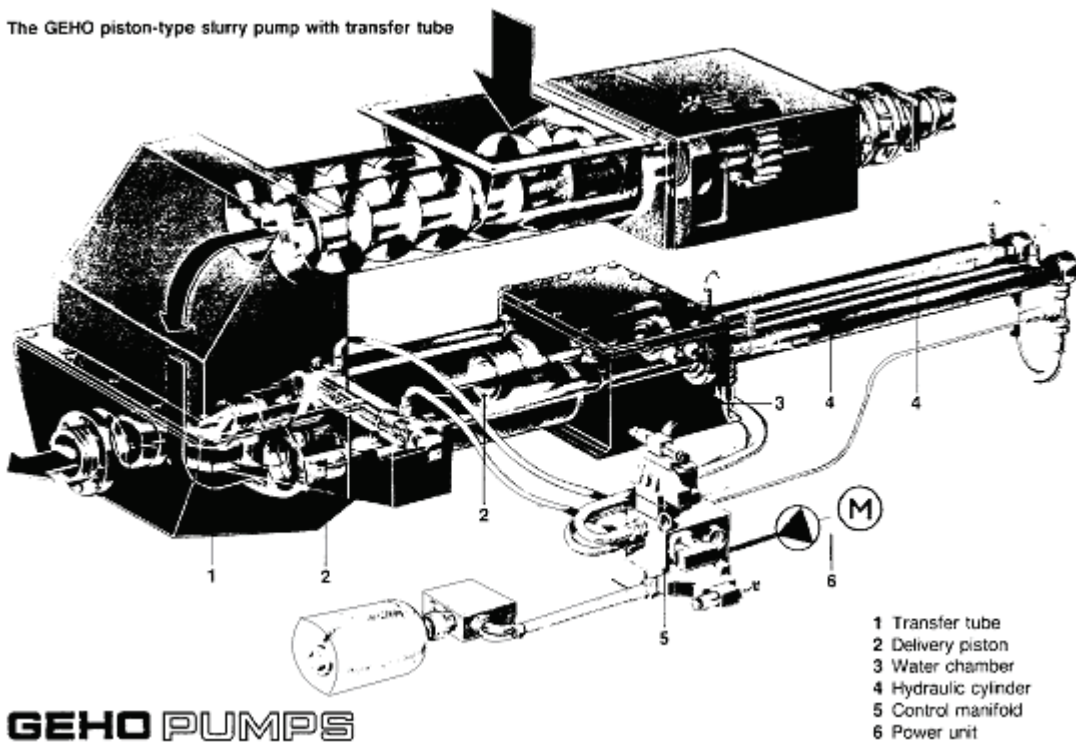


Figure 2.13 : GEHO positive displacement pump

The costs of positive displacement pumps are many times greater than those of centrifugal pumps with some pumps costing up to \$250,000. As with all pumps maintenance is a very important factor in choosing a unit. The costs involved in repair and for replacement parts can be prohibitive and a warranty protecting purchases is recommended.

The material from which the pump is manufactured is dependent on the corrosiveness and abrasivity of the slurry material being pumped. A simple rationale for pump selection could include assessment of several factors, such as:

**Abrasivity:** High >7 (on the original Mohr's scale) chrome plated steel Medium, 5 - 7 (Mohr's) rubber lined mild steel Low, <5 (Mohr's) unlined mild steel.

**Corrosivity:** Acidity or alkalinity will require pump protection by either, stainless steel or chrome plating.

The higher head (or pressure) required for pumping then the lower will be the capacity for a given pump. A high pressure positive displacement pump will require superior pipeline connections and overall higher quality, including more maintenance and supervision. Post sales service is very important when choosing a positive displacement pump since spare parts and repairs can be costly. Such machines are precisely engineered and when working in a harsh environment such engineering can be expensive to maintain.

## **2.4 Financial and technical considerations**

Cost is the primary reason why backfilling is not carried out in some underground mines. Technology is readily available to place either dry, slurry or paste backfill underground regardless of the geometry and depth of the mineral deposit and the mining method utilized. Mining methods could also be modified or adapted to facilitate backfill placement, to eliminate some of the operational problems of underground tailings disposal and to reduce backfill placement costs.

The improvement of existing practices, selective mining, the application of new processing methods and technology, the application of backfill as part of the mining cycle and the placement of backfill materials in favourable deep geological formations also represent opportunities for lessening the amount of surface tailings and their impact on the environment.

In any feasibility study, the cost of backfill placement underground must more than offset the cost of surface storage. Backfill placement costs include capital costs (modifications to mill process, storage bins and silos, pipelines and drop holes, conveyors, sumps, monitoring instrumentation, etc.) and operating costs (backfill preparation, backfill barricades and retaining bulkheads, drainage systems, pumping, etc.). Savings associated with the reduction in costs for any changed mining method, increased resource recovery or reduction in artificial support requirements must also be taken into consideration.

Implementation of a backfill system is only justifiable if productivity and safety can be enhanced with backfill and if the profitability of the operation is not greatly affected. Transportation and geotechnical issues represent two critical factors which directly affect the economic and technical feasibility of backfilling technology. Backfilling will be justifiable only if the transportation and placement costs (capital and operating) and the reduced mining costs associated with higher extraction methods, such as modified chevron, straight ahead and shortwall, are competitive with the costs of surface storage and decommissioning. Also, the number of operational benefits associated with backfilling should be considered in any analysis of alternatives. Such benefits include increased safety for workers, increased ore recovery, and reduced risk of slurry inflows, gas outbursts and rockbursts. Some underground mines have economically justified the placement of tailings underground while others have found that the required capital and operating costs would force their operation to become less competitive.

## Chapter 3

### Backfill Material Characteristics

#### 3.1 Importance material characteristics for Backfill

##### 3.1.1 Geomechanics of backfill

In order to appreciate the mechanical response of backfill within a mining stope, it is crucial to first understand the physiochemical properties of its constituent materials and their interactions. This allows engineers to optimize backfill design for maximum quality (i.e. the strength required to fulfil its role safely) while minimizing mining costs. Whether composed of tailings, alluvial sand or a coarse rockfill, backfill can be considered to be a special form of soil and therefore many soil mechanical properties and relationships can be applied to it. It should also be noted that mechanical and cure properties of backfill placed underground may change remarkably depending upon the backfill material's intrinsic properties, method of preparation, placement and the conditions of the mine environment.

This study is to investigate backfill materials and techniques suited for underground mines (e.g. underground gypsum mine in Germany, underground potash mines in Thailand, underground coal mines and coal fires in China). Therefore, primary emphasis in this study is selection of backfill materials. Design and planning considerations and evaluation of materials as well as economical and environmental factors, and other backfilling procedures are discussed where pertinent to successful backfill operations. Additionally the information in these procedures is applicable to backfilling around large and important structures and is also applicable in varying degrees to backfilling operations around all underground mine voids.

Selection of backfill materials should be based upon the engineering properties and compaction characteristics of the materials available. The results of the field exploration and laboratory test programs should provide adequate information for this purpose. The materials may come from mine waste excavation, mine tailing, or local sources. In selecting materials to be used, first consideration should be given to the maximum use

of materials from mine waste and industrial waste. If the mine waste materials are deficient in quality or quantity, other sources should be considered. Common backfill having the desired properties may be found in mine areas convenient to the site, but it may be necessary to obtain select backfill materials having particular gradation requirements, such as filter sands and gravels and pipe or residues from mineral processing sources. Anyway the use of commercial by-products, such as synthetic anhydrite, fly ash, filter dust, FGD-gypsum or slag as backfill material, may be advantageous where such products are locally available and where suitable natural materials cannot be found. The suitability of these materials will depend upon the desirable characteristics of the backfill and the engineering characteristics of the by-products.

The focus of this research is to optimize the analysis procedure of a new and promising systematic selection of backfill materials and techniques for underground mines in Germany, Thailand and China. Specifically, this study aims to achieve the following objectives:

- Attent that the primary source of backfill materials should be local to the mine. All materials generated as by-products, mine waste and tailings from the mineral processing of the mining industry and other industries with cheaply available materials e.g. fly ash and FGD-gypsum from power plants, natural and synthetic anhydrite.
- Investigate the physical, chemical and mechanical properties of different backfill materials and mixtures suitable for each underground mines.
- Apply the backfill materials and technologies investigated more in depth, paste, hydraulic and dump backfill as well as combinations.
- Evaluate backfill technical, long term safety, environmental and economical.

The investigation included three main aspects: a physical characterization, a mechanical characterization and a chemical characterization. This laboratory test program was implemented to study the relation between the water to solid ratio and compressive strength of backfill mixture based on German standard methods. As a first step, the following tests were used to characterize the backfill material; specific gravity determination, particle size measurement, bulk density, water content, differential

thermal analysis, permeability, porosity, microstructure. Then investigate chemical characterization, eluate analysis and mechanical characterization. The additional systematic selection of backfill, long term safety and economic evaluation prove to analytic calculations that the proposed combination is technically feasible.

### 3.1.1.1 Strength of materials

In most underground mining environments the predominant ground stress condition is one in which compressive stresses exist and in which failure will be predominantly caused by such stresses through the processes of compressional shear failure. By rock mechanics definition, induced rock stresses are always assumed to be positive in nature if they are compressive. Mining stress effects are mobilized three-dimensionally and the condition of "principal stress" will result in the formation of three mutually perpendicular normal stress components, or principal stresses, as shown in Figure 3.1.

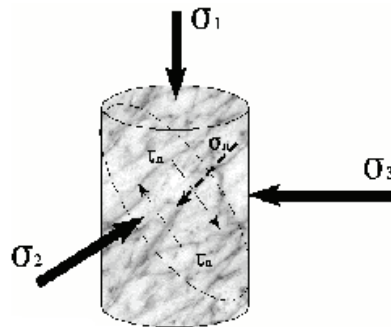


Figure 3.1: Principal stresses acting upon a backfill cylinder and resultant stress conditions upon a potential shear plane surface.

$\sigma_1$  - major principal stress (largest compressional magnitude)

$\sigma_2$  - intermediate principal stress

$\sigma_3$  - minor principal stress (smallest compressional/largest tensional stress magnitude)

In order that the stability of underground excavations in rock, of rock structures, or of backfill materials can be adequately assessed, it is important that knowledge concerning existing stress conditions within the rock or backfill masses be determined. For ease of analysis, it is common to study structures or bodies as simple two-dimensional



(biaxially stressed) elements. Should a plane of weakness exist within the cubic element which bisects the plane of stress being evaluated, but oriented other than parallel to one of the reference axial directions, then it becomes important to be able to determine the stress conditions acting on this plane. If stress components affecting the plane of weakness exceed the planar strength capabilities, then planar shear failure may be the result.

### 3.1.1.2 Component of backfill

Backfill generally consists of two or three component materials, these being solid particles mixed with water and/or air within the pores or void spaces between solid particles. It is important to understand the various physical properties of aggregate materials in order to evaluate the stability, handling, and other engineering characteristics of the wide range of backfill materials that are utilized by modern mines.

Figure 3.2 shows a representative slice through a column of backfill and the physical relationships existing between the volumes and masses of the contained solid particles, liquids and gases in the backfill column.

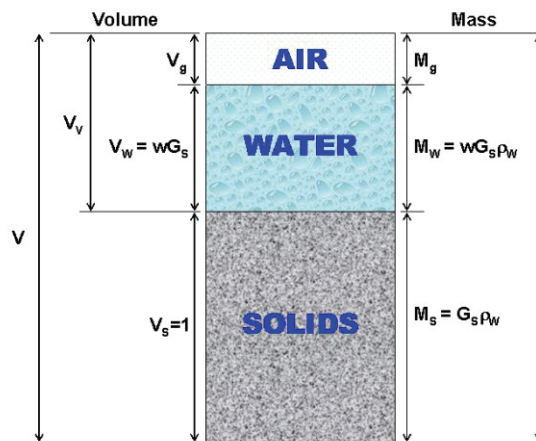


Figure 3.2: Phase diagram of backfill (Craig, 1995)

Where,

$V_g, V_w, V_s$  = volume of gas, water and solids, respectively,  $m^3$

$V_v$  = volume of void space,  $m^3$

$M_g, M_w, M_s$  = mass of gas, water and solids, respectively, kg

$w$  = water content, %

$G_s$  = specific gravity of the soil particles, dimensionless

$\rho_w$  = density of water,  $kg/m^3$

### 3.1.1.3 Particle shape and friction angle

The physical nature of solid particles, and the way they fit together, greatly influences the mechanical properties, and therefore strength condition, of a backfill material. Often, the source of the backfill material and the way in which it is processed affect the constituent particle's shape, size, and size distribution characteristics.

Due to the effects of blasting and mill grinding processes on minerals, most rock backfill and tailing particles are very angular and rough-surfaced, while alluvial sands, which are formed through weathering by water, tend to be round and smooth-surfaced.

Particle shape affects the size of voids and the connectivity of paths available for holding and transporting fluids (Herget and De Korompay, 1978), as can be seen in Figure 3.3, as well as aggregate friction angle and packing density characteristics of backfill materials, as demonstrated in Table 3.1.

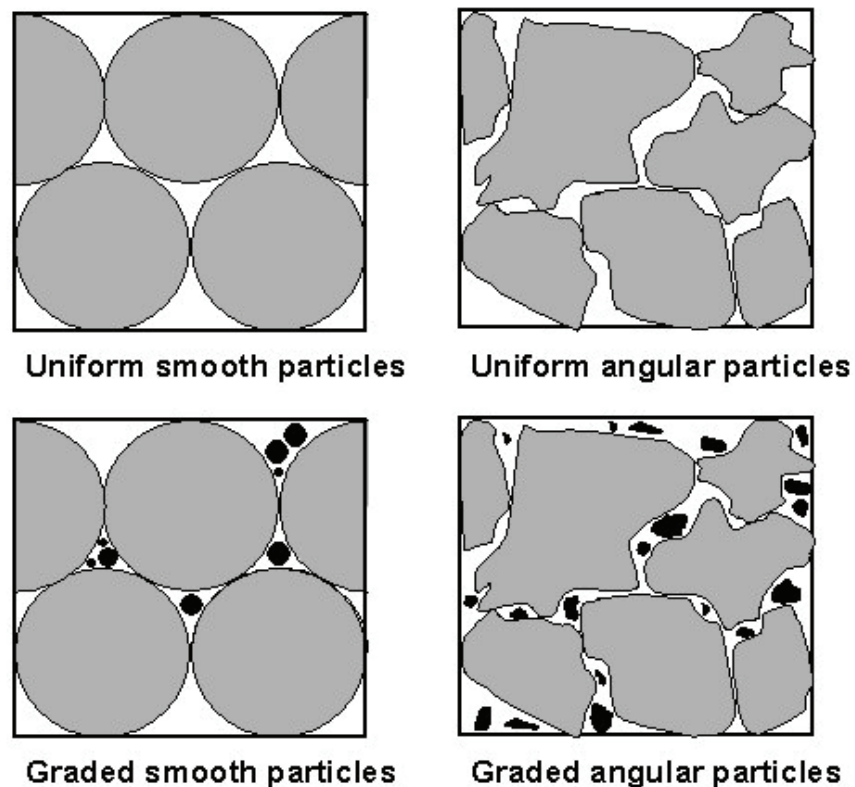










Figure 3.3: Particle shape of distribution (Herget,1978)

Table 3.1: Effect of particle shape and packing density on friction angle (Sowers, 1951)

Shape and Grading	Friction Angle ( $\Phi$ )	
	Loose Packing	Dense Packing
Rounded, uniform		
Rounded, well graded		
Angular, uniform		
Angular, well graded		

The presence of fine particles in a soil or backfill aggregate acts to increase the strength of the aggregate by backfilling in voids between coarser particles and increasing interparticle contact (frictional) forces. An increase in fine particle content can also increase the pulp density of backfill, which, during transportation, can make the slurry less likely to settle, thus allowing for lower slurry critical velocity conditions. Paste backfills take advantage of the presence of fines to promote increased backfill strength and settlement reduction of particles during transport. Alternately, slimes elimination has traditionally been adopted for slurry backfill manufacturing and use in order to improve backfill drainage and to reduce slimes handling problems in water decant systems.

#### 3.1.1.4 Particle size distribution

As can be seen in Figure 3.4, different backfill materials may consist of particles with considerably different size characteristics. In order to compare one backfill to another, backfill materials are often characterized by their particle size distribution (PSD) conditions. This distribution shows the range and frequency of particle sizes comprising

the backfill material and acts to define its material structure. Particles of different sizes within a backfill material are able to strongly influence porosity, permeability, backfill strength, and backfill transportation characteristics. Particle size distributions have traditionally been determined using a system of progressively finer sieves that trap particles of a certain size range on individual sieves. A cyclosizer, which employs gravity separation of particles, may be used for finer particle size ranges, as sieves generally become ineffective over the very fine particle size range, usually at sizes less than 400 mesh (38  $\mu\text{m}$ ). Laser-based instruments are also employed for fine- and medium-particle size measurements.

The PSD of a backfill material is commonly plotted in terms of the cumulative weight percent of the backfill material passing a certain particle size versus the particle size on a log-normal chart. As shown in Figure 3.5, a backfill material is described as being well graded if its constituent PSD demonstrates a wide range of particle sizes and is poorly graded or uniform if it demonstrates a narrow range of particle sizes. A standard set of screen openings are used to measure soil-like materials of standard Tyler sieve sizes.

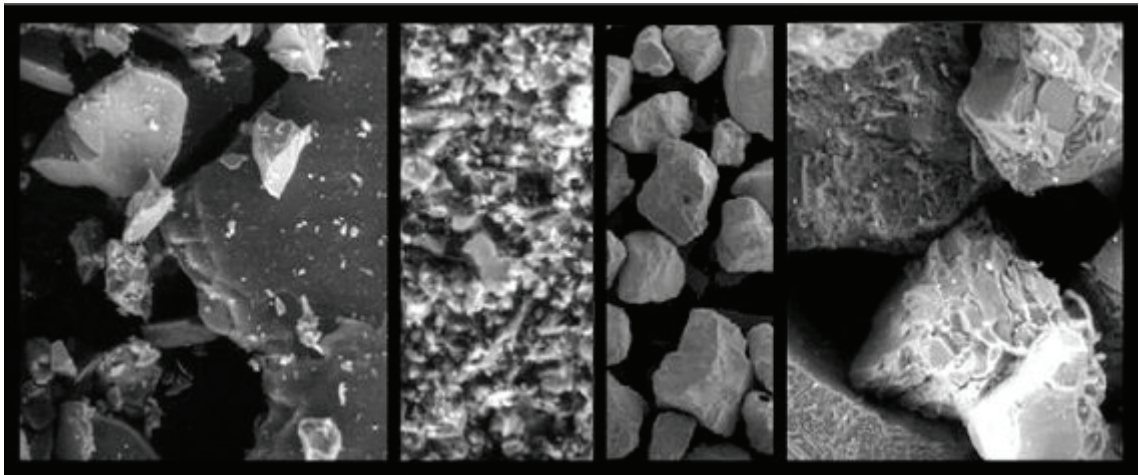


Figure 3.4: Electron microscope images (from left to right: mica bearing base metal tailings, gold tailings, construction sand and a base metal tailings) (Herget, 1981)

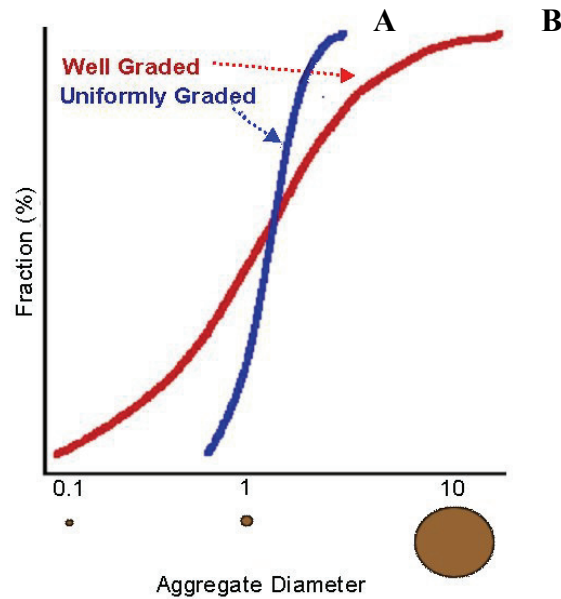


Figure 3.5: Typical particle size distribution curves for uniformly graded (A) and well graded (B) aggregate materials (Herget, 1981)

The maximum backfill grain size is generally limited by material transport restrictions. For pipeline transport of slurry backfill, for example, the maximum particle size must be less than approximately 1/3 the diameter of the pipe through which the slurry will be carried, otherwise pipeline blockage may result. In the case of conveyor transport, as is done for rock fill, the maximum aggregate size can be very large (usually ranging between 15-30 cm), though no larger than approximately 1/5 the conveyor width to prevent side spillage effects.

### 3.1.1.5 Bulk density, unit weight, and specific gravity ( $\rho$ , $g$ , $G_s$ )

Density  $\rho$  or bulk density is the ratio of the total mass  $M$  of the fill to its total volume  $V$ :

$$\rho = \frac{M}{V}, \text{ kg/m}^3 \quad (3-1)$$

The unit weight  $\gamma$  of a backfill is the ratio of its total weight  $M_g$  e.g. mass times the force of gravity to its total volume  $V$ :

$$\gamma = \frac{M_g}{V}, \text{ kN} / \text{m}^3 \quad (3-2)$$

Specific gravity  $G_s$  is defined as the ratio of the weight of a solid or liquid to the weight of an equal volume of a standard material. Water has a specific gravity of unity, by definition, and is used as the standard material. Practice indicates that most cemented backfill possesses a specific gravity ranging between 2.6 to 4.0. It is generally of prime concern in determining backfill quantities, pulp density and critical flow velocity for hydraulic transport.

$$G_s = \frac{M_s}{V_s \rho_w} = \frac{\rho_s}{\rho_w} \quad (3-3)$$

where,

$M_s$  = mass of solids, kg

$V_s$  = volume of solids,  $\text{m}^3$

$\rho_s$  = density of solids,  $\text{kg}/\text{m}^3$

$\rho_w$  = density of water,  $\text{kg}/\text{m}^3$

### 3.1.1.6 Friction angle $\Phi$ and cohesion $C$

The following two components of soil are directly responsible for backfill strength:

1. Frictional forces, proportional to the internal angle of friction  $\Phi$ , that result from interlocking solid particles and which are independent of moisture content.
2. In uncemented backfills, an apparent cohesion  $C$  results from surface tension forces in pore water that disappears when the backfill is fully dry or fully saturated. Portland cement or similar soil binders act to greatly increase actual fill cohesion by coupling the solid particles together.

Apparent cohesion results from surface tension in the water held at grain contacts within the backfill. Surface tension is inversely proportional to the radius of curvature of the free water surface at contact, and therefore for a given pair of particles increases as the amount of water held between them decreases. Net particle attractive force, however, varies with both the magnitude of surface tension (decreasing with increasing water content) and the area over which it acts (increasing with increasing water content). There exists an optimum backfill moisture content, therefore, at which apparent cohesion is a maximum. The importance of grain interlocking and hence the magnitude of the internal friction angle depends upon grain shape, overall particle size and packing density.

The strength capabilities of cohesionless materials are mobilized solely by the frictional resistance that develops along internal shear plane surfaces (Figure 3.6) within the backfill under stress ( $\sigma_1$ ,  $\sigma_3$ ). The level of frictional resistance that can develop is directly proportional to the magnitude of the normal stress  $\sigma_n$  that develops perpendicular to such failure planes. Resisting shear stress  $\tau$  develops along the failure plane, based upon the material's coefficient of sliding friction and the normal stress developed across the sliding plane (Equation 3-4). The coefficient of sliding friction is based upon a physical parameter constant that is dependent upon the measured angle of failure  $\psi$  that can be determined when backfill samples are failed in compression (Equation 3-5).

$$\tau_f = \sigma_n \tan \phi \quad (3-4)$$

$$\phi = 2(\psi - 45^\circ) \quad (3-5)$$

where,

$\tau_f$  = frictional shear stress developed along a failure plane, kPa

$\sigma_n$  = resolved stress perpendicular to the failure plane, kPa

$\phi$  = internal friction angle of fill material, °

$\psi$  = measured failure angle of backfill in compression, °

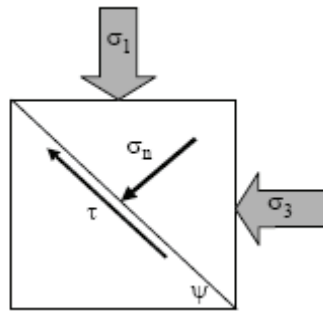


Figure 3.6: Shear plane development within backfill under load (Thomas, 1979)

### 3.1.1.7 Backfill failure

This failure mode for backfill can be plotted as shear stress versus normal stress to establish a positively sloped linear Mohr failure locus (envelope) to define the maximum tolerable backfill normal stress (Figure 3.6).

For purely cohesive materials, failure will occur along any planar orientation where the maximum generated shear stress exceeds the intrinsic bonding strength between sample grains (cohesive strength of the material). The backfill material is therefore assumed to behave as a frictionless material that will develop failure shear surfaces oriented at a constant angle of  $45^\circ$  to the direction of principal compressive stress  $\sigma_1$  application. Typical examples of Coulomb materials are: (i) structural materials such as pelletized backfill components, held in loose confinement, (ii) fractured rock having wet, slickensided or clay-filled apertures, and (iii) gelled backfill materials containing very high retained water contents.

$$\tau_c = C \quad (3-6)$$

where,

$\tau_c$  = cohesive shear stress developed along a failure plane, kPa

$C$  = cohesion, kPa

This failure mode for backfill can be plotted as shear stress versus normal stress to establish a constant Coulomb failure locus (envelope) to define the maximum tolerable backfill normal stress (Figure 3.7). In practice, backfill exhibits strength characteristics



that are mobilized both by cohesive and by frictional resistance effects as expressed by the Mohr-Coulomb relationship:

$$\tau = C + \sigma_n \tan \phi \quad (3-7)$$

where,  $\tau$  = total shear stress developed along a failure plane, kPa

For a range of triaxial conditions applied, the Mohr-Coulomb failure criteria can be represented by a linear locus of points on a shear stress versus normal stress plot as illustrated in Figure 3.7.

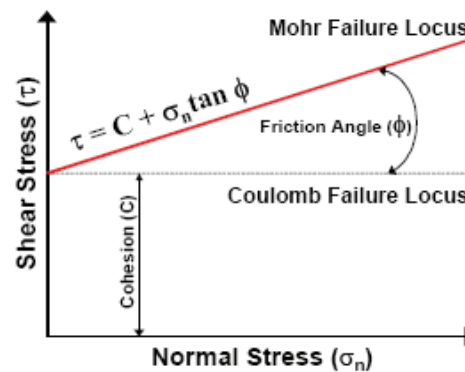


Figure 3.7: Mohr-Coulomb failure locus (Thomas, 1979)

### 3.1.1.8 Consolidation and compaction

In mining engineering, the term consolidation generally refers to a cemented or consolidated mass. However, in classical soil mechanics, and for this section, consolidation refers to the densification (i.e. closer particle packing) of a soil at a rate controlled by the flow of water from the soil. When a saturated soil is subjected to some external load, the pore water pressure will increase to resist the load and prevent particle rearrangement. If pore pressures dissipate very rapidly, as they do in sands, pore pressures may be ignored except when considering very rapid loading, such as during blasting. In practice, consolidation of initially loose, moist, cohesionless slurry backfills under low confining loads occurs very quickly with consolidation frequently being 90 % complete within approximately three seconds following load application. Paste backfill, however, is much finer and its ability to dissipate pore pressures may be insufficient under rapid loading conditions when uncemented. Compaction is similar to consolidation, but is not normally controlled by the expulsion of water. A partially

saturated or drained backfill can undergo compaction as void space is reduced due to the action of external forces, such as mobile equipment moving across it.

### 3.1.1.9 Stiffness ( $k$ )

Stiffness  $k$  relates a material's resistance to deformation, either in compression or tension, and is expressed in terms of load resistance per unit of deformation, as given:

$$k = \frac{P}{\Delta L} \quad (3-8)$$

where,

$\Delta L$  = deformation induced by the applied force, m

$P$  = applied force, N

Similarly, axial strain provides a measure of material deformability, and is expressed as the deformation per unit length when a stress is applied to the material. Axial strain  $\varepsilon$  relates a material's resistance to deformation or compression and is expressed as the deformation per unit length:

$$\varepsilon = \frac{\Delta L}{L} \quad (3-9)$$

where,

$\Delta L$  = deformation, m

$L$  = unit length, m

Stress and strain are intrinsically linked and can be related by the following expression:

$$\sigma = \varepsilon E \quad (3-10)$$

where,

$\sigma$  = Axial compressive stress, MPa

$E$  = Modulus of Elasticity (Young's Modulus), MPa

Often it is desirable, from a strength perspective, to design a backfill with as high a stiffness or Modulus of Elasticity, as possible. As can be seen from Equation 3-9, deformability of a material is proportional to its modulus of Elasticity or Deformation. The modulus of a backfill is generally several orders of magnitude less than that of the

intact rock mass surrounding it. For example, typical values of Young's Modulus for intact rock, rockfill and slurry backfill are approximately 70 GPa, 5 GPa and 0.5 GPa, respectively. Stiffness is important where the backfill is intended to limit ground convergence and/or bear some tertiary stress from adjacent pillars. The addition of a binder to backfill significantly increases its stiffness. However, it should be noted that a stiff material is also a brittle material. This makes stiff backfill more prone to cracking under blast loading and to rupturing under local rock deformation. It is recommended that forces, displacements and energy dissipation be considered in backfill design and that, in many cases, Normal Portland Cement (NPC) addition, for example, be limited to 5 % or 20:1 (i.e. 20 parts aggregate to 1 part NPC) so that exposed fill can yield without rupturing (Mitchell and Smith, 1979).

#### **3.1.1.10 Permeability and percolation rate**

Permeability and percolation rate properties are additional important slurry backfill characteristics. Both are properties of porous media, such as backfill aggregates, which define the flow properties of fluids through such media. Good backfill permeability is required to ensure that emplaced backfill will drain adequately and that there exists little potential for fill liquefaction. Effective permeability is required to ensure that excess water, used to transport slurry into stopes from the surface, drains rapidly to allow for high placement and curing rates. Permeability is not considered in the design of paste fill materials, as there usually exists too little excess water to drain following placement and the majority of water contained in paste is consumed in cement or other binder hydration, which also restricts the potential for paste fill liquefaction. The universally accepted minimum percolation rate for mine slurry backfills is 10 cm/hr, which is suggested as a good design guideline for slurry backfill placement. Percolation rate is closely related to the grain size composition and the cement content of backfill aggregate mixtures. The rate of percolation decreases rapidly with the addition of fines fractions in backfill, and may be nonexistent when cement binder additions are made to fill and within short time intervals after placement has occurred.

The detrimental effect of fines on percolation rate behaviour is the principal reason why mines have to deslime tailings material which is to be utilized for slurry backfill manufacture. Other factors which are known to influence the percolation rate of

aggregates include porosity (including particle shape), particle constituency, and composition of minerals.

Permeability of a material can be defined by Darcy's Law as:

$$K = \frac{QL\eta}{hA\gamma^2} \quad (3-11)$$

$$Q = q\gamma \quad (3-12)$$

where,

$K$  = permeability of a porous medium,  $m^2$

$Q$  = quantity rate of flow of fluid through a porous medium, N/s

$L$  = length of porous medium, in direction of flow, m

$H$  = static pressure differential across a porous medium, m

$A$  = cross-sectional area of porous medium, normal to direction of flow,  $m^2$

$\eta$  = absolute viscosity of fluid flowing, Ns/ $m^2$

$\gamma$  = unit weight of fluid flowing, N/ $m^3$

This expression for permeability is valid for conditions which typically occur during fluid flow testing and dewatering of fill materials.

The percolation rate of an aggregate material is defined as:

$$V_p = \frac{q}{A} \quad (3-13)$$

where,

$V_p$  = percolation rate, m/s

$q$  = quantity rate of flow,  $m^3/s$

$A$  = cross-sectional area of sample normal to flow direction,  $m^2$

A characteristic material permeability, in units of  $m^2$ , has no inherent physical significance. It is not surprising, therefore, that the percolation rate parameter, with its readily comprehensible units of m/s, has been adopted throughout the mining industry as an indicator of backfill drainage suitability. Percolation rate and permeability are in fact directly related, as indicated in the following equation

$$k = \frac{qL\eta}{hA\gamma} \quad (3-14)$$

where,

$k$  = permeability coefficient, m/s

If a fixed temperature condition is assumed, the term  $(\eta / \gamma)$  remains constant and the equation becomes:

$$k = \frac{qL}{hA} \quad (3-15)$$

It should be noted that permeability coefficient units are the same as those for the percolation rate. Accurate measurement of permeability or percolation rate parameters is difficult to achieve. The main problem is an inability to establish constant flow rate conditions for the test. Of three methods generally available for measuring backfill material permeability, two (constant and falling head permeameter) are used with materials that exhibit very low permeability, while the third (percolation rate tube) is more relevant to the mining industry, where high permeability slurry backfill materials are commonly encountered.

### 3.1.2 Backfill materials specification

The backfill materials which are most commonly utilized are classified into three groups; inert material (which is the major part of the backfill), the binding agent and chemical additives. The inert materials commonly used are mill plant tailings, sand or gravel, waste rock and coarse slag. Binding agents, such as Portland cement, ground slag, or fly ash, are applied in backfill technology to improve the mechanical properties of the backfill, i.e. strength. Chemical additives such as flocculants, accelerators, and retarders are employed to improve the backfill permeability, flowability of the slurry and the consolidation properties of the backfill.

These tailing materials can be used either as received or prepared 'full plant tailings' or deslimed by using hydrocyclones to meet desired percolation requirements. Their size compositions largely depend on ore processing and desliming technology. The fraction of 10 mm particles in classified tailings is usually less than 20 % of total mass by

weight. Sand from surface alluvial basins is widely used in mine backfill, and its particle size is generally less than 2 mm. Waste rock from mine development or quarries must be sized to meet transport requirements. The maximum size for pipeline transportation is less than 1/4 the diameter of the pipe; in the case of hydraulic transportation this means aggregate sizes less than about 60 mm whilst aggregates up to 30 cm can be transported by truck or conveyor.

### 3.1.2.1 Backfill binders

Backfill binders are materials that react with water to form chemical bonds that, over time, glue aggregate grains together. Backfill is said to cure with time, and its strength tends to increase with time, until it reaches its ultimate strength. The main types of binders are cements and pozzolans. Cements are primarily made up of calcium (lime) and silica (quartz) compounds. Cements can be used solely as a backfill binder, while most pozzolans require the addition of lime. Pozzolans are often used in conjunction with cements, since lime is a natural by-product of the cement reactions. However, since some slags and all pozzolans must wait for lime to first be generated by the cement reaction, they do not contribute to overall backfill strength until after a period of weeks or even months. Mining methods, stope sequencing, binder availability, and cost all influence the decision as to which binder, if any, to select. Figure 3.8 is a ternary diagram representation of the three most typically abundant compounds, silica ( $\text{SiO}_2$ ), lime ( $\text{CaO}$ ), and aluminate ( $\text{Al}_2\text{O}_3$ ), which make up a binder system and show the relative placement of major binder groups with respect to each other.



Figure 3.8: Ternary diagram of binders (Douglas and Malhotra, 1987)

Most of the pozzolanic and cementitious materials investigated for use in mine backfill have been the same as investigated by civil engineers for admixture into cement and

concrete. Natural minerals (such as sulphides and volcanic ash), iron and non-ferrous blast furnace slags, incineration ashes (such as fly or coal ash, peat ash, industrial waste ash, municipal solid waste (MSW) ash) and finely pulverized waste glass have all been studied with respect to mine backfill. One notable exception has been the implementation of silica fume, a highly pozzolanic material used as a concrete admixture, for mine backfill consolidation. Modern pozzolans can be classified into five representative groups: cementitious (quenched blast furnace slag), cementitious and pozzolanic (high calcium fly ash), highly pozzolanic (condensed silica fume), normal pozzolanic (low calcium fly ash), and weakly pozzolanic (slow cooled blast furnace slag), (Takemoto and Uchikawa, 1980). Those materials that contain both silica and lime tend to be self-cementing. Most pozzolans, however, contain relatively little lime. Although these groups have been established based primarily upon chemical composition, it should be noted that the mineralogical composition, rather than the chemical composition, determines whether a material will be chemically reactive and if so, its rate of reaction. Within this Chapter, the term pozzolan and alternative binder will be used interchangeably and will include all slags, ashes, and glasses.

### **3.1.2.2 Portland cement**

Portland cement is a crystalline material that consists primarily of  $\text{CaO}$ ,  $\text{SiO}_2$ ,  $\text{Al}_2\text{O}_3$ , and  $\text{Fe}_2\text{O}_3$ . It contains four major phases (Alite, Belite, Aluminate, and Ferrite) that, upon hydration, are responsible for its strength development and for the rate of chemical reaction. Using the following cement chemistry notation where C =  $\text{CaO}$ , S =  $\text{SiO}_2$ , A =  $\text{Al}_2\text{O}_3$ , F =  $\text{Fe}_2\text{O}_3$ , and H =  $\text{H}_2\text{O}$  these phases are expressed as  $\text{C}_3\text{S}$ ,  $\text{C}_2\text{S}$ ,  $\text{C}_3\text{A}$ , and  $\text{C}_4\text{AF}$ . Alite, or tricalcium silicate ( $\text{C}_3\text{S}$ ), represents 50 % to 70 % of Portland cement (by mass) and is important for early strength development within the first 28 days. Representing 15 % to 30 % (by mass) of Portland cement, dicalcium silicate ( $\text{C}_2\text{S}$ ) is important for long term strength development, matching the Alite phase strength within a year. The remaining two phases each represent between 5 % and 15 % (by mass) of Portland cement and are alumino-based. The considerable cost of Portland cement realized during the energy crisis of the 1970's, the remoteness of most mining operations, and the proximity of substitute materials has encouraged mining companies to investigate and implement the use of alternative binders.

### 3.1.2.3 Pozzolans

A pozzolan is „a siliceous or siliceous and aluminous material which in itself possesses little or no cementitious value but will, in finely divided form and in the presence of moisture, chemically react with calcium hydroxide (lime) at ordinary temperature to form compounds possessing cementitious properties,,. (ASTM, 1986).

### Blast furnace and non-ferrous slags

Blast furnace (BF) slag is a by-product that results from the fusion of fluxing limestone with coke ash and siliceous and aluminous residues remaining after the separation of the metal from ore. Typical BF slag makes up to 20 % (by mass) of the metal production. Blast furnace slag tends to be quite consistent in physical and chemical composition which assists in assuring reproducible product quality. Figure 3.9 is a schematic of an iron and steel blast furnace showing the stages involved in the production of the primary metals and slag by-products. As a result of selective cooling, four distinct blast furnace slag ‘products’ exist, these being: air-cooled, foamed, granulated, and pelletized which are described below based on Hooton (1987).

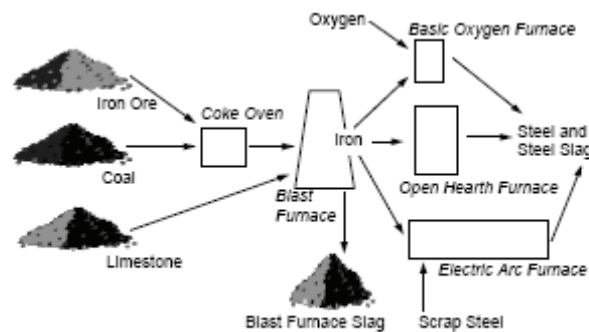


Figure 3.9: Schematic of Ferrous Blast Furnace (Emery, 1992)



## Coal ash

Coal ash is a waste product derived from the combustion of coal in thermal power generation plants. As shown in Figure 3.10, coal ash consists of fine particles known as fly ash that flow with flue gases and coarser particles, called bottom ash, which collect at the bottom of the boiler. Combusted coal results in approximately 10 % (by mass) coal ash, of which 85 % is fly ash and the remainder bottom ash. Bottom ash is considerably coarser than fly ash, ranging in particle size from about 20 mm to 200 mesh. Due primarily to its large particle size, bottom ash is weakly reactive as a binder and is typically used as an aggregate. Most fly ash is naturally fine and grinding is rarely required to activate the material.

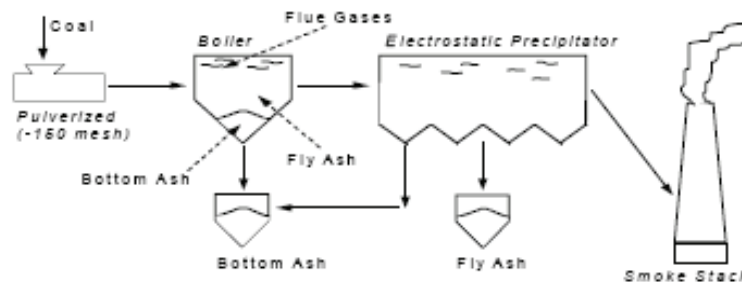


Figure 3.10: Coal ashes produced by thermal power plants (Emery, 1992)

There are two types of fly ash: Class-C, which has a high lime content, is self-cementitious and is produced when sub-bituminous or lignite coals are burned; and Class-F, which must be activated through the addition of lime and which is produced by burning bituminous coal. Typically, up to 60 % of NPC can be substituted by Class-C fly ash (Archibald et al, 1995). As fly ash typically contains toxic metals and other hazardous compounds, and may be radioactive, it is not suitable for non-cemented fill, especially near water sources.

## Silica fume

There is no known application or study of silica fume as an alternative binder for use in mining backfill. However, it has had considerable use in civil engineering practice as an alternative binder for concrete and is included for completeness. Condensed silica fume consists of ultrafine, approximately 0.1 mm diameter, spherical particles of nearly pure silica. It is a by-product of silicon metal or ferrosilicon alloy manufacturing plants. Cost

and limited supply have most likely prevented investigations into using this alternative binder for mining backfill use.

### **Natural minerals**

Natural minerals, especially those that constitute mine backfill, have been examined as possible consolidating agents incorporating a wide range of cementitious mechanisms. Typically, these enjoy only local success and are not readily transferable methods for the industry as a whole as they are dictated by regional geological circumstances. The cementation of hydraulic backfill with naturally occurring minerals has been investigated and focused primarily on the use of clays as a backfill additive material. Calcined dolomitic tailings have been observed to harden naturally, but two different mines with similar dolomitic tails experienced completely different results. Pyrrhotite, a pyrophoric mineral, has demonstrated considerable reactivity through oxidation, and has been used as a binder and backfill additive in tailings by several mines. It yields an exothermic reaction that requires oxygen and water (Falconbridge, 1990) and therefore the consolidated fill mass requires positive drainage and subsequent air circulation via perforated piping.

#### **3.1.2.4 Mixture proportions**

In practice, the mix proportions vary, depending on the properties of the individual ingredients and on the desired properties of the backfill. The properties of the ingredients of the mix are discussed below. First of all, these materials are generally cheaper than Portland cement. Secondly, these materials hydrate or react chemically somewhat later than Portland cement. Different mixture proportions are summarized in table 3.2.

Table 3.2: Details of backfill mix proportions

Mix ID	Synthetic anhydrite	Natural anhydrite	Fly ash	Filter dust	Cement	FGD gypsum	Tailing
SA	X	-	-	-	-	-	-
SA+FA	X	-	X	-	-	-	-
NA	-	X	-	-	-	-	-
NA+FA	-	X	X	-	-	-	-
C	-	-	-	-	X	-	-
C+FA	-	-	X	-	X	-	-
C+FD+FA	-	-	X	X	X	-	-
FGD-G+FA	-	-	X	-	-	X	-
C+T+FA	-	-	X	-	X	-	X

- SA- Synthetic anhydrite
- NA- Natural anhydrite
- C- Cement
- FA- Fly ash
- FD- Filter dust
- FGD-G- Flue gas desulfurization (FGD) gypsum
- T- Tailing from poash mine

## 3.2 Instrumentation of determination

### 3.2.1 Setting time of backfill

The initial and the final setting times were measured by the penetration-resistance procedure, as per the German Standard Method DIN EN 196-3. They are defined as the periods, after the initial contact of binder and water, required for the mortar sieved from the backfill mix to reach a penetration resistance of 3.5 MPa and 27.6 MPa, respectively. During the study water and solid ratios (w/s) 0.6, 0.55, 0.5, 0.45, 0.4, 0.35, 0.3, 0.25, 0.2 and 0.15 were chosen for various mixtures by Vicat test (Fig. 3.11).



Figure 3.11: Vicat test setting time of backfill

### 3.2.2 Simultaneous Thermal Analysis (STA) of backfill materials

Simultaneous thermal analysis refers to the simultaneous application of two or more thermoanalytical methods on one sample at the same time. Using simultaneous thermal analysis one has the chance to get information on the transformation energetics and the mass change on one sample in one run under identical conditions. Using the STA the comparability of characteristic temperatures measured on the TG and DSC runs is ensured. In case of inhomogeneous sample materials, problems resulting from differences in the sample composition for the TG and DSC measurements are excluded. The STA 409 PC *Luxx* at Institut für Keramik, Glas und Baustofftechnik combines the advantages of a highly sensitive toploading thermobalance and a high-temperature differential scanning calorimeter (Fig. 3.12). The maximum sample mass as well as the measurement range of the balance are 18 g. The entire measurement range can be analyzed with a resolution of 2 g (up to 0.00001 %).



Figure 3.12: STA 409 PC *Luxx*

### 3.2.3 Permeability measurement

Permeability measurements were made by using the steady-state flow method, which consists of imposing a known pore-pressure difference across the specimen and measuring the resultant flow rate, which is proportional to permeability. Pore-fluid pressures on both sides of the specimen were controlled by using high-precision, servocontrolled volumeters. Typically the equipment consists of two pressure chamber and the core holder for samples with 5 cm diameter and 5 cm length. Confining pressure up to several 100 bars can be applied (Fig. 3.13).

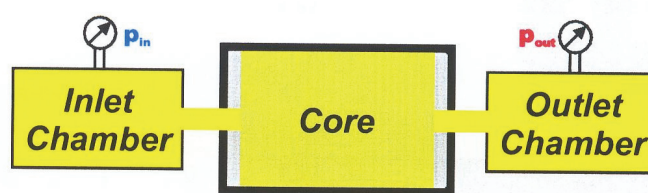


Figure 3.13: Laboratory measurement of permeability

The equilibration process with the 2 converging pressures at inlet and outlet is monitored digitally. Based on the pressure development a numerical model is used to determine permeability and porosity of the sample. A Finite-Difference model is therefore coupled with an automatic parameter identification method. The graph in

figure 3.14 as shown the measured and the simulated pressure development of a concrete plug filled with gas.

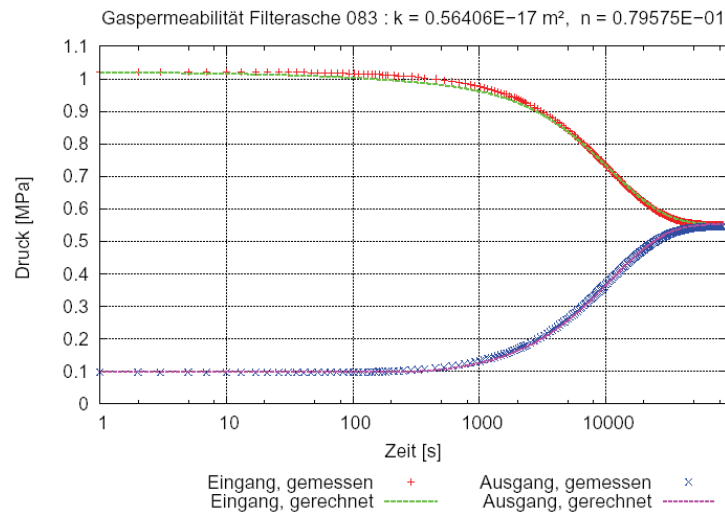


Figure 3.14: Permeability measurement

### 3.2.4 Specimen preparation and mechanical strength test

The mixing was conducted using a mortar mixer which produces a good homogenized mixture. The latter was blended for about 10 min and then poured into plastic cylinders with a diameter of 50 mm and a height of 100 mm (Fig. 3.15). After pouring the mixtures into the cylinders, these were sealed and cured in a humidity chamber and control temperature maintained for periods of 3, 7, 28 and 90 days. The resulting specimens were then tested by uniaxial compression tests to investigate compressive strength, flexural strength and tensile strength. A total of specimens were subjected to uniaxial compression tests using a mechanical press (ZD 100) having a normal loading capacity maximum of 1,000 kN (Fig. 3.16). The triaxial compression test is used to measure the shear strength, cohesion and angle friction of a backfill under controlled drainage conditions. In the conventional triaxial test, a cylindrical specimen of backfill encased in a rubber membrane is placed in a triaxial compression chamber, subjected to a confining fluid pressure, and then loaded axially to failure. Connections at the ends of the specimen permit controlled drainage of pore water from the specimen.

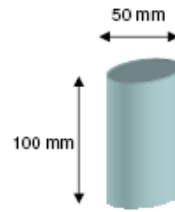


Figure 3.15: Size of specimen

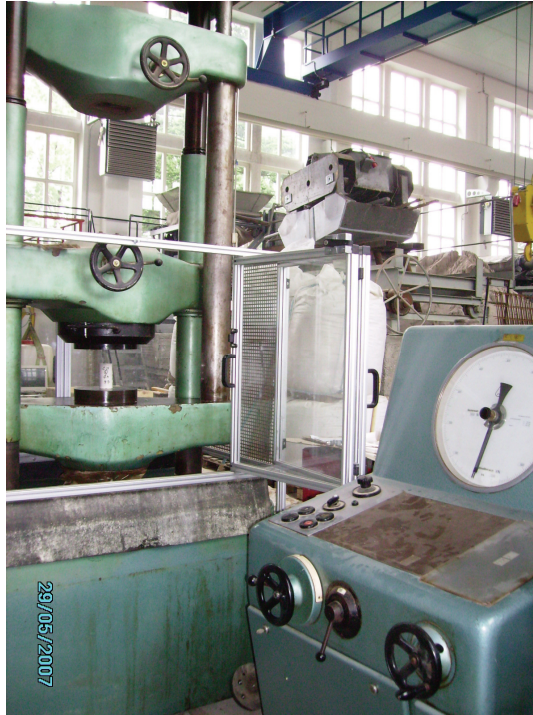


Figure 3.16: Mechanical press (ZD 100)

### 3.2.5 Ultrasonic test

Computer-based ultrasonic wave velocity measuring device, an ultrasonic-universal testing system (Fig. 3.17), was applied for testing the dynamic elastic parameters of specimens. All of specimens were subjected to ultrasonic test. Through the ultrasonic wave and its velocity, the mechanical properties of the specimens in the age of 3, 7 and 28 days, such as the dynamic elastic modulus ( $E$ ), shear modulus ( $G$ ) and poisson's ratio can be calculated.

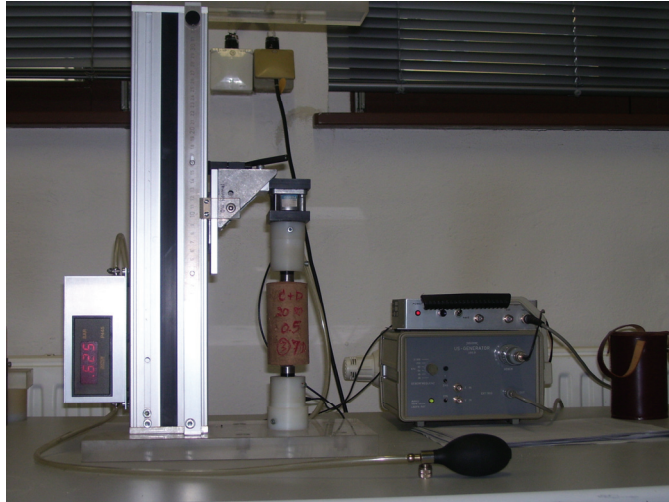


Figure 3.17: Computer-based ultrasonic wave velocity measuring device

### 3.2.6 Chemical characterization

The chemical, eluate and mineralogical analyses were completed on the solid and the interstitial solution of backfill samples. Chemical analyses were performed by induced coupled plasma spectroscopy and mineralogical characterization was analysed by the Rietveld Method at the Institute of Mineralogy. The eluate test using standard methods with AAS and/or ICP equipment.

## 3.3 Result for backfill materials investigation

### 3.3.1 Selection of materials

The primary source of backfill materials will be local to the mine. Backfill materials used for this study were obtained from by-products, mine waste and tailings from the mineral processing of the mining industry and other industries in Germany, Thailand and China. There consisted of:

#### 3.3.1.1 Synthetic anhydrite

Calcium sulphate, generated in the manufacture of hydrogen fluoride, is known as synthetic anhydrite or fluoroanhydrite (Fig. 3.18- 3.19) and this material is sent to landfill. Over the past 10 years a variety of applications have been developed utilising



synthetic anhydrite as an essential component. These include the manufacture of aerated concrete building blocks, monolithic cements and floor screeds.

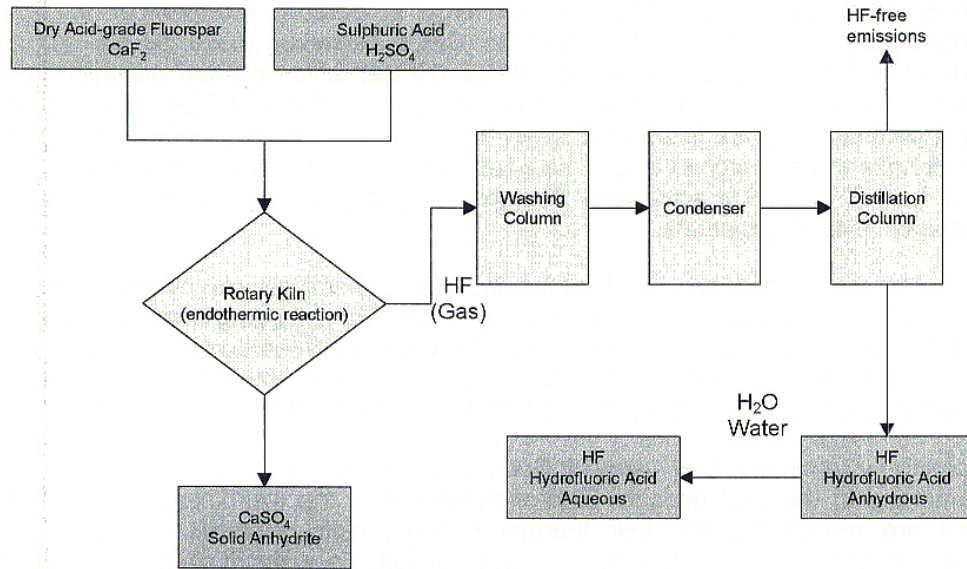


Figure 3.18: Function diagram – Production of hydrogen fluoride (HF) and hydrofluoric acid (H<sub>2</sub>SO<sub>4</sub>)



(a)



(b)

Figure 3.19: Synthetic anhydrite from Germany (a) and Thailand (b)

### 3.3.1.2 Natural anhydrite

Anhydrite is a relatively common sedimentary mineral that forms massive rock layers. Anhydrite does not form directly, but is the result of the dewatering of the rock forming mineral Gypsum (CaSO<sub>4</sub>-2H<sub>2</sub>O). This loss of water produces a reduction in volume of

the rock layer and can cause the formation of caverns as the rock shrinks. There was from Obrigheim and Ellrich (Fig. 3.20).



Figure 3.20: Natural anhydrite from Germany

### 3.3.1.3 Fly ash

Fly ash is the finely divided mineral residue by-product resulting from the combustion of powdered coal in electric generating plants. Fly ash material is solidified while suspended in the exhaust gases and is collected by electrostatic precipitators or filter bags. Since the particles solidify while suspended in the exhaust gases, fly ash particles are generally like fine-grained gray powder and range in size from 0.5  $\mu\text{m}$  to 100  $\mu\text{m}$ . They consist mostly of silicon dioxide ( $\text{SiO}_2$ ), aluminum oxide ( $\text{Al}_2\text{O}_3$ ) and iron oxide ( $\text{Fe}_2\text{O}_3$ ), and are hence a suitable source of aluminum and silicon for geopolymers. They are also pozzolanic in nature and react with calcium hydroxide and alkali to form cementitious compounds. The fly ash used in the study was obtained from Germany, China and Thailand (Fig. 3.21).

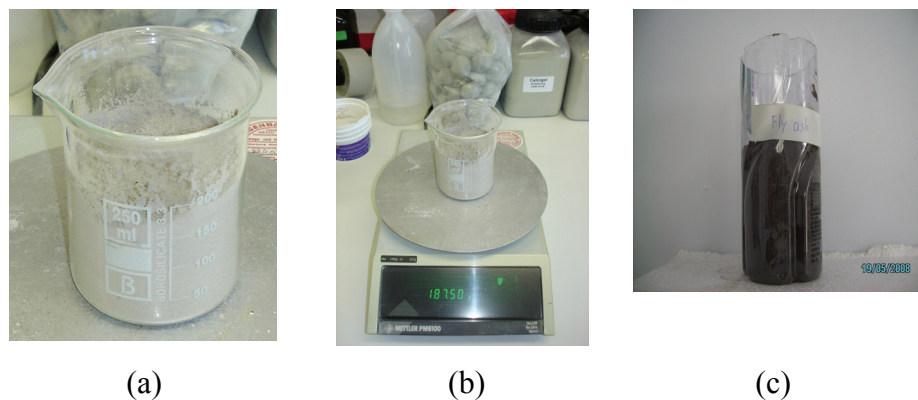


Figure 3.21: Fly ash from Germany (a), Thailand (b) and China (c)

### 3.3.1.4 Filter dust was from a cement plant (Fig. 3.22)

Filter dust is a byproduct of cement manufacture and is routinely given or sold to farmers as a soil treatment, or is discarded into pits or is piled on the ground near cement kilns. Some cement plant is disposed filter dust of each year and it buried on-site.



Figure 3.22: Filter dust from Germany

### 3.3.1.5 Cement

Cement is a binder, a substance which sets and hardens independently, and can bind other materials together (Fig. 3.23).

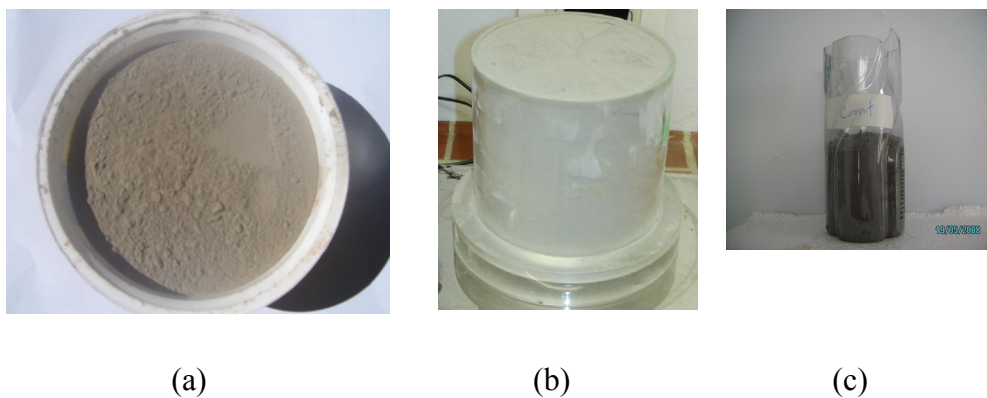


Figure 3.23: Cement from Germany (a), Thailand (b) and China (c)

### 3.3.1.6 Flue gas desulfurization (FGD) gypsum

FGD- gypsum is also known as scrubber gypsum. FGD- gypsum is the by-product of an air pollution control system that removes sulfur from the flue gas in calcium-based scrubbing systems (Fig. 3.24). It is produced by employing forced oxidation in the scrubber and is composed mostly of calcium sulfate. FGD-gypsum is most commonly used for agricultural purposes and for wallboard production. The FGD- gypsum are produced annually as a by-product material in the lignite-fired Mae Moh Power Plant in Thailand, obtaining fuel from its two opencast mines.



Figure 3.24: FGD- gypsum from Thailand

### 3.3.1.7 Tailings from potash mine in Thailand

Waste rocks removed to access the potash deposit are generally piled up next to the surface. Mineral processing pilot plant of potash ores involves flotation of the crushed salt which results in the concentration of the salt minerals and rejection of the gangue phases. The major waste products of potash processing include brines and tailings. Tailings were from potash mine in Thailand (Fig. 3.25).



Figure 3.25: Tailing from potash mine Thailand

### 3.3.1.8 Salinity water

The salinity water used to study the influence on the mechanical properties of backfill. Analysis of the composition of the water indicated that it had a Total Dissolved Solids (TDS) of 18,000 mg/l. concentration of salt in water 115-120 g/l

## 3.3.2 Results of materials characteristics

### 3.3.2.1 Physical characteristics

The density of the materials was first determined by measuring the physical dimensions of the material. That is the weight, and actual volume which the mass occupied was determined. The mass of a given volume (500 mL) of the sample of sediments was found on a grams scale. Density was found as the mass per unit volume the sediments occupied. The water content, specific gravity, mean particle size distribution were determined in using the German standard method procedure that is shown in Table 3.2. As can be seen in Figure 3.26, different backfill materials may be comprised of considerably different particle sizes. Particles of different sizes within the backfill material have effects on porosity, permeability, compressive strength and backfill transportation characteristics. The backfill materials were determined by sieve and HELOS particle size analysis with laser diffraction.

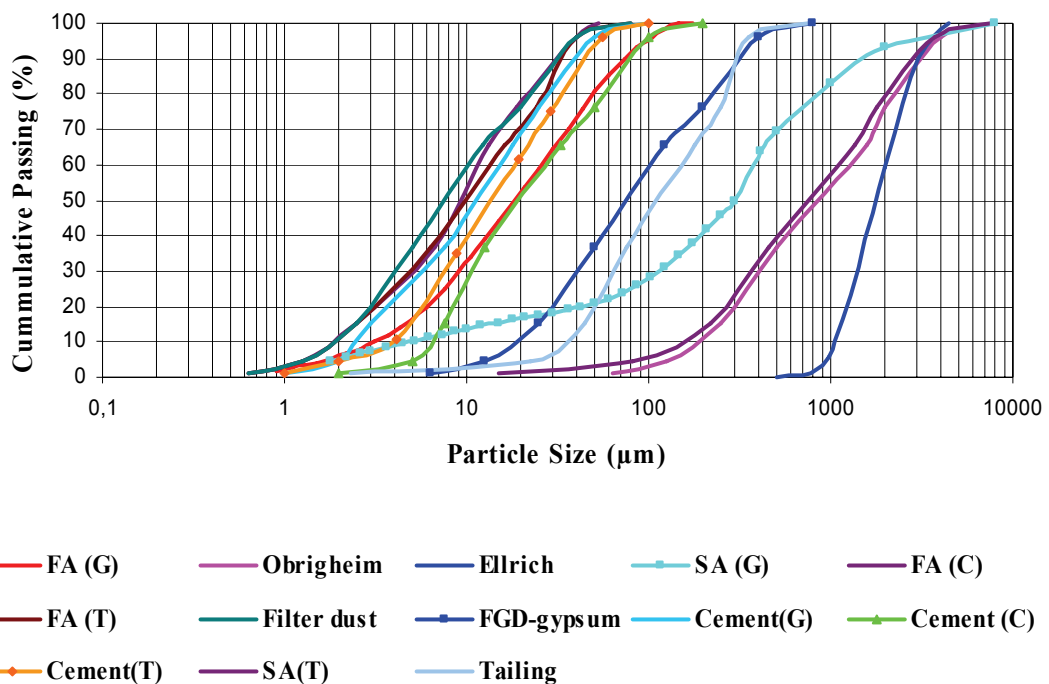


Figure 3.26: Backfill particle size distribution

Table 3.3: Physical characteristics of backfill materials

Samples	Bulk density (g/cm <sup>3</sup> )	Specific gravity (g/cm <sup>3</sup> )	Water content (%)	d <sub>50</sub>
Synthetic anhydrite (G)	1.45	2.89	1.7	0.28 mm
Synthetic anhydrite (T)	1.46	2.9	2.5	0.34 mm
Natural anhydrite (Ellrich)	1.48	2.91	2.4	0.75 mm
Natural anhydrite (Obrigheim)	1.52	2.93	2.1	1.08 mm
Cement (G)	1.58	3.15	0.6	12.4 µm
Cement (T)	1.52	3.11	0.8	10.4 µm
Cement (C)	1.51	3.04	1.4	19.5 µm
Fly ash (G)	1.08	2.15	0.9	18.5 µm
Fly ash (T)	1.1	2.24	1.4	9.8 µm
Fly ash (C)	1.2	2.05	2.2	11.5
Filter dust (G)	1.1	2.21	1.7	8.5 µm
FGD-Gypsum (T)	1.24	2.44	4.5	65 µm
Tailing (T)	1.33	2.62	3.2	0.12 mm

### 3.3.2.2 Optimal ratio of backfill

During the study water and solid ratios of backfill mixtures of 0.6, 0.55, 0.5, 0.45, 0.4, 0.35, 0.3, 0.25, 0.2 and 0.15 were chosen for various mixtures of backfill. Water was added to set the resulting backfill. The lowest suitable water solid ratio of synthetic anhydrite and natural anhydrite were 0.18 because below 0.18 the mixture could not be mixed in a satisfactory way (Fig. 3.27 - 3.28). The lowest suitable water solid ratio mixture of cement mixed fly ash, mixture of cement mixed fly ash and filter dust, mixture of FGD-gypsum and fly ash, mixture of tailings and cement were 0.4. The initial setting time of all samples increases with a decrease in water content and is below 1-2 hours for investigated conditions. The slump is used to determine the consistency of backfill mixtures as shown in figure 3.29 and table 3.4.

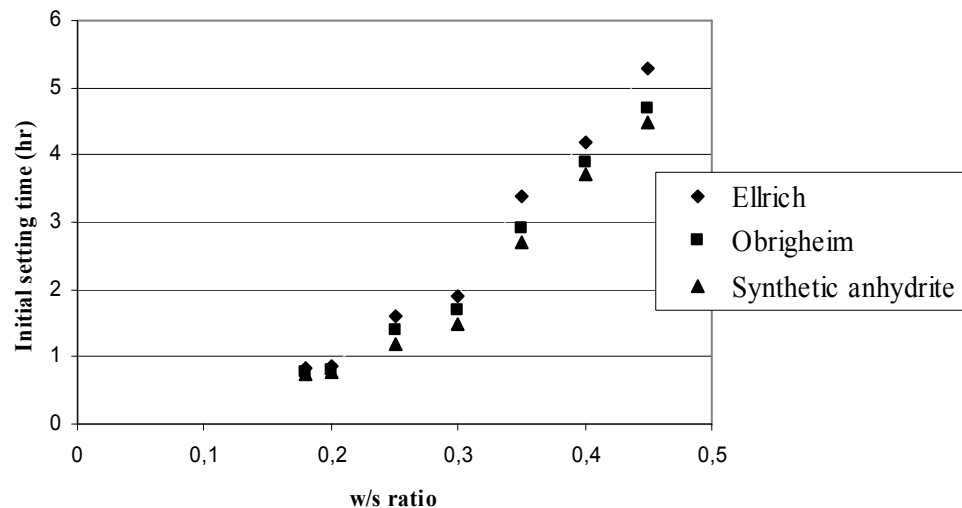


Figure 3.27: Initial setting time of backfill materials

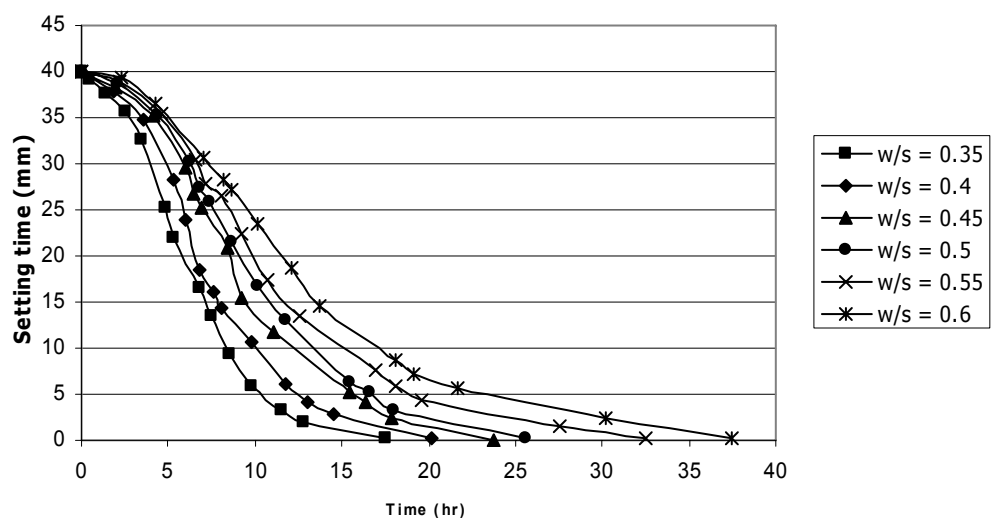


Figure 3.28: Setting time of dust filter by Vicat test



Figure 3.29: Slump test

Table 3.4: Time of setting with vicat test and slump test of backfill materials (5 % cement at w/s 0.45)

Samples	Initial setting time (min)	Final setting time (min)	Slump (cm)
100 % C (G)	50	100	10
C+FA (G)	95	120	15
C+FA+FD (G)	106	143	16
100% C (T)	55	90	11
C+FA (T)	100	150	15
100% C (C)	65	107	11
C+FA (C)	112	161	17
100% FGD-G (T)	104	173	15
10 % FGD-G + 90 %FA (T)	97	164	16
T+ C (T)	120	190	17



### 3.3.2.3 Scanning electron microscope investigations

The JEOL JSM 6400 scanning electron microscope (SEM) was used to characterize the microstructure and texture of the backfill samples after 28 days curing (Fig. 3.30-3.36). The SEM micrographs show tabular prismatic crystals of synthetic anhydrite, natural anhydrite and filter dust. The characteristic of fly ash was the abundance of spherical fly ash particles. The FGD-gypsum is irregular in shape and mostly composed of dihydrate gypsum ( $\text{CaSO}_4 \cdot 2\text{H}_2\text{O}$ ). Tailings from potash mines principally consist of tabular prismatic crystals. The SEM of cement hydration and the reactants of pozzolanic reaction, which has a laminar morphology. The mixture of backfill materials and salt water shows salt crystals because the water evaporates and the salt crystallizes. The presence of salt in sufficient concentrations can affect the strength development of backfill. Figure 3.34 show a scanning electron microscope image illustrating the significant presence of salt in the cured samples. During the curing process, a large amount of the salt crystallises. The growth of such crystals may inhibit the strength gain of paste backfill by reducing the dispersion of cement.

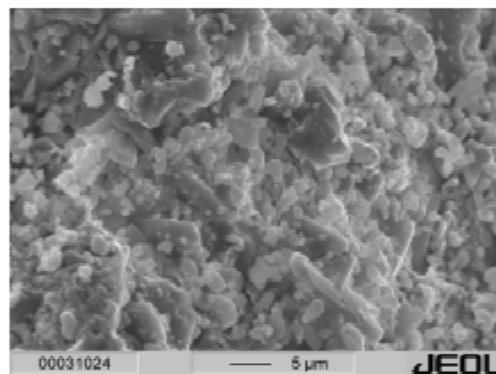


Figure 3.30: SEM image showing synthetic anhydrite

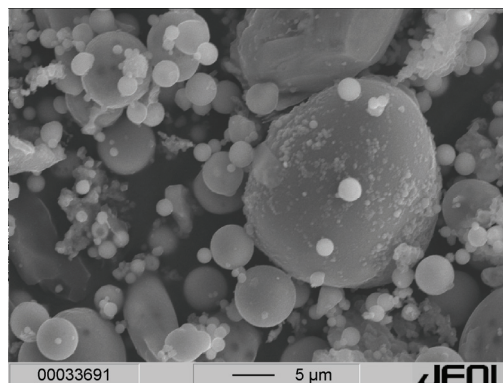


Figure 3.31: SEM image showing fly ash from Germany

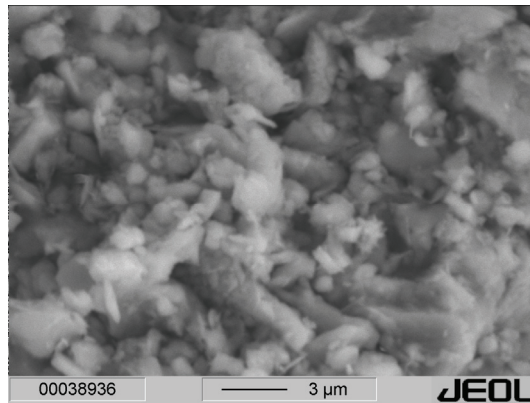


Figure 3.32: SEM image showing filter dust

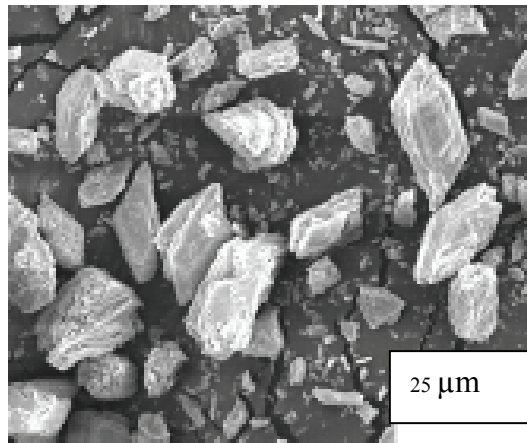


Figure 3.33: SEM image showing FGD-Gypsum

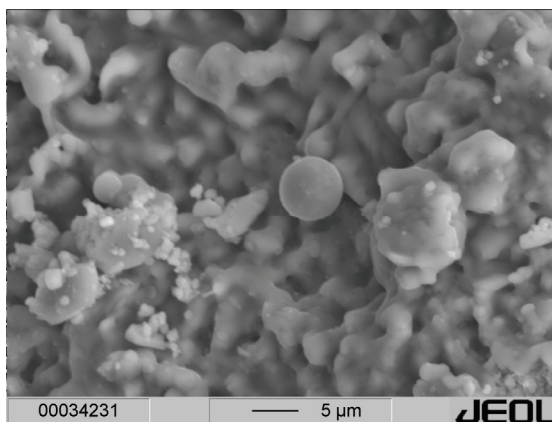


Figure 3.34: SEM image showing mixture of synthetic anhydrite, fly ash and salt solution

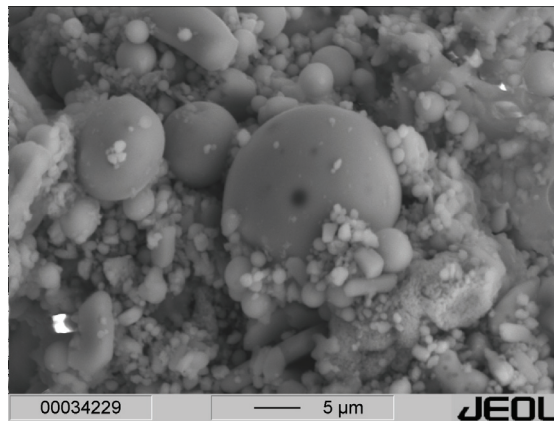


Figure 3.35: SEM image showing mixture of natural anhydrite, fly ash and salt solution

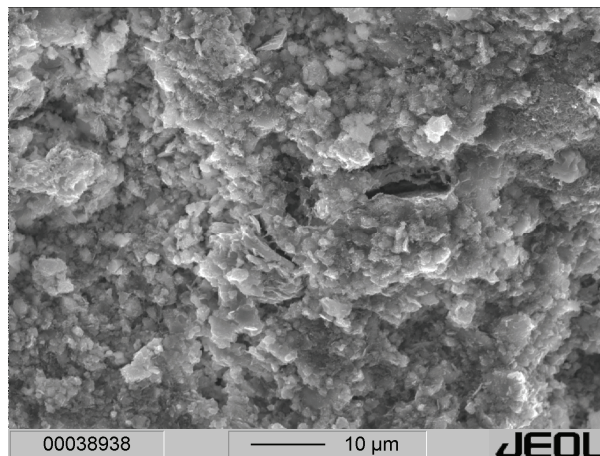


Figure 3.36: SEM image showing mixture of tailing, fly ash and salt solution

### 3.3.2.4 Simultaneous Thermal Analysis (STA)

Place 6.343 g of P1 and 6.700 g of P2 on the sample pan (Fig. 3.37) and  $\text{Al}_2\text{O}_3$  on the reference pan of the Netzsch STA 409 PC heat flux differential scanning calorimeter. The pans are made from alumina and the analysis is carried out under an  $\text{N}_2$  inert atmosphere. In a typical extended range experiment the heating rate is  $10\text{ }^\circ\text{C}/\text{min}$  over the range  $50 - 1,000\text{ }^\circ\text{C}$ , taking about 2 hours. Thermal analysis results for backfill materials are shown in figure 3.38-3.39. The Thermal gravimetric (TA) and Differential Scanning Calorimetry (DSC) plot showed continuous weight loss up to  $800\text{ }^\circ\text{C}$ . However, above this temperature, no significant loss was observed up to  $1,000\text{ }^\circ\text{C}$ . Taking into account the DTA data plotted as an arbitrary unit, a first weight loss of

about 26.58 % (P1) and 32.28 % (P2) was found below 150 °C, which is attributable to the removal of physisorbed water from the interparticle and/or intraparticle spaces. A second weight loss of 12.53 % (P1) and 4.46 % (P2) occurred between 580 and 800 °C, resulting from the moisture loss. The endothermic peak at about 107.3 and 781.8 °C of P1 indicated the moisture loss. Also the endothermic peak and exothermic peak at about 110.5 °C and 587.9 °C of P2 indicated the moisture loss. A total weight loss of about 39.32 % of P1 was reached by 800–1,000 °C and 36.85 % of P2 was reached by 600–1,000 °C.

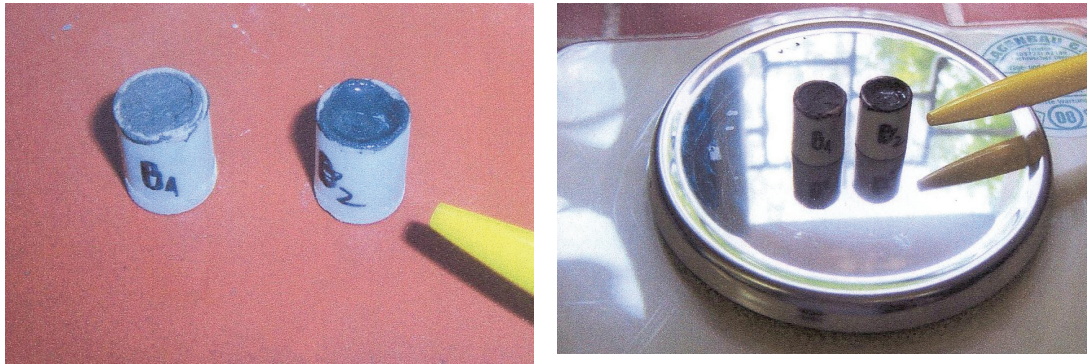


Figure 3.37: P1 and P2 samples

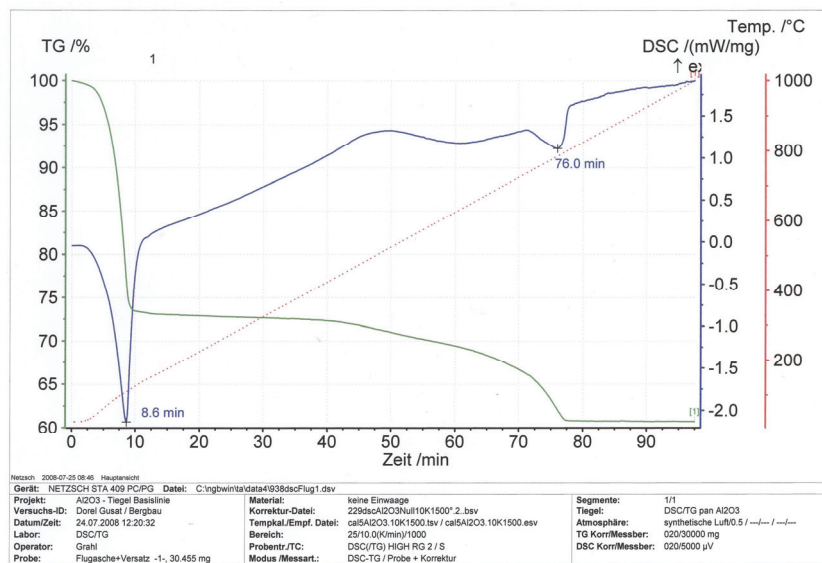
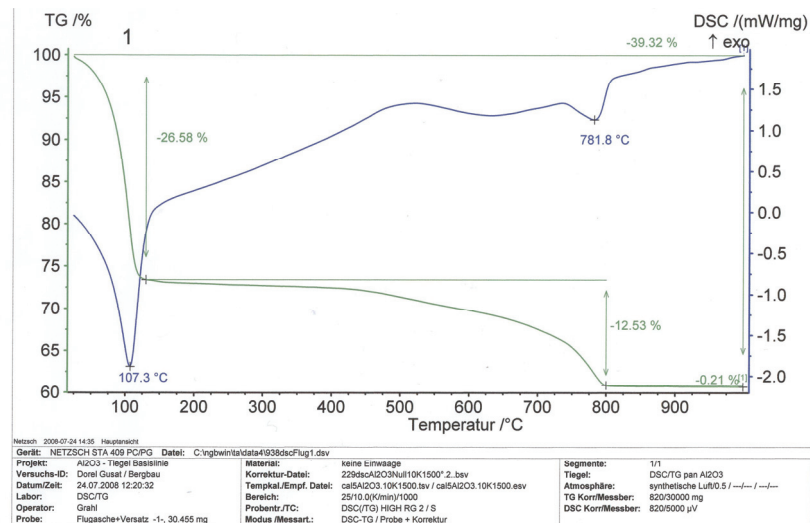


Figure 3.38: Thermogravimetry (TG) and Differential Scanning Calorimetry (DSC) curves of mixture of cement, fly ash and filter dust

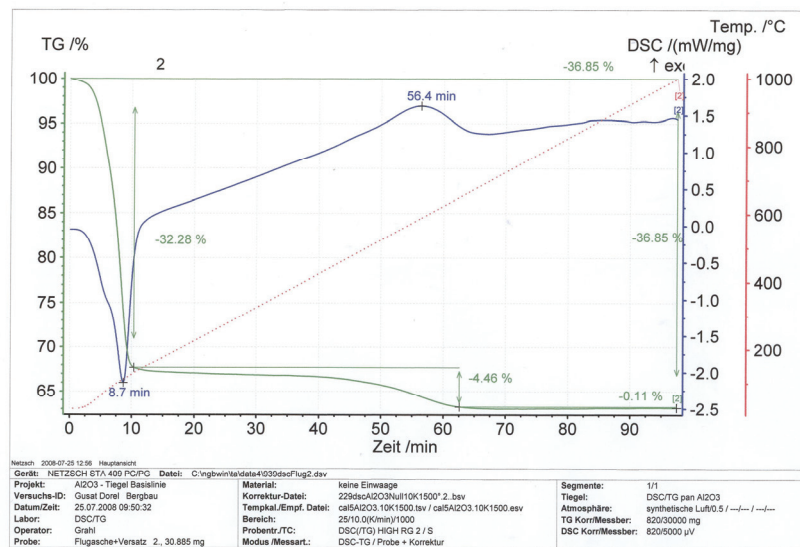
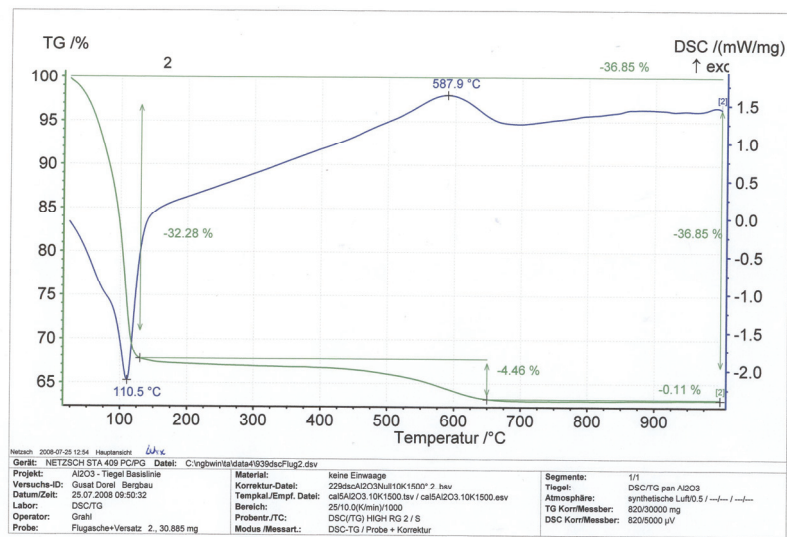


Figure 3.39: Thermogravimetry (TG) and Differential Scanning Calorimetry (DSC) curves of mixture of cement and fly ash

### 3.3.2.5 Permeability measurement

The overall permeability and porosity of backfill mixtures depends partly on the combination properties of backfill material, and partly on the possible existence of fine powder particles. The permeability of backfill mixtures increases when fly ash decreases as shown in table 3.5.

Table 3.5: Permeability measurement

<b>Samples</b>	<b>K<sub>0</sub> (m<sup>2</sup>)</b>	<b>Porosity (%)</b>
SA (G)	3.4 E-13	40
SA+FA (G)	1.5 E-15	25
NA (G)	1.7 E-10	47
NA+FA (G)	5.6 E-14	28
C (G)	2.1 E-18	23
C+FA(G)	1.7 E-18	8
C+FA+FD (G)	5.6 E-18	8
C+FA (C)	4.5 E-15	14
C+FA (T)	6.7 E-16	16
FGD-G (T)	2.7 E-13	24
FGD-G+FA (T)	6.4 E-16	13
T+C (T)	3.6 E-12	19
T+FA+C (T)	5.6 E -15	10
SA (T)	7.2 E -12	35
SA + FA (T)	5.3 E-15	21

### 3.3.2.6 Mineralogical characterization

The mineralogy of backfill materials includes a number of other characteristics, such as water retention, strength, settling characteristics and abrasive action. Different backfill types with different mineral assemblages can result in different backfill properties. The mineralogy can also affect the final strength of backfill by influencing chemical reactions that promote strength or produce additional chemical reactions. The mineralogical characterization was analysed by the Rietveld Method and shown in Table 3.6.

Table 3.6: Mineralogical characterization of backfill materials

Samples	SA (G)	NA (EL)	NA (OB)	SA (T)	FA (G)	FA (T)	FA (C)	FGD-G (T)
Quartz (%)	-	-	-	-	10	12	-	1
Anhydrite (%)	89	95	90	90	-	-	95	4
Magnetite (%)	-	-	-	-	2	1	-	1
Mullite (%)	-	-	-	-	21	20	-	-
Gypsum (%)	8	4	10	6	-	-	4	92
Fluorite (%)	3	-	-	4	-	-	-	2
Magnesite (%)	-	1	-	-	-	-	1	-
Amorphous (%)	-	-	-	-	67	61	-	-

### 3.3.2.7 Uniaxial compressive strength (UCS) tests and evolution of the dynamic elastic parameters

For the study, the backfill mixtures were poured into plastic cylinders with a diameter of 50 mm and a height of 100 mm (Fig. 3.40). After pouring the mixtures into the cylinders, then sealed and cured in a humidity chamber maintained for periods of 3, 7, 28 and 90 days. The resulting backfill specimens were then tested by uniaxial compression tests, split tensile strength test and flexural strength test. All of the backfill specimens were subjected to uniaxial compression tests using the mechanical press (ZD 100) having a normal loading capacity maximum of 1,000 kN.



Before test

After test

Figure 3.40: Compression test of mixture of cement (20 %) and filter dust (80 %) after 7 days (w/s = 0.4)



The results are shown in figure 3.41 the compressive strength of the backfill specimens (mixture of synthetic anhydrite and fly ash) continued to increase with increasing curing time. It was found the maximum compressive strength of synthetic anhydrite from Germany was 15.4 MPa mixed with fly ash 16 % by weight, the maximum compressive strength of synthetic anhydrite from Thailand was 14.9 MPa mixed with fly ash 19 % by weight. The tests of dynamic elastic parameters (E-modulus, G-modulus and Poisson's ratio) were performed on two specimens from six specimens and the mean values of the two readings were calculated. The dynamic elastic parameters E-modulus and G-modulus show that for the specimens, it was found the maximum E and G - modulus of synthetic anhydrite from Germany was 2.2 GPa mixed with fly ash 11 % by weight and 0.85 GPa mixed with fly ash 10 % by weight respectively. The E and G - modulus of synthetic anhydrite from Thailand was 2.1 GPa mixed with fly ash 12 % by weight and 0.7 GPa mixed with fly ash 10 % by weight respectively.

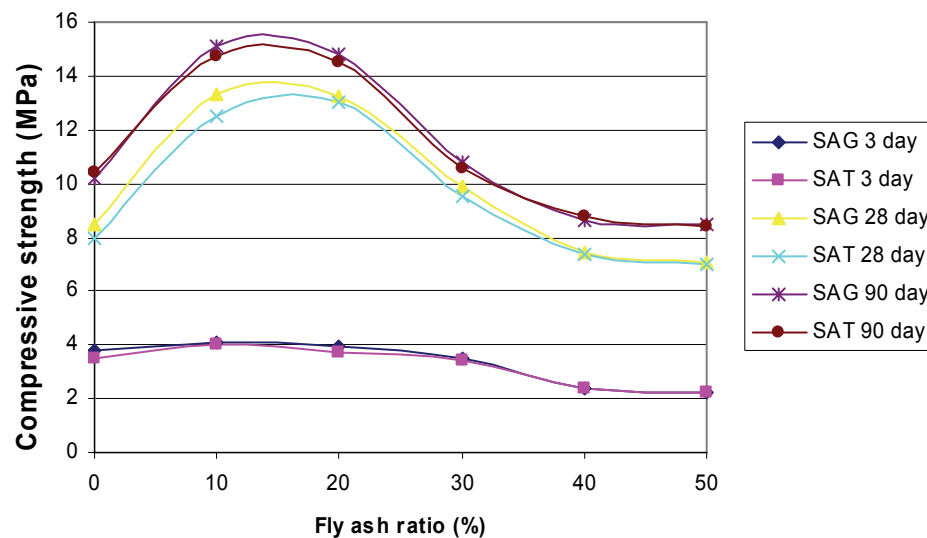


Figure 3.41: Compressive strength of synthetic anhydrite

The results are shown in figure 3.42. The compressive strength of the backfill specimens (mixture of natural anhydrite and fly ash) continued to increase with increasing curing time. It was found the maximum compressive strength of natural anhydrite from Obrigheim (particle size less than 4 mm) was 13.4 MPa mixed with fly ash 18 % by weight, the maximum compressive strength of natural anhydrite from

Obrigheim (particle size less than 8 mm) was 11 MPa mixed with fly ash 19 % by weight, the maximum compressive strength of natural anhydrite from Ellrich (particle size less than 4 mm) was 11.6 MPa mixed with fly ash 19 % by weight. The tests of dynamic elastic parameters (E-modulus, G-modulus and Poisson's ratio) were performed on two specimens from six specimens and the mean values of the two readings were calculated. The dynamic elastic parameters E-modulus and G-modulus show that for the specimens, it was found the maximum E and G -modulus of natural anhydrite from Ellrich was 0.96 GPa mixed with fly ash 18 % by weight and 0.5 Gpa mixed with fly ash 20 % by weight respectively. The E and G -modulus of natural anhydrite from Obrigheim (particle size less than 4 mm) was 0.95 GPa mixed with fly ash 13 % by weight and 0.5 Gpa mixed with fly ash 18 % by weight respectively. The E and G -modulus of natural anhydrite from Obrigheim (particle size less than 8 mm) was 0.9 GPa mixed with fly ash 15 % by weight and 0.46 Gpa mixed with fly ash 17 % by weight respectively.

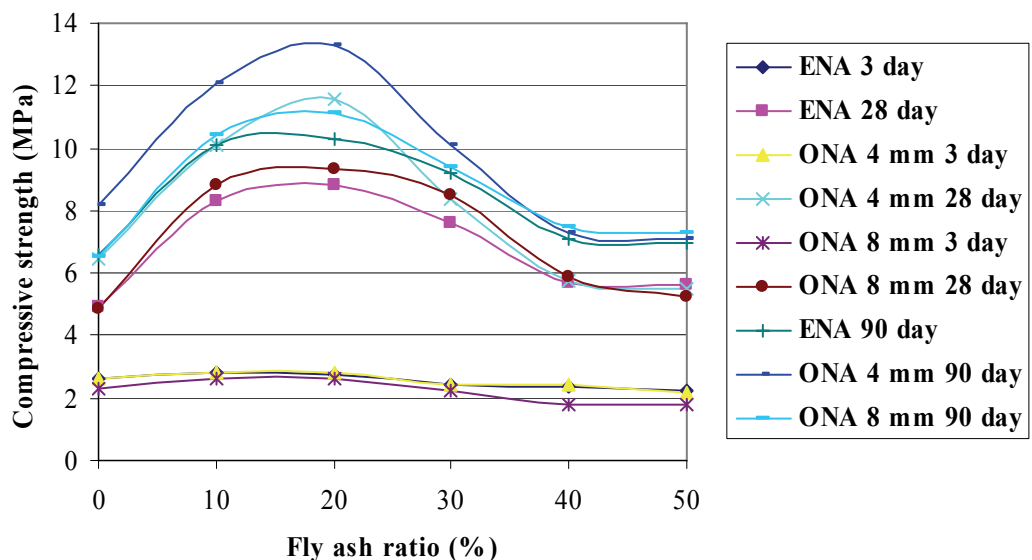


Figure 3.42: Compressive strength of natural anhydrite

Figure 3.43 shows the compressive strength of the mixtures of FGD-gypsum and fly ash specimens continued to increase with increasing curing time. It was found the maximum compressive strength of FGD-gypsum was 14.8 MPa mixed with 18 % fly ash mixing a w/s ratio 0.45, the maximum compressive strength was 14.2 MPa mixed with 12 % fly ash mixing a w/s ratio 0.4, the maximum compressive strength was 12.6 MPa mixed

with 11 % fly ash mixing a w/s ratio 0.5. The tests of dynamic elastic parameters (E-modulus, G-modulus and Poisson's ratio) were performed on two specimens from six specimens and the mean values of the two readings were calculated. The dynamic elastic parameters E-modulus and G-modulus show that for the specimens, it was found the maximum E and G -modulus of mixture of FGD-Gypsum and fly ash (w/s 0.4) was 4.2 GPa mixed with fly ash 20 % by weight and 2 Gpa mixed with fly ash 20 % by weight respectively. The E and G -modulus of w/s 0.45 was 5.4 GPa mixed with fly ash 12 % by weight and 2.7 GPa mixed with fly ash 13 % by weight respectively. The E and G -modulus of w/s 0.5 was 4.6 GPa mixed with fly ash 12 % by weight and 2.5 Gpa mixed with fly ash 13 % by weight respectively.

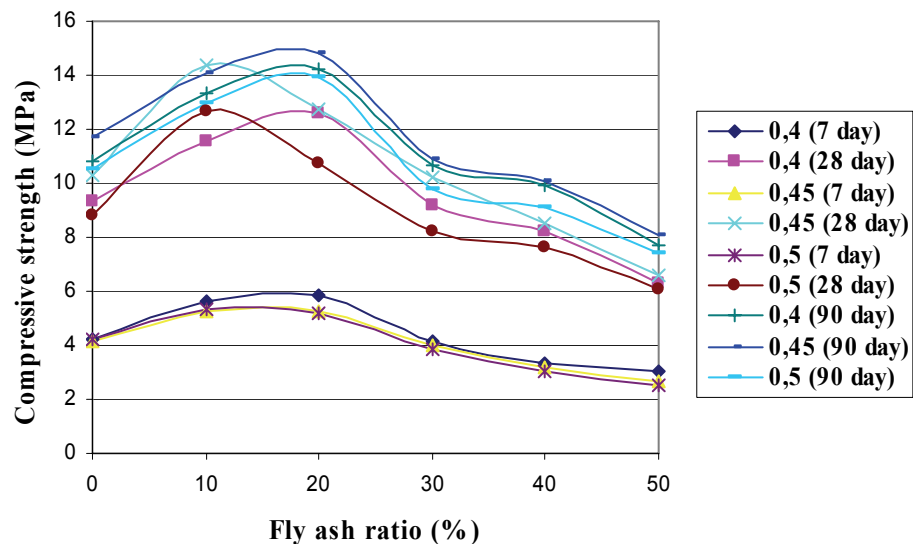


Figure 3.43: Compressive strength of FGD-gypsum (T)

Table 3.7 shows the compressive strength of the mixture of cement and water specimens continued to increase with increasing curing time. It was found the maximum compressive strength of cement mixing a w/s ratio 0.4 from Germany, Thailand and China were 41.75 MPa , 38.25 MPa and 31.83 respectively.

Table 3.7: Compressive strength of cement

w/s ratio	Mix ID	7 days				28 days				90 days UCS (MPa)
		UCS (MPa)	E (kN/mm <sup>2</sup> )	G (kN/mm <sup>2</sup> )	Poisson's ratio	UCS (MPa)	E (kN/mm <sup>2</sup> )	G (kN/mm <sup>2</sup> )	Poisson's ratio	
0.4	CG	23.51	12.64	5.36	0.245	41.75	23.32	9.15	0.276	43.5
	CC	15.47	9.81	4.14	0.213	31.83	18.62	6.42	0.241	32.7
	CT	20.22	10.52	5.11	0.234	38.25	20.24	8.74	0.253	40.1
0.45	CG	20.42	11.71	5.19	0.241	36.88	23.41	9.17	0.277	38.5
	CC	14.85	9.23	3.95	0.208	33.67	17.43	6.24	0.234	35.2
	CT	18.75	11.24	4.86	0.227	35.64	22.53	8.53	0.247	37.7
0.5	CG	18.73	10.55	5.21	0.234	33.42	23.12	9.11	0.265	35.1
	CC	12.57	8.46	3.27	0.202	29.25	16.28	6.07	0.228	31.1
	CT	17.22	9.25	5.22	0.217	32.45	22.71	8.15	0.237	34

Figures 3.44 - 3.49 show the compressive strength and dynamic elastic parameters (E-modulus, G-modulus and Poisson's ratio) of the mixtures of cement and fly ash specimens continued to increase with increasing curing time and decrease with increasing fly ash replacement.

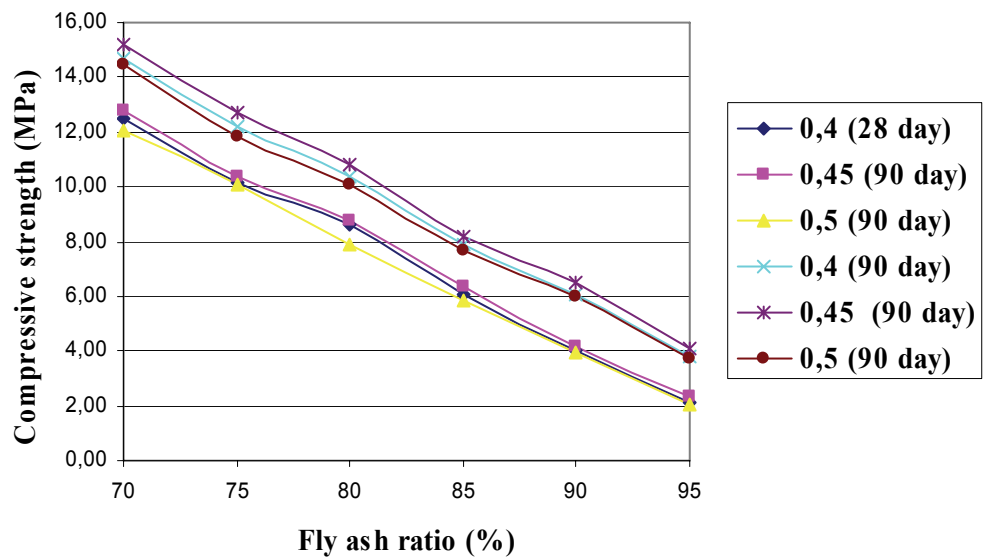


Figure 3.44: Compressive strength of cement and fly ash (G) mixtures

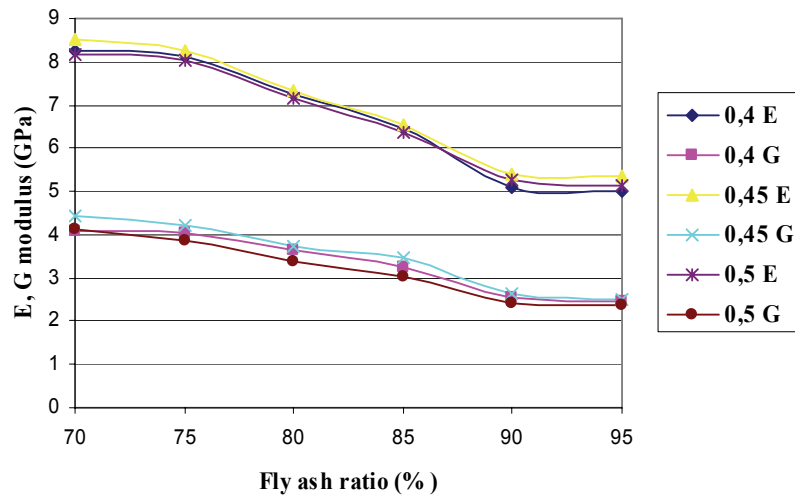


Figure 3.45: E and G modulus of cement and fly ash (G)

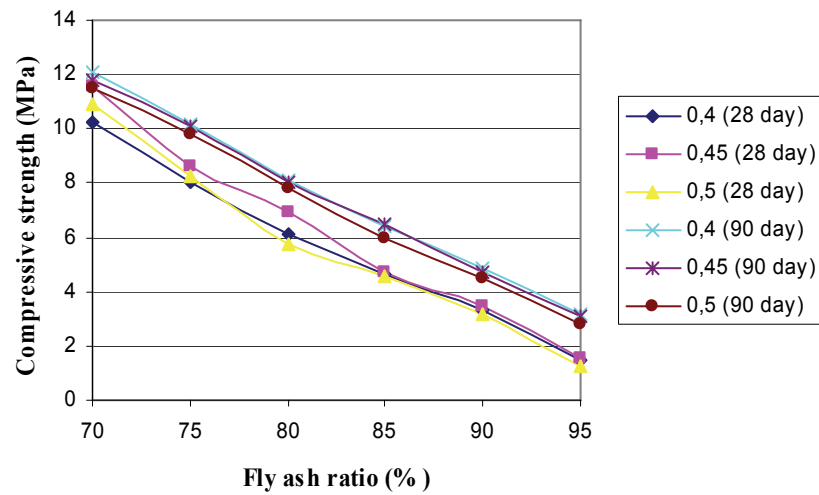


Figure 3.46: Compressive strength of cement and fly ash (C)

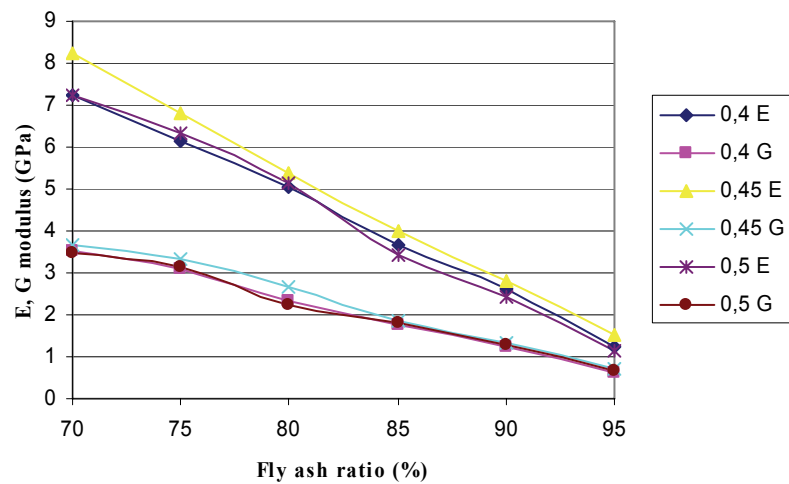


Figure 3.47: E and G modulus of cement and fly ash (C)

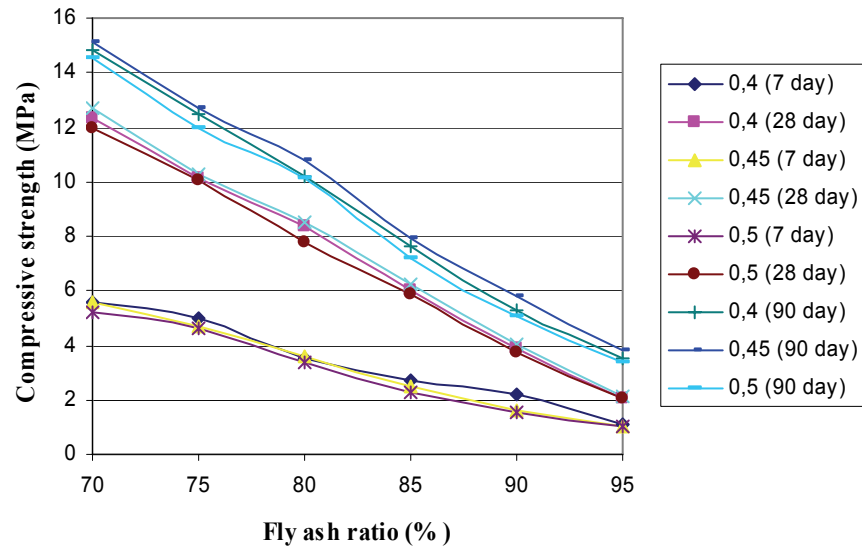


Figure 3.48: Compressive strength of cement and fly ash (T)

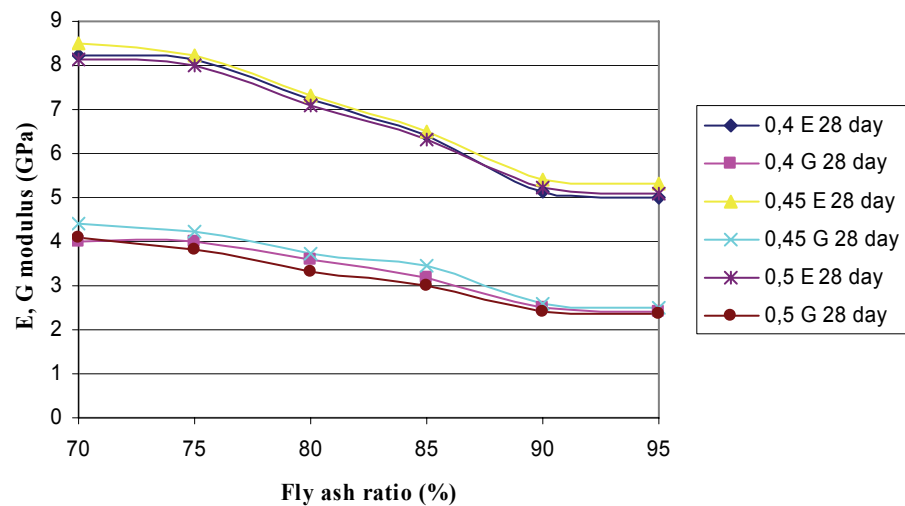


Figure 3.49: E and G modulus of cement and fly ash (T)

Figure 3.50 – 3.51 show the compressive strength and dynamic elastic parameters (E-modulus, G-modulus and Poisson's ratio) of the mixtures of cement and filter dust specimens continued to increase with increasing curing time and decrease with increasing filter dust replacement.

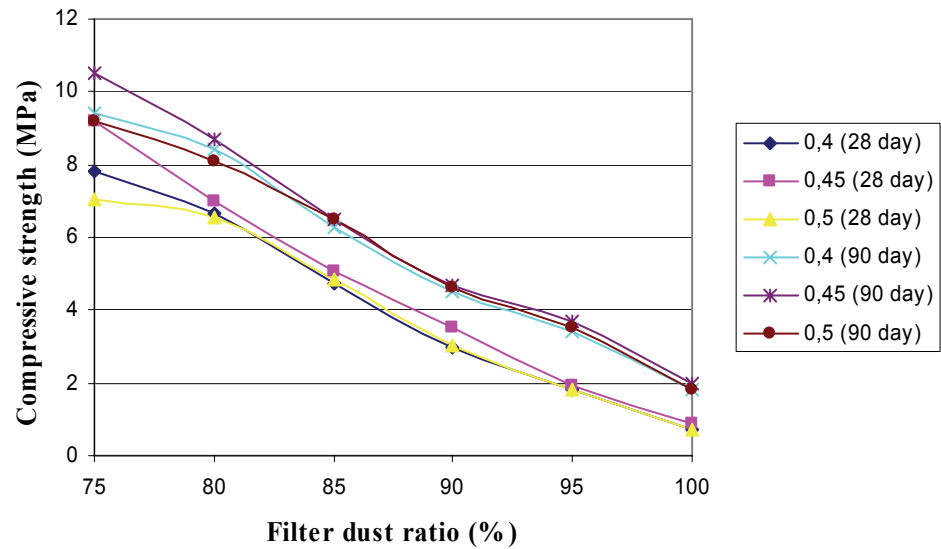


Figure 3.50: Compressive strength of cement and filter dust (G)

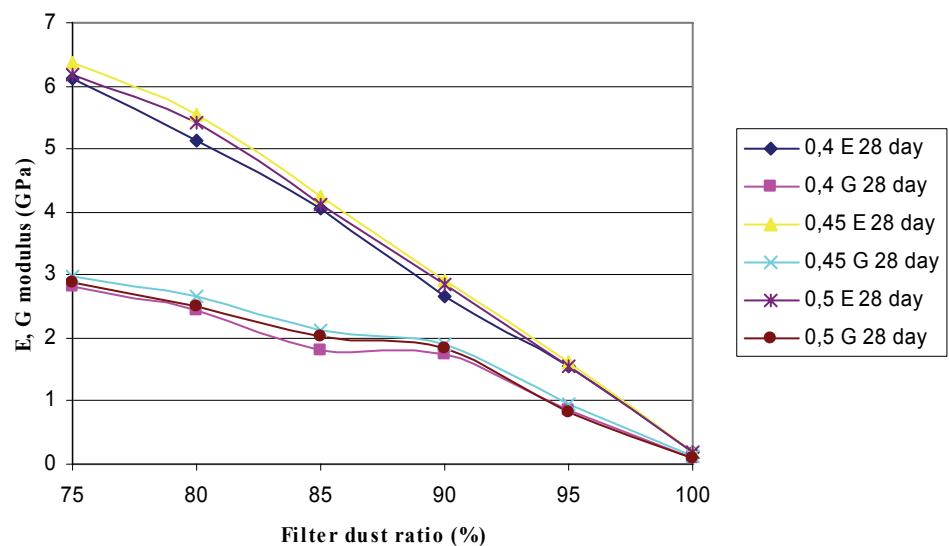


Figure 3.51: E and G modulus of cement and filter dust (G)

The compressive strength and dynamic elastic parameters (E-modulus, G-modulus and Poisson's ratio) of the mixtures of cement, fly ash and filter dust specimens continued to increase with increasing curing time and decrease with increasing filter dust replacement. The dynamic elastic parameters E-modulus and G-modulus show that for the specimens with higher w/s ratio (0.5), the evolution of E-modulus and G-modulus in the mixture is much faster than in the specimens with a lower w/s ratio (0.4) with curing time 7 and 28 days. The effects of mixtures with different w/s ratios and curing time for Poisson's ratio shows that for the specimens with higher w/s ratio (0.5), the evolution of

Poisson's ratio in the mixture is much faster than in the specimens with a lower w/s ratio (0.4) with curing time 7 and 28 days.

The compressive strength and dynamic elastic parameters (E-modulus, G-modulus and Poisson's ratio) of the mixtures of cement, fly ash and tailings specimens continued to increase with increasing curing time and decrease with increasing tailings replacement. The dynamic elastic parameters E-modulus and G-modulus show that for the specimens with higher w/s ratio (0.5), the evolution of E-modulus and G-modulus in the mixture is much faster than in the specimens with a lower w/s ratio (0.4) with curing time 7 and 28 days. The effects of mixtures with different w/s ratios and curing time for Poisson's ratio show that for the specimens with higher w/s ratio (0.5), the evolution of Poisson's ratio in the mixture is much faster than in the specimens with a lower w/s ratio (0.4) with curing time 7 and 28 days.

### 3.3.2.8 Effects of water salinity on backfill properties

Tap water and saline water were used to make the backfill specimens (synthetic anhydrite, natural anhydrite, cement and fly ash) in order to make a comparison between the mechanical properties of tap water based backfill and saline water based backfill. A comparison between the compressive strength of backfill samples made with different water types is presented in figures 3.52 - 3.53. The results show that a significant negative impact was imposed on backfill strength development by using saline mine water.

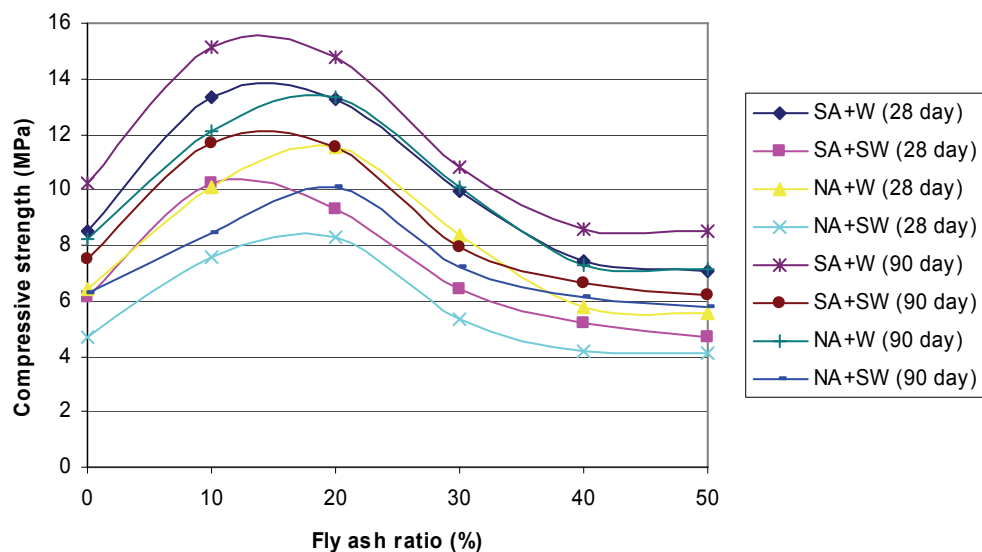


Figure 3.52: Influence of water quality on backfill (anhydrite) properties



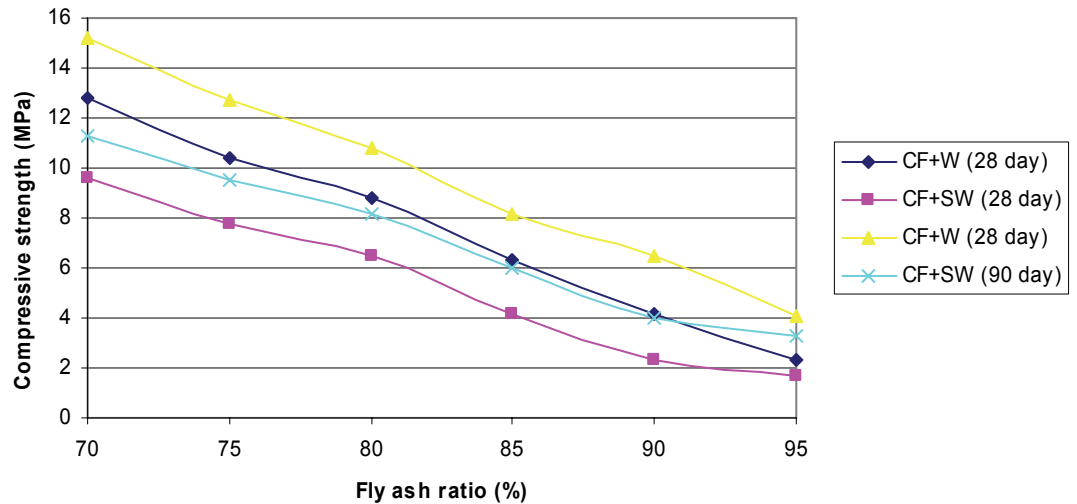


Figure 3.53: Influence of water quality on backfill (cement and fly ash) properties

### 3.3.2.9 Triaxial compression test of backfill specimens

Triaxial compression testing can be used to assess the failure criterion of the backfill at different confining pressures and moisture contents. Shear strength parameters can be used in the estimation of both active and passive lateral support that the backfill provides to remnant mine pillars. Drainage during the compression test can be controlled to simulate conditions which exist in actual mining applications. It is expected that the backfill will be placed in a loose state, and that there will be a large amount of grain displacement as the backfill is compacted by failing mine roof and pillars. After a slip movement has occurred in the backfill, the slip surface forms a permanent plane of weakness. The shear strength that can be mobilized along this plane corresponds to the residual shear strength of the material, which may be significantly lower than the peak strength. In this situation, an appropriate triaxial compression test would be one which measures residual shear strength parameters. This can be accomplished by 'failing' the sample, increasing the confining pressure, and then bringing the sample to failure again. The test can also be used to determine changes in the modulus of deformation of the backfill. Table 3.8 shows the triaxial compression test of the mixture of backfill specimens that lowest cost available (synthetic anhydrite, natural anhydrite, cement, filter dust, tailings, FGD-gypsum and fly ash).

Table 3.8 Triaxial test of backfill materials

Specimens	Triaxial compressive strength test	
	C (MPa)	Friction angle (°)
SA (G)	0.63	42
SA+F (G)	0.91	47
NA (G)	0.24	35
NA+FA (G)	0.47	38
SA (T)	0.57	40
SA+FA (T)	0.88	44
C+FA (G)	0.72	39
C+FA (C)	0.37	36
C+FA (T)	0.64	38
C+FA+FD (G)	0.83	42
FGD-G (T)	0.64	40
FGD-G+FA (T)	0.72	41
C+T (T)	0.41	37

### 3.3.3 Chemical composition

#### 3.3.3.1 Chemical composition

All chemical analyses of backfill materials and mixing water (Table 3.9 - 3.11) were done using an ICP AES spectrometer which is an emission spectrophotometric technique, exploiting the fact that excited electrons emit energy at a given wavelength as return to ground state. The fundamental characteristic of this process is that each element emits energy at specific wavelengths peculiar to its chemical character.

Table 3.9: Chemical composition of backfill materials

Chemical composition (%)	SA (G)	SA (T)	NA (EL)	NA (OB)	FA (T)	FA (G)	FA (C)	FGD -G (T)	FD (G)	C (G)	C (C)	C (T)	T (T)
CaSO <sub>4</sub>	>99	>98	-	-	-	-	-	-	-	-	-	-	-
SiO <sub>2</sub>	<0.1	0.5	0.07	-	42.86	56.61	62.8	1.10	46.2	20.7	46.1	21.8	21.8
Al <sub>2</sub> O <sub>3</sub>	<0.1	0.4	0.12	0.11	23.05	21.05	11.2	0.52	6.29	6.12	6.43	6.2	6.2
Fe <sub>2</sub> O <sub>3</sub>	0.1	0.1	0.22	0.66	8.75	5.58	3.4	0.70	1.77	2.51	2.4	2.43	2.43
CaO	-	0.1	44.31	44.19	10.13	7.55	0.42	46.7	39	62.4	34.2	61.2	61.2
MgO	0.1	0.1	-	-	2.93	1.3	0.25	0.39	1.25	2.78	1.48	2.65	2.65
Na <sub>2</sub> O	-	-	-	0.66	0.2	0.62	0.1	0.08	0.15	0.167	0.17	0.15	0.15
K <sub>2</sub> O	-	-	0.23	-	2.55	4.68	0.33	0.05	2.98	1.65	0.7	1.73	1.73
MnO <sub>2</sub>	-	-	-	-	-	-	0.02	-	-	-	0.04	-	-
P <sub>2</sub> O <sub>5</sub>	-	-	-	-	-	-	0.06	-	-	-	0.04	-	-
TiO <sub>2</sub>	-	-	-	-	-	-	0.07	-	-	-	0.02	-	-
SO <sub>3</sub>	-	-	54.89	54.86	1.17	-	0.56	1.47	1	2.77	2.44	2.56	2.56

Table 3.10: Trace elements in mixing water

<b>Element</b>	<b>Element</b>	<b>Unit</b>	<b>Value</b>
Zinc	<i>Zn</i>	µg/l	34.3
Bromine	<i>Br</i>	µg/l	35
Strontium	<i>Sr</i>	µg/l	113
Arsenic	<i>As</i>	µg/l	1.4
Barium	<i>Ba</i>	µg/l	39.6
Cadmium	<i>Cd</i>	µg/l	0.4
Aluminium	<i>Al</i>	µg/l	214.7
Manganese	<i>Mn</i>	µg/l	11.5
Iron	<i>Fe</i>	µg/l	105
Copper	<i>Cu</i>	µg/l	4.4
Nickel	<i>Ni</i>	µg/l	1.0
Uranium	<i>U</i>	µg/l	4.5
Lead	<i>Pb</i>	µg/l	0.6
Rubidium	<i>Rb</i>	µg/l	3.4

Table 3.11: pH and conductivity of backfill materials

<b>Samples</b>	<b>pH</b>	<b>Conductivity (<math>\mu\text{S/cm}</math>)</b>
Synthetic anhydrite (G)	11.56	2,940
Synthetic anhydrite (T)	10.87	2,760
Natural anhydrite (Ellrich)	9.74	1,780
Natural anhydrite (Obrigheim)	9.65	1,740
Cement (G)	12.1	14,760
Cement (T)	12.5	12,470
Cement (C)	12.6	11,800
Fly ash (G)	12.3	4,440
Fly ash (T)	11.6	2,540
Fly ash (C)	10.2	1,160
Filter dust (G)	8.99	5,700
FGD-Gypsum (T)	10.5	2,130
Tailing (T)	8.7	1,580

### **3.3.3.2 Elute analysis**

Mine wastes or industrial wastes may only be utilised to produce backfill materials and/or for direct use as backfill materials for long-term safety. The limit values for solids and backfill correlation values as listed in Table 3.12-3.13 was necessary to control arsenic in fly ash and mercury in filter dust. The use of the backfill materials does not lead to harmful pollution of the groundwater or surface water or any other negative impact on the quality of water bodies. In this context the limit values in eluates as listed in Appendix C may not be exceeded in the stowage materials.







## Chapter 4

### Discussion of the Results

Backfill materials were sampled from different sources and local materials in each country. Each sample was taken from randomly selected points on the surface. To achieve as representative a sample as possible, a large amount of material was collected from many locations in each country and then mixed to obtain a representative sample.

Various investigation can be performed to help assess the potential performance of mining industrial waste and industrial waste as a backfill material. The systematic selection of backfill materials can be determined with materials available, mining methods and backfill technologies. Certain engineering properties can be measured with the uniaxial and triaxial compression tests. Chapter 3 provides a summary of the desired properties based on both placement and engineering performance considerations.

#### 4.1 Effect of different parameters on backfill behavior

##### 4.1.1 Grain size analysis

Assuming that there was not significant segregation of the different grain sizes during and following backfilling, one can analyse particle sizes to help predict, in a qualitative way, how a backfill composed of a given material may be expected to behave with respect to strength, settlement and permeability. A backfill which contains well graded particles should offer more resistance to displacement and settlement than one with uniformly graded particles, all other factors being equal. It has been shown that the amount of water flow through mine waste can be empirically related to its gradation and void ratio. Permeability decreases with a decrease in the effective size of the material, which is the 10 % passing size according to the grain size distribution. Therefore, one would expect backfill materials with a high percentage of minus 75  $\mu\text{m}$  material to have a low permeability. A size analysis is also required to determine the suitability of a material for a particular backfill system, and whether or not crushing and screening of the material is needed. An indication of the gradation of the materials can be computed from a grain size distribution curve for grain sizes larger than the 75  $\mu\text{m}$  sieve using the

coefficient of uniformity ( $C_u$ ) and coefficient of curvature ( $C_c$ ). Both values can be calculated provided that not more than 10 % of the grain sizes are less than 75  $\mu\text{m}$ .

#### **4.1.2 Age of specimens**

Chapter 3 shows the effect of the age of the specimens on mechanical behavior of backfill. In general, for the tests with the same confining pressures, the peak or maximum value of stress ratio (or axial stress) increases with an increase of the age of the specimens. This phenomenon is more evident in low confining pressures. The elastic modulus of mixture of backfill specimens increases with an increase of the age of the specimens. It also shows that when the age of the specimens increases, the elastic modulus augmentation is almost equal for different confining pressures.

The evolution of triaxial strength effective parameters with the age of the specimens are shown in Table 3.8. It can be clearly seen that when the age of the specimens increases, cohesion parameter increases and the internal friction angle slightly increases. Therefore, it can be concluded that the increase of the compressive strength of backfill due to the completion of the cement hydration and the strengthening of the bonds between cement paste and backfill materials is reflected on the triaxial strength parameters by increasing the cohesion parameter, although the internal friction is slightly increases. The same trend of evolution of the triaxial strength parameters of specimens as a function of its compressive strength was noted. The rate of augmentation of the cohesion and increase of the internal friction is smaller for the mixed low cement, which its water to cement ratio is greater than other specimens.

#### **4.1.3 Binder factor and water to binder ratio**

The effect of binder factor on uniaxial strength parameters of backfill is shown in chapter 3. It shows that increasing the binder factor increases the cohesion parameter and slightly increase the internal friction angle of the material. This effect does not have the same intensity for the different mixes. As for normal concrete, the compressive strength depends on the binder factor as well as the water to binder ratio. Increasing the binder factor or decreasing water to binder ratio, the compressive strength increases.

The results in chapter 3 shows clearly this effect of water to binder ratio evolution on the compressive strength for the backfill specimens. Generally, obtained results show that an increase of binder factor leads to an increase of compression strength, triaxial strength and elastic modulus.

#### **4.1.4 Fly ash and filter dust content**

Effect of the fly ash content on the mechanical behavior of backfill ss shown in chapter 3 shows the evolution of the compressive strength of the specimens, that the difference between them is only their fly ash contents. It shows that when the fly ash content is mixed with anhydrite or FGD-gypsum the compressive strength of the backfill specimens increase and this is more important when the age of the specimens increases. As explained before, this is due to the higher fly ash content more than the bonding between the binder and fly ash. In chapter 3 shows that the elastic modulus was also affected by the fly ash content. Evolution of the elastic modulus of the mentioned specimens show that when the fly ash content mixed with anhydrite or FGD-gypsum of the specimens increases the elastic modulus increases and the difference between the elastic modulus of the different specimens is more important when the age of the specimens increases.

When the fly ash and filter dust content increases mixed with cement the compressive strength of the backfill specimens decrease and this is more important when the age of the specimens increases. As explained before, this is due to the higher fly ash content that more than the bonding between the backfill materials and cement paste. In chapter 3 shows that the elastic modulus was also affected by the fly ash and filter dust content. Evolution of the elastic modulus of the mentioned specimens show that when the fly ash and filter dust content mixed with cement of the specimens increases the elastic modulus increases and the difference between the elastic modulus of the different specimens is more important when the age of the specimens increases.

#### **4.1.5 Fly ash and filter dust content on permeability**

The effect of fly ash and filter dust content on permeability is shown in table 3.5. It shows that increasing fly ash and filter dust content results in decreases in the

permeability of the specimens. Generally the results of this study show that increasing the fly ash and filter dust content initially reduces the permeability but after adding more fly ash and filter dust content because of increasing the water required in the mixture to maintain backfill workability, the dry density decreases and the permeability increases. The increased water tends to counterbalance the increased fly ash and filter dust.

#### **4.1.6 Backfill technology**

In this study, paste backfill was suited to be utilized in underground mines because this backfill was mixed of fine solid particles, binder and water, containing between 72 % and 85 % solids by weight. The paste backfill provides ground support to the pillars and walls, but also helps prevent caving and roof falls, and enhances pillar recovery, which enhances productivity. Thus, the backfill placement provides an extremely flexible system for coping with changes in geometry of the orebody, that result in changing stope width, dip, and length. The method of the backfill delivery depends upon the amount of energy required to deliver the backfill material underground which depends on its distribution cone. The backfill is usually transported underground through reticulated pipelines. Analysis of the backfill stability must consider the geometric boundaries of the backfill for the best economic use of paste backfill. Mine openings and exposed backfill faces in large underground mines vary in shape from high and narrow to low and wide. Additionally, wall rock next to the backfill may be either steeply dipping or relatively flat-lying. The stoping sequence can be modified to reduce the number of backfilled stopes, or the stope geometries could be revised to reduce the strength required of backfill exposures. Once the required strength has been determined, the mix variables can be optimized to provide the desired mix, which achieves the target strength with the lowest cement usage. The mix variables under consideration include the binder content and type, mill tailings grain size distribution and mineralogy, solids concentration, and the mixing-water chemistry. For the design of a certain uniaxial compressive strength, these variables can be adjusted to produce an optimal mix design.

#### **4.1.7 Costs**

In general, higher backfill strengths are achieved by adding more binder, so costs are higher. However, any required strength can usually be achieved using a number of

different mixes, so testing is necessary to identify the optimum mix from the available materials. The relative prices of portland cement and pozzolans, the cost-effectiveness of chemical additives and the potential savings from disposal of tailings or waste rock as backfill must all be incorporated into the determination of operating costs. Capital costs also vary widely for different backfill types and from site to site, depending on the availability and quality of the potential backfill materials and their proximity to the mine.

#### **4.1.8 Eluate and metals concentration in backfill**

The public in every country has expressed concern about the pollution of backfill materials from mining industries and other industries. A great amount of the heavy metal such as arsenic, chromium, mercury, copper, lead and zinc are persistent in the aquatic system, with high toxicity to the flora and fauna. Due to their inherent hazardous nature, the indiscriminate release of materials from these industries to the environment has in the past adversely affected the normal well-being of life and continue to be a permanent danger to the hydrologic cycle and our food chain. Prior to disposal and backfill, such wastes demand some stabilization or immobilization, but high treatment cost often limits viable options for safe disposal.

For this study synthetic anhydrite and fly ash, there were potential environmental concerns for some eluation (As and Cr) and metals. Total metals concentration in FGD-gypsum appears lower than in fly ash. So far, cement or binder solidification is one of the most cost effective and widely used techniques to treat heavy metal. Solidification of heavy metals in cementitious matrices can transform the waste into the form of the insoluble hydroxides or may sometime be absorbed in the cement matrix reducing the water leachability. Cement paste is highly alkaline with high adsorption capacity for metals.

A wide variety of pozzolanic materials such as amorphous form of fly ash, hydrated lime and silicafume can be applied to improve the stability of cement-waste material. Active pozzolanic materials present in the amorphous form of fly ash by-products generate from pulverized coal power plants can chemically react with calcium

hydroxide as cement hydration product. Thus calcium silicate hydrate emulsion possessing can lead to good cementitious properties improving the heavy metal binder.

#### **4.1.9 Thermal analysis**

In Figure 3.38-3.39. the Thermal gravimetric (TA) and Differential Scanning Calorimetry (DSC) plot showed continuous weight loss up to 800 °C. However, the results of the temperature, no significant loss was observed up to 1,000 °C. Taking into account the DTA data plotted as an arbitrary unit, a first weight loss of about 26.58 % (P1) and 32.28 % (P2) was found below 150 °C, which is attributable to the removal of physisorbed water from the interparticle and/or intraparticle spaces. A second weight loss of 12.53 % (P1) and 4.46 % (P2) occurred between 580 and 800 °C, resulting from the moisture loss.

#### **4.1.10 Benefits of backfill containing fly ash**

Fly ash replaced some of the more expensive cement in the backfill mixture, thereby reducing the cost per cubic metre. When used with cement, fly ash improves flowability and increases compressive strength. It improves flowability because the spherical particles act like ball bearings. This allows the backfill to move more freely and the small particle size promotes better backfilling of voids. The cementitious properties of fly ash increase compressive strength. Contract specifications for backfilling projects in potash mine in Thailand presently require that the unconfined compressive strength of backfill be at least 5 MPa at 28 days. Use of fly ash also reduces shrinkage and slows set-up time, an important factor if backfill pumping must be interrupted for a few hours. Another important reason for using fly ash is recycling: every ton of fly ash used beneficially is one not disposed in a landfill.

Fly ash can potentially pose environmental and health risks. It contains trace amounts of several toxic elements including arsenic, chromium, copper, lead and zinc. These elements could contaminate soil, water and underground water. Portland cement also contains these elements and they can occur naturally in soil and water. If used responsibly, fly ash is a safe product and can be used safely with very limited chances of polluting soils, water and underground water. After backfill containing fly ash

hardens it is fairly inert. In this study it was found that backfill mixes using fly ash often leached lower concentrations of trace minerals than cement-only backfill. This study also indicated that, depending on the source of fly ash, leachate from hardened backfill could meet safe drinking water standards for heavy metal concentrations.

Fly ash will continue to be produced as long as coal-fired electricity is generated. Coal is an abundant and relatively cheap resource. Although concerns about fly ash use and disposal are valid, some environmental groups have sensationalized these concerns of fly ash as a hazardous waste. This could severely limit fly ash recycling and its beneficial uses and result in higher energy costs. The use of fly ash as a backfill component has resulted in improved performance and significant cost savings in pressurized backfilling projects in each country. This study indicates that sources differ markedly in chemistry and performance of their fly ash. These differences result from properties of the coal itself and the method of coal processing and combustion. A responsible user should thoroughly test fly ash from each potential source to ensure that it is appropriate for its intended use.

## Chapter 5

### Application of New Method

#### 5.1 Application of Backfill in underground potash mines in Thailand

Thailand is developing two major potash underground mines in the northeastern province: one in the Khorat sub-basin at Bam Net Narong Chaiyaphum province (the ASEAN project) and the other one is the Somboon mine at Udon Thani province, the APPC-Asian Pacific Potash Corporation Project (Fig. 5.1). Both projects will use room and pillar as mining method because this needs relatively low investment and it can provide good control of subsidence. The ASEAN project is constructed of a decline access into the potash deposit and plans to produce up to one million metric tons of  $K_2O$  equivalent product per year, whereas the APPC project is waiting for government decision and plan to produce two million tons of  $K_2O$  equivalent product per year (Masniyom, 2007).

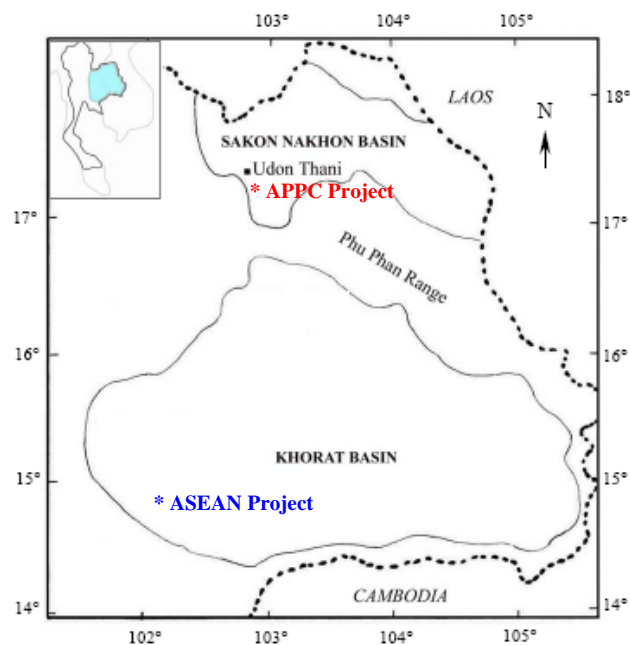


Figure 5.1 Locations of ASEAN and APPC Potash mine project in Sakon Nakhon Basin and Khorat basin in the northeast of Thailand



### 5.1.1 Mining method of ASEAN potash project

Room and Pillar Mining is used for this project because it is appropriate for a thickness of carnallite seam of 10-15 m (Fig. 5.2). Mining equipment will be mainly used to excavate into the ore body in order to keep the top and bottom of the tunnel smooth and unscathed. Then, orthogonal tunnels will be excavated 20 m apart. By connecting parallel tunnels, the pillars and rooms are generated. The dimensions of the pillars are 20 by 20 m and rooms are 15 m wide for the total length of 400 m.

The ASEAN Potash Mining Project awarded a \$15 million contract to Trafalgar House Construction Mining of the United Kingdom to take over and restart construction of a decline access into the Bamnet Narong potash mine in the Bamnet Narong District of Chaiyaphum. The mine will be a room and pillar layout. Construction work was stopped in 1993 when the original contractor hit a brine aquifer that caused flooding in the area. Trafalgar House Construction Mining demonstrated that the company could safely penetrate the aquifer on an incline shaft to the depth of 180 m. The 180 m deep shaft would connect between the potash processing plant on the surface and the underground deposits. Construction work was scheduled to begin in March 1996 and was expected to be completed in 2003 for first mainlevel. Currently this project is waiting for an investor to construct processing plant.

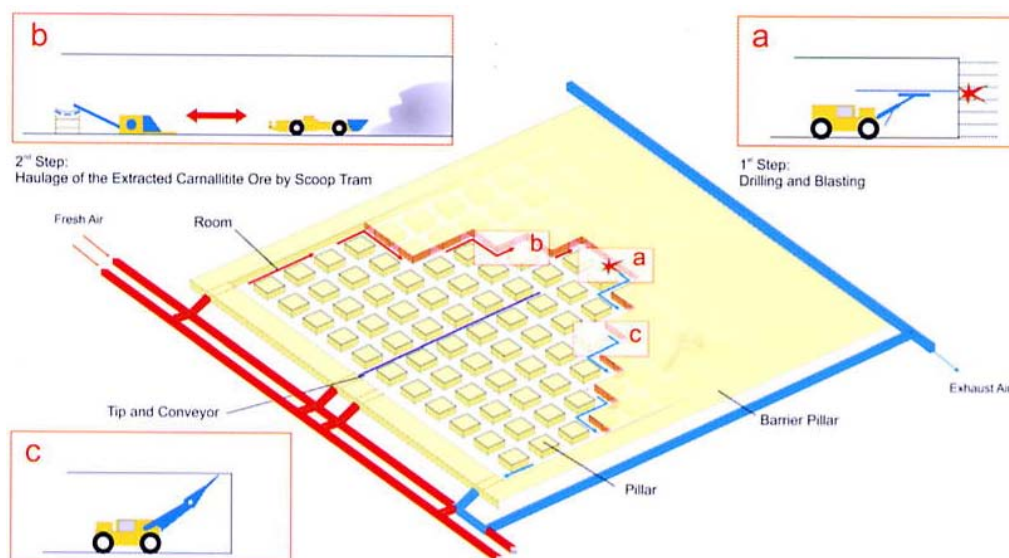


Figure 5.2: Underground mine layout of the ASEAN project (Bamnet Narong Mine)

### 5.1.2 Mining method of APPC potash project

The Udon Thani Potash Mine will be a conventional underground mine using the room and pillar method of mining to recover sylvinite ore from the variable depths of 300 to 380 m (Fig. 5.3). The room and pillar mining method as designed for the Udon South potash deposit is the only method applicable for mining the relatively thin, flat to undulating ore beds that characterize the deposit. A minimum amount of development work is required to prepare flat-lying bedded ore deposits for room and pillar mining. Roadways or panel entries are established for ore transport, ventilation and communication within the production panels. Excavation of the panel entries are combined with ore production. Mined out rooms can then serve as transport or perhaps air intake or out take routes.

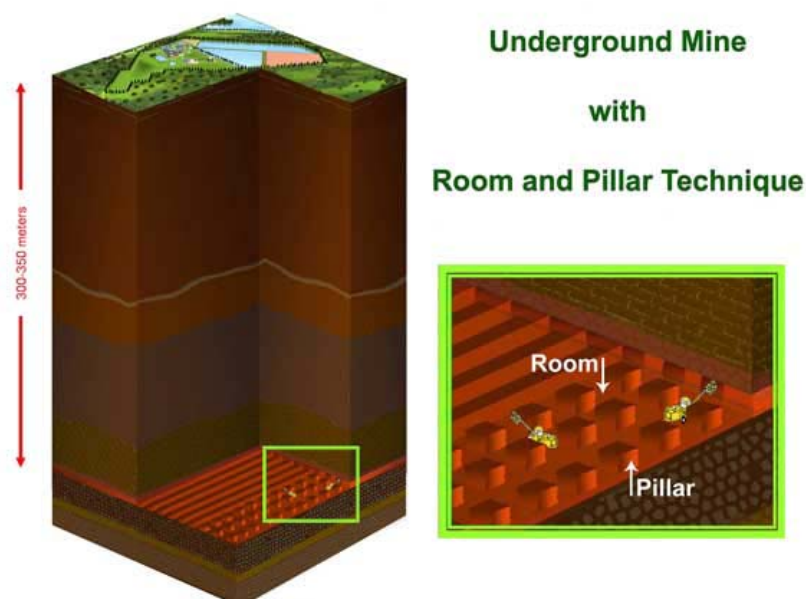


Figure 5.3: Underground mine layout of the APPC project (Udonthani Potash Mine)

### 5.1.3 Application of backfill in potash mine

Tailings, the waste of potash processing, is predominantly NaCl as salt. The tailings produced during the processing of potash ore will be pumped from the concentrator to store above the ground in a HDPE-lined containment area designed in accordance with

international best practice prior to disposal. Backfilling of tailings generated during the processing of potash ore is proposed to begin in the sixth year of operation when sufficient underground storage room for backfilling placement is already made available during the first 5 years of operation. Tailings stored in the surface tailings pile will reach the maximum amount of approximately 10 million tonnes in the ninth year, after which tailings will be transported underground for backfilling. It is designed such that after 22 years of operation, no tailings will remain on the surface.

According to by-product of the Electricity Generating Authority of Thailand (EGAT) statistics, 3 Million tons of fly ash, 0.7 Million tons of bottom ash and 1.5 Million tons of FGD-Gypsum have been produced in 2006. There is 200,000 tons of synthetic anhydrite by product from the chemical industry in 2006. For this study, the backfill system selected must be capable of potash backfilling mined voids at a rate that will not interrupt the mining schedule. All of the backfill materials being used to backfill as part of a stabilization in underground potash mines depend on cost of transportation. This will have the added benefit of minimizing subsidence, enhances the stability of the mine and environmental considerations.

## **5.2 Application of Backfill in coalfield fires and underground coal mines in China**

Coal fires are known from different coalfields worldwide. China, India, USA, Australia, Indonesia and South Africa are the main countries affected by coal fires. Normally, the mineworkers and the people living in the surrounding area are affected by large amounts of aerosols and toxic gases, like carbon monoxide or sulphur oxides. But also greenhouse relevant gasses are being released in large amounts and affect the environment. Additional hazards include land-subsidence, contamination of drinking water and damage of flora and fauna around the fires. Protecting the economically valuable coal resources and the environment is of great relevance on a national and international level (Li Jing et al, 2005).

Enormous resources of coal are present in China. Coal is one of the most important contributors to the development of the national economy. China is the largest exporter of coal in the world. However, many coal mines in China are seriously endangered by

coal fire. These fires occur within a region that stretches over 5,000 km east to west and 750 km north to south (Fig. 5.4). About 100-200 million tons of coal is being lost because of coal fires each year. The main regions in China effected by coalfield fires are: Xinjiang, Gansu, Qinghai, Ningxia, Shaanxi, Shanxi, Wuda Inner Mongolia, Sichuan, Chongqing and Fujian.

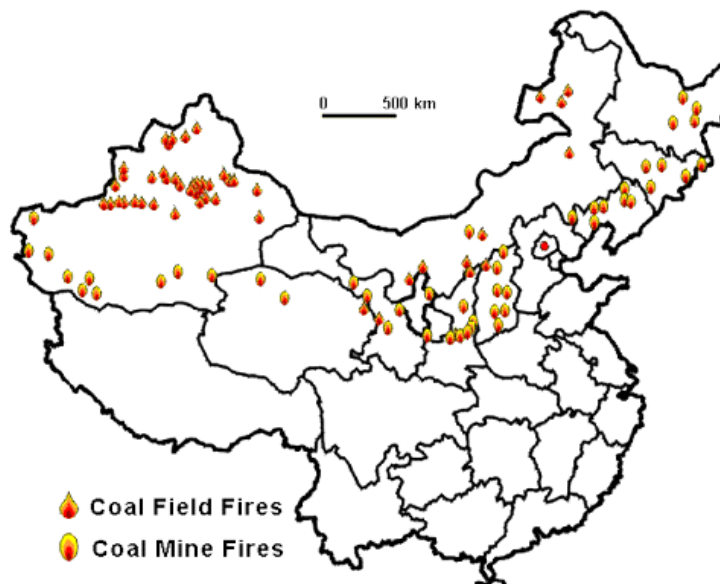


Figure 5.4: Localization of coal fires in China (Jing, 2005)

The Wuda Inner Mongolia coalfield is located NE of the Helan Mountain range in a desert-like environment with elevations ranging between 1,100 and 1,300 m msl (Fig. 5.4). The coal layers of the Wuda coalfield belong to the Upper Carboniferous and Lower Permian Taiyuan and Shanxi Formation. The coal bearing strata was deposited in marine near coastal swamps. 24 coal seams with a thickness of 0.2 m to 6m are exposed in a 10 km long and 4 km wide N-S striking syncline. The coal quality is in the range of medium volatile bituminous coal. The surface of the Wuda coalfield is strongly mined and mainly covered by sandstone's or loose sand. Coal fires affect an area of 280,000 m<sup>2</sup>. Most coal fires occur underground and can be related to small-scale mining operations. These fires is thermally intensive and cause numerous sinkholes, large-scale subsidence, air pollution, global warming, loss of mining productivity and increasing safety risk. Currently there are 3 underground coal mines in Wuda (Huang Baici, Su Haitu and Wu Hushan).

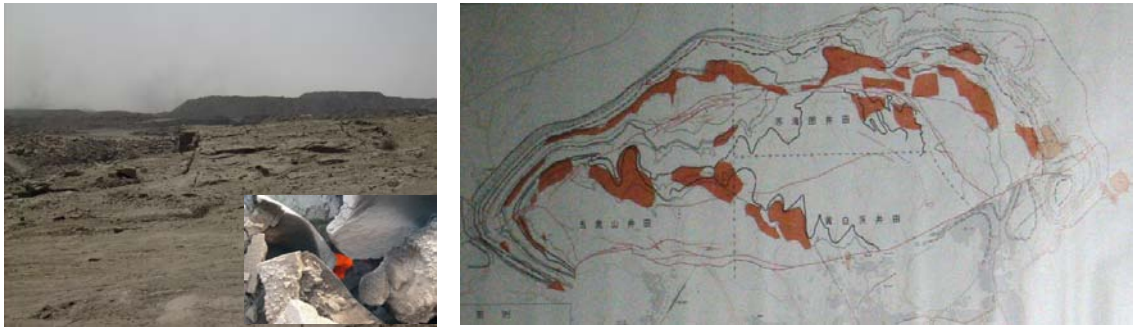


Figure 5.5: Localization of coal fires in Wuda Inner Mongolia

The Wuda has been selected as a possible test area for paste backfill. The traditional methods, executed by fire fighting teams, by covering the coalfire areas with soil, blasting burning coal outcrops and injecting water in the subsurface fire pockets are continuously improved and extended. Initiatives to introduce modern techniques, such as backfill placement at fracture and borehole (Fig. 5.7-5.8), to cool down the burning coal and cut off the air supply.

The boreholes of 12 m. deep and 98 mm. in diameter were drilled from the surface at coal fires zone and then measured the temperature inside (Fig. 5.6). Borehole coordinates were measured by a GPS positioning devices the coordinates of which are shown in table 5.1. The results of temperature measurements in borehole shown in table 5.2.



Figure 5.6: The borehole site

Table 5.1: Borehole coordinates

Borehole	Latitude	Longitude	Elevation (m)
BH-1	39° 31' 19''	106° 37' 50''	1,234

Table 5.2: Results of temperature measurements in borehole

Depth (m)	Temperature (° C) before paste backfill placement	Temperature (° C) after paste backfill placement
0	95	70.4
2	110.8	89.8
4	136.3	110.2
6	143.6	130.4
8	139.1	121.6
10	99.1	90.5

Source of backfill materials were from local mine and power plant. The mixtures of backfill are mixed at the mixing area to be used to fight the coal fire. The paste backfill was placed to underground openings through fracture and boreholes and distributed around the source of the coal fire (Fig. 5.7-5.8 ). The basic behavior of coal fires depends on the transport and supply of oxygen in the subsurface and therefore mainly on the permeability, thermal conductivity and specific heat capacity of the material. Because of this, systematic experiments, carried out in the laboratory on backfill samples, yield the functional dependency of these parameters on the salt content of the material. The experiments have shown that if backfill mixture of cement, fly ash and water or mixture of cement, fly ash and salt water are placed into high temperature zones of burning coal or even used for rewetting an oxygen isolating sand cover, water will evaporate and the salt will crystallize. Besides the cooling effect, the pores of the permeable rock will be partially closed by salt crystals (Fig. 3.34). The resulting lower permeability will prevent further oxygen transport. Besides that, the salt significantly increases the thermal conductivity in the mostly fractured rock/coal and heat flow is enhanced. The results clearly demonstrate the advantage of salt water over freshwater injections for fire fighting.



Figure 5.7: Paste backfill placement in fracture



Figure 5.8: Paste backfill placement in borehole

## Chapter 6

### Conclusions and Recommendations for Further Research

#### 6.1 Conclusions

Backfill is an increasingly important component of underground mining operations. As mines get deeper, the need for improved ground control and maximised resource recovery is essential to their safe and economic operation. The new method has a wide range of backfill materials used in systematic selection of backfill, including development mullock, total mill tailings, mine wastes, binders such as portland cement, gypsum and pozzolans (e.g. power station fly ash or FGD-gypsum) and chemical additives. Water is required for transport of hydraulic materials, hydration of binders and for dust control in dry systems. The total management of waste materials at the mine site needs to be engineered into the design of the mine. Increasingly, environmental considerations are showing that improved waste management procedures have benefits to the mining operations. Regulators are increasingly requiring the prior planning of final site restoration as part of the initial mine plan. The choice of a system often depends on the cost and availability of the necessary constituents at the particular site. The selection of a backfill system involves a cost/benefit analysis of those systems that meet the basic technical and operational requirements. Some systems can usually be eliminated because the materials required are not available locally, or because they are not applicable to the particular mining methods being considered. In some instances, environmental considerations may significantly narrow the range of options. There are usually several systems and/or variations that are capable of satisfying the operational and geotechnical requirements for safe and efficient extraction of the orebody. These are then short listed by considering specific local conditions such as projected mine life, production rate, treatment plant location, availability of waste rock, aspect ratio and any other constraints. Those systems that remain are then subjected to a detailed comparison in which technical, operational, environmental and economic aspects are assessed and ranked. The testwork may be required to confirm the suitability of available materials for a particular system. In summary, the systematic selection of backfill materials from by-products, mine wastes and tailings from the mineral processing of mining industry and other industries was suited as a backfill material for underground mines.



## **6.2 Recommendations for further research**

### **6.2.1 Chemical effect in backfill**

Backfill derived from tailings, mine industry and other industries that have been processed contain toxic chemicals. It may pose a pollution potential as a result of leaching. However, this can be rectified by disposal below the water table, where the backfill will eventually become saturated. Permanent saturation of the refuse reduces or eliminates the oxidation that might produce acid mine drainage. On the other hand, saturated backfill may not have the desired strength and stiffness for ground control requirements, so incorporating cementing admixtures into the mine waste may be a more appropriate solution to the pollution problem.

### **6.2.2 Backfill transportation**

For backfill transportation design is required to ensure a full line which reduces hammer and wear, in turn reducing the risk of plugging the line. For surface disposal, the transportation issues are more straightforward, normally related to finding a pump that can provide the necessary driving force with the required availability to operate 24 hours a day. Positive displacement pumps can provide the necessary pressure and capacity. The pressure gradient for pipeline transportation of paste backfill is much higher than the gradient for dilute slurries. Much more pumping energy is therefore required to deliver the backfill from the mineral processing plant to the tailings deposit. As discussed above, additives have the potential to reduce friction losses. Experience gained to date has been inconclusive but this may be because commercially available plasticisers were developed for concrete pumping and act on the cement fines. For paste backfill, cement content is minimal and for the surface disposal of backfill, there is unlikely to be any cement.

### **6.2.3 Environmental effect of acid generating tailings**

Of all potential advantages, associated with disposal of mine waste, acid-generating tailings and by product from industry in backfill form, the environmental effects are amongst the most promising. As regulatory and societal demands on the mining industry continue to increase, use of backfill technology may provide an avenue for

minimizing or even eliminating various environmental issues. The environmental effects of disposal of acid generating tailings in backfill form are several. First, very little free water is available for generation of a leachate, thereby reducing potential impacts on receiving waters and biological receptors. In addition, the permeability of a poorly-sorted, run-of-mill backfill is significantly lower than that of classified, well-sorted tailings. This limits infiltration of rainfall and snowmelt, which also results in a reduction of the seepage volume. When placed underground, the backfill may represent a hydraulic barrier to groundwater flow, thereby limiting interaction between backfill and groundwater. Second, the higher degree of saturation within the backfill retards the ingress of oxygen, which reduces the potential for generation of acid mine drainage (AMD). Third, the backfill production technology allows for production of an engineered material by modifying the backfill geochemistry in such a manner that environmental benefits result. Fourth, co-disposal of other waste materials with backfill is made feasible by the backfill production technology. In particular, encapsulation of acid generating tailings in appropriately-designed backfill may provide significant benefits in terms of environmental control and waste management.

#### **6.2.4 Other backfill materials in underground mines**

The implementation of backfill technology in underground mining operations must take into account the physical and chemical stability of the backfill mixture sent underground, which may vary with time. There are great advantages associated with the correct and successful use of other materials from mining industry or commercial industry in backfill operations. In recent years, mining has been hit hard economically by environmental regulations and concerns. It is the common belief that finding solutions for environmental problems associated with mine waste disposal is highly cost intensive. In addition, backfill technology holds promise in altering the public perception of mining wastes and the mining industry in general. Comprehensive geochemical characterization of backfill is crucial to evaluation of paste designs and disposal alternatives. Especially, the use of large-scale field cells is proving to be of great value in determining and predicting the long-term environmental stability of paste. When choosing a particular waste material for a backfilling system, one should examine the material's long term mechanical properties and expected behaviour following placement. This will allow an assessment of the backfill's ability to act as a ground

support material. Important properties for the in situ backfill are strength, deformability, ability to dissipate pore pressure, primary and secondary consolidation characteristics, and slake durability. An analysis of these properties will help to determine if the design objectives of the backfill will be met.

## References

1. Amaratunga, L. M., 1995, Cold-bond agglomeration of reactive pyrrhotite tailings for backfill using low cost binders: gypsum  $\beta$ -hemihydrate and cement, *Minerals Engineering*, Vol. 8. No. 12, pp. 1455-1465.
2. Amaratunga, L.M. and Yaschyshyn, D.N., 1997, Development of a high modulus paste fill using fine gold mill tailings, *Geotechnical and Geological Engineering*, Vol. 15, No. 3, September, 1997, pp. 205-219.
3. Archibald, J.F. and Nantel, J.H., 1986, Frozen fill for underground support, *CIM Bulletin*, 1986, Vol. 79, No. 885, pp. 45-49.
4. Aref, K., Hassani, F.P., Churcher, D., 1989, A study on liquefaction potential of paste backfill, *Proceedings of 4<sup>th</sup> international symposium on mining with backfill*, *Innovations in mining technology*, Montreal 2-5 October, 1989, pp. 405-414.
5. Arioglu, E., 1983, Engineering properties of cemented aggregate fill mixes for Uludag Tungsten Mine of Turkey, *Proceedings of the 1<sup>st</sup> International Symposium on Mining with Backfill*, Lulea (Sweden), A.A. Balkema (Rotterdam), 7-9 June 1983, pp. 3-9.
6. Askew, J E, McCarthy, P L and Fitzgerald, D J, 1978, Backfill Research for Pillar Extraction at ZC/NBHC, *Mining with Backfill*, 12<sup>th</sup> Canadian Rock Mechanics Symposium, Sudbury, Ontario, May, *CIM Special Volume*, pp. 1-12.
7. ASTM, 1986, Standard Specifications for Blended Hydraulic Cements, ASTM C 595-86, American Society for Testing and Materials, Philadelphia, Pennsylvania, revised 1986.
8. Baldwin, G. and Grice A.G., 2000, Engineering the New Olympic Dam Backfill System, in *Proceedings Massmin 2000*, pp 705-711 (The Australasian Institute of Mining and Metallurgy: Melbourne). Reprinted with permission of The Australasian Institute of Mining and Metallurgy.
9. Bandt, G., Posnatzki, B. and Beckers, K-A., 2003, Final Disposal of Radioactive Waste in Germany :Plan Approval Process of Konrad Mine and Acceptance Requirements, *Proceedings of the WM'03 Conference*, February 23-27, 2003, Tucson, AZ, USA.

10. Barret, J., 2000, Paste fill development in Australia-Lessons and Surprises, Australian Centre for Geomechanics, Paste Technology 2000 Seminar. Perth, Australia, 13-14 April, 2000.
11. Beddoes, R.J., Roulston, B.V. and Streisel, J., 1989, Field monitoring of salt tailings used as backfill in cut-and-fill potash mining, *Innovations in Mining Backfill Technology*, Proceedings of the 4<sup>th</sup> International Symposium on Mining with Backfill, Montreal:Balkema, pp. 343-348.
12. Belem, T. and Benzaazoua, M., 2008, Design and Application of Underground Mine Paste Backfill Technology, *Geotechnical and Geological Engineering*, Vol. 26, No. 2 ,April, 2008, pp. 147-174.
13. Bell, F.G., Donnelly, L.J., Genske, D.D. and Ojeda, J., 2005, Unusual cases of mining subsidence from Great Britain, Germany and Colombia, *International Journal of Environmental Geology*, Vol. 47, pp. 620–631.
14. Benzaazoua, M., Belem, T. and Bussiere, B., 2002, Chemical factors that influence the performance of mine sulphidic paste backfill, *Cement Concrete Res* 32:1133–1144.
15. Benzaazoua, M., Fall, M. and Belem, T., 2004, A contribution to understanding the hardening process of cemented pastefill, *Minerals Engineering* 17, pp. 141–152.
16. Benzaazoua, M., Fiset, J.F., Bussiere, B., Villeneuve, M. and Plante, B., 2005, Sludge recycling within cemented paste backfill: Study of the mechanical and leachability properties, *Minerals Engineering* 17, pp. 141–152.
17. Benzaazoua, M., Marion, P., Picquet, I. and Bussiere, B., 2004, The use of pastefill as a solidification and stabilization process for the control of acid mine drainage, *Minerals Engineering* 17, pp. 233–243.
18. Benzaazoua, M., Ouellet, J., Sevant, S., Newman, P. and Verburg, R., 1999, Cementitious backfill with high sulfur content physical, chemical, and mineralogical characterization, *Cement Concrete Res* 29:719–725.
19. Berry, P., 1981, Geomechanical investigations for the design of cemented fill, *Proceedings of the of Application of Rock Mechanics to Cut and Fill Mining*, Lulea (Sweden), Institution of Mining and Metallurgy, London, pp. 79-92.

20. Bharatkumar, B.H., Raghuprasad, B.K., Ramachandramurthy, D.S., Narayanan, R. and Gopalakrishnan, S., 2005, Effect of fly ash and slag on the fracture characteristics of high performance concrete, *Materials and Structures*, Vol.38. pp. 63-72.
21. Biurrun, E., and Hartje, B., License for the Konrad Deep Geological Repository, 2003, Proceedings of the WM'03 Conference, February 23-27, Tucson, AZ, USA.
22. Bloss, M.L. and Greenwood, A.G., 1998, Cemented rock fill research at Mount Isa Mines Limited 1992-1997, *Minefill 1998: Proceedings of the 6<sup>th</sup> International Symposium on Mining with Backfill*, Brisbane (Australia), M. Bloss Ed., Australian IMM (Brisbane), 14-16 April, pp. 207-215.
23. Bodenstein, J., Rauche, A.M.H., Schreiner, W. and Eulenberger, K. H., 2001, Reduction of surface subsidence and brine inflow prevention in potash mines by subsequent backfilling, Proceedings of the 8<sup>th</sup> International Conference on Tailings and Mine Waste' 01, Fort Collin, Colorado, USA, 16-19 January, pp. 171-176
24. Bollingerfehr, W., Bechthold, W. and Rothfuchs, T., 2004, The BAMBUS Project in the Asse Mine (Germany) Full Scale Testing of the Direct Disposal of Spent Fuel Elements in Salt Formations, Proceedings of the WM'04 Conference, February 29 - March 4, Tucson, AZ. USA.
25. Brackebusch, F.W., 1994, Basics of paste backfill systems, mining engineering. *Mining Engineering Journal* 46(10):1175–1178.
26. Brechtel, C. E., Hardy, M.P., Baz-Dresch, J. and Knowlson, J.S., 1989, Application of High-Strength Backfill at the Cannon Mine, *Innovations in Mining Backfill Technology: Proceedings of the 4<sup>th</sup> International Symposium on Mining with Backfill*, ed. by F. P. Hassani, M. J. Scobie, and T. R. Yu (Montreal, PQ, Oct. 2-5, 1989). Balkema, pp. 105-117.
27. Brennecke, P. and Schrimpf, C., 2004, Disposal of Waste in Mines – An Introduction to Morsleben, Proceedings DisTec, Disposal Technologies and Concepts, International Conference on Radioactive Waste Disposal, 26-28 April, Berlin, pp. 278 - 290.

28. Chan, H.T., Johnston, H.M., Konecny, L., Hooton, R.D. and Dayal, R., 1989, Use of Flue-Gas Desulphurization By-product for Stabilizing Hydraulic mine Backfill, *Innovations in Mining Backfill Technology*, Hassani et al (editors), Balkema, Rotterdam, pp. 63-69.
29. Chen, L.J., Millette, D.G. and Annor, A., 1999, A new development in paste backfill technology, *Tailings and Mine waste'99*, Rotterdam, pp. 159-167.
30. Contini, B., Iabichino, G., Mancini, R. and Pelizza, S., 1983, A study on the possible uses of waste calcium sulphate from chemical industry as a mine fill material, *Proceedings of the 1<sup>st</sup> International Symposium on Mining with Backfill*, Lulea (Sweden), A.A. Balkema (Rotterdam), 7-9 June, pp. 9-20.
31. Cowling, R., 1998, 25 Years of Mine Filling: Development and Directions, *Minefill 1998: Proceedings of the 6<sup>th</sup> International Symposium on Mining with Backfill*, Brisbane (Australia), M. Bloss Ed., Australian IMM (Brisbane), 14-16 April, pp. 3-10.
32. Craig, R.F., 1995. *Soil mechanics*. Fifth Edition, Chapman and Hill Publishing, London, 427 p.
33. Crandall, W.E., 1992, *Backfilling Methods*, SME Mining Engineering Handbook, 2<sup>nd</sup> edition, Vol. 2, pp. 1769-1772.
34. Crosby, K. S., 2005, Overview of the Geology and Resources of the APPC Udon Potash (Sylvinite) Deposits, Udon Thani Province, Thailand, *International Conference on Geology, Geotechnology and Mineral Resources of Indochina (GEOINDO 2005)*, 28-30 November, Khon Kaen, Thailand, pp. 283-299.
35. De Souza, E., 1995, Backfill in potash mines - transportation and geotechnical issues. *Mine Planning and Equipment Selection. Proceedings of the 4<sup>th</sup> International Symposium*. Calgary:Balkema, pp. 857-863.
36. Dorricott, M.G. and Grice, A.G., 2000, Impact of Stop Geometry on Backfill Systems for Bulk Mining, in *Proceedings Massmin 2000*, pp. 705-711, (The Australasian Institute of Mining and Metallurgy: Melbourne). Reprinted with permission of The Australasian Institute of Mining and Metallurgy.
37. Dorricott, M.G. and Grice, A.G., 2002, Backfill – The Environmentally Friendly Tailings Disposal System, in *Proceedings Green Processing 2002*, (The

- Australasian Institute of Mining and Metallurgy: Melbourne). Reprinted with permission of The Australasian Institute of Mining and Metallurgy, pp. 265-270.
38. Douglas, E. and V.M. Malhotra, 1987, A Review of the Properties and Strength Development of Non-ferrous Slag - Portland Cement Binders, Supplementary Cementing Materials for Concrete, V.M. Malhotra (editor) CANMET, SP 86-8E, Chapter 7, pp. 371-428.
  39. Eilers, G., Mauke, R., Gläß, F., Preuss, J., Fischle, W., Linn, M., Schmidt, H., Müller-Hoepe, N. and Schrimpf, C., 2003, Sealing of the Morsleben Repository, Germany, Proceedings of the WM'03 Conference, February 23-27, Tucson, AZ, USA.
  40. Emery, J., 1992, Mineral Aggregate Conservation-Reuse and Recycling, John Emery Geotechnical Engineering Ltd, Aggregate and Petroleum Resource Section, 68 p.
  41. Fall, M. and Benzaazoua, M., 2005, Modeling the effect of sulphate on strength development of paste backfill and binder mixture optimization, Cement and Concrete Research 35, pp. 301–314.
  42. Fall, M., Belem, T., Samb, S. and Benzaazoua, M., 2007, Experimental characterization of the stress–strain behaviour of cemented paste backfill in compression, Journal of Materials Science, Vol. 42, No. 11 / June, pp. 3914-3922.
  43. Fall, M., Benzaazoua, M. and Ouellet, S., 2004, Effect of tailings properties on paste backfill performance, Minefill 2004: Proceedings of the 8<sup>th</sup> International Symposium on Mining with Backfill, 19-21 September, Beijing, China, pp.193-202.
  44. Fall, M., Benzaazoua, M., and Ouellet, S., 2005, Experimental characterization of the influence of tailings fineness and density on the quality of cemented paste backfill, Minerals Engineering 18, pp. 41–44.
  45. Farmer, I.W., “Room and Pillar Mining,” SME Mining Engineering Handbook, 2nd Edition, Port City Press, Baltimore, 1992, pp. 1681-1703.
  46. Federal Environmental Ministry, New Rules for Underground Waste Disposal, The Ordinance on Underground Waste Stowage entered into force on 30 October 2002.



47. Federal Environment Agency, Background paper on permanent storage in salt mines, 29 July 2004, Berlin, Germany.
48. Finn, D. And Dorricott M.G., 2002, Cemented Rockfill For Extraction of High Grade Crown Pillars at Crusader Gold Mine, in Proceedings 8<sup>th</sup> AusIMM Underground Operators' Conference. Townsville July 2002, Reprinted with permission of The Australasian Institute of Mining and Metallurgy, pp. 177-180.
49. Gerhardt, H., 1983, Some aspects of using cemented filling in the ore mining of the GDR, Proceedings of the 1<sup>st</sup> International Symposium on Mining with Backfill, Lulea (Sweden), A.A. Balkema (Rotterdam), 7-9 June, pp. 133-140.
50. Golosinski, T.S., Wang, C. and Ganeswaran, R., 1999, Studies of high water and quick setting (HWQS) cementitious mine backfill, Mining Science and Technology'99, Rotterdam, pp. 579-584.
51. Gray, T.A., Kyper, T.N. and Snodgrass, J.L., 1997, Disposal of coal combustion byproducts in underground coal mines, *Energieia*, Vol. 8, No. 6, pp. 4-6.
52. Grice, A.G., 1987, Secrets of the Open Stope – A Study of the Fill Process *minmag*, Vol. 1, pp. 14-16. Ed Jan Patterson.
53. Grice, A.G., 1989, Fill research at Mount Isa Mines Limited, *Innovations in Mining Backfill Technology: Proceedings of the 4<sup>th</sup> International Symposium on Mining with Backfill*, ed. by F. P. Hassani, M. J. Scobie, and T. R. Yu (Montreal, PQ, Oct. 2-5, 1989). Balkema, pp. 15-22.
54. Grice, A.G., 1998, Stability of Hydraulic Backfill Barricades, *Minefill 1998: Proceedings of the 6<sup>th</sup> International Symposium on Mining with Backfill*, Brisbane (Australia), M. Bloss Ed., Australian IMM (Brisbane), 14-16 April, pp. 117-120.
55. Grice, A.G., 1998, Underground Mining with Backfill, *The Proceedings of 2<sup>nd</sup> Annual Summit, Mine Tailings Disposal Systems*, Brisbane, Australia, Australasian Institute of Mining and Metallurgy, Carlton South, Australia, p. 14.
56. Grice, A.G., 2001, Recent Minefill Developments in Australia, *Proceedings of the 7<sup>th</sup> international symposium on mining with backfill*, Seattle, Washington, pp. 351-358.

57. Grice, A.G., Finn, T. and Smith P.A., 1999, Innovative use of backfill to enable continuous longwall mining through old headings at Homestead Colliery - Wambo Mining, Adapted for the Australian Coal Review, October.
58. Hassani, F. and Quellet, J., 2005, Sustainability and development of paste fill technology "Mining and Sustainable Development" 20<sup>th</sup> World Mining Congress & Expo 2005, 7 – 11 November, Tehran, Iran, pp. 33-42.
59. Hassani, F., Razavi, S.M. and Isagon, I., 2007, Effect of Sodium Silicate on Physical and Mechanical Behavior of Mine Backfill, Mine Planning and Equipment Selection. Proceedings of the 16<sup>th</sup> International Symposium. Bangkok, Thailand, pp. 339-409.
60. Henderson, A., Jardine, G. and Woodall, C., 1998, The Implementation of Paste Fill at The Henty Gold Mine, Minefill 1998: Proceedings of the 6<sup>th</sup> International Symposium on Mining with Backfill, Brisbane (Australia), M. Bloss Ed., Australian IMM (Brisbane), 14-16 April, pp. 229-304.
61. Herget, G. and Munroe, S.R., 1989, Utilization of salt tailings backfill at Denison- Potacan Potash Company'. Innovations in Mining Backfill Technology, Proceedings of the 4<sup>th</sup> International Symposium on Mining with Backfill. Montreal: Balkema, pp. 335-342.
62. Herget, G. and de Korompay, V., 1978, In-situ drainage properties of hydraulic backfills. Canadian Rock Mechanics Symp., Proc. 12th Mining with Backfill, Sudbury, Ontario, 23-25 May, CIM Special Volume 19, pp.117-123.
63. Hussmann, J. und Klee, H., 2000, Versatz im Steinkohlenbergbau, GDMB-Schriftenreihe, Heft 90 „Stand der Abfallverwertung im Bergbau unter Tage” s. 49-56.
64. Hustrulid, W., Qianyuan, Y. and Krauland, N., 1989, Modeling of cut-and-fill mining systems – Näsliden revisited. Innovation in Mining Backfill Technology, F.P. Hassani, M.J. Scoble, and T.R. Yu (eds.). Balkema, Rotterdam, pp. 147-164.
65. Jain, M.K. and Sastry, B.S., 2003, Properties of some Indian fly ash relating to mine fill applications, National Seminar on Status of Environmental Management in Mining Industry, India, pp. 305-313.

66. Japakasetr, T., 1985, Review on rock salt and potash exploration in Northeast of Thailand, Conference on Geology and Mineral Resources Development of the Northeast, Thailand, Khon Kaen University, Khon Kaen, 26-29 November.
67. Japakasetr, T., and Jarnyaharn, P., 1992, Thailand's mineral potential and investment opportunity, in Piancharoen, C., ed., Proceedings of a National Conference on Geologic Resource of Thailand: Potential for Future Development, DMR, Bangkok, pp. 641-652.
68. Jing, L., Voight, S., Kunzer, C., Bol, Y., Jianzhong, Z., Yianmin, Z., Bing, K. and Songmeil, Z., 2005, The Progress in Detecting of Coal Fire on Remote Sensing, The First Result of The Joint SINO-German Research Project on Innovative Technologies for Exploration, Extinction and Monitoring of Coal Fires in North China, Proc. 2005 Dragon Symposium "Mid-Term Results", Santorini, Greece 27 June – 1 July, 7 p.
69. Kamp, N., 1989, Backfilling on gold mines of the Gold Fields group, Proceedings of the 4<sup>th</sup> International Symposium on Mining with Backfill, Montreal, Canada, pp. 39-52.
70. Kaskiw, L.M., Morgan, R.M. and Ruse, D.C., 1989, Backfilling at IMC Canada K-2 potash mine'. Innovations in Mining Backfill Technology. Proceedings of the 4<sup>th</sup> International Symposium on Mining with Backfill. Montreal:Balkema, pp. 315-325.
71. Keren, L. and Kainian, S., 1983, Influence of tailings particles on physical and mechanical properties of fill, Proceedings of the 1<sup>st</sup> international symposium on mining with backfill, Lulea 7-9 June, pp. 21-30.
72. Kesimal, A., Yilmaz, E. and Ercikdi, B., 2004, Evaluation of paste backfill mixtures consisting of sulphide-rich mill tailings and varying cement contents, Cement and Concrete Research, Vol. 34, pp. 1817–1822.
73. Kind, H.J., 1991, Die Untertagedeponie Herfa-Neurode, Glückauf, 127:922-926.
74. Knissel, W. and Helms, W., 1983, Strength of cemented rockfill from washery refuse- Results from laboratory investigations, Proceedings of the 1<sup>st</sup> International Symposium on Mining with Backfill, Lulea (Sweden), A.A. Balkema (Rotterdam), 7-9 June, pp. 31-38.

75. Knissel, W., 1999, Entsorgungsbergbau in Deutschland, ERZMETAL 52, s. 666-672.
76. Komine, H., 2004, Simplified evaluation on hydraulic conductivities of sand-bentonite mixture backfill, Applied Clay Science 26, pp. 13– 19.
77. Koskela, V. A., 1983, Consolidated Backfilling at Outokumpu Oy's Vihanti, Keretti and Vammala Mines, Proceedings of the First International Symposium on Mining with Backfill, Lulea (Sweden), A.A. Balkema (Rotterdam), 7-9 June, pp. 151-160.
78. Kratzsch, H., 1983, Mining Subsidence Engineering, Springer-Verlag New York, 543 p.
79. Kuenzer, C., 2007, Uncontrolled coal fires and their environmental impacts: Investigating two arid mining regions in north-central China, Applied Geography, Vol. 27, pp. 42–62.
80. Kuganathan, K. and Sheppard, I.A., 2001, A non-segregating “Rocky Pastefill” (RPF) produced by co-disposal of cemented de-slimed tailings slurry and graded rockfill, Minefill 2001: Proceedings of the 7<sup>th</sup> International Symposium on Mining with Backfill, D. Stone Ed., Society for Mining, Metallurgy and Exploration (SME), pp. 27-41.
81. Kwong, J., 2004, Chemical stability of two tailings backfill materials with two types of binder, Minefill 2004: Proceedings of the 8<sup>th</sup> International Symposium on Mining with Backfill, 19-21 September, Beijing, China, pp.219-223.
82. Lamos, A.W. and Clark, I.H., 1989, The Influence of Material Composition and Sample Geometry on the Strength of Cemented Backfill, Innovations in Mining Backfill Technology: Proceedings of the 4<sup>th</sup> International Symposium on Mining with Backfill, ed. by F. P. Hassani, M. J. Scobie, and T. R. Yu (Montreal, PQ, Oct. 2-5, Balkema, pp. 89-94.
83. Lempert, J.P., 1999, Geological disposal of radioactive waste the basis of the German waste management concept, International Congress ‘Mining for Torrow’s World’ Düsseldorf, Germany, June 8-10, pp. 243-246.
84. Lidkea, W. and Landriault, D., 1993, Tests on pastefill at INCO, Minefill 1993: Proceedings of the 5<sup>th</sup> International Symposium on Mining with Backfill,

- Johannesburg (South Africa), H.W. Glen Ed., South African IMM (Johannesburg), September, pp. 337-347.
85. Lindloff, U., 1999, High density slurry stowage in potash mines, International Congress 'Mining for Tomorrow's World' Düsseldorf, Germany, June 8-10, pp. 239-242.
86. Lux, K.H., 2000, Langzeitsicherheit im Salinar, GDMB-Schriftenreihe, Heft 90 „Stand der Abfallverwertung im Bergbau unter Tage“ s. 73-108.
87. Manca, P.P., G. Massacci, L. Massidda, and G. Rossi, 1983, Mill Tailings and Various Binder Mixtures for Cemented Fill: Analysis of Properties Related to Mining Problems. Proceedings of 1<sup>st</sup> the International Symposium on Mining with Backfill, Luleå, 7- 9 June, pp. 39-47.
88. Mark, R., Corrigan, R., and Cochrane, L., 1990, Internal Report INCO Ltd., Ontario Division, Third Report to Lucky Friday Mine regarding High Density Backfill, 7 p.
89. Martens, P.N. and Kaufmann, M., 1997, Backfill operation planning utilising power plant ashes to minimize mine damages, Mine Planning and Equipment Selection 1997, Balkema, Rotterdam, pp. 889-895.
90. Martens, P.N. and Laumert, G. 1993, Untertägige Entsorgung in der Bundesrepublik Deutschland. Glückauf. 129:283-290.
91. Marx, H., Lack, D. and Krauke, W., 2005, Substantial Aspects of the Recycling of Industrial Wastes as Backfilling Material in Salt Mines, "Mining and Sustainable Development" 20<sup>th</sup> World Mining Congress & Expo 2005, 7 – 11 November, Tehran, Iran, pp. 141-144.
92. Masniyom, M., 2007, Potash Mining in Thailand – Backfill Materials and Technologies Mine Planning and Equipment Selection, Proceedings of the 16<sup>th</sup> International Symposium. Bangkok, Thailand, pp. 578-598.
93. Menninger, D. und Militzer, J., 2003, Bergbau und Metallurgie im Erzgebirge, ERZMETALL 56, Nr. 9. ss. 563-565.
94. Minkley, W., Baumert, H., Mühlbauer, J. und Geißler, D., 2006, Sicherung von carnallitischen Abbaufeldern in der stillgelegten Grube Merkers, Kali und Steinsalz, Heft 2/2006, pp. 12-20.

95. Mine Subsidence. Singh, Madan M. ed. Society of Mining Engineers, Littleton, CO, 1986, AIME, pp.73-143.
96. Mischo, H., Untersuchungen an Baustoffen auf Steinsalz- Anhydrit- Basis für Dammbauwerke im Salzgebirge, TU Clausthal, Shaker Verlag, Diss. 2002.
97. Mishra, M.K. and Karanam, R.U.M., 2006, Geotechnical characterization of fly ash composites for backfilling mine voids, Geotechnical and Geological Engineering, Volume 24, Number 6 / December, pp.1749-1765.
98. Mitchell, R.J. and Smith, J.D., 1979, Mine backfill design and testing, CIM Bulletin, 72(8018), January, pp. 82-89.
99. Mohrmann, R. und Wagner, R.M., 1995, Einsatz von BFA im Bergbau, Handbuch der Verwertung von Braunkohlenfilteraschen in Deutschland, ss. 563-576.
100. Herausgeber: Bundesverband der Gipsindustrie e.V, 2003, Gips – Datenbuch, Darmstadt.
101. Nandy, S.K. and Szwilski, A.B., 1986, Disposal and utilization of mineral waste as mine backfill, Proceeding of the International Symposium on Underground Mining Methods and Technology, England, Sept. 8-13, pp. 241-252.
102. Nantel, J., 1998, Recent developments and trends in backfill practices in Canada, Minefill '98, Proceedings of the 6<sup>th</sup> International Symposium on Mining with Backfill, Brisbane:AIMM. 11-14.
103. Neindorf, L.B., 1983, Fill operating practices at Mount Isa Mines, Proceedings of the 1<sup>st</sup> International Symposium on Mining with Backfill, Lulea, Sweden, 7-9 June, pp. 179-187.
104. Nieminen, P. and Seppänen, P., 1983. The Use of Blast Furnace Slag and Other By-products as Binding Agents in Consolidated Backfilling at Outokumpu Oy's Mines. Proceedings of the 1<sup>st</sup> International Symposium on Mining with Backfill, Luleå, 7-9 June, pp. 49-59.
105. Norm DIN 1045 April 1997, Beton und Stahlbeton - Bemessung und Ausführung, (Zurückziehungsdatum 07.2001).
106. Norm DIN 1048-1 Juni 1991, Prüfverfahren für Beton - Teil 1: Frischbeton.

107. Norm DIN 18121 – 2 – Wassergehalt, Baugrund, Untersuchung von Bodenproben - Teil 2: Bestimmung durch Schnellverfahren, August 2001.
108. Norm DIN 18121-1 April 1998, Wassergehalt, Baugrund, Untersuchung von Bodenproben - Teil 1: Bestimmung durch Ofentrocknung.
109. Norm DIN 4208: 1997-04, Anhydritbinder, Deutsches Institut für Normung Taschenbuch 33, pp. 106-111.
110. Norm DIN 4208: April 1997, Anhydritbinder, (Zurückziehungsdatum 01. 2005).
111. Norm DIN 4226-3: April 1983, Zuschlag für Beton - Teil 3: Prüfung von Zuschlag mit dichtem oder porigem Gefüge.
112. Norm DIN 52450 – Bestimmung des Schwindens und Quellens an kleinen Probekörpern – Prüfung anorganischer nichtmetallischer Baustoffe, August 1985.
113. Norm DIN 66137-2 Dezember 2004, Bestimmung der Dichte fester Stoffe - Teil 2: Gaspyknometrie.
114. Norm DIN EN 1097-3 Juni 1998, Prüfverfahren für mechanische und physikalische Eigenschaften von Gesteinkörnungen - Teil 3: Bestimmung von Schüttdichte und Hohlraumgehalt; Deutsche Fassung EN 1097-3.
115. Norm DIN EN 12390-5 Februar 2001, Prüfung von Festbeton - Teil 5: Biegezugfestigkeit von Prüfkörpern; Deutsche Fassung EN 12390-5: 2000.
116. Norm DIN EN 12390-6 Februar 2001, Prüfung von Beton - Teil 6: Spaltzugfestigkeit von Prüfkörpern; Deutsche Fassung EN 12390-6: 2000.
117. Norm DIN EN 14227-14 Februar 2004, Ungebundene und hydraulisch gebundene Gemische – Anforderungen - Teil 14: Bodenverbesserungen mit Flugasche; Deutsche Fassung EN 14227-14: 2003.
118. Norm DIN EN 196-1 Mai 2005, Prüfverfahren für Zement - Teil 1: Bestimmung der Festigkeit; Deutsche Fassung EN 196-1: 2005.
119. Norm DIN EN 196-3 Mai 2005, Prüfverfahren für Zement - Teil 3: Bestimmung der Erstarrungszeiten und der Raumbeständigkeit; Deutsche Fassung EN 196-3.
120. Norm DIN EN 206-1 Juli 2001, Beton - Teil 1: Festlegung, Eigenschaften, Herstellung und Konformität, Deutsche Fassung EN 206-1: 2000.

121. Norm DIN EN 450-1 Mai 2005, Flugasche für Beton - Teil 1: Definition, Anforderungen und Konformitätskriterien; Deutsche Fassung EN 450-1: 2005.
122. Ouellet, J. and Servant, S., 1998, Numerical Simulation of the Drainage in a Mining Stope Filled with Hydraulic Backfill, Minefill 1998: Proceedings of the Sixth International Symposium on Mining with Backfill, Brisbane (Australia), M. Bloss Ed., Australian IMM (Brisbane), 14-16 April, pp 105 - 110.
123. Özarslan, A., Martens, P.N., Olbrich, T. and Röhrlich, M., 2001, Underground Disposal of Hazardous Wastes in German Mines, 17<sup>th</sup> International Mining Congress and Exhibition of Turkey- IMCET 2001, pp. 479-484.
124. Palarski J., 1994, Design of backfill as support in Polish Coal Mines, The Journal of The South African Institute of Mining and Metallurgy, Vol. 94, No.8, pp.218-226.
125. Palarski J., 2003, Underground Utilization of Waste in Poland, 19<sup>th</sup> World Mining Congress. 1-5 Nov. 2003, New Delhi, pp. 1351-1362.
126. Palarski J., 2006, Polish experience best practice in Poland – underground waste utilization. INFRA 22944 - TAIEX Workshop on EU Legislation as it affects mining; Tallin; November 30.
127. Palarski J., 2007, Waste disposal and backfill technology in underground mines, Mining and the Environment 2007, Baia Mare/Romania, 8-10 November, page 95-104.
128. Palarski, J., 1989, The experimental and practical results of applying backfill, Proceedings of the 4<sup>th</sup> International Symposium on Mining with Backfill, Montreal, Canada, pp. 33-38.
129. Palarski, J., 1993, The Use of Fly-ash, Tailings, Rock and Binding agents as Consolidated Backfill for Coal Mines, Minefill 93, SAIMM, Johannesburg 1993.
130. Paynter, J.T. and Dodd, J.C., 1997, The Design, Commissioning and Operation of the Golden Giant Paste Backfill Plant, Proceedings of the 29th annual meeting of the Canadian Mineral Processors (Division of the CIM), Ottawa, Ontario, 21-23 January, pp. 382-403.



131. Peila, D. and Pelizza, S., 1995, Civil Reuses of Underground Mine Openings: a Summary of International Experience, *Tunnelling and Underground Space Technology*, Vol. 10, No. 2, pp. 179-191.
132. Petrolito, J., Anderson, R.M. and Pigdon, S.P., 1998, The Strength of Backfills Stabilised with Calcined Gypsum, *Minefill 98*, AusIMM, April 14-16, Brisbane.
133. Pfeifer, P., Kohlhase, L. and Tischbein, U., 2001, Verbringung von Abfällen mineralischen Ursprungs mittels Spülversatztechnologie als Pflichtversatzaufgabe in der Nachbetriebsphase im Bergwerk Bleicherode: *Freiberger Forschungshefte A 855 Bergbau und Geotechnik*, 93-113.
134. Pierce, M. E., 2004, PFC3D Modeling of Inter-Particle Percolation in Caved Rock Under Draw, in *Numerical Modeling in Micromechanics Via Particle Methods- 2004*, Proceedings of the 2nd International PFC Symposium, Kyoto, Japan, October, pp. 149-156. Y. Shimizu et al., Eds. Leiden: Balkema, 2004.
135. Pierce, M. E., Cundall, P. A., Hout G. J and Lorig, L., 2002, PFC3D Modeling of Caved Rock Under Draw, in *Numerical Modeling in Micromechanics via Particle Methods*, Proceedings of the 1<sup>st</sup> International PFC Symposium, Gelsenkirchen, Germany, November, pp. 11-217. H. Konietzky, Ed. Lisse: Balkema, 2003.
136. Pierce, M., Bawden, W. and Paynter, J., 1998, Laboratory Testing and Stability Analysis of Paste Backfill at the Golden Giant Mine, *Minefill 1998: Proceedings of the Sixth International Symposium on Mining with Backfill*, Brisbane (Australia), M. Bloss Ed., Australian IMM (Brisbane), 14-16 April, pp. 159-165.
137. Potvin, Y., Thomas, E. and Fourie, A., 2005, *Handbook on Mine Fill*, Australian Centre for Geomechanics, 179 pp.
138. Preuss, A., Gruen, E., Herzog, C. and Bock, J., 2002, The use of pneumatic stowing in Germany considering subsidence aspect, 21<sup>st</sup> International conference on ground control in Mining, Morgantown, WV, USA , 2002.
139. Preuss, J., Eilers, G., Mauke, R., Müller-Hoeppe, N., Engelhardt, H-J., 2002, Kreienmeyer, M., Lerch, C. and Schrimpf, C., "Post Closure Safety of the Morsleben Repository", Proceedings of the WM'02 Conference, Feb. 24-28, Tucson , AZ., USA.

140. Raffield, M.P., James, J.V. and Pethos, S.Z., 1998, Monitoring of the performance of a crushed waste/classified tailings backfill for shaft pillar pre-extraction in the south deep section, Western Areas Gold Mine. Minefill 1998: Proceedings of the 6<sup>th</sup> International Symposium on Mining with Backfill, Brisbane (Australia), M. Bloss Ed., Australian IMM (Brisbane), 14-16 April, pp. 185-190.
141. Rankine, K. J., Sivakugan, N., Cowling, R., 2006, "Emplaced geotechnical characteristics of hydraulic fills in a number of Australian mines," *Geotechnical and Geological Engineering*, Springer, 24(1), 1-14.
142. Rankine, M.R. and Sivakugan, N., 2007, Geotechnical properties of cemented paste backfill from Cannington Mine, Australia, *Geotechnical and Geological Engineering*, Vol. 25, No. 4 / August, pp. 383-393.
143. Rauche, A.M.H., and Fulda, D., 2001, Tailings and disposal brine reduction- Design criteria for potash production in the 21<sup>st</sup> century, Proceedings of the 8<sup>th</sup> International Conference on Tailings and Mine Waste' 01, Fort Collin, Colorado, USA, 16-19 January, pp. 85-91.
144. Rohlfiing, I., 1983, Slinger belt stowing technique for cemented backfill at the Meggen mine, Proceedings of the 1<sup>st</sup> International Symposium on Mining with Backfill, Lulea (Sweden), A.A. Balkema (Rotterdam), 7-9 June, pp. 189-198.
145. Schade, H., 2000, Der Beitrag des deutschen Bergbaus zu der nach europäischem und deutschem Recht gebotenen Abfallverwertung, *ERZMETALL* 53, Nr. 3, pp. 147-158.
146. Schreck, P., 1998, Environmental impact of uncontrolled waste disposal in mining and industrial areas in Central Germany, *Environmental Geology*, Vol. 35 (1), pp. 66-72.
147. Schulz, D., 1996, Recultivation of Mining Waste Dumps in the RUHR Area, Germany, *Water, Air, & Soil Pollution Journal*, Vol. 91, Numbers 1-2 / September, pp. 89-98.
148. Senyur, G., 1989, The Time Effect on Flow Through Mine Backfill Materials, *Innovations in Mining Backfill Technology*, Proceedings of 4<sup>th</sup> International Symposium on Mining With Backfill, ed. by F. P. Hassani, M. J. Scoble, T. R. Yu (Montreal, PQ, Oct. 2-5, 1989). Balkema, pp. 415-423.

149. Sitz, P., Eulenberger, K.H., Ehrhardt, K. and Gruner, M., 2000, New materials for backfill, sealing and load-distribution for underground use, Underground Construction 2000, Krskow, 25-27 September, pp. 475-483.
150. Sivakugan, N. and Rankine, K., 2006, "A simple solution for drainage through a 2-dimensional hydraulic fill stope," Geotechnical and Geological Engineering, Springer, 24(5), 1229-1241.
151. Skeeles, B.E.J., 1998, Design of Paste Backfill Plant and Distribution System for the Cannington Project, Minefill 1998: Proceedings of the 6<sup>th</sup> International Symposium on Mining with Backfill, Brisbane (Australia), M. Bloss Ed., Australian IMM (Brisbane), 14-16 April, pp. 59-64.
152. Smith, J. D., Dejongh, C. L. and Mitchell, R. J., 1983, Large scale model tests to determine backfill strength requirements for pillar recovery at the Black Mountain Mine, Proceedings of the 1<sup>st</sup> International symposium on mining with backfill, Lulea, June 7-9. pp. 413- 423.
153. Souza, E.D., 1995, Backfill in potash mines: Transportation and geotechnical issues, Mine Planning and Equipment Selection 1995, Balkema, Rotterdam, pp. 857-863.
154. Sowers, 1951, Structures. Proc. Conf. Sponsored by Geotech. Eng. Div. Of the ASCE and the SME of AIME, held at Colorado State University, Fort Collins, Colorado.
155. Spearing, A.J.S., Millette, D. and Gay, F., 2000, The potential use of foam technology in underground backfilling and surface tailings disposal, MassMin 2000, pp. 193-197.
156. Springer, H. und Haase, R., 2000, Versatzverfahren in Kalibergbau, Bergwerk „Glückauf ” Sondershausen, GDMB-Schriftenreihe, Heft 90 „Stand der Abfallverwertung im Bergbau unter Tage” s. 65-72.
157. Städtler, G., 2000, Abfallverwertung im Kalibergbau am Beispiel der Untertageverwertung Unterbreizbach, GDMB-Schriftenreihe, Heft 90 „ Stand der Abfallverwertung im Bergbau unter Tage” s. 27-40.
158. Straskraba, V. and Abel, J.F., 1994, The differences in underground mines dewatering with the application of caving or backfilling mining methods, Mine Water and The Environment, Vol. 13, No. 2, pp. 1-20.

159. Sturm, G.L., 2006, Disposal of Mine Wastes by Backfill of Existing Mine Excavations at an Abandoned Lead Mine in Montana, the 2006 National Association of Abandoned Mine Land Programs 28<sup>th</sup> Annual Conference, September 25-27, Billings, MT.
160. Suwanich, P., 1986, Potash and Rock Salt in Thailand, Nonmetallic Mineral Bulletin No. 2, Economic Geology Division, DMR, 339 P.
161. Suwanpal, A., 1992, Potash mine: a co-operative project among ASEAN countries and private sectors, in Piancharoen, C., ed., Proceedings of a National Conference on Geologic Resource of Thailand: Potential for Future Development, DMR, Bangkok, pp. 159-164.
162. Tesarik, D. R., Seymour, J.B. and Vickery, J.D., 1989, Instrumentation and Modeling of the Cannon Mine's B-North Ore Body, Innovations in Mining Backfill Technology: Proceedings of the 4<sup>th</sup> International Symposium on Mining with Backfill, ed. by F. P. Hassani, M. J. Scobie, and T. R. Yu (Montreal, PQ, Oct. 2-5, 1989). Balkema, pp. 119-128.
163. Thein, J. und Veerhoff, M., 2000, Langzeitsicherer Versatz mit bergbaufremden Abfällen in Festgestien, GDMB-Schriftenreihe, Heft 90 „ Stand der Abfallverwertung im Bergbau unter Tage“ s. 109-130.
164. Udd, J. E., 1989, Backfill Research in Canadian Mines, Innovations in Mining Backfill Technology: Proceedings of the 4<sup>th</sup> International Symposium on Mining with Backfill, ed. by F. P. Hassani, M. J. Scobie, and T. R. Yu (Montreal, PQ, Oct. 2-5, 1989). Balkema, pp. 3-13.
165. Ultha-aroon, C., 1993, Continental origin of the Maha Sarakham evaporites, northeastern Thailand, Journal of Southeast Asian Earth Sciences, Vol. 8, No.1-4, pp. 193-203.
166. Vallieres, D. and Greiner, A., 1995, Paste Backfill Implementation at the Chimo Mine, 12th Underground Operator Conference, CIM, Timmins, Canada, February.
167. VDI 2296, 1987, Emission Control, Production of Hydrogen Fluorine, Hydrofluoric Acid and Cryolite, Germany.
168. Voss, K.H., 1983, The state of development of pneumatic stowing in the hard coal industry of the Federal Republic of Germany, Proceedings of the 1<sup>st</sup>

- International Symposium on Mining with Backfill, Lulea (Sweden), A.A. Balkema (Rotterdam), 7-9 June, pp. 281-292.
169. Wang, C. and Villaescusa, E., 2001, Factors influencing the strength of cemented aggregate fill, Minefill 2001: Proceedings of the 7<sup>th</sup> International Symposium on Mining with Backfill, Seattle (USA), D. Stone Ed., Society for Mining, Metallurgy and Exploration (SME), pp. 81-87.
170. Wegener, W., 1993, Waste disposal in a German rock salt mine, Engineering and Mining Journal, 194 (4), pp. 32-35.
171. Wendland, E. and Himmelsbach, T., 2002, Underground waste repositories in Exhausted Coal Mines-Recent Developments, Mine Water and the Environment Vol. 21, pp. 160-167.
172. Whittaker, B.N., and D.J. Reddish, 1989, Subsidence: Occurrence, prediction and control: Developments in geotechnical engineering: New York, New York, Elsevier, v. 56, 528 p.
173. Wingrove, A.C., 1993, The Tailings-Aggregate Backfilling Project at South-Deep Mine. Minefill 1993: Proceedings of the 5<sup>th</sup> International Symposium on Mining with Backfill, Johannesburg (South Africa), H.W. Glen Ed., South African IMM (Johannesburg), pp. 275-288.
174. Xiao, Z.Z., Wang, X.M. and Zhang, Q.I., 2004, Experimental study on phosphogypsum cemented backfilling in Kaijiang Phosphorite Mine, Minefill 2004: Proceedings of the 8<sup>th</sup> International Symposium on Mining with Backfill, 19-21 September, Beijing, China, pp. 128-131.
175. Yamaguchi, U. and Yamatomi, J., 1989, An Experimental Study to Investigate the Effect of Backfill for Ground Stability, Innovations in Mining Backfill Technology: Proceedings of the 4<sup>th</sup> International Symposium on Mining with Backfill, A.A. Balkema, Rotterdam, 71-80.
176. Yilmaz, E., Kesimal, A. and Ercikdi, B., 2004, Strength development of paste backfill samples at long term by using two different binder, Minefill 2004: Proceedings of the 8<sup>th</sup> International Symposium on Mining with Backfill, 19-21 September, Beijing, China, pp.281-285.

177. Youwai, S. and Bergado, D.T., 2004, Numerical analysis of reinforced wall using rubber tire chips–sand mixtures as backfill material, *Computers and Geotechnics* 31, 2004, pp. 103–114.
178. Zhang, Q.I., Wang, X.M., Gu, D.S., Xiao, Z.Z., Chen, J.S. and Tian, M.H., 2004, A Study of fly ash backfill technology in Xinqiao Pyrite Mine, *Minefill 2004: Proceedings of the 8<sup>th</sup> International Symposium on Mining with Backfill*, 19-21 September, Beijing, China, pp. 99-103.
179. Zimmels, Y., Kirzhner, F., Lux, K.H. and Zeller, T., 2006, Underground disposal of hazardous waste in Israel- Design principles and conceptual approach, *Tunnelling and Underground Space Technology*, Vol. 21, Issue 1, January, pp. 68-78.

## Appendix A: Results of backfill mechanical properties

Table A.1: Mechanical properties of mixture of synthetic anhydrite (G) and fly ash at w/s 0.18

Mix ID	SA (%)	Fly ash (%)	3 days						28 days						90 days	
			UCS (MPa)	Flexural (MPa)	Split (MPa)	E (GPa)	G (GPa)	Poisson's ratio	UCS (MPa)	Flexural (MPa)	Split (MPa)	E (GPa)	G (GPa)	Poisson's ratio	UCS (MPa)	Poisson's ratio
SAG1	100	0	3.8	0.57	0.38	0.63	0.273	0.154	8.5	1.51	0.95	0.86	0.355	0.212	10.2	
SAG2	90	10	4.1	0.49	0.41	0.81	0.349	0.162	13.32	2.59	1.25	2.15	0.890	0.208	15.1	
SAG3	80	20	3.96	0.43	0.32	0.67	0.296	0.132	13.25	2.12	1.31	1.53	0.622	0.229	14.8	
SAG4	70	30	3.5	0.42	0.3	0.52	0.231	0.127	9.91	1.73	1.04	0.92	0.381	0.206	10.8	
SAG5	60	40	2.4	0.26	0.21	0.43	0.193	0.112	7.45	1.42	0.84	0.71	0.293	0.213	8.6	
SAG6	50	50	2.2	0.22	0.17	0.39	0.174	0.119	7.05	1.23	0.73	0.65	0.269	0.207	8.5	

Table A.2: Mechanical properties of mixture of synthetic anhydrite (T) and fly ash (w/s 0.18)

Mix ID	SA (%)	Fly ash (%)	3 days						28 days						90 days	
			UCS (MPa)	Flexural (MPa)	Split (MPa)	E (GPa)	G (GPa)	Poisson's ratio	UCS (MPa)	Flexural (MPa)	Split (MPa)	E (GPa)	G (GPa)	Poisson's ratio	UCS (MPa)	Poisson's ratio
SAT1	100	0	3.5	0.55	0.35	0.54	0.236	0.146	8	1.48	0.93	0.75	0.310	0.208	10.4	
SAT2	90	10	4	0.46	0.42	0.73	0.315	0.157	12.5	2.55	1.22	2.04	0.824	0.238	14.7	
SAT3	80	20	3.7	0.42	0.3	0.61	0.262	0.163	13.05	2.15	1.33	1.45	0.591	0.227	14.5	
SAT4	70	30	3.4	0.41	0.31	0.47	0.206	0.143	9.56	1.72	1.02	0.9	0.370	0.217	10.6	
SAT5	60	40	2.4	0.25	0.2	0.37	0.163	0.136	7.4	1.44	0.82	0.73	0.295	0.236	8.8	
SAT6	50	50	2.2	0.21	0.15	0.35	0.153	0.143	7	1.2	0.71	0.62	0.255	0.218	8.4	

Table A.3: Mechanical properties of mixture of Ellich natural anhydrite and fly ash (w/s 0.18)

Mix ID	ENA (%)	Fly ash (%)	3 days						28 days						90 days	
			UCS (MPa)	Flexural (MPa)	Split (MPa)	E (GPa)	G (GPa)	Poisson's ratio	UCS (MPa)	Flexural (MPa)	Split (MPa)	E (GPa)	G (GPa)	Poisson's ratio	UCS (MPa)	Poisson's ratio
ENA1	100	0	2.6	0.31	0.26	0.45	0.22	0.114	4.92	0.62	0.45	0.75	0.34	0.161	6.6	
ENA2	90	10	2.81	0.34	0.29	0.48	0.23	0.13	8.31	0.87	0.56	0.92	0.48	0.19	10.1	
ENA3	80	20	2.78	0.31	0.27	0.44	0.21	0.12	8.83	0.95	0.59	0.96	0.49	0.19	10.3	
ENA4	70	30	2.46	0.29	0.24	0.41	0.21	0.11	7.62	0.81	0.51	0.82	0.43	0.183	9.2	
ENA5	60	40	2.37	0.28	0.22	0.38	0.2	0.11	5.71	0.62	0.46	0.791	0.41	0.194	7.1	
ENA6	50	50	2.24	0.25	0.2	0.35	0.2	0.1	5.63	0.61	0.45	0.749	0.356	0.188	7	

Table A.4: Mechanical properties of mixture of Obrighem natural anhydrite (&lt; 4 mm) and fly ash (w/s 0.18)

Mix ID	ONA (%)	Fly ash (%)	3 days						28 days						90 days	
			UCS (MPa)	Flexural (MPa)	Split (MPa)	E (GPa)	G (GPa)	Poisson's ratio	UCS (MPa)	Flexural (MPa)	Split (MPa)	E (GPa)	G (GPa)	Poisson's ratio	UCS (MPa)	Poisson's ratio
ONA1	100	0	2.62	0.29	0.22	0.37	0.17	0.124	6.43	0.55	0.43	0.74	0.32	0.175	8.2	
ONA2	90	10	2.84	0.31	0.24	0.41	0.18	0.132	10.12	0.58	0.44	0.95	0.46	0.186	12.1	
ONA3	80	20	2.8	0.34	0.25	0.43	0.2	0.154	11.54	0.62	0.46	0.91	0.49	0.203	13.3	
ONA4	70	30	2.45	0.31	0.23	0.3	0.14	0.152	8.37	0.49	0.42	0.76	0.35	0.196	10.1	
ONA5	60	40	2.4	0.26	0.2	0.25	0.11	0.143	5.76	0.36	0.35	0.62	0.31	0.187	7.3	
ONA6	50	50	2.2	0.21	0.17	0.21	0.12	0.132	5.52	0.31	0.3	0.53	0.25	0.183	7.1	



Table A.5: Mechanical properties of mixture of Obrigheim natural anhydrite (&lt; 8 mm) and fly ash (w/s 0.18)

Mix ID	ONA (%)	Fly ash (%)	3 days					28 days					90 days		
			UCS (MPa)	Flexural (MPa)	Split (MPa)	E (GPa)	G (GPa)	Poisson's ratio	UCS (MPa)	Flexural (MPa)	Split (MPa)	E (GPa)	G (GPa)	Poisson's ratio	UCS (MPa)
ONA1	100	0	2.31	0.27	0.19	0.31	0.16	0.111	4.86	0.51	0.4	0.61	0.31	0.171	6.5
ONA2	90	10	2.62	0.29	0.2	0.35	0.18	0.123	8.84	0.54	0.41	0.87	0.41	0.175	10.4
ONA3	80	20	2.6	0.3	0.2	0.36	0.18	0.125	9.35	0.6	0.43	0.88	0.42	0.181	11.1
ONA4	70	30	2.22	0.24	0.15	0.22	0.16	0.124	8.53	0.48	0.38	0.75	0.34	0.18	9.4
ONA5	60	40	1.79	0.21	0.11	0.16	0.14	0.122	5.89	0.37	0.34	0.54	0.29	0.174	7.5
ONA6	50	50	1.76	0.17	0.1	0.12	0.11	0.111	5.25	0.28	0.28	0.42	0.24	0.173	7.3

Table A.6: Mechanical properties of mixture of cement (T) and fly ash (w/s 0.4)

Mix ID	Cement (%)	Fly ash (%)	7 days					28 days					90 days		
			UCS (MPa)	Flexural (MPa)	Split (MPa)	E (GPa)	G (GPa)	Poisson's ratio	UCS (MPa)	Flexural (MPa)	Split (MPa)	E (GPa)	G (GPa)	Poisson's ratio	UCS (MPa)
CFT1	5	95	1.08	0.15	0.14	1.3	0.61	0.185	2.04	0.32	0.2	5	2.41	0.224	3.5
CFT2	10	90	2.2	0.27	0.15	1.48	0.81	0.183	3.86	0.54	0.34	5.13	2.52	0.215	5.3
CFT3	15	85	2.7	0.36	0.21	2.32	1.1	0.176	6.02	0.81	0.52	6.42	3.2	0.221	7.6
CFT4	20	80	3.5	0.5	0.3	3.4	1.52	0.211	8.4	0.9	0.64	7.21	3.61	0.243	10.2
CFT5	25	75	5	0.7	0.45	3.82	1.7	0.213	10.1	1.31	0.81	8.12	4	0.248	12.5
CFT6	30	70	5.6	0.81	0.62	4.5	2.1	0.191	12.3	1.65	0.9	8.24	4	0.267	14.8

Table A.7: Mechanical properties of mixture of cement (T) and fly ash (w/s 0.45)

Mix ID	Cement (%)	Fly ash (%)	7 days						28 days						
			UCS (MPa)	Flexural (MPa)	Split (MPa)	E (GPa)	G (GPa)	Poisson's ratio	UCS (MPa)	Flexural (MPa)	Split (MPa)	E (GPa)	G (GPa)	Poisson's ratio	
CFT1	5	95	1.04	0.14	0.11	1.24	0.6	0.177	2.15	0.32	0.21	5.33	2.5	0.228	3.8
CFT2	10	90	1.65	0.2	0.13	1.44	0.83	0.179	4.03	0.56	0.4	5.4	2.61	0.229	5.8
CFT3	15	85	2.5	0.31	0.18	2.21	1.1	0.214	6.25	0.9	0.66	6.51	3.44	0.241	7.9
CFT4	20	80	3.6	0.45	0.26	3.12	1.42	0.201	8.51	1	0.81	7.3	3.71	0.245	10.8
CFT5	25	75	4.7	0.6	0.4	3.6	1.61	0.216	10.3	1.35	0.9	8.21	4.21	0.266	12.7
CFT6	30	70	5.55	0.74	0.51	4.11	1.92	0.215	12.7	1.71	1.11	8.5	4.42	0.265	15.1

Table A.8: Mechanical properties of mixture of cement (T) and fly ash (w/s 0.5)

Mix ID	Cement (%)	Fly ash (%)	7 days						28 days						
			UCS (MPa)	Flexural (MPa)	Split (MPa)	E (GPa)	G (GPa)	Poisson's ratio	UCS (MPa)	Flexural (MPa)	Split (MPa)	E (GPa)	G (GPa)	Poisson's ratio	
CFT1	5	95	1.04	0.12	0.11	1.12	0.6	0.185	2.02	0.3	0.2	5.11	2.35	0.217	3.4
CFT2	10	90	1.55	0.15	0.13	1.33	0.75	0.196	3.75	0.5	0.42	5.21	2.4	0.221	5.1
CFT3	15	85	2.3	0.28	0.17	2.14	1.1	0.211	5.88	0.75	0.5	6.34	3.02	0.236	7.2
CFT4	20	80	3.4	0.4	0.21	3	1.42	0.22	7.76	0.85	0.63	7.11	3.32	0.247	10.1
CFT5	25	75	4.6	0.53	0.35	3.34	1.55	0.221	10.02	1.1	0.72	8.01	3.83	0.255	12
CFT6	30	70	5.2	0.65	0.41	4.01	1.82	0.221	12	1.42	0.85	8.12	4.11	0.265	14.5

Table A.9: Mechanical properties of mixture of cement (G) and fly ash (w/s 0.4)

Mix ID	Cement (%)	Fly ash (%)	7 days						28 days						90 days	
			UCS (MPa)	Flexural (MPa)	Split (MPa)	E (GPa)	G (GPa)	Poisson's ratio	UCS (MPa)	Flexural (MPa)	Split (MPa)	E (GPa)	G (GPa)	Poisson's ratio	UCS (MPa)	Poisson's ratio
CFG1	5	95	1.2	0.18	0.11	1.34	0.67	0.158	2.10	0.3	0.21	5.02	2.48	0.212	3.8	
CFG2	10	90	2.3	0.28	0.15	1.52	0.85	0.176	4.05	0.55	0.37	5.11	2.56	0.211	6.1	
CFG3	15	85	2.98	0.39	0.22	2.36	1.13	0.164	6.08	0.86	0.53	6.47	3.25	0.234	7.9	
CFG4	20	80	3.76	0.51	0.32	3.41	1.54	0.204	8.64	0.93	0.67	7.23	3.64	0.262	10.4	
CFG5	25	75	5.1	0.72	0.47	3.85	1.73	0.201	10.14	1.35	0.84	8.14	4.05	0.275	12.2	
CFG6	30	70	5.92	0.84	0.61	4.52	2.12	0.195	12.51	1.67	0.92	8.27	4.1	0.264	14.7	

Table A.10: Mechanical properties of mixture of cement (G) and fly ash (w/s 0.45)

Mix ID	Cement (%)	Fly ash (%)	7 days						28 days						90 days	
			UCS (MPa)	Flexural (MPa)	Split (MPa)	E (GPa)	G (GPa)	Poisson's ratio	UCS (MPa)	Flexural (MPa)	Split (MPa)	E (GPa)	G (GPa)	Poisson's ratio	UCS (MPa)	Poisson's ratio
CFG1	5	95	1.1	0.15	0.1	1.28	0.61	0.168	2.31	0.34	0.25	5.36	2.51	0.223	4.1	
CFG2	10	90	1.85	0.19	0.14	1.48	0.82	0.183	4.15	0.58	0.43	5.41	2.63	0.224	6.5	
CFG3	15	85	2.96	0.33	0.2	2.25	1.11	0.212	6.34	0.92	0.67	6.54	3.47	0.236	8.2	
CFG4	20	80	4.14	0.46	0.29	3.14	1.43	0.204	8.78	1.03	0.84	7.33	3.75	0.248	10.8	
CFG5	25	75	4.87	0.62	0.41	3.65	1.67	0.213	10.37	1.38	0.92	8.25	4.23	0.264	12.7	
CFG6	30	70	5.73	0.77	0.52	4.13	1.95	0.212	12.82	1.73	1.14	8.52	4.45	0.267	15.2	

Table A.11: Mechanical properties of mixture of cement (G) and fly ash (w/s 0.5)

Mix ID	Cement (%)	Fly ash (%)	7 days					28 days					90 days		
			UCS (MPa)	Flexural (MPa)	Split (MPa)	E (GPa)	G (GPa)	Poisson's ratio	UCS (MPa)	Flexural (MPa)	Split (MPa)	E (GPa)		G (GPa)	Poisson's ratio
CFG1	5	95	1.03	0.12	0.1	1.14	0.61	0.183	2.04	0.31	0.22	5.14	2.38	0.214	3.7
CFG2	10	90	1.75	0.17	0.12	1.35	0.78	0.197	3.95	0.51	0.41	5.26	2.41	0.225	6
CFG3	15	85	2.49	0.29	0.18	2.17	1	0.214	5.87	0.78	0.52	6.38	3.01	0.234	7.7
CFG4	20	80	3.68	0.41	0.24	3.05	1.44	0.221	7.92	0.86	0.62	7.15	3.37	0.246	10.1
CFG5	25	75	4.82	0.55	0.37	3.38	1.58	0.224	10.11	1.11	0.75	8.05	3.86	0.251	11.8
CFG6	30	70	5.52	0.69	0.43	4.06	1.86	0.223	12.05	1.41	0.88	8.16	4.12	0.262	14.5

Table A.12: Mechanical properties of mixture of cement (C) and fly ash (w/s 0.4)

Mix ID	Cement (%)	Fly ash (%)	7 days					28 days					90 days		
			UCS (MPa)	Flexural (MPa)	Split (MPa)	E (GPa)	G (GPa)	Poisson's ratio	UCS (MPa)	Flexural (MPa)	Split (MPa)	E (GPa)		G (GPa)	Poisson's ratio
CFC1	5	95	0.76	0.09	0.06	0.73	0.41	0.154	1.47	0.17	0.11	1.26	0.61	0.235	3.2
CFC2	10	90	1.62	0.21	0.12	1.25	0.73	0.167	3.31	0.36	0.25	2.64	1.24	0.241	4.9
CFC3	15	85	2.41	0.31	0.19	1.86	0.98	0.158	4.64	0.55	0.34	3.65	1.76	0.238	6.4
CFC4	20	80	3.3	0.42	0.23	2.42	1.36	0.168	6.13	0.72	0.43	5.07	2.35	0.261	8.1
CFC5	25	75	4.11	0.49	0.37	3.15	1.61	0.189	8.05	0.95	0.62	6.14	3.11	0.257	10.2
CFC6	30	70	5.21	0.67	0.42	3.92	2.14	0.212	10.25	1.2	0.81	7.23	3.52	0.264	12.1

Table A.13: Mechanical properties of mixture of cement (C) and fly ash (w/s 0.45)

Mix ID	Cement (%)	Fly ash (%)	7 days						28 days						90 days	
			UCS (MPa)	Flexural (MPa)	Split (MPa)	E (GPa)	G (GPa)	Poisson's ratio	UCS (MPa)	Flexural (MPa)	Split (MPa)	E (GPa)	G (GPa)	Poisson's ratio	UCS (MPa)	Poisson's ratio
CFC1	5	95	0.71	0.08	0.06	0.62	0.34	0.164	1.55	0.17	0.13	1.51	0.72	0.225	3.1	
CFC2	10	90	1.48	0.19	0.13	1.08	0.65	0.168	3.46	0.41	0.31	2.83	1.33	0.236	4.7	
CFC3	15	85	2.23	0.26	0.17	1.65	0.84	0.175	4.72	0.57	0.39	4.02	1.85	0.243	6.5	
CFC4	20	80	3.05	0.39	0.2	2.26	1.22	0.192	6.94	0.9	0.51	5.36	2.65	0.265	8	
CFC5	25	75	3.97	0.43	0.31	2.72	1.43	0.201	8.62	1.02	0.65	6.82	3.33	0.258	10.1	
CFC6	30	70	4.75	0.61	0.38	3.51	2.04	0.223	11.54	1.28	0.95	8.22	3.65	0.267	11.8	

Table A.14: Mechanical properties of mixture of cement (C) and fly ash (w/s 0.5)

Mix ID	Cement (%)	Fly ash (%)	7 days						28 days						90 days	
			UCS (MPa)	Flexural (MPa)	Split (MPa)	E (GPa)	G (GPa)	Poisson's ratio	UCS (MPa)	Flexural (MPa)	Split (MPa)	E (GPa)	G (GPa)	Poisson's ratio	UCS (MPa)	Poisson's ratio
CFC1	5	95	0.64	0.07	0.04	0.57	0.33	0.172	1.28	0.14	0.11	1.16	0.65	0.241	2.8	
CFC2	10	90	1.35	0.16	0.11	0.95	0.57	0.167	3.18	0.36	0.26	2.43	1.28	0.236	4.5	
CFC3	15	85	2.05	0.24	0.15	1.55	0.78	0.183	4.55	0.52	0.33	3.45	1.81	0.255	6	
CFC4	20	80	2.54	0.33	0.19	2.17	1.11	0.194	5.75	0.63	0.48	5.14	2.24	0.263	7.8	
CFC5	25	75	3.85	0.46	0.27	2.57	1.32	0.215	8.26	0.94	0.68	6.32	3.15	0.261	9.8	
CFC6	30	70	4.52	0.47	0.31	3.28	1.99	0.234	10.89	1.2	0.86	7.25	3.48	0.263	11.5	

Table A.15: Mechanical properties of mixture of cement (G) and filter dust (w/s 0.4)

Mix ID	Cement (%)	Filter dust (%)	7 days						28 days						90 days UCS (MPa)
			UCS (MPa)	Flexural (MPa)	Split (MPa)	E (GPa)	G (GPa)	Poisson's ratio	UCS (MPa)	Flexural (MPa)	Split (MPa)	E (GPa)	G (GPa)	Poisson's ratio	
CDG1	0	100	0.36	0.05	0.03	0.09	0.05	0.1	0.71	0.08	0.05	0.2	0.11	0.102	1.8
CDG2	5	95	0.85	0.13	0.08	0.75	0.32	0.201	1.79	0.22	0.15	1.54	0.87	0.233	3.4
CDG3	10	90	1.54	0.28	0.15	1.26	0.68	0.223	2.96	0.38	0.22	2.65	1.74	0.243	4.5
CDG4	15	85	2.57	0.36	0.24	1.95	1.04	0.215	4.72	0.66	0.38	4.07	1.81	0.238	6.3
CDG5	20	80	3.85	0.55	0.34	2.47	1.32	0.217	6.68	0.86	0.46	5.14	2.43	0.241	8.4
CDG6	25	75	4.7	0.68	0.42	3.04	1.67	0.224	7.82	1.01	0.62	6.1	2.81	0.245	9.4

Table A.16: Mechanical properties of mixture of cement (G) and filter dust (w/s 0.45)

Mix ID	Cement (%)	Filter dust (%)	7 days						28 days						90 days UCS (MPa)
			UCS (MPa)	Flexural (MPa)	Split (MPa)	E (GPa)	G (GPa)	Poisson's ratio	UCS (MPa)	Flexural (MPa)	Split (MPa)	E (GPa)	G (GPa)	Poisson's ratio	
CDG1	0	100	0.55	0.06	0.04	0.08	0.04	0.112	0.88	0.1	0.05	0.2	0.12	0.114	2
CDG2	5	95	0.98	0.11	0.06	0.64	0.3	0.216	1.95	0.25	0.17	1.62	0.95	0.229	3.7
CDG3	10	90	1.72	0.22	0.15	1.18	0.59	0.223	3.51	0.42	0.29	2.9	1.89	0.228	4.7
CDG4	15	85	2.84	0.36	0.19	1.78	1	0.225	5.04	0.7	0.43	4.25	2.11	0.244	6.5
CDG5	20	80	4.04	0.56	0.32	2.26	1.12	0.243	7	0.91	0.61	5.53	2.66	0.243	8.7
CDG6	25	75	6.27	0.81	0.4	2.86	1.45	0.248	9.21	1.34	0.77	6.37	2.98	0.255	10.5

Table A.17: Mechanical properties of mixture of cement (G) and filter dust (w/s 0.5)

Mix ID	Cement (%)	Filter dust (%)	7 days						28 days						90 days	
			UCS (MPa)	Flexural (MPa)	Split (MPa)	E (GPa)	G (GPa)	Poisson's ratio	UCS (MPa)	Flexural (MPa)	Split (MPa)	E (GPa)	G (GPa)	Poisson's ratio	UCS (MPa)	
CDG1	0	100	0.34	0.04	0.03	0.08	0.04	0.11	0.7	0.08	0.04	0.18	0.09	0.11	1.8	
CDG2	5	95	0.76	0.09	0.07	0.61	0.31	0.209	1.81	0.21	0.16	1.55	0.83	0.24	3.5	
CDG3	10	90	1.26	0.16	0.13	1.07	0.55	0.211	3.05	0.42	0.26	2.85	1.85	0.235	4.6	
CDG4	15	85	2.17	0.28	0.22	1.53	0.97	0.227	4.83	0.62	0.4	4.12	2.02	0.242	6.5	
CDG5	20	80	3.77	0.52	0.31	2.13	1.08	0.246	6.55	0.72	0.55	5.43	2.51	0.247	8.1	
CDG6	25	75	3.94	0.51	0.35	2.58	1.35	0.235	7.04	0.91	0.62	6.17	2.88	0.251	9.2	

Table A.18: Mechanical properties of mixture of cement (G), fly ash and filter dust (w/s 0.4)

Mix ID	Cement (%)	Filter dust (%)	Fly ash (%)	7 days						28 days						90 days UCS (MPa)
				UCS (MPa)	Flexural (MPa)	Split (MPa)	E (GPa)	G (GPa)	Poisson's ratio	UCS (MPa)	Flexural (MPa)	Split (MPa)	E (GPa)	G (GPa)	Poisson's ratio	
CFDG1	5	47.5	47.5	1.2	0.13	0.08	0.65	0.38	0.16	2.10	0.23	0.15	1.67	0.85	0.2	3.7
CFDG2	5	50	45	1.01	0.11	0.07	0.62	0.34	0.17	2.06	0.19	0.13	1.58	0.71	0.21	3.4
CFDG3	5	45	50	1.25	0.13	0.09	0.67	0.42	0.19	2.34	0.25	0.16	1.71	0.92	0.21	3.5
CFDG4	10	45	45	2.3	0.25	0.18	0.87	0.49	0.21	4.05	0.46	0.3	2.82	1.53	0.22	5.8
CFDG5	10	50	40	2.04	0.19	0.15	0.81	0.47	0.22	3.87	0.4	0.27	2.77	1.41	0.24	5.5
CFDG6	10	40	50	2.43	0.26	0.18	0.9	0.55	0.22	4.31	0.51	0.32	2.89	1.62	0.23	5.6
CFDG7	15	42.5	42.5	2.98	0.33	0.22	1.21	0.72	0.24	6.08	0.71	0.45	3.21	1.74	0.24	8.1
CFDG8	15	50	35	2.62	0.3	0.21	1.2	0.68	0.23	5.52	0.65	0.43	3.14	1.68	0.23	7.8
CFDG9	15	35	50	3.11	0.35	0.24	1.25	0.79	0.24	6.37	0.73	0.47	3.35	1.82	0.25	7.6
CFDG10	20	40	40	4.16	0.48	0.32	1.57	0.83	0.22	8.64	1.01	0.64	4.25	2.25	0.24	10.2
CFDG11	20	50	30	3.82	0.41	0.31	1.49	0.81	0.23	8.16	0.96	0.61	4.08	2.04	0.25	9.8
CFDG12	20	30	50	4.35	0.5	0.35	1.60	0.86	0.24	8.85	1.11	0.66	4.34	2.35	0.25	9.7



Table A.19: Mechanical properties of mixture of cement (G), fly ash and filter dust (w/s 0.45)

Mix ID	Cement (%)	Filter dust (%)	Fly ash (%)	7 days						28 days						90 days UCS (MPa)
				UCS (MPa)	Flexural (MPa)	Split (MPa)	E (GPa)	G (GPa)	Poisson's ratio	UCS (MPa)	Flexural (MPa)	Split (MPa)	E (GPa)	G (GPa)	Poisson's ratio	
CFDG1	5	47.5	47.5	1.1	0.11	0.08	0.52	0.34	0.17	2.31	0.25	0.17	1.78	0.92	0.21	3.9
CFDG2	5	50	45	0.95	0.09	0.06	0.49	0.3	0.2	2.07	0.21	0.16	1.71	0.85	0.23	3.7
CFDG3	5	45	50	1.15	0.12	0.08	0.58	0.36	0.18	2.53	0.28	0.19	1.86	1.03	0.24	3.7
CFDG4	10	45	45	1.85	0.21	0.15	0.74	0.41	0.21	4.15	0.49	0.33	3.35	1.67	0.22	6.1
CFDG5	10	50	40	1.72	0.18	0.14	0.69	0.38	0.21	4.08	0.43	0.31	3.24	1.59	0.22	5.7
CFDG6	10	40	50	1.98	0.22	0.17	0.81	0.45	0.22	4.46	0.54	0.35	3.46	1.72	0.23	5.8
CFDG7	15	42.5	42.5	2.96	0.3	0.2	1.03	0.65	0.24	6.34	0.75	0.49	3.84	1.87	0.25	8.5
CFDG8	15	50	35	2.55	0.28	0.18	0.95	0.61	0.25	6.17	0.71	0.46	3.72	1.76	0.26	8
CFDG9	15	35	50	3.07	0.33	0.21	1.15	0.68	0.25	6.55	0.81	0.51	3.92	1.98	0.24	8.2
CFDG10	20	40	40	3.94	0.43	0.29	1.33	0.77	0.24	8.78	1.02	0.7	4.45	2.36	0.24	10.5
CFDG11	20	50	30	2.65	0.41	0.27	1.24	0.74	0.24	8.42	1	0.68	4.38	2.27	0.25	10
CFDG12	20	30	50	4.13	0.45	0.3	1.42	0.79	0.23	8.98	1.25	0.73	4.58	2.53	0.23	10.2

Table A.20: Mechanical properties of mixture of cement (G), fly ash and filter dust (w/s 0.5)

Mix ID	Cement (%)	Filter dust (%)	Fly ash (%)	7 days						28 days						
				UCS (MPa)	Flexural (MPa)	Split (MPa)	E (GPa)	G (GPa)	Poisson's ratio	UCS (MPa)	Flexural (MPa)	Split (MPa)	E (GPa)	G (GPa)	Poisson's ratio	
CFDG1	5	47.5	47.5	1.03	0.11	0.07	0.5	0.34	0.19	2.04	0.22	0.15	1.65	0.84	0.22	3.4
CFDG2	5	50	45	0.88	0.08	0.06	0.43	0.31	0.17	1.95	0.18	0.13	1.6	0.71	0.23	3.1
CFDG3	5	45	50	1.09	0.11	0.07	0.58	0.36	0.17	2.16	0.23	0.16	1.71	0.96	0.23	3.3
CFDG4	10	45	45	1.75	0.2	0.14	0.71	0.4	0.21	3.95	0.43	0.29	2.75	1.51	0.24	5.7
CFDG5	10	50	40	1.64	0.17	0.12	0.67	0.39	0.22	3.71	0.39	0.25	2.62	1.35	0.24	5.5
CFDG6	10	40	50	1.95	0.21	0.15	0.78	0.42	0.23	4.12	0.45	0.29	2.81	1.59	0.22	5.4
CFDG7	15	42.5	42.5	2.49	0.28	0.18	1.01	0.63	0.22	5.87	0.68	0.44	3.15	1.68	0.26	7.6
CFDG8	15	50	35	2.14	0.24	0.16	0.96	0.58	0.26	5.58	0.61	0.41	3.01	1.61	0.23	7.4
CFDG9	15	35	50	2.65	0.29	0.18	1.16	0.67	0.21	5.98	0.7	0.45	3.29	1.72	0.23	7.6
CFDG10	20	40	40	3.68	0.41	0.27	1.29	0.74	0.23	7.92	0.91	0.64	4.21	2.09	0.22	9.6
CFDG11	20	50	30	3.41	0.38	0.24	1.21	0.69	0.22	7.64	0.88	0.6	4.05	2.01	0.22	9.1
CFDG12	20	30	50	3.79	0.43	0.28	1.34	0.77	0.22	8.23	0.97	0.66	4.38	2.27	0.22	9.3

Table A.21: Mechanical properties of mixture of cement (C), fly ash and filter dust (w/s 0.4)

Mix ID	Cement (%)	Filter dust (%)	Fly ash (%)	7 days						28 days						90 days	
				UCS (MPa)	Flexural (MPa)	Split (MPa)	E (GPa)	G (GPa)	Poisson's ratio	UCS (MPa)	Flexural (MPa)	Split (MPa)	E (GPa)	G (GPa)	Poisson's ratio	UCS (MPa)	Poisson's ratio
CFDC1	5	47.5	47.5	0.95	0.12	0.08	0.32	0.17	0.189	1.74	0.22	0.14	0.66	0.34	0.195	3.2	
CFDC2	5	50	45	0.9	0.08	0.07	0.25	0.15	0.201	1.71	0.2	0.12	0.62	0.31	0.204	3	
CFDC3	5	45	50	1.1	0.13	0.1	0.38	0.2	0.199	1.8	0.25	0.17	0.71	0.39	0.197	3.1	
CFDC4	10	45	45	1.75	0.23	0.14	0.58	0.31	0.211	3.51	0.41	0.29	1.3	0.62	0.221	4.2	
CFDC5	10	50	40	1.62	0.18	0.12	0.51	0.28	0.225	3.42	0.37	0.25	1.24	0.57	0.243	4	
CFDC6	10	40	50	1.83	0.25	0.15	0.65	0.35	0.263	3.58	0.47	0.32	1.36	0.67	0.226	4.2	
CFDC7	15	42.5	42.5	2.61	0.34	0.24	0.71	0.37	0.235	5.15	0.59	0.42	1.98	1.04	0.218	6.8	
CFDC8	15	50	35	2.48	0.31	0.21	0.65	0.36	0.247	5.07	0.53	0.38	1.92	1.01	0.247	6.4	
CFDC9	15	35	50	2.75	0.38	0.27	0.79	0.39	0.268	5.23	0.64	0.45	2.12	1.1	0.246	6.5	
CFDC10	20	40	40	3.71	0.45	0.29	0.85	0.45	0.267	7.34	0.85	0.58	2.64	1.31	0.253	9	
CFDC11	20	50	30	3.51	0.41	0.27	0.81	0.41	0.259	7.29	0.81	0.55	2.57	1.26	0.244	8.7	
CFDC12	20	30	50	3.88	0.52	0.33	0.91	0.49	0.248	7.42	0.92	0.61	2.72	1.38	0.256	8.8	

Table A.22: Mechanical properties of mixture of cement (C), fly ash and filter dust (w/s 0.45)

Mix ID	Cement (%)	Filter dust (%)	Fly ash (%)	7 days						28 days						90 days	
				UCS (MPa)	Flexural (MPa)	Split (MPa)	E (GPa)	G (GPa)	Poisson's ratio	UCS (MPa)	Flexural (MPa)	Split (MPa)	E (GPa)	G (GPa)	Poisson's ratio	UCS (MPa)	Poisson's ratio
CFDC1	5	47.5	47.5	0.87	0.09	0.07	0.3	0.15	0.213	1.93	0.24	0.16	0.75	0.38	0.201	3.5	
CFDC2	5	50	45	0.81	0.11	0.05	0.28	0.12	0.205	1.88	0.22	0.14	0.72	0.35	0.211	3	
CFDC3	5	45	50	0.92	0.07	0.08	0.33	0.17	0.207	1.97	0.28	0.17	0.78	0.42	0.209	3.1	
CFDC4	10	45	45	1.71	0.2	0.13	0.51	0.26	0.216	3.87	0.45	0.31	1.42	0.73	0.224	4.5	
CFDC5	10	50	40	1.56	0.18	0.11	0.48	0.24	0.218	3.81	0.41	0.3	1.38	0.7	0.238	4	
CFDC6	10	40	50	1.85	0.23	0.16	0.55	0.29	0.225	3.95	0.49	0.33	1.49	0.78	0.229	4.2	
CFDC7	15	42.5	42.5	2.53	0.3	0.21	0.65	0.32	0.243	5.42	0.63	0.44	2.16	1.13	0.246	7.1	
CFDC8	15	50	35	2.45	0.28	0.2	0.63	0.3	0.246	5.35	0.6	0.41	2.12	1.1	0.247	6.7	
CFDC9	15	35	50	2.67	0.34	0.24	0.67	0.35	0.252	5.53	0.67	0.48	2.21	1.2	0.245	6.8	
CFDC10	20	40	40	3.43	0.41	0.27	0.75	0.41	0.253	7.91	0.88	0.62	2.83	1.42	0.258	9.3	
CFDC11	20	50	30	3.38	0.38	0.24	0.71	0.38	0.255	7.86	0.84	0.6	2.78	1.38	0.251	8.8	
CFDC12	20	30	50	3.62	0.45	0.31	0.78	0.45	0.248	8.12	0.92	0.67	2.89	1.49	0.256	8.9	

Table A.23: Mechanical properties of mixture of cement (C), fly ash and filter dust (w/s 0.5)

Mix ID	Cement (%)	Filter dust (%)	Fly ash (%)	7 days					28 days					90 days UCS (MPa)		
				UCS (MPa)	Flexural (MPa)	Split (MPa)	E (GPa)	G (GPa)	Poisson's ratio	UCS (MPa)	Flexural (MPa)	Split (MPa)	E (GPa)		G (GPa)	Poisson's ratio
CFDC1	5	47.5	47.5	0.74	0.08	0.06	0.28	0.14	0.197	1.62	0.19	0.12	0.66	0.35	0.212	3.1
CFDC2	5	50	45	0.71	0.07	0.05	0.25	0.12	0.186	1.55	0.17	0.1	0.64	0.33	0.206	3
CFDC3	5	45	50	0.79	0.11	0.08	0.29	0.15	0.193	1.7	0.2	0.13	0.69	0.37	0.218	3
CFDC4	10	45	45	1.56	0.18	0.12	0.45	0.24	0.214	3.48	0.42	0.27	1.35	0.67	0.234	4.1
CFDC5	10	50	40	1.51	0.15	0.1	0.41	0.22	0.206	3.41	0.38	0.25	1.31	0.64	0.228	4
CFDC6	10	40	50	1.59	0.21	0.15	0.48	0.27	0.214	3.55	0.47	0.29	0.37	0.69	0.219	3.9
CFDC7	15	42.5	42.5	2.36	0.26	0.19	0.61	0.31	0.227	5.22	0.61	0.41	1.94	1.07	0.241	6.7
CFDC8	15	50	35	2.31	0.24	0.18	0.58	0.3	0.226	5.15	0.57	0.39	1.91	1.04	0.236	6.4
CFDC9	15	35	50	2.4	0.3	0.21	0.65	0.34	0.214	5.33	0.65	0.45	1.99	1.11	0.247	6.5
CFDC10	20	40	40	2.95	0.36	0.24	0.71	0.39	0.217	6.73	0.78	0.53	2.69	1.3	0.243	8.8
CFDC11	20	50	30	2.88	0.33	0.22	0.67	0.37	0.233	6.72	0.72	0.51	2.61	1.25	0.244	8.5
CFDC12	20	30	50	3.11	0.41	0.27	0.78	0.42	0.214	6.85	0.82	0.58	2.73	1.36	0.242	8.6

Table A.24: Mechanical properties of mixture of FGD-gypsum (T) and fly ash (w/s 0.4)

Mix ID	FGD-G (%)	Fly ash (%)	7 days					28 days					90 days		
			UCS (MPa)	Flexural (MPa)	Split (MPa)	E (GPa)	G (GPa)	Poisson's ratio	UCS (MPa)	Flexural (MPa)	Split (MPa)	E (GPa)	G (GPa)	Poisson's ratio	UCS (MPa)
FGD1	100	0	4.21	0.51	0.32	1.48	0.77	0.213	9.36	1.11	0.75	3.23	1.71	0.228	10.8
FGD2	90	10	5.65	0.74	0.41	1.53	0.79	0.185	11.54	1.23	0.89	3.74	1.84	0.216	13.3
FGD3	80	20	5.82	0.76	0.42	1.66	0.83	0.213	12.61	1.45	0.95	4.16	2.05	0.234	14.2
FGD4	70	30	4.12	0.52	0.32	1.35	0.65	0.216	9.17	1.1	0.72	3.14	1.63	0.211	10.7
FGD5	60	40	3.32	0.44	0.3	1.24	0.61	0.223	8.25	0.95	0.64	2.87	1.52	0.195	9.9
FGD6	50	50	3.04	0.35	0.25	1.21	0.55	0.201	6.33	0.72	0.45	2.53	1.21	0.202	7.7

Table A.25: Mechanical properties of mixture of FGD-gypsum (T) and fly ash (w/s 0.45)

Mix ID	FGD-G (%)	Fly ash (%)	7 days					28 days					90 days		
			UCS (MPa)	Flexural (MPa)	Split (MPa)	E (GPa)	G (GPa)	Poisson's ratio	UCS (MPa)	Flexural (MPa)	Split (MPa)	E (GPa)	G (GPa)	Poisson's ratio	UCS (MPa)
FGD1	100	0	4.16	0.48	0.33	1.44	0.75	0.227	10.27	1.2	0.91	4.07	2.24	0.234	11.7
FGD2	90	10	5.23	0.65	0.41	1.62	0.81	0.216	14.35	1.62	1.11	5.34	2.66	0.212	14.1
FGD3	80	20	5.27	0.62	0.4	1.55	0.77	0.195	12.71	1.47	0.93	4.85	2.51	0.235	14.8
FGD4	70	30	4.02	0.45	0.31	1.31	0.62	0.212	10.24	1.24	0.83	4.15	2.23	0.218	10.9
FGD5	60	40	3.15	0.41	0.31	1.24	0.62	0.218	8.51	1.04	0.71	3.62	1.87	0.204	10.1
FGD6	50	50	2.67	0.32	0.24	1.06	0.54	0.214	6.62	0.73	0.45	3.11	1.65	0.201	8.1

Table A.26: Mechanical properties of mixture of FGD-gypsum (T) and fly ash (w/s 0.5)

Mix ID	FGD-G (%)	Fly ash (%)	7 days					28 days					90 days		
			UCS (MPa)	Flexural (MPa)	Split (MPa)	E (GPa)	G (GPa)	Poisson's ratio	UCS (MPa)	Flexural (MPa)	Split (MPa)	E (GPa)	G (GPa)	Poisson's ratio	UCS (MPa)
FGD1	100	0	4.19	0.48	0.31	1.45	0.73	0.216	8.85	1.03	0.73	3.51	1.78	0.223	10.5
FGD2	90	10	5.31	0.62	0.39	1.64	0.81	0.195	12.63	1.43	0.92	4.61	2.45	0.212	13
FGD3	80	20	5.16	0.58	0.33	1.47	0.77	0.186	10.73	1.25	0.9	4.22	2.31	0.237	13.9
FGD4	70	30	3.88	0.46	0.3	1.28	0.62	0.224	8.24	0.96	0.66	3.43	1.72	0.215	9.8
FGD5	60	40	3.06	0.36	0.24	1.21	0.55	0.198	7.64	0.91	0.61	3.17	1.61	0.211	9.1
FGD6	50	50	2.52	0.3	0.22	1.02	0.51	0.204	6.08	0.71	0.48	2.64	1.42	0.203	7.4

Table A.27: Mechanical properties of mixture of tailing (T), cement and fly ash (w/s 0.4)

Mix ID	Cement (%)	Tailing (%)	Fly ash (%)	7 days						28 days						90 days	
				UCS (MPa)	Flexural (MPa)	Split (MPa)	E (GPa)	G (GPa)	Poisson's ratio	UCS (MPa)	Flexural (MPa)	Split (MPa)	E (GPa)	G (GPa)	Poisson's ratio	UCS (MPa)	
T1	5	47.5	47.5	1.25	0.23	0.17	0.41	0.24	0.209	2.4	0.39	0.32	0.85	0.55	0.248	3.5	
T2	5	50	45	1.1	0.22	0.17	0.38	0.21	0.213	2.3	0.4	0.28	0.81	0.51	0.243	3	
T3	5	45	50	1.3	0.26	0.18	0.44	0.26	0.224	2.3	0.41	0.33	0.88	0.56	0.231	3.6	
T4	10	45	45	1.8	0.36	0.25	0.63	0.35	0.215	4	0.61	0.45	1.4	0.68	0.228	5.1	
T5	10	50	40	1.8	0.36	0.24	0.61	0.32	0.227	3.8	0.57	0.41	1.35	0.61	0.241	5	
T6	10	40	50	2.1	0.42	0.29	0.74	0.38	0.233	4.2	0.64	0.48	1.46	0.7	0.247	5.3	
T7	15	42.5	42.5	2.9	0.58	0.4	0.94	0.44	0.241	5.9	0.87	0.65	1.95	0.95	0.253	7.2	
T8	15	50	35	2.5	0.5	0.36	0.88	0.42	0.227	5.7	0.83	0.6	1.91	0.91	0.264	6.9	
T9	15	35	50	3.2	0.64	0.44	0.96	0.48	0.231	5.6	0.88	0.69	2.1	1.1	0.248	7.4	
T10	20	40	40	4.1	0.82	0.56	1.33	0.58	0.211	8	1.34	0.87	2.57	1.33	0.257	9.1	
T11	20	50	30	3.9	0.78	0.55	1.21	0.52	0.228	8	1.22	0.81	2.51	1.27	0.253	8.7	
T12	20	30	50	4.2	0.84	0.58	1.42	0.59	0.234	8.2	1.41	0.91	2.65	1.35	0.261	9.4	



Table A.28: Mechanical properties of mixture of tailing (T), cement and fly ash (w/s 0.45)

Mix ID	Cement (%)	Tailing (%)	Fly ash (%)	7 days						28 days						90 days UCS (MPa)
				UCS (MPa)	Flexural (MPa)	Split (MPa)	E (GPa)	G (GPa)	Poisson's ratio	UCS (MPa)	Flexural (MPa)	Split (MPa)	E (GPa)	G (GPa)	Poisson's ratio	
T1	5	47.5	47.5	1.1	0.19	0.14	0.35	0.19	0.212	2.5	0.42	0.35	0.94	0.61	0.233	3.9
T2	5	50	45	1.1	0.16	0.11	0.31	0.15	0.214	2.2	0.38	0.31	0.91	0.55	0.247	3.1
T3	5	45	50	1	0.2	0.15	0.37	0.2	0.218	2.6	0.44	0.38	0.98	0.63	0.236	3.5
T4	10	45	45	1.8	0.32	0.21	0.55	0.3	0.223	4.3	0.64	0.51	1.49	0.75	0.248	5.5
T5	10	50	40	1.6	0.29	0.2	0.48	0.25	0.224	3.9	0.6	0.5	1.42	0.71	0.263	5.1
T6	10	40	50	1.65	0.33	0.24	0.56	0.32	0.217	4	0.66	0.54	1.55	0.79	0.242	5.6
T7	15	42.5	42.5	2.8	0.55	0.37	0.89	0.39	0.237	6.2	0.88	0.68	2.05	1.15	0.245	7.5
T8	15	50	35	2.6	0.51	0.33	0.82	0.34	0.244	5.8	0.85	0.64	1.96	1.1	0.228	7.1
T9	15	35	50	2.6	0.56	0.38	0.89	0.41	0.232	6	0.89	0.7	2.1	1.18	0.236	7.7
T10	20	40	40	4	0.75	0.5	1.14	0.51	0.246	8.5	1.4	0.92	2.62	1.41	0.244	9.4
T11	20	50	30	3.8	0.7	0.45	1.05	0.48	0.258	7.9	1.35	0.88	2.57	1.34	0.257	9.1
T12	20	30	50	3.6	0.77	0.52	1.2	0.52	0.251	8.2	1.48	0.97	2.69	1.45	0.249	9.6

Table A.29: Mechanical properties of mixture of tailing (T), cement and fly ash (w/s 0.5)

Mix ID	Cement (%)	Tailing (%)	Fly ash (%)	7 days						28 days						90 days	
				UCS (MPa)	Flexural (MPa)	Split (MPa)	E (GPa)	G (GPa)	Poisson's ratio	UCS (MPa)	Flexural (MPa)	Split (MPa)	E (GPa)	G (GPa)	Poisson's ratio	UCS (MPa)	Poisson's ratio
T1	5	47.5	47.5	0.9	0.16	0.11	0.29	0.15	0.215	2.1	0.31	0.25	0.78	0.47	0.255	3	
T2	5	50	45	0.77	0.15	0.1	0.24	0.11	0.224	1.9	0.27	0.21	0.69	0.44	0.238	2.8	
T3	5	45	50	1	0.18	0.13	0.3	0.16	0.218	2.2	0.33	0.28	0.81	0.48	0.247	3.1	
T4	10	45	45	1.7	0.27	0.18	0.47	0.25	0.236	3.8	0.55	0.37	1.26	0.61	0.241	4.5	
T5	10	50	40	1.6	0.24	0.15	0.42	0.21	0.237	3.5	0.51	0.33	1.21	0.6	0.252	4.2	
T6	10	40	50	1.9	0.28	0.19	0.49	0.28	0.236	3.9	0.58	0.39	1.3	0.65	0.239	4.8	
T7	15	42.5	42.5	2.6	0.47	0.34	0.71	0.32	0.224	5.9	0.74	0.56	1.86	0.88	0.262	7	
T8	15	50	35	2.4	0.44	0.31	0.68	0.3	0.237	5.5	0.71	0.53	1.8	0.82	0.247	6.5	
T9	15	35	50	2.7	0.49	0.37	0.66	0.35	0.219	5.9	0.75	0.59	1.92	0.93	0.255	7.2	
T10	20	40	40	3.7	0.68	0.44	1.05	0.41	0.215	7.5	1.24	0.78	2.44	1.14	0.238	8.8	
T11	20	50	30	3.5	0.63	0.41	1	0.38	0.225	7.3	1.15	0.71	2.38	1.08	0.239	8.5	
T12	20	30	50	3.8	0.7	0.45	1.12	0.43	0.237	7.8	1.29	0.8	2.48	1.19	0.245	9	

## Appendix B

### Scanning electron microscope investigations

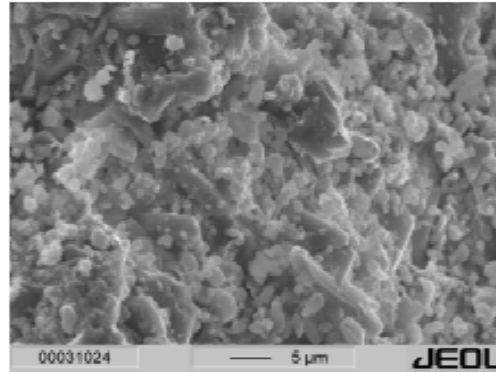


Figure B.1: SEM image showing synthetic anhydrite

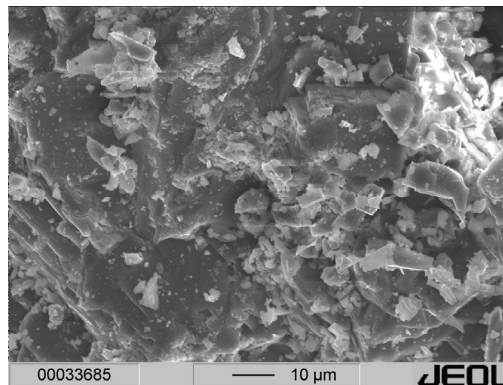


Figure B.2: SEM image showing natural anhydrite from Ellrich

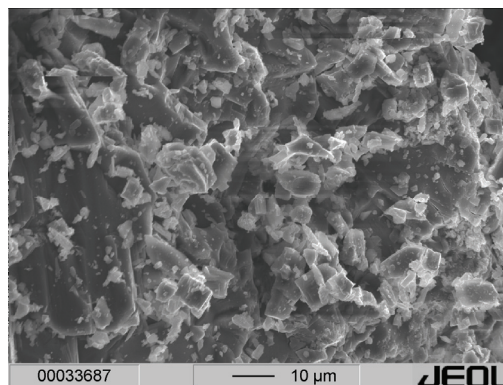


Figure B.3: SEM image showing natural anhydrite from Obrigheim

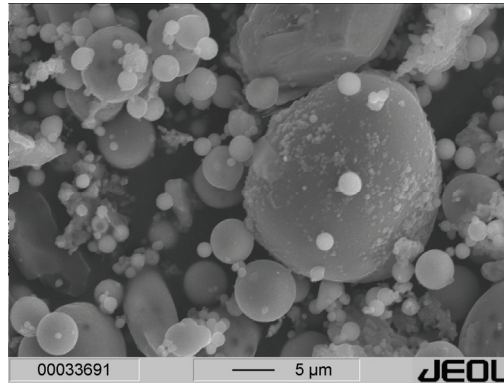


Figure B.4: SEM image showing fly ash from Germany

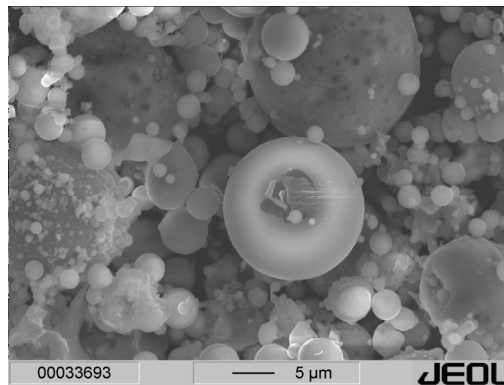


Figure B.5: SEM image showing fly ash from China

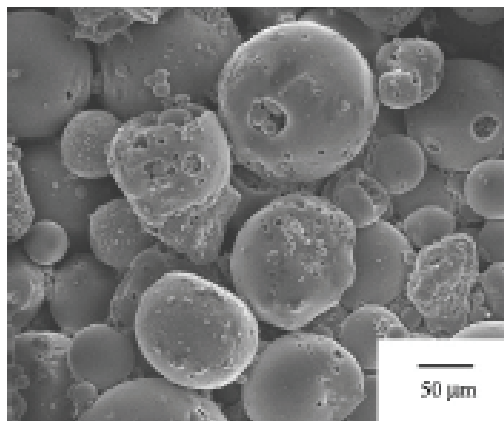


Figure B.6: SEM image showing fly ash from Thailand

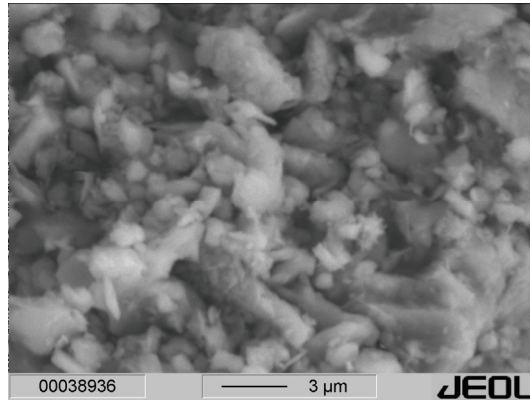


Figure B.7: SEM image showing filter dust

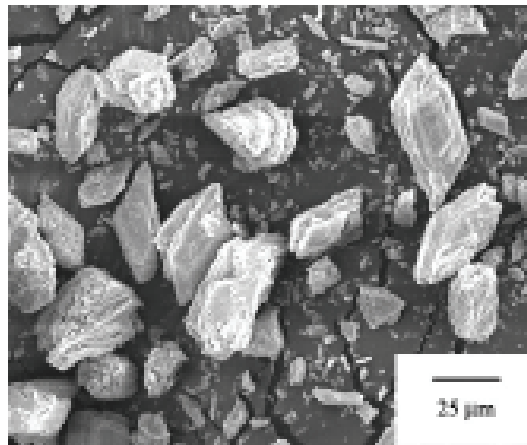


Figure B.8: SEM image showing FGD-Gypsum

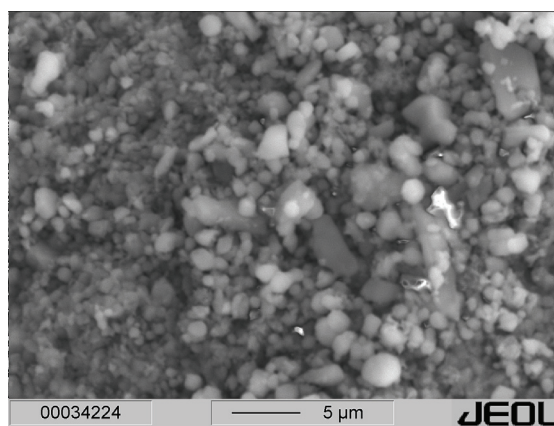


Figure B.9: SEM image showing mixture of synthetic anhydrite and fly ash

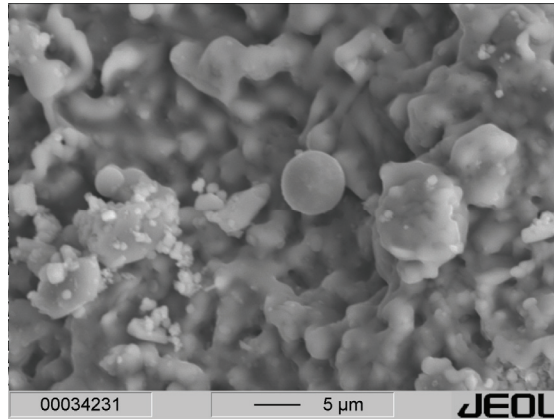


Figure B.10: SEM image showing mixture of synthetic anhydrite, fly ash and salt solution

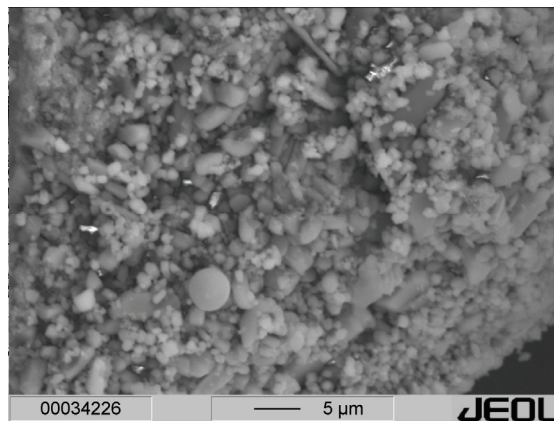


Figure B.11: SEM image showing mixture of natural anhydrite and fly ash

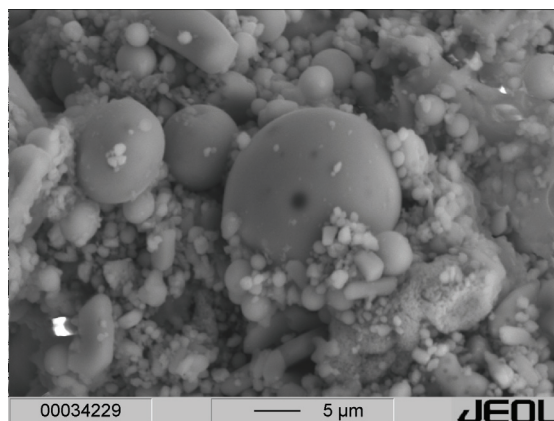


Figure B.12: SEM image showing mixture of natural anhydrite, fly ash and salt solution

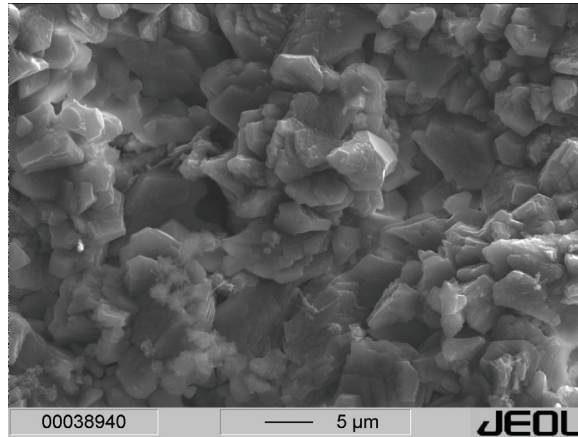


Figure B.13: SEM image showing mixture of cement(G)

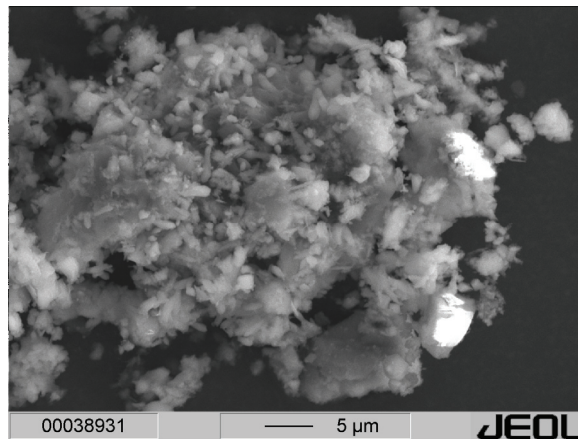


Figure B.14: SEM image showing mixture of cement(G) and fly ash

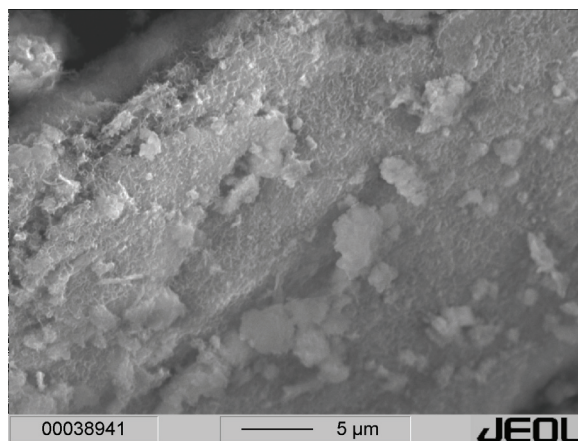


Figure B.15: SEM image showing mixture of cement (G), fly ash and salt solution

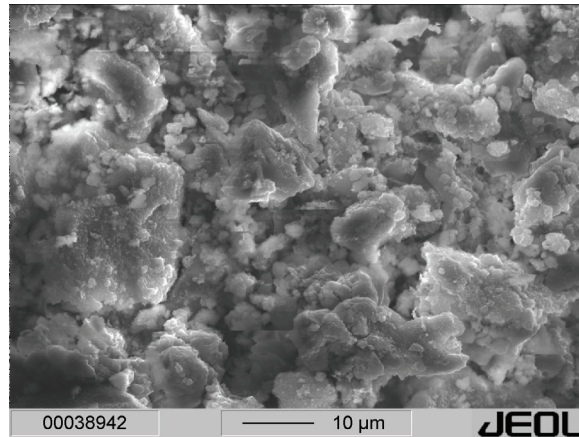


Figure B.16: SEM image showing mixture of cement (C) and fly ash (C)

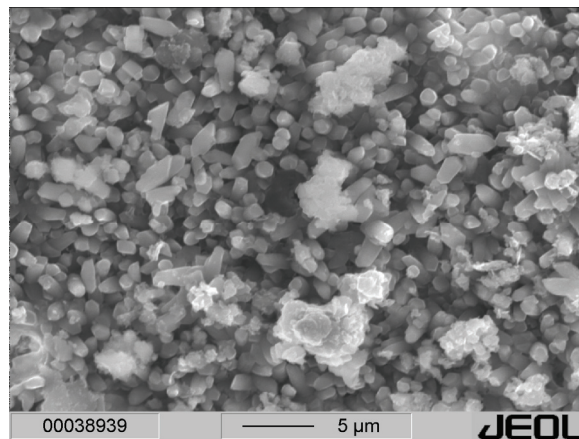


Figure B.17: SEM image showing mixture of cement (C), fly ash (C) and salt solution

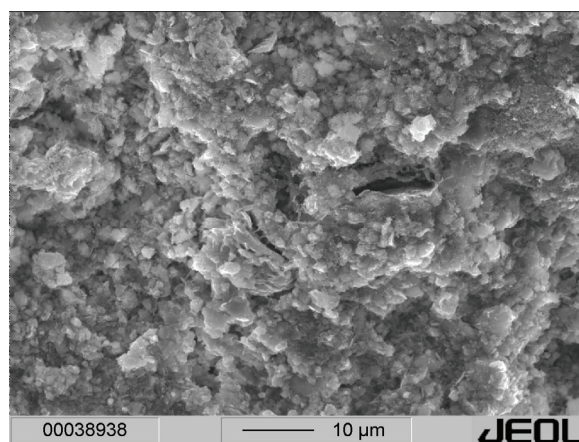


Figure B.18: SEM image showing mixture of cement and filter dust



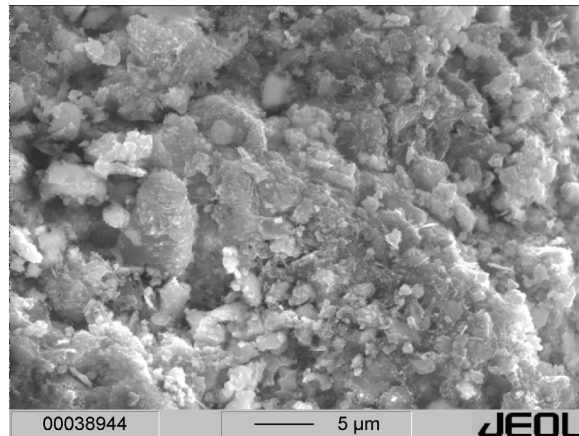


Figure B.19: SEM image showing mixture of cement, filter dust and fly ash

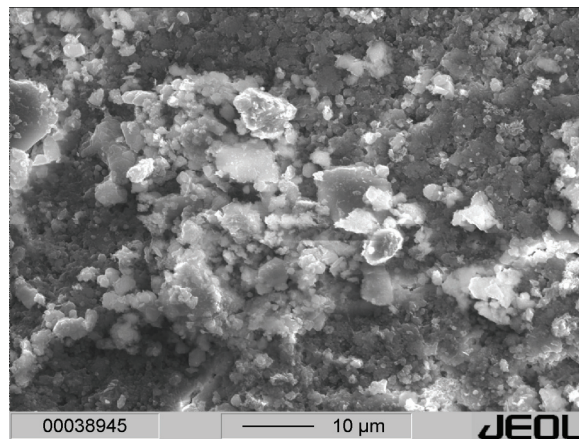


Figure B.20: SEM image showing mixture of cement, filter dust, fly ash and salt solution

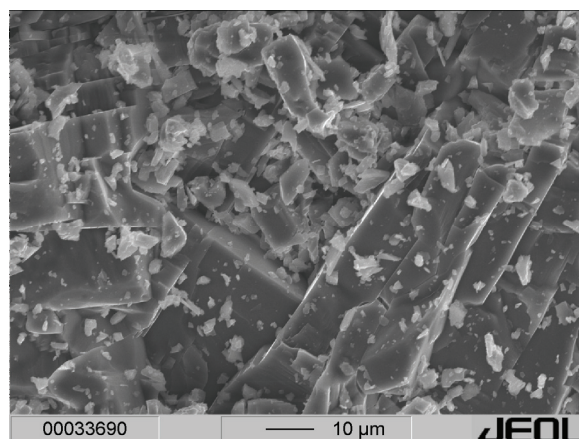


Figure B.21: SEM image showing mixture of FGD-Gypsum and fly ash

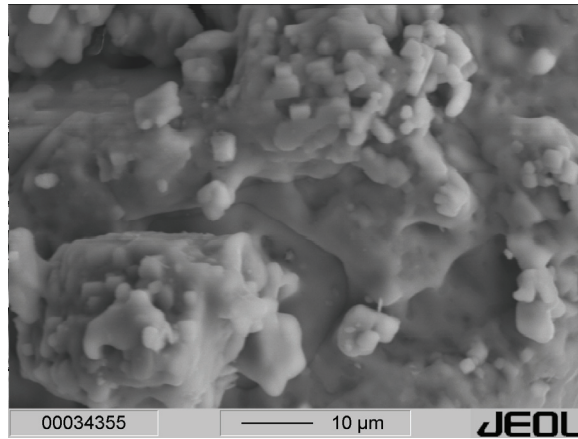


Figure B.22: SEM image showing mixture of FGD-Gypsum, fly ash and salt solution

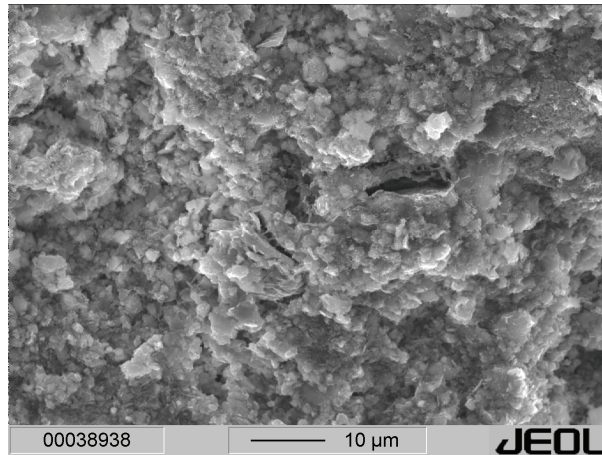


Figure B.23: SEM image showing mixture of tailing, fly ash and salt solution

## Appendix C

### German standard of underground waste stowage

**Table C.1: Limit value concentrations for metals in wastes**

Elements	Concentration (g/kg)
Zinc ( <i>Zn</i> )	>= 100
Lead ( <i>Pb</i> )	>= 100
Copper ( <i>Cu</i> )	>= 10
Tin ( <i>Sn</i> )	>= 15
Chromium ( <i>Cr</i> )	>= 150
Nickel ( <i>Ni</i> )	>= 25
Iron ( <i>Fe</i> )	>= 500

**Table C.2: Limit value for solids**

Elements/compound	Concentration (mg/kg dry in mass)
Mineral hydrogen carbon	1,000
BTEX (Aromatic compound)	5
LHKW (Highly volatile halogenated hydrocarbons)	5
PAHs (Polychluclear aromatic hydrocarbons)	20
PCB (Polychlorinated biphenyls)	1
Arsenic ( <i>As</i> )	150
Lead ( <i>Pb</i> )	1,000
Cadmium ( <i>Cd</i> )	10
Chromium, total ( <i>Cr total</i> )	600
Copper ( <i>Cu</i> )	600
Nickel ( <i>Ni</i> )	600
Mercury ( <i>Hg</i> )	10
Zinc ( <i>Zn</i> )	1,500
Cyanide, total ( <i>CN<sup>-</sup> total</i> )	100

**Table C.3: Correlation values for solids**

Elements/compounds	Concentration in (mass %)
Organic proportion of the dry residue of the original substance , detesmined as	
TOC	<= 6
LOI	<= 12

**Table C.4: Limit values for eluates**

Inorganic substances	Concentration in ( µg/l )
Arsenic ( <i>As</i> )	10
Lead ( <i>Pb</i> )	25
Cadmium ( <i>Cd</i> )	5
Chromium, total ( <i>Cr</i> )	50
Hexavalent chromium ( <i>Cr VI</i> )	8
Copper ( <i>Cu</i> )	50
Nickel ( <i>Ni</i> )	50
Mercury ( <i>Hg</i> )	1
Zinc ( <i>Zn</i> )	500
Cyanide, total ( $CN^-$ )	50
Cyanide, readily releasable ( $CN^-$ )	10

Organic substances	Concentration in ( µg/l )
PAHs, total	0.2
-Naphthalene	2
Highly volatile halogenated hydrocarbons, total	10
PCB, total	0.05
Mineral oil hydrocarbons	200
BTEX	20

## Appendix D

### Methods of Analysis

**Table D.1: Methods of analysis – solids**

Analysis parameter	Method	Standard	Publication date
pH	soil quality	DIN ISO 10390	May 1997
dry matter	soil quality, determination of dry matter and water content on a mass basis- Gravimetric method	DIN ISO 11465	December 1996
cyanide, total	soil quality	E DIN ISO 11262	June 1995
arsenic	determination of arsenic by atomic absorption spectrometry (AAS) – hydride technique	DIN EN ISO 11969	November 1996
cadmium chromium copper nickel lead zinc	atomic absorption spectrometry (AAS) for all metals  inductively coupled plasma atomic emission spectroscopy (ICP-AES) for all metals	DIN ISO 11047  DIN EN ISO 11885	June 1995  April 1998
mercury	water analysis AAS cold vapour technique	DIN EN 1483 DIN EN ISO 12338	August 1997 October 1998
mineral oil hydrocarbons	n-alkanes (in the range of C10 - C39), isoalkanes, cycloalkanes and aromatic hydrocarbons (gas chromatography)	DIN EN 14039	Draft December 2000
highly volatile halogenated hydrocarbons	sum of the halogenated C1 and C2 hydrocarbons gas chromatography with electron capture detector (GC-ECD)	DIN EN ISO 10301	August 1997
benzene and its derivatives (BTEX)	BTEX-highly volatile halogenated hydrocarbons (benzene, toluene, xylene, ethylbenzene, styrene, cumen)	DIN 38407, Part 9	May 1991
polynuclear aromatic hydrocarbons (PAC)	soil quality, method using high-performance liquid chromatography (HPLC) HPLC or gas chromatography with mass spectrometer (GC-MS)	DIN ISO 13877  Code of practice no.1,LUA-NRW *)	January 2000  1994
polychlorinated biphenyls (PCB)	German standard methods for the examination of water, waste water and sludge – Sludge and sediments (group S)	DIN 38414, Part 20	January 1996
TOC	determination of organic and total carbon after dry combustion (elementary analysis). This standard refers to soil and is therefore also applicable to mineral wastes.	DIN ISO 10694	August 1996
loss on ignition		DIN 38414, Part 3	November 1985

**Table D.2: Methods of analysis– eluates**

Analysis parameter	Method	Standard	Publication date
pH	German standard methods for the examination of water, waste water and sludge; physical and physico-chemical parameters (group C); determination of the pH-value (C5)	DIN 38404, Part 5	January 1984
electrical conductivity	German standard methods for the examination of water, waste water and sludge; water quality; determination of electrical conductivity	DIN EN 27888	November 1993
total solids residue	German standard methods for the examination of water, waste water and sludge; general measures of effects and substances (group H); determination of the total solids residue, the filtrate solids residue and the residue on ignition (H 1)	DIN 38409, Part 1	January 1987
cyanide, total cyanide, readily releasable	German standard methods for the examination of water, waste water and sludge; anions (group D); determination of cyanides (D 13) spectral photometry	DIN 38405, Part 13 E DIN ISO 11262 E DIN ISO 14403 DIN 38405, Part 13 DIN 38405, Part 14	February 1981 June 1995 May 1998 February 1981 December 1988
arsenic	water quality - determination of arsenic with atomic absorption spectrometric method (hydride technique)	DIN EN ISO 11969	November 1996
lead cadmium chromium, total hexavalent chromium (Cr VI) copper nickel zinc	German standard methods for the examination of water, waste water and Sludge cations (group D) -determination by atomic absorption spectrometry (AAS) -determination by inductively coupled plasma atomic emission spectrography (ICP-AES)	DIN 34806, Part 6 DIN EN ISO 5961 DIN EN 1233 DIN EN ISO 10304-3 DIN 38406, Part 7 DIN 38406, Part 11 DIN 38406, Part 8 for all elements: DIN EN ISO 11047 DIN EN ISO 11885	July 1998 May 1995 August 1996 November 1997 September 1991 September 1991 October 1980 June 1995 April 1998
mercury	water quality AAS cold vapour technique	DIN EN 1483	August 1997
BTEX	GC-FID	DIN 38407, Part 9	May 1991
PCB, total	GC-ECD GC-ECD or (GC-MS)	DIN EN ISO 6468 DIN 51527, Part 1 DIN 38407, Part 3	February 1997 May 1987 July 1998
PAHs, total DIN		38407, Part 8	October 1995
naphthalene	GC-FID or GC-MS	DIN 38407, Part 9	May 1991
mineral oil hydrocarbon	extraction by petroleum ether, GC-FID	ISO/TR 11046	June 1994

# Practical techniques to improve the air quality in underground stone mines

R. H. Grau III, T. P. Mucho, S. B. Robertson, A. C. Smith & F. Garcia  
*National Institute for Occupational Safety and Health (NIOSH), Pittsburgh Research Laboratory, Pittsburgh, PA, USA*

**ABSTRACT:** Researchers working for the National Institute for Occupational Safety and Health (NIOSH) at the Pittsburgh Research Laboratory are developing ways to protect the health of miners. Part of that effort is devoted to improving the air quality in underground stone mines by developing ventilation techniques that can be used in these types of operations. The air quality in these large opening nonmetal mines can be significantly improved by using diesel particulate matter (DPM) controls along with sufficient ventilation quantities to remove contaminants. Practical methods of ventilating these underground stone mines can be accomplished by using mine layouts that course and separate ventilation air through the use of stoppings. The design, construction, and maintenance of effective stoppings in large openings have been a real challenge to mine operators. Several different types of stoppings have and can be used for this application. The choice of stopping design, material used, and construction techniques should be dependent upon a number of factors such as the intended life and effectiveness desired.

## 1 INTRODUCTION

The National Institute for Occupational Safety and Health (NIOSH) conducts research into various mining health and safety issues to provide the basis for improvements to U.S. miners' health and safety. As part of this role, researchers at the NIOSH Pittsburgh Research Laboratory (PRL) are developing methods and technologies to improve the air quality for large opening underground metal/nonmetal mines. This paper discusses NIOSH/PRL research dealing with ventilation techniques that will be applicable to large opening mining operations. Furthermore, the paper describes concepts that can be incorporated into the overall ventilation design of these mines. The most common underground large opening mines are underground stone mines followed by underground rock salt mines. Surveillance data from the Mine Safety and Health Administration (MSHA) for the year 2000 shows that there were 162 active nonmetal underground mines in the United States, of which, 117 were stone mines and 13 were rock salt mines.

The continuing and emerging air quality issues in metal/nonmetal mines include silica dust, diesel particulate, fog and fumes. The concentration of these contaminants can be effectively reduced by utilizing various control technologies along with adequate air quantities and proper ventilation methods. A growing concern by various health agencies is the health risks

associated with exposure to diesel particulate matter (DPM). It is generally accepted by various regulatory agencies, ACGIH (2001), NIOSH (1988), EPA (2000), and confirmed by the United States Congress, as to the health hazards of exposure to diesel particulate matter. As this concern grows, the mining community is confronted with new DPM regulatory exposure limits. MSHA recently addressed these health concerns by promulgating underground diesel regulations for coal and metal/nonmetal mines, MSHA (2001). The standard was developed to reduce the health risks associated with exposure to DPM. Our view is that the metal/nonmetal DPM exposure limits proposed by the regulations of  $400_{10} \mu\text{g}/\text{m}^3$  on July 19, 2002 and a more stringent limit on January 12, 2006 to  $160_{10} \mu\text{g}/\text{m}^3$  will impel the use of diesel emissions control technology, and in many cases, some form of ventilation improvement to meet these new air quality standards. The most common ventilation knowledge and techniques that are utilized in coal and some metal mines are not readily adaptable to large opening mines. The large openings in many mines offer little ventilation resistance to air flow. However, this low resistance permits large air quantities to move through the large opening mines at extremely small mine (fan) pressures. From an engineering design perspective, this large air quantity, small pressure scenario should play an integral part in the overall mine ventilation design scheme.

## 2 FUNDAMENTALS OF IMPROVING VENTILATION IN LARGE OPENING MINES

Previous literature (Head 2001; Grau 2002) has documented the necessity for the large air volumes that are required to effectively dilute DPM concentrations to meet the proposed regulatory standards established by MSHA. In addition to the large air requirements, effective planning for the placement of ventilation equipment and control devices, such as fans and stoppings are necessary to effectively ventilate the large opening mines. Determining the required air quantity throughout the mine is the first and most important elements for planning effective underground mine ventilation. Although many mining activities produce contaminants that enter the mine air, the greatest concern is with the DPM created from the diesel engines used to power the equipment operating in these U.S. mines. Most likely, if the DPM concentrations are reduced or diluted to concentrations that comply with the proposed regulatory standards, the other contaminant concentrations will also be in compliance. The research at NIOSH indicates that there is no single fix or approach to reduce DPM concentrations within these large opening mines, however, providing at least the minimum ventilation quantities to areas with operating diesel equipment plays a crucial role in diluting DPM concentrations. Therefore, we believe, that for the foreseeable future, the eventual DPM regulatory exposure limits will be the dominant parameter driving ventilation requirements for these mines.

## 3 DESIGNING EFFICIENT VENTILATION SYSTEMS

The fundamental principle of mine ventilation is that air movement is caused by differences in air pressure. The pressure difference results from either natural ventilation pressures or a mechanical fan(s) or a combination of both. There are currently large variations in the methods used by U.S. underground large opening mine operators to develop air movement. The methods vary from reliance on natural ventilation forces to the use of main mine fan(s) or combinations of both. In addition, auxiliary jet fans (free standing) are often used in most of these systems for local areas or to assist and direct the main mine currents. Since natural ventilation is a product of the differences in densities of air columns in and around mine openings, natural ventilation is largely variable and uncontrolled. The direction and magnitude of natural ventilation will change frequently, often several times in a day and certainly seasonally in temperate climates. Therefore, mines that rely solely on natural ventilation as the primary source of

ventilation have a highly uncontrolled ventilation system. It should be noted that natural ventilation is better than no ventilation and natural ventilation may provide satisfactory air exchanges in some circumstances or in some parts of the mine. Natural ventilation has been helpful in some large opening drift stone mines with multiple entries and in parts of mines that have been extensively benched. Even with small differences in elevation, natural ventilation alone can promote large volume air movement and mine air exchanges, although in an uncontrolled manner. In areas that have become extensively benched, the large void created may actually create an "air reserve." Although this air reserve can become gradually contaminated with DPM, the natural ventilation does provide some ventilation relief during working hours and clean out the system during off shift times. Jet fans positioned in proper locations may enhance this exchange process. However, jet fans in other portions of the mine are often positioned working against the natural ventilation flow direction. This results in inadequate air flow and uncontrolled recirculation. In most cases, using natural ventilation as a primary ventilation source is a haphazard affair usually with unknown results.

To effectively improve the air quality in these underground mines, sound ventilation planning needs to be incorporated into the overall mine planning process. For instance, mechanical main mine fans, auxiliary fans, stoppings, and a general ventilation concept should be integrated into mine layouts and mining sequences. Also, special ventilation considerations, such as production faces, shops, benching areas, and haulage routes should be considered in this mine planning process. Criteria for proper fan selection, installation and operation for both main mine fans and auxiliary fans should be considered. Fan characteristics of pressure and quantity should be matched for the operation. Fan effectiveness is increased dramatically when used in conjunction with stoppings. Utilizing stoppings to build air walls helps control the mine ventilation flow, i.e., efficiently directing the air to where it's needed the most. The air walls also separate the intake and return airways. Stoppings can be made from man-made materials, leaving areas of intact rock to act as stoppings, or by filling an opening with waste material.

Fan and stopping locations need to be an integral part of the mine layout. Stopping and air wall locations will often need to be built, taken down or moved with changes in mining areas and/or in concert with a predetermined sequence of a mining and accompanying ventilation scheme. This would include methods to ventilate the active faces, while providing adequate ventilation to any special needs area noted above. The overall ventilation concepts for these types ventilation concepts are discussed more fully in Grau (2002). Other important factors that reduce DPM at



the face area are selecting cleaner burning diesel engines and planning the truck haulage routes. Effective planning of haulage routes will reduce DPM from truck haulage which is the single largest source of DPM in many underground stone mines.

#### 4 DETERMINING SUFFICIENT AIR REQUIREMENTS

The first step to designing an effective ventilation system in underground stone mines is to determine the total air quantity that is needed for effective dilution of DPM and other contaminants. As previously noted, although many different mining activities emit noxious contaminants and require dilution, the result of the new DPM regulations will be that the overriding ventilation design parameter is for the dilution of DPM. In addition, even though the total theoretical air quantity needed to dilute these contaminants can be estimated for adequate dilution, sufficient quantities of air must be distributed to areas where contaminants are being generated. Therefore, certain mining operations may require auxiliary fans to adequately dilute the DPM at the source. Methods to determine the mine air requirements for DPM dilution are described by both Haney (1998); Grau (2002). Grau (2002) reported that the estimated air quantity required for the equipment currently operating in an underground stone mine producing 113 million metric tons (1.25 million tons) is 401 m<sup>3</sup>/s (850,000 cfm) to dilute to a 400 µg/m<sup>3</sup> concentration and 990 m<sup>3</sup>/s (2,100,000 cfm) to dilute to a 160 µg/m<sup>3</sup> concentration. These conclusions were based on the current equipment, controls, etc being used. The air quantities may be too high for practical mine ventilation, however the required air quantity is highly dependent upon the engines in use and as previously described, the extremely large volume of the bench area may reduce the air flow required. It should be noted that engines of an older vintage are less efficient. As an engine ages, the combustion process degrades, which lowers the fuel economy and promotes higher emissions. Mine operators can dramatically decrease air requirements by selectively replacing the engines with a lower DPM emissions or by adding control measures to engines that emit the most DPM. This significant difference defines why additional research is needed to define more accurate estimates of air requirements.

The goal for many mine operators in the near future will be to have their mine be in compliance with the DPM regulations. We expect that, over time, this will be a process of implementing both DPM control measures and ventilation techniques. Operators are looking at different scenarios in both areas to determine where the most DPM reduction can be achieved in the best practical way. As they move

through this iterative process, they will likely make ventilation changes to their mine and also gradually replace the older high DPM emitting engines with new cleaner burning engines. The operators should factor these scenarios into their mine planning process.

#### 5 FAN SELECTION

Many underground limestone mines are drift mines developed from previous quarry operations. Typically, these room and pillar mines have entries that are 6.1 m (20 feet) or higher and at least 12.2 m (40 feet) wide. These large dimensions lead to a very small pressure loss, even when significant air quantities move through the mine. This is especially true of the drift mine operations where our observations found that pressure differences of less than a 24.9 Pa ((0.1 in of water gauge, (w.g.)) are not uncommon, no matter whether these mine are ventilated by natural ventilation, a mechanical fan(s) or combinations of both. Our observations also indicate that the underground stone mines with slope/decline and shaft operations that are less than 70 m (200 ft) in depth, have small mine pressure differences, usually less than 746 Pa (3 in w.g). These differences are or could be much lower if the proper consideration was given to the contribution that the slope/decline and shaft provide to the overall mine resistance.

The low pressure loss present in these large opening mines is actually an advantage compared to other type mines and should be treated as such. The ventilation principles, concepts and techniques used to ventilate these mines are different from the techniques used in mines with larger pressure losses. For example, axial vane fans have predominately been used where higher pressures are required. However, in large opening mines with low pressure requirements, propeller fans offer an alternative. The propeller fans can develop large air volumes under low pressure conditions. Propeller fans can be used as either main mine fans or as free standing auxiliary (jet) fans. Free-standing fans are commonly used to promote air movement as shown in Figure 1.

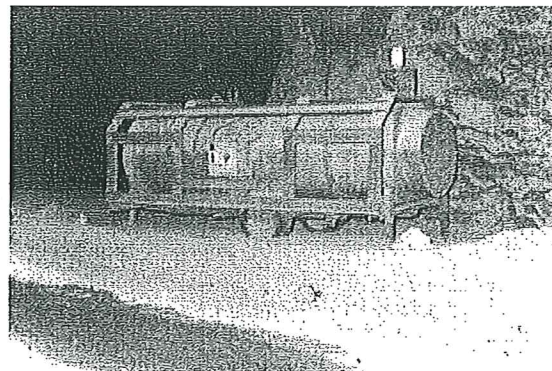


Figure 1. Jet fan.

Ventilation studies by Matt et al. (1978), Agaipito (1985), Goodman (1992) and Foster-Miller (1980) have measured the performance of jet fans (usually axial vane free standing) either in single headings or ventilating portions of the main airways. The research found that the most important aspect for jet fan performance is that the jet fan should be positioned in the intake incoming main air stream so that there is sufficient intake air for the fan. Other important results from these tests showed that the performance of these fans was enhanced by adding a nozzle to the fan. Results were also significantly improved by angling the fan upward and located against a rib when ventilating a dead-ended opening.

## 6 VENTILATION CONTROLS (STOPPINGS)

In order to adequately deliver proper air flows to the face areas, good air controls in the form of stoppings are necessary. Stoppings are physical barriers that separate the intake air from the return air. Since air flows through a mine due to differential pressure between travel points, a pressure difference always exists between the intake and return airways. The stoppings act as a barrier allowing for this pressure differential to exist and circumvent short circuiting of intake air to return air. Currently, in most U.S. large opening mines, stoppings and fans are the only control measures used. Most of these operations are currently using or strive to produce a primary, single mine air current to the active mining faces. However, there are a number of variations, especially for drift operations where natural ventilation and sometimes a number of openings, yields secondary air currents. This single split concept currently eliminates the need for other control measures such as overcasts, regulators and air doors. In many underground mines with large openings, the auxiliary fans are the only control devices used to distribute the air to the face working area.

Stoppings have not been widely used in large opening stone mines. Unfortunately, capital expense, construction, and maintenance problems have impeded this segment of the mining industry from building stoppings. This is particularly problematic in the larger, more established mines. In those mines, stoppings were never incorporated into the mining plan. Retrofitting the mines with stoppings to course the air requires building many stoppings with a corresponding investment in time and construction cost.

Design criteria for stoppings include minimizing the leakage between the intake and return air, withstanding the fan pressure differentials and withstanding or relieving the pressure from face production blasting. Table 1 shows the criteria that are

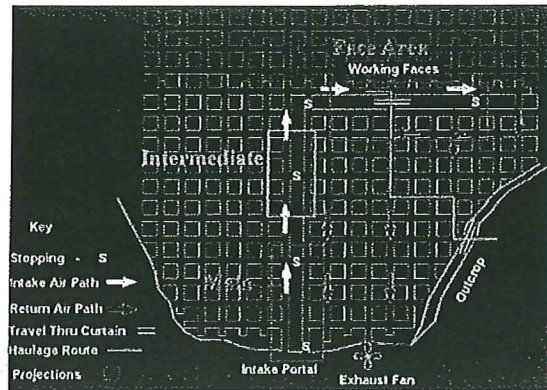


Figure 2. Stopping locations in a typical room and pillar stone mine.

the most important in different parts of the mine. There are three main areas of the mine to consider in determining the type or quality of stopping, the main, intermediate, and the face areas. These areas are shown in Figure 2 for a typical underground stone mine. The stoppings in the main airways will typically have less blast pressure, but since they are usually located near the main mine fan, they are subject to the highest constant pressure differential and thus have the potential for the highest leakage. The stoppings in the main entry will also need to survive the life of the mine, hopefully requiring little maintenance. Minimizing leakage in the main airways prevents a direct short circuit of air to or from the fan. For these reasons, the stoppings located in the main areas of the mine should be substantially constructed. For these stoppings, some form of pressure relief may be needed from production face shots, especially early in their life. This need will often diminish as the active mining advances further away, causing the blast pressures to dissipate with ventilation relief (other openings) and distance.

Table 1 - Stopping criteria for locations in an underground stone mine.

Location in the mine	Fan pressure difference	Blast pressure	Acceptable leakage
Main	Greatest	Little	Low
Intermediate	Significant	Some	Intermediate
Face Area	Lowest	Greatest	Moderate

For underground large opening stone drift mines with multiple entries, the pressure across intake and return air is generally less than 62 Pa (0.25 inch w.g.) as found by Grau (2002). From theoretical ventilation calculations, this pressure differential is greatest near the fan.

Pressures from face production blasts far exceed the ventilation pressure. Tests performed by NIOSH, (Mucho, 2001) found pressures from two different

production face shot, ranged from 8.2738 kPa (1.20 psi) to 9.3769 kPa (1.36 psi) at distances of 200-500 ft from the face shot as shown in Figure 3. The face shots were generated with 400 lbs of ANFO, 169 lb of dynamite and 50 lb of Datagel. Research is continuing at NIOSH to further bracket expected blasting pressures that stoppings could be expected to experience in these types of mines and to define the controlling parameters such as distance and the impact of venting to adjacent openings.

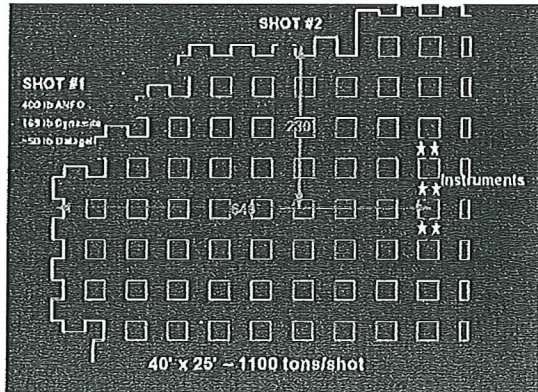


Figure 3. Schematics of tests for measure pressure from face production shots.

Some mines have had success in developing stoppings designed to provide relief from blast pressure. Techniques such as leaving the brattice loose at the floor (and sometimes ribs), using tear away VELCRO strips (Timko 1987), creating openings in the stoppings prior to blasting, and using a combination of used mine belt and brattice have been used. The brattice left loose at the floor simply allows the brattice to fly up when the face shot pressure passes by and returns to the floor when the pressure is through. This technique has been used in some mines near face areas where leakage is not as critical and pressure differentials are lower. Brattice stoppings sealed with VELCRO strips have been developed and used on brattice stoppings in oil shale mines (Timko 1987) and in the NIOSH Lake Lynn Laboratory (Mayercheck 2002). The VELCRO strips separate during the impact of the face shot but they immediately reseal. If sealing is not immediately accomplished, the VELCRO strip seals are manually reconnected after the mine blast. Although they exhibited good success in the Lake Lynn conditions, at least one mine has discontinued their use because of mud and dirt filling the VELCRO and reducing the sealing effectiveness.

## 7 TYPES OF LARGE OPENING STOPPINGS

Stoppings are built from a variety of construction materials. The construction materials are chosen based upon the desired performance, construction time and

ease, and material cost. Construction materials that have typically been used in these mines for stoppings include steel sheeting, cementious-covered fiber matting, mine brattice cloth, used mine belting and piled waste stone.

Used conveyor belting that is no longer useful for material transport can be used to make stoppings. The combination of used belting and brattice have been used effectively in stoppings for both sealing, production face shot relief, and flyrock or other physical damage protection. It has been successfully used as blast relief in a main mine fan bulkhead. Prior to utilizing the mine belt as shown in Figure 4, the mine had several stoppings blown over during production face shots. The mine belt weight and strength allow it to be strong enough to withstand the pressure wave from the face shot but flexible enough to give and act as a pressure relief. Belting hung in this manner should be hung in an overlapping concave pattern to promote interlocking of belting. This technique will minimize air leakage. Figure 5 shows used mine conveyor belt supplementing conventional mine brattice in a stopping. This combination minimizes leakage while providing protection, blast relief, and a more substantial stopping. Conveyor belts could also be used to shield conventional brattice stoppings from the fly rock damage shown in Figure 6.

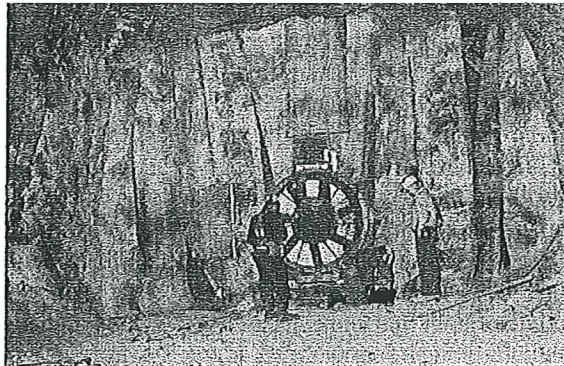


Figure 4. Used mine belt used pressure relief.

Certainly one of the most durable, but also the most costly, for both construction and materials are the corrugated steel panels reinforced with a steel frame as shown in Figure 7. This is the most durable stopping and can be effectively sealed on roof and rib by making a template of the rib and cutting the corrugated sheet to match. The remaining spaces can be filled with expanding foam. One advantage of this stopping is that a swing door can be incorporated into it. This allows for personnel and equipment passage, as well as for blast relief. Besides the cost and time required to install, a disadvantage of this door is that leakage can occur at the door bottom. This might be corrected by adding some type of door sweep.

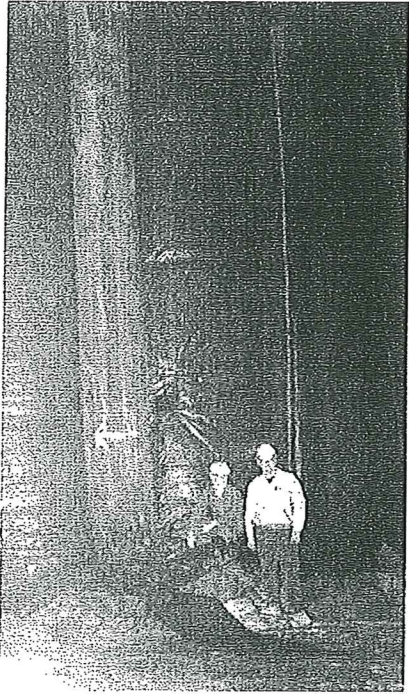


Figure 5. Used mine conveyor belt supplementing conventional mine brattice in a stopping.

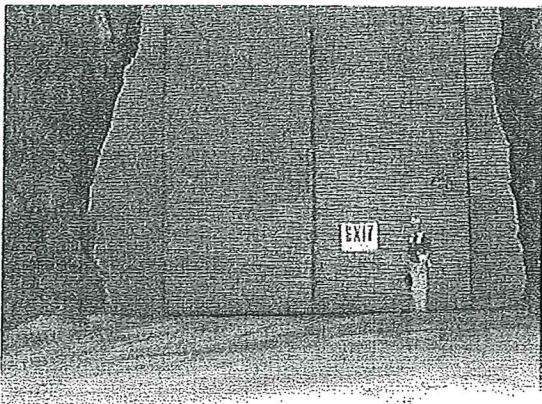


Figure 7. Stopping made for corrugated steel panels reinforced with a steel frame.

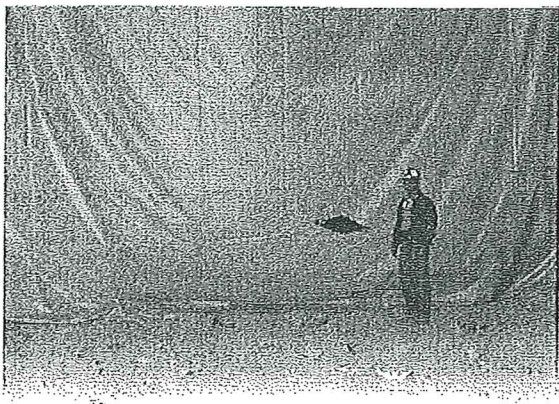


Figure 6. Fly rock damage in brattice cloth.

A less elaborate, but still rigid, stopping is a fiber/mesh covered with cementitious grout as shown in Figure 8. This type of stopping is currently being evaluated in an operating underground limestone mine. This stopping is installed by hanging fabric backed by grid and then sealed by spraying with a water-based cementitious grout on both sides using high pressure grout pumps. Stoppings of this type are still being evaluated for effectiveness by NIOSH researchers.

A prototype stopping being researched by NIOSH is a tension brattice stopping. The stopping is similar to the tension membrane construction methods used to create various fabric covered, large dome stadiums throughout the country. In this stopping, currently being installed and tested at NIOSH's Lake Lynn Laboratory, a brattice material is tensioned and attached to the various steel framework supports, thereby increasing the strength of the structure.

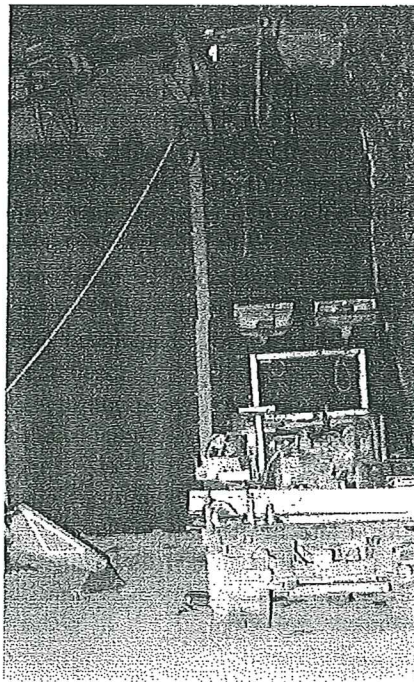


Figure 8. Fabric-grid material sprayed with cementitious material.

## 8 NATURAL ROCK STOPPINGS

Leaving rock in place to form natural rock stoppings has several advantages. By using the natural rock stopping, leakage, construction, and maintenance costs are eliminated. The rock stoppings are created by leaving at least the last face shot that would normally break through two adjoining openings. This keeps a natural rock integrity between the two adjoining pillars. Similar to constructed stoppings, natural rock stoppings between future independent pillars can be strategically oriented to direct the ventilation air. In

order to direct the air, the rock stoppings are oriented parallel to the ventilation flow. Stone production may be temporarily compromised because the stone in the rock stopping is not immediately mined. However, the rock stoppings can be pre-drilled and mined through at a later time for stone recovery, or for other reasons when the particular stopping line is no longer required to course the air.

When using lines of rock stoppings to separate and course the air, openings need to be created every few crosscuts to meet practical mining needs. However, often the natural rock can be left in place along the ribs and back of the final cut that creates these long pillars to serve as a natural framework for the stoppings and to minimize the size of the stoppings. These too can be pre-drilled for future enlargement to normal opening size when the stopping line is no longer needed and/or the area is to be benched. A caution when using this method is the mining horizon for the top or back rock must be carefully chosen so that a ground control problem is not created.

#### 9 CONCLUSIONS

NIOSH is researching various ways to improve ventilation in large opening mines in an effort to assist with methods and techniques to improve the air quality in these mines and therefore the health of miners. NIOSH is currently focusing on fan applications, air coursing, intake and return airway separation using stoppings, and implementing mine ventilation techniques and concepts into the mine planning to accomplish this goal.

Many U.S. underground stone mines are large opening mines that generally feature small ventilation head losses compared to other types of underground mining. Propeller fans are generally well suited to efficiently produce large air quantities under low pressure requirements. Stoppings are necessary to direct and control the mine air. A variety of stopping choices exist for these types of applications and depend upon the quality of the stopping needed. Different portions of the mine may be better suited to different types of stoppings. The use of stone stoppings is being investigated, especially as it relates to their deployment in various stages of the mine

layout. Operators of all underground stone mines should find that this information will improve their ventilation in the underground workings.

#### REFERENCES

- American Conference of Governmental Industrial Hygienists (ACGIH), 2001. Threshold limit values for chemical substances and physical agents and biological exposure indices.
- Grau, III, R.H., Robertson, S.B., Mucho, T.P., Garcia, F., & Smith, A.C. 2002. NIOSH research addressing diesel emissions and other air quality issues in nonmetal mines. In *2002 Society for Mining, Metallurgy and Exploration Annual Meeting, Feb. 26-28, Phoenix AZ.*
- Haney, R., & Saseen, G. 1998. Estimation of diesel particulate concentrations in underground mines. *Preprint 98-146, presented at the Society for Mining, Metallurgy and Exploration Annual Meeting March 9-11, Orlando, FL.*
- Head, R. 2001. Calculating underground mine ventilation fan requirements. *Aggregates Manager, April 2001: 6(3):17-19.*
- Mayercheck, W. 2002. Personnel Communication. Mine Safety and Health Administration (MSHA), U.S. Department of Labor 2001. *Final Rule 30 CFR Part 57. January.*
- Mucho, T.P., Grau, R.H., Robertson, S.B. 2001. Practical mine ventilation. *Presentation at the Safety Seminar for Underground Stone Mines, Louisville, KY, Dec. 5.*
- National Institute for Occupational Safety and Health (NIOSH), Department of Health and Human Services 1988. Carcinogenic effects of exposure to diesel exhaust. *Publication 88-116.*
- Timko, R.J. & Thimons, E.D. 1987. Damage resistant brattice stoppings in mines with large entries. *Engineering Mining Journal: 188(5):34-36.*
- U.S. Environmental Protection Agency (EPA) 2000. Health Assessment Document for Diesel Exhaust. Report EPA/600/8-90/057E, July.

# **USE OF COAL COMBUSTION PRODUCTS IN MINE-FILLING APPLICATIONS: A REVIEW OF AVAILABLE LITERATURE AND CASE STUDIES**

DOE Award No: 99-CBRC

Final Report

(November 1999 – March 2005)

*Prepared by:*

Ishwar P. Murarka

Ish Inc.  
804 Salem Woods Drive, Suite 201B  
Raleigh, NC 27615-3313

Jim Erickson

GeoTrans Inc.  
363 Centennial Parkway  
Louisville, CO 80027

October 2006

## **DISCLAIMER**

This report was prepared as an account of work sponsored by an Agency of the United States Government. Neither the United States Government nor an agency thereof, nor any of their employees, makes any warranty, express or implied, or assumes any legal liability or responsibility for the accuracy, completeness, or usefulness of any information, apparatus, product, or process disclosed, or represents that its use would not infringe privately owned rights. Reference herein to any specific commercial product, process, or service by trade name, trademark, manufacturer, or otherwise does not necessarily constitute or imply its endorsement, recommendation, or favoring by the United States Government or any agency thereof. The views and opinions of authors expressed herein do not necessarily state or reflect those of the United States Government or any agency thereof.

## **ACKNOWLEDGEMENT**

The authors are grateful for funding for this technical report preparation provided by the following organizations:

DOE-CBRC

Public Service Company of Colorado

American Coal Ash Association (ACAA)

McDonald Farms

Utility Solid Waste Activities Group (USWAG)

Ish Inc.

Geo Trans Inc.

# TABLE OF CONTENTS

EXECUTIVE SUMMARY .....	iii
1.0 INTRODUCTION.....	1
1.1 Scope of the Research.....	2
1.2 Report Contents .....	2
2.0 PHYSICAL AND CHEMICAL COMPOSITION OF CCPs .....	2
2.1 Physical Characteristics .....	2
2.2 Chemical Composition and Leaching Characteristics.....	3
2.3 Physical and Hydraulic Characteristics of Mine Spoils .....	3
2.4 Premined Area Water Quality .....	4
2.5 Water Quality in Mined Areas.....	4
2.6 CCP Mine Placement Sites.....	4
3.0 GEOCHEMISTRY OF COAL MINE DRAINAGE AND INTERACTIONS WITH CCPs .....	5
3.1 Coal Mine Drainage.....	5
3.2 INTERACTIONS BETWEEN CCPs AND COAL MINE DRAINAGE .....	5
4.0 CCPs IN COAL MINES .....	6
4.1 Wyodak Mine (WY).....	7
4.1.1 Background.....	7
4.1.2 Local Geology .....	7
4.1.3 Local Hydrogeology and Hydrology.....	8
4.1.4 Ash-Leaching Characteristics.....	8
4.1.5 Groundwater Quality .....	9
4.2 Keenesburg Mine (CO).....	11
4.2.1 Local Geology .....	11
4.2.2 Local Hydrology.....	12
4.2.3 Ash Chemical Characteristics.....	12
4.2.4 Groundwater Quality .....	12
4.3 Trapper Mine (CO).....	13
4.3.1 Hydrogeology .....	14
4.3.2 Ash Chemical Characteristics.....	15
4.3.3 Groundwater Quality .....	16
4.4 Savage Mine (MT).....	17
4.4.1 Local Geology .....	18
4.4.2 Local Hydrogeology .....	18
4.4.3 Ash Leaching Characteristics .....	19
4.4.4 Groundwater Quality .....	19

Continued . . .



**TABLE OF CONTENTS (continued)**

4.5 Storm Strip Mine (WV) ..... 21

4.6 Universal Mine (IN) ..... 22

    4.6.1 Hydrogeology ..... 23

    4.6.2 Chemical Composition of Coal Ash and Leachates ..... 23

    4.6.3 Water Quality-Monitoring Program ..... 24

    4.6.4 Groundwater Quality Results ..... 25

    4.6.5 Surface Water Quality ..... 27

    4.6.6 Summary and Conclusions ..... 28

4.7 Midwestern Abandoned Mine (IN) ..... 29

4.8 The Arnold Willis “City” Underground Coal Mine (IN) ..... 30

4.9 Harwick Mine Complex (PA)..... 31

    4.9.1 Introduction..... 31

    4.9.2 History of Ash Injection in Mine..... 31

    4.9.3 Ash Sluicing and Water Pumping of Operations..... 31

    4.9.4 Coal Ash Characteristics..... 32

    4.9.5 Mine Effluent Characteristics ..... 32

4.10 Clinton County (PA)..... 32

4.11 Big Gorilla Pit (PA)..... 33

    4.11.1 Introduction..... 33

    4.11.2 Mining and Reclamation..... 33

    4.11.3 Regional Acid Mine Drainage Chemistry ..... 34

    4.11.4 Ash Placement and Characterization ..... 34

    4.11.5 Chemical Evolution of the Big Gorilla Mine Lake ..... 35

    4.11.6 Groundwater-Monitoring Well Chemistry ..... 37

    4.11.7 Conclusions..... 38

4.12 Red Oak Mine (OK) ..... 38

4.13 Winding Ridge Demonstration Project at Frazee Mine (MD)..... 39

    4.13.1 Introduction..... 39

    4.13.2 Characteristics of Frazee Mine ..... 39

    4.13.3 Geology and Hydrogeology..... 39

    4.13.4 CCP Grout Mix..... 40

    4.13.5 Grout Injection..... 40

    4.13.6 Pre- and Postinjection Monitoring..... 40

    4.13.7 Conclusion..... 41

5.0 REFERENCES ..... 41

# USE OF COAL COMBUSTION PRODUCTS IN MINE FILLING APPLICATIONS: A REVIEW OF AVAILABLE LITERATURE AND CASE STUDIES

## EXECUTIVE SUMMARY

### **Background**

Surface and underground mining combine to produce over 800 million tons of coal annually, and the vast majority of this coal is burned in utility boilers to generate electricity. Combustion of coal in the utility boilers produces coal combustion residues or products (CCPs) in the form of fly ash, bottom ash, boiler slag, and flue gas desulfurization (FGD) sludge. In the year 2003, U.S. electric utilities produced approximately 122 million tons of CCPs. Coal fly ash constituted about 70 million tons, the bottom ash/boiler slag accounted for about another 20 million tons, and the remaining 30.8 million tons was FGD material. Approximately 62% of the CCPs generated are land disposed. About 38% of the fly ash generated was used within cement/concrete/grout, structural fill, waste stabilization/solidification, mining applications, and road base/subbase, accounting for most of the fly ash volume utilized. About 45% of bottom ash was used mostly in structural fills, road base, snow and ice control, mining application, and cement/raw feed for clinkers. About 96% of the boiler slag was utilized mostly for blasting grit and roofing granules. About 70% gypsum was used mostly for wallboard production. FGD material generated by wet scrubbers was utilized only about 2.75% and dry scrubber-generated FGD material accounted for about 13.5% use.

### *Use of CCPs in Mines*

CCPs possess several physical and chemical properties/characteristics that are beneficial both from environmental and economic standpoints. Mine reclamation represents a potential beneficial use of CCPs that has been receiving increased attention in recent years. Coal mining operations have produced both open pits and deep underground cavities that can be filled by CCPs. Placement of CCPs into deep mines can provide structural support to abate subsidence, and placement of CCPs in surface mines or other open pits can aid in restoring mined land to beneficial use. The use of CCPs as mine backfill may provide the additional potential benefit of limiting impacts of acid mine drainage (AMD). Many CCPs are alkaline materials that can neutralize acidic groundwater and/or inhibit production of acid. Placement of CCPs also may reduce the permeability of mine strata and divert water away from acid-generating materials. Although CCPs possess several beneficial physical and chemical properties, there are concerns from regulators and environmental groups regarding potential for release of toxic chemicals in the leachates from the CCPs. Therefore, scientifically sound information is needed so that environmental concerns can be adequately and reliably identified and addressed.

### *CBRC and Cofunders*

Ish Inc. and GeoTrans, Inc., were selected by the Combustion Byproducts Research Consortium (CBRC) to conduct research that will compile and synthesize information from several case studies involving CCP usage for mine applications for dissemination to inform regulators,

environmental interest groups, and the generators of CCPs about the benefits and impacts of CCP use for mine filling. CBRC provided funding for this research project, with additional cofunding by the Public Service Co. of Colorado, McDonald Farms, American Coal Ash Association, Utility Solid Waste Activities Group, GeoTrans, Inc., and Ish Inc.

### **Report Content and Results of Literature Search**

This report contains information gleaned from literature on chemical and physical characteristics of CCPs produced in the United States along with some information on mine spoil material. This report also contains background information on coal mines and a brief discussion of the geochemistry of coal mines particularly to describe the formation of AMD. A summary of available data on water quality characteristics of mined areas is presented. A brief description of the geochemical interactions between the AMD water and CCPs is also presented in this report.

A summary list is presented of mine sites where CCPs are being utilized for filling the mined land and/or for abating AMD conditions.

Beneficial use of CCPs for coal mine reclamation occurs in varying degrees across the United States. Injection of CCPs into deep mines has been performed to provide structural support for subsidence abatement, and placement of CCPs in surface mines has been utilized to reclaim mined land to original grade and to mitigate AMD. Such practices have been employed at both active and abandoned coal mines.

Several surface and deep mines in the midwestern and western United States that have utilized CCPs for reclamation are identified in this report. These mines include the Keenesburg and Trapper Mines (CO); Wyodak, Glen Rock, and Rock Springs Mines (WY); Midwestern Abandoned Mine and Arnold Willis City Mine (IN); Big Gorilla Pit (PA); Winding Ridge Frazee Mine (MD); Savage Mine (MT); and Universal Mine (IN). Active mining operations continue to occur at the Trapper, Wyodak, and Savage Mines. Types of CCPs placed at these mines include fly ash, bottom ash, and FGD materials.

Thirteen mines were selected based on availability of site-specific data required to perform a reasonable evaluation of the benefits and impacts of CCP placement on groundwater quality. Tables and graphs are included, when available, to illustrate important aspects of each case study. These case studies represent a large range of CCP uses from filling of mine pits to using CCP grout mix to minimizing/eliminating acid mine drainage. A brief summary of each case study follows:

1. Placement of fly ash, bottom ash, and scrubber ash in mined areas at Wyodak Mine began in 1978. Approximately 5,000,000 yd<sup>3</sup> of ash has been placed in 13 separate pits. Results indicate that the average groundwater quality throughout the Wyodak site compares favorably with the Wyoming Department of Environmental Quality (DEQ) Class III (livestock use) standard. Mean concentrations for all of the measured constituents in wells are at or below Class III standards.

2. Reclamation at the Keenesburg site is being performed using fly ash and bottom ash derived primarily from combustion of Keenesburg coal. Ash was placed at least 5 feet above the premining groundwater table, and reclamation includes placement of a vegetative final cover consisting of at least 5 feet of compacted overburden and 3 feet of topsoil material. Upon comparison of water quality in upgradient versus downgradient wells and for sampling events prior to ash placement (1978–1986) relative to sampling events following ash placement (1988–2000), there is little evidence indicating that elevated levels of regulated constituents in site groundwater are a direct result of leaching from the ash.
3. Trapper Mine is a surface coal mine located approximately 6 miles south of Craig, Colorado. Trapper Mine began operation in 1977 and produces up to 2.8 million tons of coal annually. Deposition of CCPs in the mined out areas of A Pit began in 1984. Trapper Mine has managed approximately 390,000 tons of CCPs per year since 1984 with total disposal quantities approaching 7 million tons to date. Current ash placement practices involve deposition of sufficient overburden material into the pit bottom such that the ash is placed above the expected postmining groundwater table. Overburden materials are placed above the ash and revegetated as part of the final reclamation plan. Comparison of the historic groundwater concentration data with Colorado standards indicates little or no evidence of groundwater impacts associated with most of the analyzed constituents.
4. Savage Mine has been in operation since 1958 as a surface lignite mine and currently produces 250,000 tons of lignite annually. Savage Mine began utilizing fly ash and bottom ash as backfill in 1987. The annual volume of ash received by the Savage Mine is variable and dependent upon the amount of coal burned by Holly Sugar in relation to the quantity of sugar beets processed. The estimated cumulative volume of ash placed between 1987 and 2000 is approximately 130,000 cubic yards.
5. The Mount Storm case study is about placement of coal ash in an active coal strip mine. The downgradient groundwater-monitoring data reveal no evidence of contamination over the 10-year period of operation. Coal ash (both bottom ash and fly ash) is being placed at a rate of about 800,000 tons annually in an active strip mine near an electric power plant in West Virginia. The strip mine provides coal for the power plant and is located on the plant property. Ash placement began in 1987. No ash has been placed below the water table because the groundwater table is deeper than the mine floor.
6. In 1988, PSI Energy, Inc. (now Cinergy Corporation) acquired a portion of the Universal Mine site containing the final cut pit for the express purpose of coal ash deposition and surface mine reclamation. Indiana Department of Natural Resources (DNR) issued a permit to PSI Energy to dispose of fly ash/bottom ash from its nearby Wabash River Station to fill and reclaim the mine pit. Between April 1989 and the end of October 2001, Cinergy placed approximately 1.6 million tons of coal ash from a nearby power plant to completely fill the open pit. The monitoring data to date indicate that the alkaline coal ash leachate has been effective in improving AMD water

quality that was present at the site. The coal ash leachate neutralized the acidic pH, increased alkalinity, essentially eliminated acidity, and significantly decreased manganese, iron, and sulfate concentrations. There were no indications of any other trace metal migration via the mine seep. However, the coal ash leachate did significantly increase boron concentrations in the mine seep water.

7. The Midwestern Abandoned Mine is a case study where a state agency elected to place CCPs with a Poz-O-Tec (a mixture of FGD sludge, fly ash, and quicklime) cap, which resulted in reduced infiltration and improvement in water quality by neutralization. The Midwestern Abandoned Mine consists of approximately 550 acres of previously mined land, which in some instances intersects with abandoned deep mining of the same coal seam. Based on the monitoring results, Branam et al. (1999) it was concluded that using CCPs to reclaim the Midwestern Abandoned Mine has resulted in the reduction of AMD leaving the site. This response is ascribed to the reduction in vertical recharge of oxygenated water by the fixated scrubber sludge cap and the neutralization provided by the alkaline CCPs.
8. The Arnold Willis City Underground Coal Mine in Indiana is an example in which fixated scrubber sludge (FSS) has been successfully injected into an abandoned underground coal Mine for stabilization by filling mine voids. Groundwater-monitoring data indicated that trace metals and sulfide remained unaffected by the placement of FSS. An FSS grout consisting of a mixture of FGD scrubber sludge, fly ash, lime, and water was developed for injection into the abandoned deep mine to abate surface subsidence and reduce acid mine drainage. A total of 12,502 m<sup>3</sup> of FSS was injected over an 8-week period, resulting in filling of about 5 acres of the mine.
9. The Harwick Mine Complex includes the Monarch, Old Harwick and Cornell Mines covering approximately 7000 acres. This coal mine is a deep mine and was operated from about 1932 through 1970. The mine disposal operation consists of a wet ash-handling system to pump 10% solids slurry for a distance of approximately 8000 ft to two operating injection boreholes at the Harwick Mine Complex. Approximately 3 to 4 million gallons per day of the slurry is conveyed. Approximately 150,000 tons of coal ash is injected annually into the mine along with millions of gallons of water. The water quality data from samples of the mine water indicate no adverse effect on the water in the Harwick Mine Complex.
10. The Clinton County, Pennsylvania, Mine provides an example of the placement of fluidized-bed combustor (FBC) ash in a closed surface coal mine resulting in beneficial effects on water quality because of the favorable geochemistry that occurs. The alkaline FBC ash neutralizes the acidic AMD waters, resulting in precipitous decreases in arsenic, cadmium, and aluminum concentrations as a result of lower solubility and precipitation of solids. Results indicate that the injection of grout caused a temporary increase in pH from about 2.3 to about 9 as the alkaline FBC ash neutralized the acidic AMD waters. However, within a short time the pH again became acidic, with sulfate and aluminum returning to the pregrouting concentrations, although arsenic and cadmium remained at much lower levels.

11. In eastern Pennsylvania, there are several preact stripping pits in the middle of an anthracite coal basin where active strip and deep mining for coal was practiced since the 1800s. The strip mined pit known as Big Gorilla was one such location. The Pennsylvania Department of Environmental Protection's Regional Mining office in conjunction with the Wilkes-Barre Regional office issued a demonstration permit for the placement of cogeneration-derived dry fly and bottom ash into standing water in the Big Gorilla Pit. Ash deposition has taken place since August 1997. Over 3 million tons of ash was used to completely fill the pit which contained an acid mine water pool. The Big Gorilla water has maintained a consistently high pH value in response to the placement of ash. Iron, manganese, magnesium, aluminum, and zinc all have decreased significantly. One long-term effect of ash placement in the former Big Gorilla Mine pool will be the prevention of acidic water production through the surface mine pool.
12. The Red Oak Coal Mine was operated from 1907 to 1925 utilizing the room-and-pillar extraction method. The mine which covers approximately 46.5 acres contains water pools or reservoirs of AMD. The University of Oklahoma and the Oklahoma Conservation Commission injected 418 tons of FBC ash in 15 hours into this acidic (pH 4.3) flooded mine to chemically alter the mine water.
13. The Maryland Department of Natural Resources Power Plant Research Program and the Maryland Department of Environment Bureau of Mines launched a joint effort with private industry to demonstrate large-volume beneficial uses of CCPs to create flowable grouts for placement in abandoned, underground coal mines to reduce acid formation. In April 1995, this multiyear project initiative started with the Winding Ridge Demonstration project involving injection of a 100% CCP grout into the Frazee Mine, located near Friendsville, Garrett County, MD. The Winding Ridge Demonstration project at the Frazee Mine has shown that CCP grout mixture can be beneficially used for abandoned underground coal mines to reduce acid formation as well to fill mine voids with a high-strength, low-permeability material that would control mine subsidence. The placement of the CCP grout appears to have not caused an unacceptable water quality impact either.

## **Conclusions**

This literature review report on the use of CCPs in mine-filling activities provides a readily available resource for regulators, the general public, environmental interest groups, and potential users of CCPs by synthesizing technical information on a range of case studies. Each case study is different in several details and provides the readers insights into the use of CCPs from benefits and limitations standpoints. The technical information can be used to determine and decide on environmentally compatible uses of CCPs in surface and underground coal mines.

# USE OF COAL COMBUSTION PRODUCTS IN MINE FILLING APPLICATIONS A REVIEW OF AVAILABLE LITERATURE AND CASE STUDIES

## 1.0 INTRODUCTION

Coal is a widely distributed fossil fuel across the United States. Surface and underground mining combine to produce over 800 million tons of coal annually, and the vast majority of this coal is burned in utility boilers to generate electricity. Combustion of coal in the utility boilers produces coal combustion residues or products (CCPs) in the form of fly ash, bottom ash, boiler slag, and flue gas desulfurization (FGD) sludge. In the year 2003, U.S. electric utilities produced approximately 122 million tons of CCPs. Coal fly ash constituted about 70 million tons, the bottom ash/boiler slag accounted for about another 20 million tons, and the remaining 30.8 million tons was FGD material (American Coal Ash Association [ACAA], 2004). Approximately 62% of the CCPs generated are land disposed. About 38% of the fly ash generated was used in cement/concrete/grout, structural fill, waste stabilization/solidification, mining applications, and road base/subbase, accounting for most of the fly ash volume utilized. About 45% of bottom ash was used mostly in structural fills, road-base, snow and ice control, mining application, and cement/raw feed for clinkers. About 96% of the boiler slag was utilized mostly for blasting grit and roofing granules. About 70% gypsum was used mostly for wallboard production. FGD material generated by wet scrubbers was utilized only about 2.75% and dry scrubber-generated FGD material accounted for about 13.5% use.

The CCPs possess several physical and chemical properties/characteristics that are beneficial both from environmental and economic standpoints. For example, fly ash has been used in the manufacture of portland cement, as a cement substitute in concrete, and as a stabilizing agent in road bases and subbases because of its wide availability and pozzolanic nature. Compacted fly ash also is considered a good candidate for structural fill on compressible ground since it is strong and durable but lighter than conventional fill materials. Gray et al. (1991) investigated the use of fly ash in slurry wall backfill mixtures and observed that these mixtures can exhibit high sorptive capacity for nonpolar organic pollutants. In addition, other researchers have investigated the potential use of CCPs in waste containment liners and have shown that it is possible to achieve hydraulic conductivity values below  $10^{-7}$  cm/s using compacted fly ash alone or in conjunction with sand and/or bentonite (Gray et al., 1991).

Mine reclamation represents another potential beneficial use of CCPs that is receiving increasing attention in recent years. Coal-mining operations have produced both open pits and deep underground cavities that can be filled by CCPs. In addition, non-coal-mining operations (e.g., limestone, clay, sand and gravel) result in the creation of open pits. Placement of CCPs into deep mines can provide structural support to abate subsidence, and placement of CCPs in surface mines or other open pits can aid in restoring mined land to beneficial use. Use of CCPs as mine backfill may provide the additional potential benefit of limiting impacts of acid mine drainage (AMD). Many CCPs are alkaline materials that can neutralize acidic groundwater and/or inhibit production of acid. Placement of CCPs also may reduce the permeability of mine strata and divert water away from acid-generating materials (Kim and Cardone, 1997).

## **1.1 Scope of the Research**

Mine reclamation has been identified as a long-term, large-volume beneficial use market for CCPs. Nonetheless, the use of CCPs in mine reclamation currently is performed on a limited basis relative to the overall quantity of CCPs generated each year. Only 0.68 million tons of fly ash, 1.2 million tons of bottom ash and about 0.39 million tons of FGD materials were used in mining applications in year 2003 (ACAA, 2004). Although CCPs possess several beneficial physical and chemical properties, there are concerns from regulators and environmental groups regarding potential for release of toxic chemicals in the leachates from the CCPs. Therefore, scientifically sound information is needed so that environmental concerns can be adequately and reliably identified and addressed.

Ish Inc. and GeoTrans, Inc., were selected by the Combustion Byproducts Research Consortium (CBRC) to conduct research that will compile and synthesize information from several case studies involving CCP usage for mine application for dissemination to inform regulators, environmental interest groups, and the generators of CCPs about the benefits and impacts of CCP uses for minefilling. CBRC provided funding for this research project, with additional cofunding by the Public Service Co. of Colorado, McDonald Farms, ACAA, the Utility Solid Waste Activities Group, GeoTrans, Inc., and Ish Inc.

## **1.2 Report Contents**

This report contains compilation, synthesis, and limited evaluation of the available information from a number of mine sites where CCPs have been or are being used to fill the mined lands. This report contains a brief summary of physical and chemical composition of CCPs produced in the United States along with some information on mine spoil material. This information is presented in Section 2. Section 2 also contains a summary list of mine sites where CCPs are being utilized for filling the mined land and/or for abating AMD conditions. Section 3 contains a brief discussion of geochemistry in coal mines particularly to describe the formation of acid mine drainage. A brief description of the geochemical interactions between the AMD water and CCPs is also presented in this section. Section 4 contains summaries of case studies for which environmental monitoring information was obtained from the operators/owners of the sites. In Section 5, conclusions and recommendations are presented.

## **2.0 PHYSICAL AND CHEMICAL COMPOSITION OF CCPS**

### **2.1 Physical Characteristics**

CCPs include fly ash, bottom ash, FGD materials, and boiler slag. These different types of CCPs represent approximately 58%, 15%, 25%, and 1.5%, respectively, of the total CCPs produced in the United States in 2000 (ACAA, 2004). The smaller ash particles contained in flue gas are referred to as fly ash and are collected by air pollution control equipment such as electrostatic precipitators. The fly ash consists primarily of particles between 5 and 100  $\mu\text{m}$  in size. Fly ash comprises spherical, glassy particles comparable in size to silt and/or fine sand. Larger particles that fall to the bottom of the boiler result in the production of bottom ash or



boiler slag. Bottom ash is a coarser-grained material, with particle sizes comparable to sands and gravels. Boiler slag and bottom ash consist of particles ranging from 100  $\mu\text{m}$  to 10 mm. FGD materials are generated when some of the sulfur in the flue gas is removed. Wet FGD systems generate waste with a particle size range of 0.001 to 0.05 mm, whereas the dry systems produce waste with particle size in the 0.002- to 0.074-mm range. FGD gypsum is also produced at some of the power plants from sulfur removal activities.

The physical properties of CCPs have been well characterized. Fly ash particle morphology has been extensively investigated by scanning electron microscopy with four general categories describing most particles: 1) cenospheres, 2) plerospheres, 3) spherical particles with crystals, and 4) irregularly shaped solid particles. The fly ash exhibits light to dark colors. The bottom ash and boiler slag are black or gray in color.

Reported specific gravity for most coal fly ash and bottom ash falls between 2.2 and 2.6, and the bulk density ranges between the values of 80 and 90  $\text{lb}/\text{ft}^3$ . Crushed boiler slag has been reported to have high hydraulic conductivity (permeability) equivalent to that of fine gravel. Bottom ash permeability ranges from  $10^{-3}$  to  $10^{-1}$   $\text{cm}/\text{sec}$ . Fly ash material exhibits permeability typically in the range of  $10^{-6}$  to  $10^{-4}$   $\text{cm}/\text{sec}$  that is similar to that for silty-clay soils.

## **2.2 Chemical Composition and Leaching Characteristics**

Numerous studies have been completed to provide data on the chemical composition of CCPs. Oxides of silicon, iron, aluminum, and calcium account for about 95% of the weight of the bottom ash, fly ash, and boiler slag. Magnesium, potassium, and sodium are also present in the ash. The FGD sludge is composed mostly of calcium and sulfur when limestone/lime is used to scrub the flue gas. All CCPs also contain trace amounts of many metals. A comprehensive elemental characterization study of samples of fly ash, bottom ash, and FGD sludge was completed by the Electric Power Research Institute (EPRI) in 1987. Table 2.1 provides the summary of the chemical concentration data from the EPRI study. This study did not contain data on Boron in CCPs. The presence of boron in CCPs, however, is well documented.

Western coal fly ash and FGD sludge are typically alkaline and possess acid neutralization properties which make them useful materials for abating acid mine drainage and for filling mined land for reclamation. Additional available chemical characteristic data and information on alkaline CCPs and their use in minefilling are included in the individual case study summaries later in this report.

## **2.3 Physical and Hydraulic Characteristics of Mine Spoils**

Both underground and surface mines generate mine spoils of varying physical and chemical composition. In the surface mine setting, the mine pits are reclaimed by the replacement of the spill material as well as in permitted cases by CCPs. The mine spoil material is composed of excavated overburden sandstone, clays, and shale as well as coal remnants. The mine spoil material can contain pyritic material and/or high-sulfur reject material. The mine spoil is a heterogeneous and anisotropic material leading to the presence of variable hydraulic conductivity. Aljoe and Hawkins (1994) reported that increasing percentages of sandstone and

decreasing percentages of shale in mine spoil appear to yield higher-hydraulic-conductivity values. This may be due to the presence of larger-sized rock fragments in the sandstone-rich spoil zones than shale-rich zones. Shales break into smaller fragments and readily weather to create silt and clay particles which yield lower hydraulic conductivities. Aljoe and Hawkins (1994) also reported that hydraulic conductivity of the mine spoils may increase with spoil age. They observed that reclaimed mine spoil 30 months or less old had a significantly lower median hydraulic conductivity than reclaimed mine spoil that was over 30 months old. Rehm et al. (1980) reported that spoil permeability decreases with age. Their results are from the northern Great Plains region, compared to the Aljoe and Hawkins (1994) results from eastern coal fields. Hydraulic conductivity for surface mine spoils exhibits a broad range of values. A summary table (Table 2.2) prepared by Hawkins (2002) captures the available hydraulic conductivity data for surface mine spoils.

#### **2.4 Premined Area Water Quality**

Groundwater and surface water quality data for premined areas are sparsely available. Strippable coal and lignite deposits are prevalent in the Denver and Laramie Formations in the Denver Basin. Kirkham and O'Leary (1980) reported water quality data collected from monitoring wells in Watkins (Adams/Arapahoe County), Bijou Creek (Elbert County), Keenesburg (Weld County), and Matheson (Elbert County) areas. These chemical analysis results are shown in Table 2.3. Brady et al. (1996) and Hawkins et al. (1996) have given a summary of shallow groundwater quality in unmined regions of the northern Appalachian Plateau.

Examination of these premined area groundwater quality results indicates the presence of low to quite high concentrations of sulfate, sodium, iron, manganese, and total dissolved solids (TDS) in groundwater with a significant amount of alkalinity and neutral to alkaline pH.

#### **2.5 Water Quality in Mined Areas**

Numerous studies have been carried out around the United States to characterize water quality from surface and subsurface mined areas. Much of the water quality data deals with coal mine drainage. Coal mine drainage can be either acidic or alkaline. AMD is typically elevated in SO<sub>4</sub>, Fe, Mn, Al, and a few other elements.

#### **2.6 CCP Mine Placement Sites**

A survey questionnaire was developed and sent out to solicit information on CCP mine placement sites. Follow-up phone calls and individual contacts were made to identify over 100 mine sites where CCPs have been or are being placed in the previously mined areas. As a result, Table 2.4 has been developed to list the mine sites where CCPs were or are being used to fill the mined areas. Most of the identified sites are either surface or underground coal mines. Environmental monitoring data were obtained for a subset of these sites and are summarized to the extent possible in this report.

### **3.0 GEOCHEMISTRY OF COAL MINE DRAINAGE AND INTERACTIONS WITH CCPs**

#### **3.1 Coal Mine Drainage**

Coal mines represent an environmental setting where the mining of coal generates coal refuse and exposes pyritic material present in the coal. Coal mine drainage results when rainwater and drainage water undergo chemical reactions with the coal refuse, pyrites, and overburden material. AMD occurs by the oxidation of pyrite to release dissolved  $\text{Fe}^{2+}$ ,  $\text{SO}_4^{2-}$ , and  $\text{H}^+$ , followed by further oxidation of  $\text{Fe}^{2+}$  to  $\text{Fe}^{3+}$ , generating more  $\text{H}^+$ . The oxidized  $\text{Fe}^{2+}$  precipitates as iron hydroxide solid giving rise to the orange–yellow color in the areas where the precipitates are deposited.

Coal mine drainage can be acidic or alkaline, typically with relatively high concentrations of sulfate, iron, manganese, and aluminum. The pH of the coal mine drainage water commonly is either in the range of 3 to 4.5 s.u. or 6 to 7 s.u. (standard unit). Obviously, more abundant pyrite material in the overburden correlates to a more acidic pH of the coal mine drainage.

The major source of acidity is, therefore, due to the oxidation of pyrite that gets exposed to humid air and/or aerated water when mining activities break rocks and move the overburden material. AMD water contains elevated levels of dissolved  $\text{SO}_4$ , Fe, Al, and Mn, is typically low in pH, and may have elevated concentrations of arsenic, copper, nickel, and zinc (U.S. Bureau of Mines, 1994; Caruccio et al., 1994, Evangelou, 1995). Caruccio and Geidell (1978) reported that pyrite can range in grain size between 400  $\mu\text{m}$  and 5 mm. Oxidation of pyrite is a complex set of reactions involving both abiotic geochemical and biotic microbial reactions (Figure 3.1). At low pH (<4.5), pyrite is oxidized by  $\text{Fe}^{3+}$  much faster than by oxygen.

Neutral or alkaline mine drainage has alkalinity that equals or exceeds acidity because of the neutralization reactions with carbonate minerals such as calcite and dolomite. The alkalinity imparted by the dissolution of carbonate minerals promotes the removal of Fe, Al, and other dissolved metals while neutralizing the acidity. The neutral or alkaline mine drainage water still contains elevated amounts of sulfate. Table 3-1 shows median postmining water quality data for several mine sites in Pennsylvania to illustrate the acidic and alkaline coal mine drainage water quality.

#### **3.2 Interactions Between CCPs and Coal Mine Drainage**

If acidic CCPs are placed in coal mines with AMD, then the low pH and acidity in the AMD water could increase leaching or release of some metals in the CCPs. When alkaline CCPs are placed in coal mines with AMD, then the AMD is neutralized by the CCPs. The primary base cations in CCPs that provide alkalinity are calcium and magnesium. The dissolution of the base cations from CCPs results in neutralization and increase in pH of the AMD, which in turn decreases the concentrations of other heavy metals in the AMD.

The most obvious effect of alkaline CCPs on AMD is the reduction of iron. As soon as the pH of the neutralized AMD water is about 6.5 and higher, iron solubility decreases and iron oxide or iron hydroxide precipitates are formed as red or orange flocculants. The formation of iron hydroxide further helps in the coprecipitation/adsorption of metals such as As, Ni, Cd, and Cr.

However, most of the sulfate found in the AMD water is likely to remain in solution, although some precipitation of sulfate may occur when enough calcium or barium is present to precipitate gypsum or barite.

The net effect of placing alkaline CCPs in abandoned coal mines is expected to be beneficial in most situations. The pH of the water is likely to increase, and concentrations of most metals in the AMD are expected to decrease.

#### **4.0 CCPs IN COAL MINES**

Beneficial use of CCPs for coal mine reclamation occurs in varying degrees across the United States. Injection of CCPs into deep mines has been performed to provide structural support for subsidence abatement, and placement of CCPs in surface mines has been utilized to reclaim mined land to original grade and to mitigate AMD. Such practices have been employed at both active and abandoned coal mines.

Several surface and deep mines in the midwestern and western United States that have utilized CCPs for reclamation are identified in Table 2.4. These mines include Keenesburg and Trapper Mines (CO), Wyodak Mine (WY), Savage Mine (MT), Midwestern Abandoned Mine and Arnold Willis City Mine (IN); Big Gorilla Pit (PA); Winding Ridge Frazee Mine (MD); and Universal Mine (IN). Active mining operations continue to occur at Trapper, Wyodak, and Savage Mines. Types of CCPs placed at these mines include fly ash, bottom ash, and FGD materials.

Several case studies to assess the advantages and disadvantages associated with beneficial use of CCPs in mine reclamation are presented in this section of the report. These mines were selected based on availability of site-specific data required to perform a reasonable evaluation of the benefits and impacts of CCP placement on groundwater quality. Tables and graphs are included, when available, to illustrate important aspects of each case study. Following is the list of case studies included in this report:

1. Wyodak Mine, WY
2. Keenesburg Mine, CO
3. Trapper Mine, CO
4. Savage Mine, MT
5. Storm Strip Mine, WV
6. Universal Mine, IN
7. Midwestern Abandoned Mine, IN
8. Arnold Willis City Mine, IN
9. Harwick Mine Complex, PA
10. Clinton County, PA
11. Big Gorilla Pit, PA
12. Red Oak Mine, OK
13. Winding Ridge Frazee Mine, MD

## **4.1 Wyodak Mine (WY)**

### ***4.1.1 Background***

The Wyodak Mine is an active, above-ground coal mine located approximately 5 miles east of Gillette, Wyoming. Approximately 69 million tons of coal was mined at Wyodak between 1922 and 1990, and the estimated remaining minable quantity of coal within the permit boundary exceeds 100 million tons. The total permitted area of the mine is 5811 acres. The Wyodak coal seam is classified as subbituminous and ranges between 20 and 100 feet in thickness. The overburden thickness above the coal seam ranges from 20 to 200 feet, with thin overburden (i.e., 20–100 ft) in the southern area of the site and thicker overburden (i.e., 100–200 ft) in the northern area of the site.

Placement of fly ash, bottom ash, and scrubber ash in mined areas at Wyodak Mine began in 1978 and is expected to continue through 2009. The ash is received from three nearby power plants, i.e., Neil Simpson I, Neil Simpson II, and Wyodak. Annual quantities of each ash type generated at the three power plants are listed in Table 4.1.

Bottom ash currently is slurried to an on-site disposal pond that is dredged periodically to remove material for use as mine backfill. Fly ash from the Neil Simpson I power plant is mixed with bottom ash and either slurried to the disposal pond or placed directly in the pits. The commingled fly/bottom ash also may be intermixed with spoil material prior to backfilling. Scrubber ash (i.e., mixed fly ash and FGD sludge) is obtained from the Wyodak and Neil Simpson II power plants and is placed directly as pit backfill. Upon completion of ash placement, backfilled mine areas are covered with soil and revegetated. Approximately 5,000,000 yd<sup>3</sup> of ash has been placed in 13 separate pits listed in Table 4.2.

Active ash placement operations are ongoing in Area 4 (1998–2009) near the center of the site at an annual placement rate of nearly 250,000 yd<sup>3</sup>. Ash-filling operations began at the base of each mined-out pit. As indicated in Table 4.2, pits filled from 1980 to 1982 in Area 2 represent “unencapsulated” cells in which no soil liner was constructed at the base of the cells prior to ash placement. In the southern area of the site, pits filled with ash prior to 1980 (Area 1) and after 1983 (Area 3) were lined with compacted clay materials selected from appropriate overburden, interburden, and/or underburden soils. Clay liners with a maximum hydraulic conductivity of  $5 \times 10^{-7}$  cm/s were required for these mines as a result of a relatively thin layer of overburden (i.e., less than 20 feet) between the mined-out pit floors and the groundwater table. The unlined pits (Area 2) and the lined pit filled in 1983 (Area 3) are located beneath the floodplain of Donkey Creek.

### ***4.1.2 Local Geology***

The Wyodak site is located within the Powder River Basin. The Eocene Wasatch Formation comprises the overburden at the site ranging from 10 to 200 feet in thickness and consisting primarily of fine-grained clays and siltstones with discontinuous cross-bedded sandstone and scoria beds. The scoria beds were formed from baked and fused shale and clay in the Wasatch. The Wyodak coal seam forms outcrops in the eastern side of the permit region and

generally comprises the uppermost Paleocene Fort Union Formation unit. Approximately 400 feet of interbedded claystone, siltstones, and shale underlies the coal. The coal and underlying sedimentary units form outcrops in the eastern portion of the site.

#### ***4.1.3 Local Hydrogeology and Hydrology***

The shallow hydrologic system in the Powder River Basin primarily comprises five permeable units: 1) lenticular sands in the Fort Union Formation, 2) the Wyodak coal seam, 3) lenticular sands in the Wasatch Formation, 4) scoria beds in the Wasatch formation, and 5) Quaternary alluvium. Each of these water-bearing units produces water at the site. The most significant source of shallow groundwater within the Fort Union Formation at the site is a sandstone unit that is less than 100 feet thick and occurs 360 to 380 feet beneath the Wyodak coal seam. Interbedded claystones, siltstones, and shale are located between the coal seam and sandstone unit. The Wasatch Formation is saturated in the mine permit area, although it is not considered to be a significant source of groundwater because of its relatively low permeability. Secondary permeability created by fracturing has produced yields for some domestic and stock wells. However, groundwater from the coal beds on-site typically is not suitable for domestic use.

Surface water hydrology within the mine permit boundary is controlled by Donkey Creek, which is located in the southern portion of the permit region and has a drainage area of about 77 square miles upgradient of the permit area. Donkey Creek flows to the east and is a tributary of the Belle Fourche River.

#### ***4.1.4 Ash-Leaching Characteristics***

Laboratory tests on fly ash and bottom ash samples were performed on several occasions over the past two decades in support of reclamation activities at the Wyodak Mine. In 1983, a laboratory column leaching study was performed on crushed Wyodak bottom ash and overburden material (i.e., mine spoils). The test was performed first by permeating site groundwater through a column of overburden material and analyzing the effluent for the constituents listed in Table 4.3 to establish representative postmining water quality conditions in the absence of CCP placement. The effluent from the overburden column then was passed through a column of crushed bottom ash and analyzed for the same chemical constituents.

The results provided in Table 4.3 indicate that effluent from the overburden meets Wyoming Class III livestock use standards for all constituents, but exceeds Class I domestic use standards for TDS, Mn, NH<sub>3</sub>, and SO<sub>4</sub>. Permeation through the bottom ash resulted in an increase in some of the regulated constituents, including pH, TDS, B, Cl, Cr, Cu, NO<sub>2</sub>/NO<sub>3</sub>, and SO<sub>4</sub>. Effluent from the bottom ash meets Class III standards for all constituents with exceedances occurring for B (6.97 mg/L relative to 5.0 mg/L) and SO<sub>4</sub> (3060 mg/L relative to 3000 mg/L). Concentrations of several constituents decreased upon permeation through the ash. For example, Mn exceeded the Class I domestic use standard (0.13 mg/L relative to 0.05 mg/L) in effluent from the overburden column but was not detected in the effluent after exposure to the ash.

Additional laboratory leaching analyses of Wyodak bottom ash and scrubber ash were conducted in 1997 and 1998, respectively, using a sequential batch extraction procedure in which ash samples were mixed with site groundwater at an ash-to-water ratio of approximately 1:20 (i.e., 100 g ash:2000 mL groundwater) (Aqua Terra 1997, 1998). This ash-to-water ratio in the batch test is not representative of expected field leaching conditions as compared to the ash-to-water ratio in a column test. However, the batch method of testing is considered to yield more conservative leaching results than column testing, since more of the ash surface area is exposed to the groundwater.

The results of the Wyodak ash batch leaching tests, summarized in Table 4.4, indicate that pH values tend to be elevated relative to the groundwater prior to testing. The results further indicate that maximum postextraction concentrations of all constituents in the bottom ash test, except for Mn and NH<sub>3</sub>, are below current Wyoming Class III livestock-watering standards. Concentrations of both Mn and NH<sub>3</sub> in the groundwater also exceeded the Class III limits prior to ash exposure. As observed in the column test, the concentration of Mn in the groundwater decreased from 1.29 mg/L before ash exposure to 0.07 mg/L after ash exposure, a value that is only slightly higher than the Class III standard of 0.05 mg/L.

The postextraction groundwater in the scrubber ash test was above Class III standards for pH, Cr, F, Fe, Mn, and NH<sub>3</sub>. However, concentrations of Fe, Mn, and NH<sub>3</sub> in the groundwater exceeded Class III standards prior to ash exposure. In both tests, postextraction concentrations exceed Class I domestic use standards for TDS, B, Mn, NH<sub>3</sub>, and SO<sub>4</sub>. Of these constituents, only B was below the Class I standard in the groundwater prior to ash exposure.

#### ***4.1.5 Groundwater Quality***

Groundwater quality at the site is present within alluvium, upper and lower coal, Wasatch, scoria, Fort Union Formation, and sandstone (beneath the coal) units. Groundwater quality from the coal is classified as calcium sulfate-type water with significant bicarbonate and magnesium content. Groundwater derived from the coal is used for livestock purposes and is considered to be of better quality in the northern and eastern portions of the site where the coal seam is not split. Groundwater derived from scoria at the site is magnesium–sodium sulfate-type water, and alluvial groundwater is magnesium–sodium–calcium–sulfate-type water.

Monitoring wells are distributed within the different units both inside and outside of the permit boundary and also within or near ash-filled pits. Well LF-5 is located in close proximity to unlined pits in Area 2, and Well M-11 is located within the lined pit in Area 3 that received ash in 1998 and 1999. Well M-9 is located in Area 4, which comprises the largest unlined pit and is scheduled for ash placement until 2009. It is unclear which portions of Area 4 have already received ash. Wells M-1, M-1A, M-2, M-3, M-4, M-5A, and M-8 are located in an unmined region within the permit boundary to the north of Area 4. This area may be filled with ash in the future. Wells M-6, M-6A, M-16, M-17, M-18, M-19, M-22, M-23, and M-29 are located along the southern perimeter of the site outside of the mine permit boundary.

Results of groundwater quality analyses for samples collected from several of the Wyodak mine area monitoring wells are available for the period 1981 to 1999. Metal analyses also were

performed on a more limited basis from 1977 to 1981. These results are utilized herein as a basis for evaluating the groundwater quality at the Wyodak site. Groundwater quality information prior to mining operations is not available.

A summary of groundwater quality for regulated analytes in Wyoming is presented in Table 4.5 for selected wells. Wells were selected on the basis of data availability and well proximity to ash-filled pits in order to provide a representative cross section of groundwater quality across the site (e.g., mined versus unmined regions, upgradient versus downgradient locations). Local groundwater gradients appear to follow local topographic trends northward across the site. Monitoring Wells M-1A and M-5A were selected to represent the northern unmined area downgradient of ash backfill areas. Monitoring Well M-12 is located upgradient of ash deposition activities in the southern portion of the site. Off-site monitoring Wells M-17 and M-22 are located upgradient of mining and ash backfill areas. Monitoring Well LF-5 is located adjacent to unlined ash fill in Area 2. Although numerous wells are located within Areas 1, 2, and 3, limited analytical data are available for these wells.

Historical maximum and mean value analyte concentrations in groundwater samples from the selected wells are provided in Table 4.5. The Table 4.5 results indicate that the average groundwater quality throughout the Wyodak site compares favorably with the Wyoming Department of Environmental Quality (DEQ) Class III (livestock use) standard. Mean concentrations for all of the measured constituents in wells are at or below Class III standards. The only possible exception is mercury (Hg). Unfortunately, no valid conclusions can be made regarding whether or not mean Hg concentrations exceed the Class III standard of 0.00005 mg/L, since the reported detection limit for Hg in most of the sampling events was 0.001 mg/L. However, maximum Hg concentrations (i.e., maximum of all samples shown in Table 4.5 – Wyodak Mine groundwater quality summary for selected monitoring wells analyzed over time for a particular well) in excess of the Class III standard were observed in all of the selected wells, including the off-site, upgradient wells (M-17 and M-22). These results indicate that elevated Hg levels may be present in upgradient groundwater for this area.

The results in Table 4.5 also illustrate that periodically elevated concentrations of some constituents were observed in wells located near the southern ash-filled pits. For example, the maximum concentrations of TDS and chromium (Cr) measured in Well LF-5 from 1987 through 1999 exceed current Wyoming DEQ Class III standards. Concentrations of As, Cl, Mn, and SO<sub>4</sub> do not exceed Class III standards but appear to be elevated in Well LF-5 relative to the other wells. Well LF-5 is located in the backfill near the unlined ash-filled pits.

Elevated maximum concentrations of Cr and B were observed from 1977 to 1981 in Well M-12, located upgradient of the ash-filled pits in the southern portion of the site. However, these elevated Cr and B concentrations likely are not due to ash placement, since pits closest to M-12 were not filled until 1985 or later. Also, historically high Cr concentrations in off-site, upgradient Well M-17 indicate that elevated Cr may be naturally occurring in this area.

Temporal groundwater quality trends observed in Wells M-1A, M-5A, LF-5, M-17, and M-22 from approximately 1981 to 1999 for B, SO<sub>4</sub>, Mn, and TDS shown in Figures 4.1–4.4. The results indicate that SO<sub>4</sub>, Mn, and TDS concentrations tend to be elevated in Well LF-5, the



nearest well to the unlined pits in the southern portion of the site, relative to the upgradient and downgradient wells. However, LF-5 concentrations in excess of the Wyoming Class III standards were observed only for TDS. Also, lower values of these constituents in downgradient Wells M-1A and M-5A indicate that ash placement has not resulted in significant impacts to regional groundwater quality within the permit boundary to date.

## **4.2 Keenesburg Mine (CO)**

The Keenesburg Mine is located approximately 7 miles north of Keenesburg, Colorado, in Weld County, Sections 25, 26, 35, and 36 of Township 3 North, Range 64 West. The permit area was recently extended to include Sections 2, 11, and 14, Township 2 North, Range 64 West, in 2000 (Correspondence dated 10-30-00 from Byron Walker of the State of Colorado DNR to Colorado Department of Health HMWMD). Coors Energy Company operated coal extraction at the Keenesburg Mine between 1980 and 1988. Approximately 1000 tons was mined from the site daily (Correspondence dated 11-14-86 from John Althouse of Coors Energy Co. to Weld County Commissioners).

Reclamation at the Keenesburg site is being performed using fly ash and bottom ash derived primarily from Keenesburg coal and generated by the Coors Brewery in Golden, Colorado. Ash placement operations began at the Site A pit that is configured in an east-west direction approximately within the mining boundary established in 1985. Ash also was deposited in the north and south ends of B pit after completion of mining operations in 1988. As of 1993, approximately 172,000 tons of ash had been placed in A and B pits at a rate of nearly 30,000 tons/yr. Additional ash placement sites were also utilized between 1987 and 1989. Ash was placed at least 5 feet above the premining groundwater table, and reclamation plans also include placement of a vegetative final cover consisting of at least 5 feet of compacted overburden and 3 feet of topsoil material.

### **4.2.1 Local Geology**

The Keenesburg Mine is located within the Denver structural basin. Documented geologic units at the site include the following, in descending stratigraphic order: quaternary deposits, the Laramie Formation, the Fox Hills Sandstone, and the Pierre Shale. The total thickness of these sedimentary units at the site is estimated at 10,000 feet (Doty and Associates, 1998). Quaternary deposits include Ennis Draw alluvium and dune sand. The Laramie Formation is considered the uppermost bedrock unit at the site and is comprised of yellow-brown and gray to blue-gray, soft, carbonaceous shale and clay-shale interbedded with sand and shaley sand. The lower portion of the Laramie contains thick, continuous coal seams. The Fox Hills Sandstone consists of calcareous marine sandstone with dark gray to black sandy shale and some massive white sandstone. The thickness of the Fox Hills Sandstone reportedly ranges between 60 and 300 feet (Doty and Associates, 1998). Pierre Shale is considered the deepest water-bearing unit of interest at this site. This unit comprises fossiliferous marine shale, silt, and clayey sandstone and is estimated to be over 8000 feet thick.

#### **4.2.2 Local Hydrology**

The major aquifer at the Keenesburg site is the Laramie–Fox Hills Aquifer, with sandstone at the base of the Laramie and the upper portion of the underlying Fox Hills Sandstone. Groundwater flow across the site prior to mining was to the northeast at a prevailing hydraulic gradient of 0.002. Recharge to aquifers within the Denver Basin primarily occurs via outcrop infiltration, while shale deposits in the upper Laramie Formation largely prohibit deep vertical recharge. The estimated average hydraulic conductivity for the Laramie–Fox Hills Aquifer is 0.05 feet/day, with a transmissivity of 8 ft<sup>2</sup>/day (Doty and Associates, 1998). The average hydraulic gradient across the site is 0.002 ft/ft, resulting in an average groundwater flow velocity of about 0.2 ft/yr (assuming 15% porosity).

Sedimentary units that are considered to be of hydraulic significance at the site include the sand and alluvial deposits, overburden, coal, and clayey backfill material (mine spoils) (Doty and Associates, 1998). The sand deposits above the shale are unsaturated and have an estimated hydraulic conductivity of  $1.0 \times 10^{-3}$  cm/s. The Quaternary alluvium is saturated at the site with an estimated hydraulic conductivity of  $10^{-4}$  cm/s. The water-bearing silty claystones and sandstones above the coal deposit in the upper Laramie Formation appear to be hydraulically connected to the alluvium. Coal deposits at the site are saturated, and the estimated geometric mean hydraulic conductivity of the coal is  $9 \times 10^{-5}$  cm/s. The hydraulic conductivity of the spoil material was not available.

#### **4.2.3 Ash Chemical Characteristics**

Chemical analyses were performed on fly ash and bottom ash samples prior to disposal at the Keenesburg Mine. For example, the results of a 1989 extraction analysis on saturated fly ash and bottom ash pastes with an ash-to-water ratio of approximately 1 g to 0.42 g are shown in Table 4.6 (Hazen Research Inc., 1989). The results indicate that the ash samples contain appreciable amounts of alkali/alkaline-earth metals (Ca, Na, K, Mg), sulfate (SO<sub>4</sub>), and trace metals (e.g., B, Cr, Cu, Fe, Pb, Mo, Se, Zn). The fly ash appears to contain greater amounts of many of the analyzed constituents, most notably As, B, Cd, Cr, Mo, Se, and SO<sub>4</sub>. The toxicity characteristic leaching procedure (TCLP) tests performed on fly ash and bottom ash samples indicate that the leached concentrations of the Resource Conservation and Recovery Act (RCRA) metals (Ag, As, Ba, Cd, Cr, Hg, Pb, and Se) would classify these ashes to be a nonhazardous solid waste as shown in Table 4.7 (Hazen Research Inc., 1991).

#### **4.2.4 Groundwater Quality**

Groundwater quality data were collected at the Keenesburg site since the late 1970s, primarily for monitoring Wells AMW-1, AMW-2, DH-96, DH-122, DH-133, DH-172, FPW, and SMW-2. Wells FPW, DH-96, DH-122, DH-133, and DH-172 were completed in the Ennis Draw alluvial aquifer. Wells SMW-2 and AMW-2 were completed in the reclaimed spoil, and Well AMW-1 was completed in undisturbed overburden. Assuming a prevailing northeastern groundwater flow direction, monitoring Wells DH-122 and DH-133 are located upgradient (south to southwest) of ash placement areas, whereas monitoring Wells AMW-1, AMW-2, FPW, DH-96, and SMW-2 are located downgradient (north to northeast) of ash placement areas.

Historic maximum and mean groundwater concentrations measured in monitoring wells prior to ash placement (i.e., 1978–1986) and after ash placement (i.e., 1988–2000) are compared to drinking water and agricultural standards from the Colorado Department of Public Health and Environment (CDPHE) Regulation No. 41 “Basic Standards for Groundwater” in Table 4.8. Regulated analytes for which site data are available include As, Ba, Cl, Fe, Mn, NO<sub>3</sub>, Se, SO<sub>4</sub>, and TDS. The results in Table 4.8 indicate that, on average, concentrations of these analytes historically have exceeded the regulatory standards in at least one of the site wells. Ba is the only analyte that has consistently remained below Colorado Groundwater Protection Standards both prior to and after the placement of ash.

However, upon comparison of water quality in upgradient versus downgradient wells and for sampling events prior to ash placement (1978–1986) relative to sampling events following ash placement (1988–2000), there is little evidence indicating that elevated levels of regulated constituents in site groundwater are a direct result of leaching from the ash. For example, elevated arsenic concentration (0.11 mg/L) was observed in both upgradient Well DH-122 and downgradient Well DH-96. Elevated concentrations of Fe, Mn, NO<sub>3</sub>, and SO<sub>4</sub> also have been measured in upgradient Well DH-122. The results in Table 4.8 also indicate that average concentrations of Cl, Fe, SO<sub>4</sub>, and TDS in downgradient Well SMW-2 for the years prior to ash placement are similar to, if not higher than, concentrations of these constituents measured in the years following ash placement. Thus the results for SMW-2 likely represent impacts to groundwater quality as a result of mining activities rather than placement of ash, which also may be responsible for the elevated concentrations of SO<sub>4</sub> and TDS measured in Wells AMW-1 (downgradient of B pit) and AMW-2 (downgradient of A pit) after 1988. Unfortunately, chemical analysis data prior to ash placement are not available for Wells AMW-1 and AMW-2.

Based upon the above analyses, the groundwater quality at the Keenesburg Mine does not appear to be impacted by placement of CCPs. Moreover, Coors Energy Company was chosen as the 1999 Small Operation Reclamation Award winner as a result of reclamation efforts at the Keenesburg Mine. Currently, the mine is operating under a reclamation-only permit.

### **4.3 Trapper Mine (CO)**

The Trapper Mine is a surface coal mine located on the north slope of the Williams Fork Mountains, approximately 6 miles south of Craig, Colorado. The Trapper Mine began operation in 1977 and produces up to 2.8 million tons of coal annually. A majority of this coal is utilized by the Craig Generating Station, an electric power plant located near the mine.

Surface-mining operations were initiated in the Ashmore Pit (A Pit) in June of 1977. The Queen Anne, the first of three draglines to be put into service at Trapper during the late 1970s, began uncovering two coal seams in the westernmost portion of A Pit. The upper coal seam averaged from 4 to 6 feet in thickness and was typically encountered at overburden depths ranging from approximately 30 to 110 feet. The underlying coal seam varied from 5 to 9 feet in thickness and was separated from the upper seam by approximately 30 feet of overburden. Mining depths for the lower seam ranged from 50 to approximately 160 feet.

Deposition of CCPs in the mined out areas of A Pit began in 1984 with the first ash placement sites located in the Johnson drainage just east of the No Name watershed divide and the No Name drainage. CCP placement at these sites occurred from 1984 through 1986. Additional ash placement sites were subsequently developed just north of the original disposal sites in the Johnson drainage and along the eastern flank of the Johnson drainage. These locations served as ash deposition sites during 1987 and 1988. Ash deposition further south along the eastern flank of the Johnson Gulch drainage began in 1989, progressed to the top of the Johnson drainage in 1993, and followed the mine workings into the East Pyeatt portion of A Pit beginning in 1994 and continuing until today.

The Trapper Mine has managed approximately 390,000 tons of CCPs per year since 1984, with total disposal quantities approaching 7 million tons to date (personal communication with Karl Koehler, Trapper Mining Inc., 2001). Current ash placement practices involve deposition of sufficient overburden material into the pit bottom such that the ash is placed above the expected postmining groundwater table. Overburden materials are placed above the ash and revegetated as part of the final reclamation plan.

#### ***4.3.1 Hydrogeology***

The geology in the vicinity of the Trapper Mine is dominated by the Williams Fork formation that represents the upper portion of the Mesa Verde Group in northwestern Colorado. The Williams Fork Formation is divided into a lower unit, Twenty Mile Sandstone (middle unit), and an upper unit. The Trapper Mine is located on an outcrop of this upper unit, which extends to a depth of approximately 850 feet in the vicinity of the Trapper Mine. Coal seams at the Trapper Mine are located within the upper 20 to 160 feet of the Upper Williams Fork Formation.

The Upper Williams Fork unit primarily consists of siltstones and shale and essentially acts as an aquitard to the Twenty Mile sandstone unit that represents the most productive aquifer in the area. Coal seams and sandstone units within the Upper William Fork Formation also may serve as aquifers for perched groundwater. The alluvial aquifer above the Upper Williams Fork Formation is associated with the Yampa River floodplain to the north and west of the mine site and has an estimated permeability of 67 to 670 ft/day (Radian Corporation, 1991). Based on groundwater levels measured in site monitoring wells in November 2000 (Trapper Mining Inc., 2001), the average groundwater flow direction is north to northwest across the site.

Groundwater recharge in the area occurs via direct infiltration, primarily from snowmelt. The rate of groundwater recharge is relatively low as a result of the climate, which is characterized by a lack of abundant precipitation and a high evaporation rate. Based on the results of a groundwater recharge study, recharge to shallow groundwater (assuming 4 feet of overburden) is estimated to be about 0.6 inches per year (Radian Corporation, 1991). Thus groundwater impacts resulting from infiltration through CCPs placed above the groundwater table are expected to be minor.

### 4.3.2 Ash Chemical Characteristics

Coal combustion products produced at the Craig Generating Station include fly ash, bottom ash, and scrubber sludge materials from combustion of bituminous coal in the boilers. Results of chemical analysis on composite samples of Craig Station fly ash and bottom ash are shown in Table 4.9 (Radian Corporation, 1991). These results illustrate that both the fly ash and bottom ash contain appreciable levels of several constituents, including Al, Ba, Ca, Fe, Mg, P, K, Si, Na, Sr, S, and Ti. Lesser amounts of other trace metals also were detected, including Ag, As, B, Cd, Cr, Cu, Mn, Mo, Ni, Pb, V, and Zn.

Analyses such as those given in Table 4.9 typically are performed by digestion of the ash samples in a strong acid solution (e.g., pH <2) and often are not representative of the expected leaching behavior of the ash, since many of the ash constituents may not be mobilized by leaching fluids that more closely approximate expected field conditions. For example, results of batch extraction tests with acetic acid (pH ~5.0) and distilled water are provided in Table 4.10. Although the results indicate that the fly ash and bottom ash tend to release measurable amounts of SO<sub>4</sub> and several trace metals (Ag, Al, B, Ba, Cr, Fe, Mn, Mo, Ni, V, Zn), comparison of constituent levels with current groundwater quality standards in Table 4.10 reveals that the fly ash tends to release elevated concentrations of only Al, B, Ba, and Cr based on distilled water extraction. No elevated concentrations were leached from the bottom ash. The alkaline nature of the ash materials is evident by final values of pH in the distilled water extraction tests that exceeded the acceptable pH range based on current standards (i.e., 6.5–8.5). Results of the RCRA extraction test indicate that the weak acid leaching tends to mobilize greater quantities of certain constituents from the fly ash. In particular, the concentration of SO<sub>4</sub> increased from <3 mg/L in the distilled water extraction to 90 mg/L in the RCRA extraction.

In order to better assess the potential impact of fly ash placement on groundwater quality, column leaching tests were conducted on fly ash and overburden materials. Column tests typically are more appropriate than batch tests for assessing potential groundwater impacts, since column tests are conducted at an ash-to-water ratio that is more representative of field conditions than the ash-to-water ratio employed in batch leaching tests. In this study, tests were conducted by passing deionized water through separate columns of Craig Station fly ash and unweathered overburden material. In addition, a third column test was conducted by passing deionized water through a fly ash column and subsequently passing the fly ash column effluent through an overburden column. The testing program provided the means to evaluate the individual leaching characteristics of the fly ash and overburden materials and to investigate the ability of the overburden to attenuate the migration of contaminants from the fly ash.

Effluent levels of pH, SO<sub>4</sub>, Al, Ba, B, Cr, Mn, and V measured during the three column leaching tests are illustrated versus cumulative effluent volume in Figures 4.5–4.12. The results indicate that effluent from the fly ash exhibited consistently higher pH and higher concentrations of Al, B, Ba, and Cr than effluent from the overburden. Effluent concentrations of pH, Ba, and Cr from the fly ash column exceeded Colorado State drinking water standards throughout the test, whereas effluent levels of these constituents from the overburden material column essentially were below (or within) the standards throughout the test duration. The test results also indicate that subsequent passage of the fly ash effluent through the overburden resulted in

reductions in pH, Ba, and Cr to below drinking water standards. The overburden also appears to attenuate Al, but exhibits little ability to attenuate B released from the fly ash. Colorado drinking water standards currently do not exist for either Al or B, although regulated agricultural use limits of 5.0 mg/L and 0.75 mg/L, respectively, have been established. Based on these limits, placement of overburden in mined pits prior to placement of fly ash may not reduce the leaching of B from the ash.

The test results also indicate that concentrations of SO<sub>4</sub>, Mn, and V were as high or higher in effluent from the overburden material column relative to the fly ash. The tendency for these constituents to be released from the overburden is illustrated further by the similar leaching trends exhibited in the overburden column test and the test in which the water is passed through the fly ash prior to passage through the overburden. Of these three constituents, SO<sub>4</sub> is the most difficult to assess in terms of groundwater impacts related to ash placement, since initial SO<sub>4</sub> leached from the fly ash and the overburden material are similar. The results in Figure 4.6 show that SO<sub>4</sub> levels may be expected to decline over time to levels below the Colorado drinking water standard (250 mg/L). However, leached concentrations of SO<sub>4</sub> in the early time were higher than the standard. In addition, SO<sub>4</sub> may be released in greater concentrations from the bottom ash based on the batch test data (see Table 4.10), as well as from the scrubber ash that tends to contain more sulfur than both fly ash and bottom ash (Radian Corporation, 1991).

#### **4.3.3 Groundwater Quality**

Groundwater quality monitoring has been performed at the Trapper Mine since 1982 but primarily since 1984, after ash deposition operations were initiated. Historic groundwater quality data are evaluated based on eight groundwater-monitoring wells identified as GD2, GD3, GF4, GF5, GF6, GF7, GF11, and GMP1. Wells GD2, GD3, GF6, and GF11 are upgradient of ash areas, whereas Wells GF4, GF5, GF7, and GMP1 are downgradient of ash disposal. Samples have been collected since 1982 in Wells GD2, GF4, and GF6. Sampling efforts were initiated in the remaining wells between 1984 and 1990. Groundwater samples were analyzed for Al, As, B, Ba, Cd, Cl, Cr, Fe, Mn, Mo, NH<sub>3</sub>, NO<sub>2</sub>+NO<sub>3</sub>, Pb, pH, SO<sub>4</sub>, and TDS. Historic maximum and mean concentrations of these constituents in each of the eight wells are listed along with the respective Colorado groundwater quality standards in Table 4.11.

Comparison of the historic groundwater concentration data with Colorado standards in Table 4.11 indicate little or no evidence of groundwater impacts associated with most of the analyzed constituents, including Al, As, B, Cd, Cl, Cr, NO<sub>2</sub> + NO<sub>3</sub>, and Pb. Historic mean concentrations of iron (Fe) also are not elevated in any of the wells, although elevated individual values have been observed periodically in groundwater Wells GD2, GD3, GF4, GF5, and GF7. None of the historic Fe concentrations measured in any of the wells exceed the agricultural use standard (5.0 mg/L).

Of all the constituents monitored at the Trapper Mine, Mn, SO<sub>4</sub>, and pH have consistently been observed at levels in excess of drinking water standards in Colorado. For example, pH values in excess of the upper limit established by Colorado drinking water standards (i.e., 8.5) historically have been measured in several of the wells, most notably in downgradient Wells GF4 and GF5. Historic maximum and mean values of pH are 9.3 and 8.86, respectively, in Well GF4,

and 9.15 and 8.06, respectively, in Well GF5. Elevated pH values in GF4 and GF5 may represent a groundwater impact related to ash placement, considering the locations of these wells relative to ash areas and the tendency for leachate from the fly ash to exhibit pH values between 10 and 12 (See Figure 4.6).

Excessive mean historic concentrations of Mn have been observed in upgradient Wells GD2, GD3, and GF11 and in downgradient Wells GF4 and GF7. The presence of elevated Mn in both upgradient and downgradient wells suggests that Mn levels reflect the overall postmining groundwater quality at the site and not an impact attributable to ash areas. This observation also is supported by the column leaching test results for Mn in Figure 4.7 that show the tendency for Mn to be mobilized from the mine spoil rather than from fly ash.

Elevated mean historic concentrations of SO<sub>4</sub> are evident in upgradient Wells GD3 and GF11 and in downgradient Well GF7. Historically high SO<sub>4</sub> levels in both upgradient and downgradient wells indicate that elevated SO<sub>4</sub> is characteristic of the overall postmining groundwater quality at the site. However, the historic mean SO<sub>4</sub> concentration in downgradient Well GF7 (1,581 mg/L) is considerably higher than the historic mean SO<sub>4</sub> concentrations in upgradient Wells GD3 and GF11 (435 mg/L and 569 mg/L, respectively). Given that the ash represents a significant source of sulfur (see Table 4.9) and mobilization of SO<sub>4</sub> from ash samples has been observed in leaching studies (see Table 4.10 and Figure 4.6), the higher concentration of SO<sub>4</sub> in Well GF7 may be due, in part, to ash disposal operations. However, the column test results also show that significant SO<sub>4</sub> may be mobilized from the mine spoil.

#### **4.4 Savage Mine (MT)**

Knife River Corporation's Savage Mine is located approximately 20 miles southwest of Sidney, Montana, and about 4 miles northwest of Savage, Montana, close to the North Dakota border. The Savage Mine has been in operation since 1958 as a surface lignite mine, and it currently produces 250,000 tons of lignite annually. The mine primarily serves the Imperial Holly Sugar Corporation plant in Sidney, Montana.

The Savage Mine began utilizing fly and bottom ash generated by Holly Sugar as backfill in 1987. The annual volume of ash received by the Savage Mine is variable and dependent upon the amount of coal burned by Holly Sugar in relation to the quantity of sugar beets processed. The ash disposal permit does not allow annual ash disposition in the mine to exceed approximately 10,000 cubic yards (about 16,500 tons). The estimated cumulative volume of ash placed between 1987 and 2000 is approximately 130,000 cubic yards. In order to achieve the maximum dilution of ash with spoils, the ash is distributed over as much pit length as possible. The typical annual pit length requirement is 700 feet for storage and disposal activities. Ash placement at the Savage Mine is performed in accordance with the following procedures:

- Ash placement occurs above the saturated zone of the anticipated postmine groundwater table. This level is achieved by placing 25 to 30 feet of ash-free spoils material at the pit bottom prior to ash placement.
- The dragline distributes the ash over the length of the pit.

- The dragline alternates buckets of ash with as many buckets of spoil material as possible to achieve maximum mixing and homogeneous dilution.
- Ash disposal will be kept to a minimum depth of 8 feet below the final postmine surface.

#### ***4.4.1 Local Geology***

The regional geology surrounding the Savage Mine is characterized by broad gravel-capped uplands between wide troughlike valleys. At least five terrace gravel deposits have been identified in proximity to the Savage Mine and are attributed to river deposits that were transported into the eastern portion of Montana from mountains in the western and central parts of the state. The permit area of the Savage Mine is located on the east-central portion of a remnant terrace from the Yellowstone River known as Breezy Flat.

Surficial sediments in the vicinity of the Savage Mine are derived from the Tongue River Member of the Fort Union Formation primarily comprising light yellow to gray, massive to cross-bedded sand and light gray, silty clay. These unconsolidated deposits ranging from about 30 to 60 feet thick form approximately one-half of the total overburden thickness at the site. The lower portions of the site overburden comprise mostly gravel and sand. The Tongue River Member also contains several thick and laterally continuous lignite beds and limestone. Lignite from the Tongue River Member is removed during mining operations. The lignite ranges in thickness from 15 to 25 feet.

#### ***4.4.2 Local Hydrogeology***

Groundwater is derived primarily from sands and gravels that cap terraces in areas around the Savage Mine and serves both livestock and domestic needs. Typical shallow aquifer yields are on the order of 5 to 20 gallons per minute (gpm). Groundwater is considered to be of good quality, with sandstone aquifers producing groundwater with softer and more mineralized characteristics as compared to the lignite aquifers.

The permit area is recharged by direct infiltration during snowmelt and rainfall events and by lateral underflow from adjacent unmined areas. Transmissivities calculated from pumping test data collected from Wells OB-1 and OB-2 are from 0.13 to 16 ft<sup>2</sup>/day. The limited transmissivity of the Pust coal has been attributed to a limited recharge area, highly variable topographic relief of the coal bed, and limited fracturing in the coal.

The stratigraphy of the Fort Union Formation and the overlying sediments at the Savage Mine and adjacent regions dictate local groundwater flow patterns. Potential water-bearing units disturbed by mining operations include the surficial sand and gravel and the Pust coal. Postmining protocol involves replacing these units with a saturated zone at the base of the spoils. The surficial sand and gravel at the site do not serve as an aquifer because of the lack of adequate recharge area, thickness, and rainfall. The unmined coal in the western part of the site is thought to form a continuous aquifer with the base of the mined-out spoil. The prevailing groundwater flow direction at the site is to the south/southeast.



Groundwater elevations in wells completed in the Pust Coal upgradient of the mine operations have remained relatively stable since 1986. Groundwater levels in Wells 261 and 284 generally have fluctuated less than 1 foot over the period of record. Groundwater levels in Wells OB-1 and OB-2 located immediately west of the mine activities have been influenced by mine-dewatering operations and have declined approximately 3 to 6 feet, respectively, over a 7-year period. Groundwater elevation declines of approximately 2 to 3 feet have been observed over the past 8 years in wells screened in mine spoils. Once mine operations cease, groundwater levels are anticipated to rise as a result of discontinuation of groundwater-dewatering operations. It is also expected that the spoils will not serve as a dependable source of water supply under postmining conditions.

#### ***4.4.3 Ash-Leaching Characteristics***

Batch-type laboratory leaching analyses on Savage coal ash are performed annually prior to placement in the surface pits. The tests are performed by mixing ash samples with water at an ash-to-water ratio of 1:1 (by weight). The test results from 1987 to 2000 and corresponding water quality standards for a range of constituents are summarized in Table 4.12. The results indicate that pH values of the leachate tend to be elevated relative to water, which is beneficial for limiting the generation of acidic leachate from the spoils. Also the average and maximum leached concentrations of most constituents, most notably As, Cr, and Pb, are below current water quality standards. On average, federal and/or state standards are exceeded for Cl, NO<sub>2</sub>+NO<sub>3</sub>, and SO<sub>4</sub>, while elevated individual values for pH and Cd have been measured. Boron (B) is present in the leachate samples. However, federal or Montana water quality standards are not established for B.

#### ***4.4.4 Groundwater Quality***

Approximately 36 wells have been identified both outside and within the mine permit boundary. All of these wells except 003, 262, OB-1, and OB-2 have temporal groundwater quality information, predominantly metals analysis. Wells 108, 108A, and 109 are no longer in service because mining operations required the removal of these wells. Wells located upgradient of the site include ETZEL NORTH, LANGE NORTH, LANGE SOUTH, 261, 262, 263, and 284. Wells located downgradient of the ash backfill areas include Wells 002, 003, 005, 286, 289, 290, 291, and ETZEL SOUTH.

General groundwater quality has been characterized in a report for ash placement in the mine. Pust coal groundwater is considered to be of very high quality for eastern Montana and ranges from slightly basic to slightly acidic (i.e., <6.4 to 7.7). The groundwater also is classified as calcium, magnesium bicarbonate type water. Sulfate levels in groundwater for spoils tend to be elevated in proportion to bicarbonate. Groundwater in contact with spoils is more acidic, with a pH range of 6.3 to 7.0 in comparison to the groundwater contained in coal aquifer.

Groundwater metals analyses have been conducted on an annual basis for monitoring wells both upgradient and downgradient of ash placement. Analyses have been conducted since 1979 for TDS, SO<sub>4</sub>, Cl, NO<sub>3</sub>, Ca, Mg, Na, Fe, and Mn, while trace metal analyses (i.e., As, B, Cd, Cr, Pb, Ni) have been performed for post-ash placement conditions since 1986. Trace metals were

not analyzed prior to ash placement. However, because trace metal analysis was performed in laboratory leaching studies on the ash (see Table 4.12), qualitative assessments can be made regarding ash constituent contribution to groundwater quality.

#### *4.4.4.1 Trace Metals*

Historical groundwater concentrations (maximum and mean) of As, B, Cd, Cr, Pb, and Ni for monitoring Wells 001, 106, 261, 263, 284, 286, 289, 290, and 291 from 1986 to 2000 are compared to Montana groundwater quality standards in Table 4.13. The results indicate that, on average, trace metal concentrations are below current Montana State maximum contaminant levels (MCLs) in all of these wells, with the exception of arsenic in Well 291. The historic mean concentration of arsenic in Well 291 (0.20 mg/L) is an order of magnitude higher than the current MCL (0.02 mg/L). The MCL for arsenic also has been exceeded on occasion in Well 290. Well 290 is approximately 700 feet downgradient (east) of Pit 3, and Well 291 is located immediately downgradient (east) of Pit 4. However, it is unclear whether the elevated arsenic levels in these wells are due to release of arsenic from the ash. Historic ash-leaching test results given in Table 4.12 indicate that the amounts of arsenic mobilized from the ash are not sufficient to account for the elevated arsenic concentrations in Wells 290 and 291, particularly considering that the ash is mixed with mine spoils during placement. Although no chemical analyses of the spoils are available for this study, the spoil material itself may contain arsenic that could be released into site groundwater.

Historic arsenic concentrations in Wells 286, 289, 290, and 291 versus time are plotted in Figure 4.13. Well 290 demonstrated slight arsenic exceedances of the Montana MCL in September 1995 (0.021 mg/L) and in October 2000 (0.023 mg/L), whereas elevated levels of arsenic has been observed in Well 291 for nearly all of the sampling events since 1986. Overall, arsenic levels in Wells 290 and 291 have fluctuated over time but generally have increased since ash placement. Surprisingly, arsenic levels in downgradient Wells 286 and 289 historically have remained below the Montana MCL, even though these wells also are located within 500 feet of the pits.

The results in Table 4.13 also indicate that concentrations exceeding the Montana MCL were observed periodically for Cd and Pb in nearly all of the selected wells, including upgradient wells. Thus elevated Cd and Pb concentrations in downgradient wells likely are not due to leaching and migration of these constituents from the ash. However, no conclusions can be made regarding the impacts of ash placement on groundwater quality since the reported detection limit (i.e., 0.01 mg/L) for Cd in most of the historic analyses is higher than the current Montana MCL (i.e., 0.005 mg/L). Elevated nickel was observed during a single sampling event in upgradient Well 284 and in downgradient Well 106. Chromium has not been detected in any of the wells since 1986.

#### *4.4.4.2 Other Constituents*

Analyses of SO<sub>4</sub>, Cl, NO<sub>3</sub>, Ca, Mg, Na, Fe (total and dissolved), and dissolved Mn were performed for most of the monitoring wells. Other analyses on groundwater from these wells included pH, temperature, electrical conductivity, and TDS. Consistently elevated historical

concentrations of TDS, SO<sub>4</sub>, and Fe have been observed in both upgradient and downgradient wells. The state of Montana has not established MCLs for these constituents.

Maximum and mean historical concentrations of TDS and sulfate measured in selected wells prior to and after ash placement in the mined pits are compared with the federal secondary MCLs in Table 4.14. The majority of monitoring well data shown in Table 4.14 indicates that TDS and/or SO<sub>4</sub> levels are consistently above the secondary MCL before and after ash placement. Elevated concentrations of TDS and SO<sub>4</sub> also are evident in both upgradient and downgradient wells relative to the ash-filled pits. These results indicate that the high-TDS and SO<sub>4</sub> concentrations are not due solely to the release of constituents from the ash but are indicative of postmining groundwater quality that is commonly encountered at other coal mine sites. However, increases in TDS and/or SO<sub>4</sub> levels have been observed in certain downgradient wells since ash placement operations began in 1986, most notably in Wells 286 and 291 along the western edge of Pit 4.

Iron (Fe) was detected at levels above the national secondary MCL of 0.3 mg/L for monitoring Wells 001, 105, 106, 110, and 111 prior to ash placement. Although measured Fe concentrations in the years following ash placement are not available in many of the wells, Fe concentrations in downgradient Well 001 decreased from an average of 1.32 mg/L prior to ash placement to 0.17 mg/L after ash placement. Overall, no obvious groundwater impacts due to release of Fe from the ash are evident at the site based on the available data.

#### **4.5 Storm Strip Mine (WV)**

This case study involves placement of coal ash in an active coal strip mine. The downgradient groundwater-monitoring data reveals no evidence of contamination over the 10-year period of operation.

Coal ash (both bottom ash and fly ash) is being placed at a rate of about 800,000 tons annually in an active strip mine near an electric power plant in West Virginia. The strip mine provides coal for the power plant and is located on the plant property. Ash placement began in 1987. No ash has been placed below the water table because the groundwater table is deeper than the mine floor. Monitoring Well MW1 is located deep underneath the land surface and is regarded as an upgradient well. No strip mining of coal has taken place near this well, which is screened in rock and coal about 130 ft below the ground surface. GWM2 is located upgradient of the ash fill area, and Wells MW6 and MW7 are located downgradient of the ash fill area. GWM2 is screened 40 ft below ground surface also in rock and coal. MW6 and MW7 wells are screened 25 ft and 60 ft, respectively, below ground surface. Groundwater quality-monitoring data from the four wells have been collected since 1987 for several metals, pH, alkalinity, conductivity, and sulfate. The Solid Waste Division of the state of West Virginia has issued a permit for a landfill involving the placement of coal ash in the strip mine.

Summary statistics of the monitoring results for eleven chemical parameters for aluminum, iron, pH, sulfate, and arsenic data trends or changes in these water quality parameters which may be associated with the ash placement in the coal strip mine. Aluminum concentrations in Wells MW1 and MW7 were below detection limits. Well MW6 shows aluminum below detection

limits with occasional measured concentrations between 0.2 and 0.6 mg/L. Only Well GMW2 showed aluminum concentrations above detection limits that range between 0.1 and 0.8 mg/L. There is no time trend indicated for aluminum. These aluminum data indicate that the upgradient well is the only well that contains a measurable amount of dissolved aluminum. All other monitoring wells are unaffected for aluminum, demonstrating no effects from the placement of coal ash.

Iron shows considerable variability and is measured above detection limit in upgradient Wells GMW2 and MW1. Well GMW2 appears to show an increasing trend. Both downgradient Wells MW6 and MW7 show low iron concentrations, averaging about 0.35 mg/L compared to an average concentration of about 7 mg/L for Well MW1 and an average concentration of 5.8 mg/L for Well GMW2. The time-series graph for iron in Well GMW2 indicates an increasing trend over the monitoring period of more than 10 years. The pH in this well also appeared to be decreasing, which may be related to the increasing iron concentrations. The pH at Well MW1 is nearly constant at around 7 for the entire monitoring period. There is relatively more variability in pH measured at MW6 and MW7, with averages of 6.25 and 7.70, respectively. All these monitoring data show that placement of ash in the strip mine has not affected pH in the downgradient groundwater.

Sulfate concentrations in the four monitoring wells show four different behaviors. Background Well GMW2 has an average sulfate concentration of about 12 mg/L, with a range from about 4.5 to 18.5 mg/L. There is no time trend indicated by the monitoring data. Sulfate in MW1, an upgradient well, shows an average concentration of about 225 mg/L, with a range from 7.5 to 483 mg/L. It appears that there was an increase in sulfate concentration for a period of time, followed by a decrease. Sulfate at MW6 is also low in the range of 3 to 18 mg/L. However, the sulfate concentrations show a decreasing trend over the more than 10 years of monitoring. Monitoring Well MW7 has consistently shown measured sulfate concentrations to be near 5 mg/L. However, there are four values out of 47 observations that are in the range of 55 to 200 mg/L.

Arsenic data show that it is not above detection limits in all four wells. Arsenic concentrations above detection limits were observed only twice in over 160 measurements.

#### **4.6 Universal Mine (IN)**

The Universal coal Mine site is located about 5 miles north-northwest of Terre Haute, Indiana in Vigo County. The site is adjacent to the eastern boundary of the eastern region, Interior Province coalfields of Illinois and southwestern Indiana. These mine fields have typically produced medium-to-high-volatility bituminous coals of Pennsylvanian and Permian geologic age. The south embankment of the Universal site ridge was augur-mined during the 1940s and 1950s. Peabody Mining Company began and completed highwall mining operations at the Universal site along a north-south line in the mid-1980s, creating a final cut pit which was approximately 1920 feet long, 325 feet wide, and about 90 feet deep.

In 1988, PSI Energy, Inc. (now Cinergy Corporation), acquired a portion of the Universal Mine site containing the final cut pit for the express purpose of coal ash deposition and surface

mine reclamation. Indiana DNR issued a permit to PSI Energy to dispose of fly ash/bottom ash from its nearby Wabash River Station to fill and reclaim the mine pit. The permit allowed for approximately 1.448 million cubic yards of CCPs to be disposed of with ash deposit thickness ranging from 30 to 75 feet. Between April 1989 and the end of October 2001, Cinergy placed approximately 1.6 million tons of coal ash from a nearby power plant to completely fill the open pit. Table 4.15 shows the annual tonnage of coal ash and coal gasification slag placed in the mine pit at the Universal site during the 13.5 years of mine-filling operation. Cinergy has been conducting quarterly monitoring of groundwater and surface water at the Universal ash fill site since early 1988.

The coal ash was hauled by triaxle road-going trucks and placed dry in the mine pit. The coal ash was deposited in the mine pit until the height of the filled area corresponded to the approximate original topographic contour. A 5-foot noncompacted soil cap and vegetation are being established as a final cover. The reclaimed mine pit land is to be maintained as a wildlife refuge.

#### ***4.6.1 Hydrogeology***

The geology of the premined consolidated strata consisted of a thin layer of fine clay overlain by an 18-inch-thick coal seam that was overlain by shaley limestone, shale, and a thick deposit of loess. The exposed high wall at the Universal site showed a mantle of about 12 to 16 feet of pre-Wisconsin till and Wisconsin loess over the bedrock. The Universal site area is part of an upland landscape north of Coal Creek and west of the Wabash River. The upland rises about 100 feet above the Coal Creek flood plain and was well dissected before surface mining altered the topography.

The water level elevation data from the groundwater-monitoring wells at the Universal site indicate that the groundwater from the unmined east side of the ash fill area is flowing to the west into the ash that has resulted in approximately 30 ft of saturated zone in the reclaimed mine pit. The groundwater then flows in a radial manner to the west, north, and south. This groundwater flow field implies that monitoring Well MW-4 is the upgradient well and that all other wells are hydraulically downgradient of the placed coal ash.

#### ***4.6.2 Chemical Composition of Coal Ash and Leachates***

Between May 1988 and December 2001, 25 samples of coal ash were collected and analyzed for total chemical concentrations and for 18-hour and 30-day leachate concentrations. Table 4.16 provides a statistical summary given by mean, median, maximum, and minimum values based on the measured concentrations for the bulk ash samples. Table 4.19 provides a statistical summary for the 18-hour and 30-day leaching tests completed on the same ash samples. Table 4.18 contains a statistical summary of field leachate composition data based on 17 samples collected and analyzed from leachate monitoring Well MW-8 installed in 1997.

The coal ash deposited at the Universal site contains aluminum, iron, potassium, calcium, magnesium, sulfate, sodium, and boron at average concentrations of greater than 240 mg/kg. Manganese, zinc, barium, arsenic, vanadium, nickel, chloride, lead, chromium, copper, and

fluoride are present in the average concentration range of 18 to 128 mg/kg. Molybdenum, selenium, cadmium, silver, and mercury are found to range from nondetect to an average of about 5 mg/kg. The coal ash is alkaline, with an average pH above 9.0 has a net neutralization capacity of about 17.6T/1000T, and contains about 5.8% total organic carbon.

The laboratory-generated leachates as well as the field leachate data show that all leachates contain sulfate as the most abundant constituent released from the coal ash. Aluminum, boron, sodium, and calcium were the next most abundant constituents in the laboratory-generated leachates. The field leachates, however, showed that calcium, sodium, chloride, boron, and potassium were the next most leached constituents (Table 4.18). The laboratory-generated leachates contained no silver, mercury, nickel, or lead. The field leachates contained no dissolved cadmium, chromium, copper, iron, lead, mercury, nickel, selenium, silver, or zinc. Field and laboratory leachates also showed arsenic, with some variability in concentration.

Time-series plots for pH, sulfate, boron, and arsenic in leachate monitoring Well MW-8 are given in Figures 4.14 through 4.17. These plots show that ash leachate has a pH of over 9 throughout the monitoring period of 1997–2001, with no measurable acidity. The sulfate concentration in the ash leachate appears to be holding at about 1700 mg/L, and boron is present at a concentration of about 45 mg/L. The field leachate data indicate that ash leachate at the Universal site is highly alkaline and contains about 200 to 300 mg/L each of chloride and sodium. However, both sodium and chloride concentrations in the leachate show a rapid decrease over the monitoring period, indicating a near depletion of these constituents in the fly ash. MW-8 monitoring data show an initial increase in arsenic concentration in the ash leachate followed by a steady concentration ranging between 180 and 250 µg/L.

#### ***4.6.3 Water Quality-Monitoring Program***

Both groundwater and surface water are monitored on a quarterly basis for the compliance-monitoring program by Cinergy. The Universal site originally installed four groundwater-monitoring wells (i.e., MW-1, MW-2, MW-3, and MW-4) in May 1988, approximately 1 year before the placement of coal ash began in April 1989. MW-4 is an upgradient well installed in the undisturbed bedrock formation and has been monitored for water level and water quality since May 1988 on a quarterly basis.

Monitoring Well MW-1 was installed to the northeast side of the ash fill and had a long screen covering both the bedrock and the overlying spoil material. The MW-1 well was replaced in December 2000 by two new wells designated as MW-1BR and MW-1UR. Monitoring Well MW-2 was installed at the edge of the mine fill to the west presumably in the downgradient direction of the groundwater flow. This monitoring well was replaced by a new Well MW-2A in 1997 which was properly screened in the mine spoil material to the west and downgradient of the ash fill. Original Well MW-3 was installed to the south of the ash fill area, approximately 30 ft downgradient in the mine spoil material. This well was replaced by MW-3R in December 2000. In 1997, additional compliance Wells MW-5, MW-6, and MW-7 were installed in the mine spoil material downgradient of the ash fill. In 1997, MW-8 was installed in the ash fill to monitor chemical composition of the ash leachate. Therefore, the longest series of groundwater-monitoring data is available from monitoring Wells MW-1, MW-3, and MW-4, with a somewhat

shorter time-series of monitoring data from Wells MW-2, MW-2A, MW-5, MW-6, MW-7, and MW-8. Replacement Wells MW-1BR, MW-1UR, and MW-3R are relatively new and have the shortest set of time-series data.

As part of the compliance-monitoring effort, Cinergy has also been sampling and analyzing surface water samples from an old mine seep location since 1988. Cinergy has since then added five more surface water quality-monitoring locations to its compliance-monitoring program. These sampling locations are designated as North Pond, Ash Pit-Water Pond, Plug Seep, and two locations in the Coal Creek. In this summary paper, we will only present and discuss the mine-seep water quality data to depict the benefits and impacts of coal ash placement on surface water at the Universal site.

Table 4.19 provides a list of parameters that have been measured in the water quality samples collected in the groundwater- and surface water-monitoring program at the Universal site.

#### ***4.6.4 Groundwater Quality Results***

Groundwater quality-monitoring data from Wells MW-1, MW-2, MW-2A, MW-3, MW-4, MW-5, MW-6, and MW-7 were evaluated for time trends and changes in concentrations that may be related to the placement of ash. It was determined that aluminum, cadmium, chromium, copper, mercury, nickel, and silver concentrations in groundwater in these wells during the period 1988 through 2001 were at or below analytical detection limits. Therefore, no further discussion of these constituents is included in this report. The data analysis also indicated that sulfate concentrations in groundwater at Wells MW-2, MW-2A, MW-3, MW-5, MW-6, and MW-7 are significantly higher than those found at MW-1 and MW-4. Boron concentrations in monitoring Wells MW-1, MW-2, MW-2A, MW-3, MW-5, and MW-6 are significantly higher than those found in groundwater at Wells MW-4 and MW-7. The groundwater pH in most wells is near neutral, with a narrow range of 6.8 to 7.2. However, MW-3 groundwater has the lowest average pH, at about 6.4. The nearly 13 years of quarterly groundwater-monitoring data also show that the waters are alkaline, with notable concentrations of chloride, magnesium, and sodium. The groundwater at the site also contains several mg/L of total organic carbon.

The groundwater quality-monitoring data also show no significant differences in concentrations of barium, cadmium, chromium, copper, fluoride, lead, mercury, nickel, selenium, silver, and zinc. Sulfate is present at low levels in monitoring Wells MW-4 and MW-1, but is found at concentrations between 500 to 2,000 mg/L in Wells MW-2, MW-2A, MW-3, MW-5, MW-6, and MW-7. MW-3 contains higher levels of iron, manganese, and boron. Boron concentrations are also higher in groundwater at MW-1, MW-2, MW-2A, MW-5, and MW-6 compared to those found in Wells MW-4 and MW-7. The pH in groundwater wells at the site generally falls in the range of 6.8 to 7.2 except for MW-3, which showed a slightly more acidic pH of about 6.4.

Since MW-3 and MW-4 wells data contain water quality measurements both before and during ash placement from 1988 through the end of 2001, we focused on presenting and discussing those data in this report. The quarterly monitoring data for pH, acidity, alkalinity,

manganese, iron, sulfate, chloride, boron, and arsenic are presented in Figures 4.18 through Figures 4.26 as time-series plots. There are several observations that can be extracted from these time-series plots. The pH time-series plot (Figure 4.17) indicates that throughout the 13.5 years of monitoring, pH in groundwater at downgradient Well MW-3 is somewhat acidic compared to the near-neutral pH in upgradient Well MW-4. Groundwater in Well MW-3 contains about 200 mg/L of acidity, whereas MW-4 contains essentially no acidity (Figure 4.18). Both MW-3 and MW-4 groundwater contains over 350 mg/L alkalinity with MW-3 groundwater being more alkaline than MW-4 from the 1988 through 1998 time period. Both MW-3 and MW-4 have alkalinity of about 450 mg/L between 1998 through 2001 (Figure 4.20).

Figure 4.21 shows the time-series plot of manganese concentrations. The upgradient well shows no measurable amounts of manganese for the entire monitoring period, whereas MW-3 has shown manganese being present in several mg/L concentrations. There appears to be a decrease in manganese concentrations in MW-3 groundwater over the 13-year monitoring period. These monitoring results indicate that dissolved manganese was present at about 5 mg/L level in groundwater downgradient of the ash fill area before the ash was placed and, therefore, the observed manganese concentrations in MW-3 are not associated with the placement of ash in the mine pit.

Figure 4.22 shows the time-series plot of dissolved iron in groundwater at monitoring Wells MW-3 and MW-4. Upgradient Well MW-4 shows an absence of dissolved iron in the groundwater, whereas downgradient Well MW-3 shows an average of about 20 mg/L iron. Dissolved iron at this elevated concentration was present in Well MW-3 before ash placement. The monitoring data lead us to recognize that groundwater in downgradient Well MW-3 contains elevated dissolved iron concentrations that are not associated with the placement of coal ash in the Universal mine pit.

Figure 4.23 shows the time-series plot of sulfate in groundwater at Wells MW-3 and MW-4. The upgradient groundwater measured in MW-4 in an undisturbed geological setting has an average concentration of about 53 mg/L of sulfate, whereas the groundwater in downgradient Well MW-3 screened in the mine spoil material has sulfate concentrations of around 1500 mg/L. It is noted that sulfate was present at these elevated concentrations at MW-3 in water samples collected before ash placement and that subsequent to ash placement the sulfate levels has not increased in the period from 1989 through 2001. This time-series behavior leads us to conclude that even though sulfate is an ash leachate constituent, it has not impacted the downgradient groundwater at MW-3 at the Universal site.

Figure 4.24 shows the time-series plot of measured chloride concentrations in groundwater at MW-3 and MW-4. The average chloride concentration in upgradient Well MW-4 is about 11 mg/L, and downgradient Well MW-3 contains about 18 mg/L. Chloride in groundwater at these two wells is pretty low and requires no further discussion.

Figure 4.25 shows the time-series plot for boron concentrations in groundwater at Wells MW-3 and MW-4. This plot indicates that background Well MW-4 contains an average concentration of about 0.4 mg/L of boron. The boron concentrations in groundwater at MW-3 do show an increase after early 1990 lasting through 1997 before showing a decrease during 1998



through 2001. The average boron concentration in groundwater at MW-3 is about 2.1 mg/L. Boron is a known leachate constituent associated with coal ash. The field-scale leachate-monitoring data show that boron is present in the ash leachate at the site in over 40-mg/L concentrations. Therefore, it is inferred that the elevated boron concentrations in groundwater at MW-3 may be a result of ash leachate migration even though there is an approximate 20-fold decrease in concentration between the source and downgradient monitoring Well MW-3.

Figure 4.26 shows the time-series plot for dissolved arsenic in monitoring Wells MW-3 and MW-4. The average dissolved arsenic concentration in upgradient Well MW-4 is 5  $\mu\text{g/L}$ , with over 95% of the data showing below-detection-limit values. The measured arsenic in MW-3 shows an increase during the monitoring period 1989 through 1996 and then a large variability in concentrations measured during 1997 through 2001. The maximum measured concentration of arsenic in MW-3 was 35  $\mu\text{g/L}$ , with about 43% of the data showing below-detection-limit values. The ash leachate data from MW-8 and data from the laboratory leaching tests showed arsenic concentrations to range from about 200 to 300  $\mu\text{g/L}$ . Further research at the Universal site is now evaluating the release and migration of arsenic in groundwater to accurately describe the fate of leached arsenic from coal ash.

#### ***4.6.5 Surface Water Quality***

AMD was present at the Universal site. AMD was caused by the oxidation of pyrites because of coal-mining operations. An old mine seep is present to the southeast of the ash-filled mine pit. The mine seep water flows through a surface channel into Coal Creek, located at least 1500 feet further south of the mine seep area. This old mine seep water has been sampled quarterly and analyzed for chemical parameters listed in Table 4.18. We have prepared time-series plots for pH, acidity, alkalinity, manganese, iron, sulfate, chloride, and boron measured in the old mine seep water from May 1988 through the end of 2001.

Figure 4.27 is the plot of pH which shows that prior to coal ash placement, the mine seep water was highly acidic (i.e.,  $\text{pH} < 3.5$ ) which has been completely neutralized to pH 7 by the coal ash deposit in the mine pit. The neutralization of the acidic pH is consistent with the alkaline chemical characteristic of the coal ash.

Figure 4.28 shows the time-series plot for measured acidity in the mine seep water. The AMD water contained a large amount of acidity before coal ash placement in the mine pit. Within 1 year of ash deposition, the acidity in the mine seep water was nearly eliminated, again because of the acid neutralization capacity of the coal ash placed in the Universal Mine pit.

Figure 4.29 is a time-series plot of measured alkalinity in the mine seep water. This plot shows the absence of alkalinity during 1988 to 1990, followed by a gradual increase in alkalinity through the end of 2001. Therefore, the coal ash not only neutralized acidity and increased the pH of the groundwater feeding the mine seep, it has also generated additional alkalinity to provide further improvements to water quality.

Figures 4.30 and 4.31 are the time-series plots of measured concentrations of manganese and iron, respectively, in the mine seep water. Before the coal was placed in the mine pit, the

mine seep, an AMD water, was quite high in dissolved iron (over 100 mg/L) and manganese (over 7 mg/L). But within a year of ash placement, both iron and manganese concentrations decreased significantly. The long-term monitoring further indicates that dissolved iron has continued to decrease and has essentially reached to a nondetect level, with manganese also showing a gradual decrease to a concentration of below 2 mg/L in 2001. These decreases are due to the neutralization of acidity and increase in pH achieved by the alkaline ash. Increases in pH and alkalinity have precipitated the dissolved iron and manganese. It is also possible that the lack of oxygen may have stopped the generation of AMD through oxidation of pyrites.

Figure 4.32 is a time-series plot of sulfate concentrations measured in the mine seep water. This plot shows a notable decrease in sulfate concentrations as a function of time. The sulfate levels of over 2000 mg/L in 1988 are now reduced to about 1500 mg/L in 2001. The initially high sulfate concentrations most likely were a result of pyrite oxidation which produced sulfate, iron, and acidic pH waters with low levels of calcium and other base cations in the water. The alkaline coal ash provided large amounts of calcium as well as alkalinity through the leachate. This ash leachate mixed with AMD waters and resulted in the precipitation of iron hydroxide(s) as well as gypsum, thereby creating the modified water quality of the mine seep that is now low in iron and sulfate compared to the original AMD waters. Therefore, even though sulfate is a coal ash as well as mine spoil-derived constituent, in this case there is no distinguishable impact of sulfate on the water quality in the mine seep.

Figure 4.33 shows a time-series plot of chloride measured in the mine seep water. This plot shows a slowly increasing trend in chloride concentrations, but the chloride levels were still less than about 100 mg/L in 2001.

Figure 4.34 shows a time-series plot of boron concentrations in the mine seep water samples monitored since May 1989. For the first 2 years of monitoring, boron concentrations in the mine seep water were less than 1 mg/L. Beginning in May 1991, the boron concentrations increased steadily, with the highest concentration of about 5 mg/L recorded in 2001. This time-series behavior and the documentation that coal ash leachate at this site contains over 45 mg/L of boron led to the conclusion that boron contained in the ash leachate has resulted in the elevated boron concentration in the mine seep water samples.

#### ***4.6.6 Summary and Conclusions***

This paper provides a limited summary of monitoring results on water quality at a coal ash-filled surface coal mine pit in Indiana. The over 13.5 years of quarterly water quality-monitoring data and the more recent extended spatial monitoring data provide insights on coal ash leachates and water quality changes when coal ash has filled and reclaimed a final cut mine pit at the Universal site. The monitoring data to date indicate that the alkaline coal ash leachate has been effective in improving AMD water quality present at the site. The coal ash leachate neutralized the acidic pH, increased alkalinity, essentially eliminated acidity, and significantly decreased manganese, iron, and sulfate concentrations. There were no indications of any other trace metal migration via the mine seep. However, the coal ash leachate did significantly increase boron concentrations in the mine seep water.

The groundwater quality data similarly show that coal ash leachate has not resulted in the leaching and migration of most of the trace metals contained in ash. Boron, arsenic, and sulfate are leached from the coal ash in different amounts. However, because of the presence of sulfate in groundwater in the spoil material, it is not feasible to discern the migration of sulfate contained in the coal ash leachate from the sulfate contributed by the mine spoil material.

Trace metals such as barium, chromium, cadmium, copper, lead, mercury, nickel, selenium, and silver all show no signs of leaching or impacting the groundwater and surface water quality around the site. The laboratory and field leachates do show leaching of arsenic from the coal ash, but over the nearly 13-year period of monitoring it appears that arsenic has not migrated and impacted downgradient groundwater or surface water quality. The continuing monitoring and the supplemental research at the Universal site will provide a better understanding of the benefits and impacts from the use of coal ash for mine filling in the next few years.

#### **4.7 Midwestern Abandoned Mine (IN)**

This case study is an example where a state agency elected to place CCPs with a Poz-O-Tec (a mixture of FGD sludge, fly ash, and quicklime) cap, which resulted in reduced infiltration and improvement in water quality by neutralization. The Midwestern Abandoned Mine consists of approximately 550 acres of previously mined land, which in some instances intersects with abandoned deep mining of the same coal seam. The Midwestern site is located within a 6000-acre Mill Creek Abandoned Mine Land Area which was partially reclaimed in the early 1980s as part of Indiana's Abandoned Mine Land Program. Deposits of pyritic coarse- and fine-grained refuse were surrounded by high walls associated with final cut pits; ponded water and seepage from an abandoned underground mine further characterized the site.

The Indiana Department of Natural Resources Division of Reclamation (IDNR DOR) conducted extensive evaluations including review of laboratory test results and a review of state and federal regulations to decide that CCPs could be utilized for the reclamation of abandoned mined land (AML). The reclamation project consisted of placing and compacting of CCPs and then covering with Poz-O-Tec. The technical specifications required the water to be removed from the highwall pits to facilitate proper placement of the ash into these areas. In actuality, the pits would not drain because of an interconnection to flooded underground mines and the existing groundwater table. To solve this problem, ponded ash was placed along the perimeters of the pits near the areas where the opening to the underground mines were located. This placement of the coal ash through the pit water was compacted enough to seal off the underground connection to prevent further migration of groundwater into the pits. The placement of ponded ash into these pits raised the pH of the pit water and the metals precipitated out of solution. This allowed the IDNR to pump out the pits without the use of a water treatment system before discharge, and the alkalinity in the ash replaced the need for calcium hydroxide addition for pH adjustment. Since completion of the reclamation, the groundwater has returned to the normal water level and the ash fill areas are below the water table.

The Indiana Geological Survey has conducted a monitoring program covering 1 year prereclamation baseline water quality monitoring and more than 1 year of postreclamation

monitoring. The objectives of the monitoring are to 1) determine the effectiveness of acid mine drainage abatement and 2) monitor the leaching of solutes from CCPs. Water samples from wells screened at different depths and several surface water discharge points have been analyzed for a number of chemical parameters. Figure 4.8.6 shows the location of these monitoring points for both the prereclamation and the postreclamation conditions.

Olyphant et al. (1997) provided a summary of prereclamation water quality data for a selected set of monitoring locations. Branam et al. (1999) provided a summary of postreclamation water quality data for a selected set of monitoring wells and chemical parameters. Based on the monitoring results, Branam et al. (1999) concluded that using CCPs to reclaim the Midwestern Abandoned Mine has resulted in the reduction of AMD leaving the site. The authors ascribe this response to the reduction in vertical recharge of oxygenated water by the fixated scrubber sludge cap and the neutralization provided by the alkaline CCPs.

#### **4.8 The Arnold Willis “City” Underground Coal Mine (IN)**

This case study is an example in which fixated scrubber sludge (FSS) has been successfully injected into an abandoned underground coal mine for stabilization by filling voids. Groundwater-monitoring data indicated that trace metals and sulfide remained unaffected by the placement of FSS.

Coal was mined from the Arnold Willis “City” mine from the late 1940s to early 1950s. The depth to the voids in this underground mine varied from 32 to 64 ft, and the void thickness varied from 2 to 7 ft. Borings into the mine encountered both flooded and dry mine conditions. An FSS grout consisting of a mixture of FGD scrubber sludge, fly ash, lime, and water was developed for injection in the abandoned deep mine to abate surface subsidence and reduce acid mine drainage. A total of 12,502 m<sup>3</sup> of FSS was injected over an 8-week period, resulting in filling of about 5 acres of the mine. Monitoring data show that the FSS material generally achieved unconfined compressive strengths of 100 psi or higher.

Water quality monitoring was conducted over a period of 18 months. The first 6 months of monitoring was completed prior to FSS injection, and the following 12 months of monitoring occurred after the grout was in place. Figure 32 shows the locations of the monitoring points and Tables 4-8-1 through 4-8-16 provide the groundwater quality analytical data for the various locations and chemical parameters measured.

The investigators reported that heavy metals in the water samples were relatively unaffected by the FSS injection. These metals include arsenic, cadmium, chromium, lead, selenium, aluminum, barium, and sulfide. The investigators also reported that acidity and pH did not appear to have changed as a result of the placement of FSS. However, sodium, potassium, calcium, boron, chloride, and magnesium showed some increases attributable to the FSS. Changes in sulfate, total dissolved solids, and specific conductance were also observed.

## **4.9 Harwick Mine Complex (PA)**

### ***4.9.1 Introduction***

The Harwick Mine Complex includes the Monarch, Old Harwick, and Cornell Mines, covering approximately 7000 acres. This coal mine is a deep mine and was operated from about 1932 through June 1970. The elevation of the mine varies from about 740 to 565 ft msl, with depth to coal ranging from 20 ft and 700 ft below ground surface. After coal-mining activities ceased, the mine workings were allowed to fill with water and are currently flooded. Water level in the mine is maintained by dewatering at the Monarch Mine Dewatering Station located at the Monarch Shaft. The entire mining perimeter is surrounded by a barrier of unmined coal isolating the Harwick Mine from the neighboring mines. Approximately 8 to 12 million gallons per day of mine water is pumped out, treated, and discharged to the nearby Little Deer Creek under an National Pollutant Discharge Elimination System (NPDES) permit.

The Monarch shaft is located under the lowest portion of the mine; therefore, all Harwick Mine water flows to this shaft. Coal mining was carried out by room-and-pillar or other conventional methods with varying rates of coal extraction. In some areas, caving occurred soon after mining. In other areas, substantial voids remain within the mine.

### ***4.9.2 History of Ash Injection in Mine***

Since 1970, Duquesne Light Company sluiced fly ash from its Cheswick Power Station into the abandoned Harwick Mine, which is located adjacent to the power station. Prior to the Cheswick Power Station, in July 1967, fly ash from the Colfax Station was injected as a slurry with river water to a worked out area of the Harwick Mine as an experiment, and the fly ash particles were allowed to settle. Then the water was pumped from the mine, treated, and discharged. The water treatment method employed neutralization, aeration, and clarification. The clear water was discharged to a nearby river under a mine drainage permit issued by the Pennsylvania State Sanitary Water Board. This pilot deep mine disposal operation lasted for almost 3 years and provided the basis for the sluicing of the fly ash from the Cheswick Power Station, which is the successor plant to the Colfax Station. It was noted that the use of fly ash in preventing mine subsidence was a benefit that could be derived from such an operation.

### ***4.9.3 Ash Sluicing and Water Pumping Operations***

The mine disposal operation consists of a wet ash-handling system at the Cheswick Power Station which includes two 5000+-gpm pumps connected in series and approximately 8000 ft of slurry pipeline to two operating injection boreholes at the mine. The fly ash generated at the power station is mixed with water from ash handling operations, other intermittent low-volume wastewaters generated in the vicinity of the ash-handling operations, and additional sluicing water.

The combined slurry (approximately 10% solids) is conveyed by the pipeline to an injection borehole into the Harwick Mine Complex. Approximately 3 to 4 million gallons per day of the slurry are conveyed.

Since 1970, a number of boreholes have been used as injection points until refusal. Additional locations for future boreholes have been identified, with a program for development and testing prior to use. Approximately 150,000 tons of coal ash is injected annually into the mine along with millions of gallons of water.

#### ***4.9.4 Coal Ash Characteristics***

Bulk and leachate chemical analyses of the coal ash from the Cheswick Power Station were conducted on samples collected in 1990. These results are shown in Table 4.20. These results indicate that the ash is neutral in pH and contains very low levels of leachable constituents. Even sulfate in the leachate is very low.

#### ***4.9.5 Mine Effluent Characteristics***

The utility company pumps out about 8 to 10 million gallons of water daily and treats it before discharge to the nearby river. Samples of the mine water have been collected and analyzed both before and after water treatment. Table 4.21 provides the chemical composition data from the Monarch Mine for a sample collected and analyzed in 1973.

These results indicate that the mine water before treatment is slightly acidic, high in total dissolved solids, and contains over 100 mg/L of iron, over 2000 mg/L of sulfate, about 100 mg/L of chloride, and nearly 1000 mg/L of sodium. The water treatment results in an increase of pH to about 7.5 and a reduction of iron to below 2 mg/L, with no other changes in the concentrations of other dissolved constituents.

### **4.10 Clinton County (PA)**

This case study provides an example of the placement of fluidized-bed combustor (FBC) ash in a closed-surface coal mine resulting in beneficial effects on water quality because of the favorable geochemistry that occurs. The alkaline FBC ash neutralizes the acidic AMD waters, resulting in precipitous decreases in arsenic, cadmium, and aluminum concentrations due to lower solubility and precipitation of solids.

Between 1974 and 1977, a 37-acre surface coal mine was mined and reclaimed. The upper split of coal was mined, leaving thick underclay as a pavement. Soon after the closure of the mine, acidic discharges were noted, averaging about 35 gpm and affecting water quality in the nearby streams. Schueck et al., (1996) conducted extensive studies of the site, locating piles of pyritic materials, buried refuse, and pit cleanings in the closed and reclaimed mine. A decision was made to use FBC ash, chosen for its pozzolanic properties, as a low-viscosity grout for pressure injection to encapsulate the pyritic material with a cementitious coating.

Forty-two monitoring wells were installed on and adjacent to the site. In addition, a surface discharge point was monitored for water quality. Water quality monitoring was conducted from 1990 to 1995. The grouting with the FBC ash was carried out in 1992 and 1993. The water quality data from the pregrouting period show poor water quality, characterized by pH of less than 2.5, high total dissolved solids, high sulfate, high iron, high aluminum, high manganese, and

low calcium. Cadmium, copper, and chromium were also present in the water. Table 4.10.1 contains a summary of the monitoring results as presented by Schueck et al. (1996) to show that generally the water quality at the monitoring wells improved following the grouting by the FBC ash. These results indicated limited neutralization of the AMD, but more importantly, there are no indications that the groundwater quality is adversely affected by leaching of the FBC ash under highly acidic conditions.

A monitoring well (L25) was monitored to evaluate the chemical changes that occurred as a result of the FBC ash injection into the acidic environment created by the oxidation of pyrites in the mine. The results indicated that the injection of grout caused a temporary increase in pH from about 2.3 to about 9 as the alkaline FBC ash neutralized the acidic AMD waters. The pH increase resulted in precipitous decreases in arsenic, cadmium, and aluminum concentrations, reflecting lower solubility and precipitation to solid-phase compounds. However, within a short time, the pH again became acidic, with sulfate and aluminum returning to the pregrouting concentrations, although arsenic and cadmium remained at much lower levels.

#### **4.11 Big Gorilla Pit (PA)**

##### ***4.11.1 Introduction***

In eastern Pennsylvania, there are several preact strip mine pits in the middle of the anthracite coal basin where active strip and deep mining for coal was practiced since the 1800s. The Silverbrook Basin contained two abandoned strip-mined pits. They are locally known as the “Big Gorilla” and the “Little Gorilla.” The Big Gorilla had an estimated volume of approximately 120 million gallons when the water level was at 1570 feet msl but can fluctuate by about +20 feet. It was approximately 1400 feet long, 400 feet wide, and about 90 feet deep before ash placement began. Big Gorilla pit was significantly affected by AMD.

The Big Gorilla demonstration project involved dry-to-wet ash placement into standing mine water. The objectives of this demonstration project were 1) to show that large-scale placement of ash into mine water is possible with minimal turbidity generation, 2) to develop the methodology for large-scale ash placement, and 3) to demonstrate that ash in contact with mine water will not result in adverse environmental releases. Cogeneration ash, from the Northeastern Power Company (NEPCO) that produces electricity by burning culm as fuel, was first placed in contact with the surface mine pool in August 1997, which was then entirely filled by 2004. Over 3 million tons of ash was placed from two platforms to fill the Big Gorilla mine pool.

Samples were collected and analyzed for water quality parameters from the standing water in Big Gorilla pit in 1993. Table 4.23 shows the water quality-monitoring data for before and after the placement of coal ash in Big Gorilla (Loop et al., 1999).

##### ***4.11.2 Mining and Reclamation***

The major coal beds in this region include Buck Mountain vein and Mammoth vein within the Llewellyn Formation. The Llewellyn also contains an abundance of pyrite and siderite minerals. The Silverbrook syncline is divided by the Centralia thrust fault, which surfaces at the

southern bank of the Big Gorilla mine pool. At this location, the Buck Mountain vein was deep mined at the turn of the 19th century.

In the Silverbrook Basin, surface mining of the Mammoth vein ceased before World War II. Currently, NEPCO burns culm from this location and other nearby sites. In late 1940s, the basins created by mining the Mammoth vein were filled with coal silt. This silt was later reclaimed, and the present-day Big Gorilla occupies the No. 1 Basin.

In 1994, clean fill was put into the western end of the Big Gorilla pit in order to build a terrace above the maximum high water level to prepare for dry land disposal of fly ash in accordance with existing permits and Department of Environmental Protection (DEP) regulations at that time. Filling the entire pit with clean fill was cost-prohibitive, whereas using fly and bottom ash from on-site avoided purchase and transportation cost in addition to having beneficial alkaline properties.

#### ***4.11.3 Regional Acid Mine Drainage Chemistry***

Mine discharge quality data have been collected since the 1940s in all four fields of the anthracite basin (Felegy et al., 1948; Ash et al., 1951). The Silverbrook Basin contributes to the Little Schuylkill River, and together with the other streams in the Little Schuylkill River Basin, is one of the most significant sources of sulfate in the southern field. When the Little Schuylkill River was sampled below Tamaqua, the pH was 5.4 and the sulfate concentration was 240 mg/L (Growitz et al., 1985). The water discharged from the 13 outflow sites contributing to the river was 18 cfs, approximately 23% of the flow at the sampled site below Tamaqua. Acidity values in 1975 (Growitz et al., 1985) and 1991 (Wood, 1996) were determined in the field on an ambient-temperature sample to the end points of both pH 7.0 and 8.3, and the values for the Silverbrook mine outflow increased from 80 to 234 mg/L CaCO<sub>3</sub> and from 90 to 252 mg/L CaCO<sub>3</sub>, respectively (Wood, 1996).

Thirty-eight samples of iron and sulfate concentrations between 1970 and 1993 were reported by Wood (1996). While the average concentration of iron in the Silverbrook discharge shows no apparent trend, the sulfate values have been decreasing, most notably in the 1970–1972 period and 1975, where the mean concentration decreased by over 100 mg/L.

#### ***4.11.4 Ash Placement and Characterization***

Ash was first deposited into the Big Gorilla mine pool in August of 1997. Fly ash from one silo and bottom ash from another were loaded into trucks in 45-ton loads and sprayed with water to prevent dust. They were then taken to the Big Gorilla mine pool ash platform and piled on the bank. Bulldozers were used to push the ash piles into the water from the lower platform, with the exception of the winter months, when ash was only placed from the edge of the upper platform. However, toward the end of the project, no distinction was made, as both platforms were found to be safe during the winter. When ash was pushed into the water, turbidity boils could be seen approximately 300 feet from the ash face. This indicated that at least the fine portion of the ash was flowing outward from the face, in a manner similar to that of a turbidity current. When



postplacement ash samples were taken from the bottom of the Big Gorilla, only fine material was recovered.

In NEPCO's case, ash is the by-product of burning culm and limestone to produce electricity. Approximately 1700 tons of culm and 60 tons of limestone are burned daily. Ash from the NEPCO cogeneration facility is reddish brown when wet and pinkish grey when dry. A greater variety of colors are observable in the bottom ash when compared to the fly ash. Fly ash particle sizes can be described as very fine, with a diameter in the 62–88- $\mu\text{m}$  range. Bottom ash particles range from approximately 100  $\mu\text{m}$  to 1 cm in diameter and are angular.

Both the bottom and fly ash were subjected to testing by total digestion and analysis, in addition to leaching tests by the U.S. Environmental Protection Agency (EPA) Method 1311, TCLP, and later the synthetic precipitation leaching procedure (SPLP), EPA Method 1312. Table 4.24 provides an average of the results from 10 years of testing the fly and bottom ash from NEPCO.

#### ***4.11.5 Chemical Evolution of the Big Gorilla Mine Lake***

On July 9, 1998, the entire mine pool was both horizontally and vertically homogeneous, with a pH of approximately 11.1. Four samples were collected for aqueous analysis from the Big Gorilla mine pool prior to ash placement. A surface sample was collected in June 1993, and three variable-depth samples were collected in July 1993. While the surface samples from June and July have very similar chemistry, there is very distinct stratification with depth. Conductivity, total dissolved solids, turbidity, and acidity all increased with depth. Aluminum, sulfate, iron, manganese, calcium, and magnesium concentrations all increased with depth as well. The pH values from the samples taken at depth were measured in the laboratory and showed no consistent variation. When quarterly sampling results of the Silverbrook outflow from 1993 and 1994 are compared to the preash-placement chemistry of the Big Gorilla mine pool, the Silverbrook outflow had a higher pH, in addition to higher values for acidity, iron, manganese, sodium, chloride, calcium, magnesium, and total dissolved solids.

Since October 1997, over 25,000 tons of fly and bottom ash had been placed in the Big Gorilla mine pool, and the mine pool water became alkaline. The water increased in alkalinity with increased ash input. Before the first winter, there was not a significant amount of alkalinity present, and values remained below 50 mg/L  $\text{CaCO}_3$  until June 1998. After June, there was a consistent increase in alkalinity, averaging 80 mg/L  $\text{CaCO}_3$  per month for the next 5 months. This trend ended when ash placement ceased for the winter. At that point, there was a decrease in alkalinity that was not reversed until ash placement resumed in July 1999. In early 1999, 2000, 2001 and 2002, alkalinity dropped dramatically, following significant suspensions in ash placement, indicating that the buffering capacity of the water was strongly tied to ash placement. Between March 2000 and May 2002 the Big Gorilla mine pool water did not fall below a pH value of 11.0.

Based on the June through November 1998 data, which were taken during ash placement, an average of 1.24% of the calcium in the ash is available. A large reservoir of excess CaO is present in the ash.

High sulfate concentrations are one of the key features of AMD impacted streams. Total sulfate concentrations in the Big Gorilla mine pool in November 1998 were approximately 147 mg/L. Initially, the Big Gorilla mine pool water had sulfate concentrations ranging from 55 to 79 mg/L. Since July 1998, sulfate concentrations have risen in response to ash input. The sulfate concentration in the Big Gorilla has been as high as 1021 mg/L, measured in August 2001. In four months, however, it had decreased to 800 mg/L, and within the year, it was less than 600 mg/L.

The pre-ash-placement Big Gorilla mine pool had an average iron concentration of 0.70 mg/L. Since ash placement began in 1997, total iron concentrations have dropped, often to below 0.2 mg/L. Iron concentrations respond to ash input in the Big Gorilla. Lower-iron aqueous concentrations are most likely due to the high pH, which causes the precipitation of iron.

Pre-ash-placement concentrations of manganese in the Big Gorilla ranged from 0.71 mg/L to 0.97 mg/L. With two apparently anomalous exceptions, manganese concentrations in the mine pool have been below 0.1 mg/L since October 1997 and have often been less than the 10- $\mu$ g/L detection limit.

The highest value given by Becher (1991) for arsenic in the Llewellyn and Pottsville Formations is 0.005 mg/L. No values for background concentrations of selenium were given by Becher (1991), and all measurements of selenium for the pre-ash-placement mine pool were less than the detection limit of 0.002 mg/L. The maximum concentration for these elements was 0.101 mg/L for Se and 0.022 mg/L for As between August 1997 and May 2002 in the Big Gorilla mine pool.

Maximum concentrations of cadmium and nickel measured by Becher (1991) in groundwater of the Llewellyn and Pottsville Formations were 0.002 mg/L and 0.440 mg/L, respectively. No values were given for mercury. There was no detectable change in cadmium, mercury, or nickel concentrations in the Big Gorilla mine pool between August 1997 and June 2000. The values during that period were comparable to those measured for the pre-ash-placement mine pool. The highest concentrations measured in the Big Gorilla mine pool for cadmium, mercury, and nickel were 0.018 mg/L, 0.003 mg/L, and 0.284 mg/L, respectively.

Chromium concentrations measured in the Llewellyn and Pottsville Formations by Becher (1991) were no higher than 0.02 mg/L; samples from the pre-ash-placement Big Gorilla had chromium concentrations no higher than 0.05 mg/L. Chromium concentrations in the post-ash-placement Big Gorilla mine pool were never above 0.260 mg/L.

Of the four analyses taken in 1993, the highest lead concentration was 0.002 mg/L. The highest post-ash-placement concentration of lead of 0.0274 mg/L in the Big Gorilla was measured in August 1999.

The highest concentration of copper measured in groundwater of the Llewellyn and Pottsville Formations was 0.047 mg/L (Becher, 1991). The highest value for copper in the pre-ash-placement Big Gorilla mine pool was 0.030 mg/L. The maximum concentration of copper detected in the Big Gorilla after ash placement is 0.132 mg/L.

#### ***4.11.6 Groundwater Monitoring Well Chemistry***

Five monitoring wells and three test borings on and near the NEPCO property have been sampled for water quality. Wells 1 and 2 are to the east of the Big Gorilla mine pool. Well 3 is within 100 feet of the southern boundary of the mine lake. Well 9 is to the west of the Big Gorilla and is associated with a Superfund site that is between Route 309 and the NEPCO property. Well 4, installed in July 2001, was to intersect the Buck Mountain vein. Table 4.25 presents average concentrations of a number of chemicals measured in the five monitoring wells. These results show that each well has a distinct chemical signature.

Only eight groundwater samples were collected from Well 1, but the iron concentration is significantly higher than that found in Well 2. Well 2 has higher concentrations of sodium and chloride than does Well 1. Both Wells 1 and 2 have much lower concentrations of sulfate and aluminum compared to Wells 4 and 9. Wells 4 and 9 are more heavily impacted by AMD than Wells 1 and 2. Well 4 intersects the Buck Mountain seam, and Well 9 is downgradient of surface culm piles and coal refuse.

The largest change in water quality in Well 3 occurred between mid-1999 and mid-2000. The pH value increased from 4 to 4.5–5. Sulfate and calcium concentrations dropped from about 125 to 50 mg/L and from 30 mg/L to 10 mg/L, respectively. With a change in pH, iron and aluminum concentrations dropped significantly.

From the beginning of ash input to the Big Gorilla surface mine pool, the concentrations of acidity were being reduced. In January 2000, acidity was less than 10, while the alkalinity concentration in Well 3 was 4.8 mg/L CaCO<sub>3</sub>. For the next 14 months, acidity was below 15 mg/L CaCO<sub>3</sub>, and alkalinity was 2.0 mg/L CaCO<sub>3</sub> or above. During this time, iron and aluminum concentrations remained consistently low. After May 2001, despite continuing ash placement in the Big Gorilla mine pool, acidity began to rise, and alkalinity remained low. However, in April 2003 acidity again decreased and alkalinity increased slightly.

The obvious source of alkalinity in groundwater in Well 3 is the Big Gorilla surface mine pool. At times, the alkalinity levels in the Big Gorilla have been over 600 mg/L CaCO<sub>3</sub>. However, iron concentrations in groundwater in Well 3 were initially below 0.5 mg/L, but rose to a maximum of 6.6 mg/L with the additional input of Big Gorilla water. After November 1999, iron concentrations generally remained low (<0.5 mg/L). Just as iron and alkalinity values were increasing in Well 3, sulfate and calcium concentrations began decreasing.

Two test borings were drilled into the lower ash platform, and one boring was drilled into the culm. PVC pipe was placed in each hole so that water samples could be collected. The water samples from the borings in the ash platform are very similar in chemistry to the Big Gorilla. All of the borings in the ash platform have consistently high pH and calcium values. It appears that the CaO component of the ash has raised the pH values.

#### **4.11.7 Conclusions**

The Big Gorilla mine pool project involved placement of ash to fill the mine pit containing the large amounts of AMD water. Over 3 million tons of fly ash has been beneficially used on the former acidic surface mine pool, which will no longer present a potential environmental hazard to nearby residents. In addition, abandoned culm piles are removed from local communities, resulting in a further decrease in acid mine drainage production.

While the Silverbrook outflow chemistry has changed since 1989, most likely in response to land reclamation in the basin. To date, the change in the chemistry of the Silverbrook has not been in the form of increasing heavy metal content or other toxic chemicals. The Big Gorilla water has maintained a consistently high pH value (11 to 12) in response to the placement of ash. Alkalinity varied with ash deposition. A small amount of the calcium oxide (<2%) derived from the limestone added in the fluidized-bed reactor appears to have been controlling the pH in the Big Gorilla mine pool.

Iron, manganese, magnesium, aluminum, and zinc have all decreased significantly since ash placement began. Based on the chemistry of Well 3, it appears that there were only low levels of drainage from and/or flow to the Big Gorilla. Once the area above the mine pool is returned to the approximate premining grade, very little water will flow through the ash plug in the former Big Gorilla mine pool. Thus, one long-term effect of ash placement in the former Big Gorilla mine pool will be the prevention of acidic water production through the surface mine pool and interconnected passages.

#### **4.12 Red Oak Mine (OK)**

This case study illustrates the use of CCPs for in situ chemical treatment to ameliorate the adverse impacts associated with AMD. The introduced alkalinity from the CCPs neutralized the acidity in mine pool waters, leading to an increase in pH, which in turn caused the precipitation of metals as hydroxides and carbonates within the mine, thereby improving water quality.

The Red Oak Mine was operated from 1907 to 1925 utilizing the room-and-pillar extraction method. The mine, which covers approximately 46.5 acres, contains water pools or reservoirs of AMD. The University of Oklahoma and the Oklahoma Conservation Commission injected 418 tons of FBC ash in 15 hours into this acidic (pH 4.3) flooded mine to chemically alter the mine water. Table 4.26 provides a summary of the chemical characteristics of the seep water from the mine pool.

Several chemical parameters were monitored for a 1-year postinjection period as well as during injection. Canty and Everett (1999) reported that there were three phases in the treatment of AMD water by the alkaline material. In Phase I, neutralization of existing acidity resulted in an increase in pH from 4.4 to 12.2 in 15 hours. Alkalinity (as CaCO<sub>3</sub>) increased from 0 to 950 mg/L, and precipitation of metals occurred. In Phase 2, carbonate alkalinity formed and reached a minimum of 50 mg/L for about 3 weeks and then increased to about 100 mg/L for the following several months. The pH declined (Figure 4.35) to below 7, and concentrations of Fe,

Mn, and Al increased (Figure 4.36). Phase 3 represents a near-equilibrium condition where pH and alkalinity have leveled off at approximately 6.3 and 150 mg/L as CaCO<sub>3</sub>, respectively.

A comparison of the AMD water preinjection and about 12 months after CCP injection shows that Fe decreased from 200 to 120 mg/L, Mn decreased from 7 to 4.8 mg/L, Al decreased from 6 to 2.3 mg/L, and pH increased from 4.4 to 6.3. The injection of 418 tons of CCPs has introduced a finite amount of alkalinity to the mine pool, which has resulted in an increase in pH and a decrease in the concentration of metals. However, the finite amount of added alkalinity will be depleted as the neutralization of newly produced AMD continues, and the mine water will most likely return to preinjection conditions. This is expected to occur slowly over several years. Further studies will quantify the longevity of the treatment.

Trace metals (arsenic, barium, cadmium, chromium, copper, lead, molybdenum, nickel, selenium, and zinc) were measured in seep water before and after CCP injection. These data indicate that trace metal concentrations were either less than preinjection levels or remained the same after CCP injection.

#### **4.13 Winding Ridge Demonstration Project at Frazee Mine (MD)**

##### ***4.13.1 Introduction***

The Maryland Department of Natural Resources Power Plant Research Program and the Maryland Department of Environment Bureau of Mines have launched a joint effort with private industry to demonstrate large-volume beneficial uses of CCPs to create flowable grouts for placement of abandoned, underground coal mines to reduce acid formation. In April 1995, this multiyear project initiative started with the Winding Ridge Demonstration project involving injection of a 100% CCP grout into the Frazee Mine, located near Friendsville, Garrett County, Maryland.

##### ***4.13.2 Characteristics of Frazee Mine***

The Frazee Mine is located in the Appalachian Plateau region and is overlain by about 100 ft of shale and sandstone overburden. The mine was a small mine that was used to extract coal from the Upper Freeport coal seam and was operated from 1930s through 1960. Frazee Mine is an abandoned 10-acre underground coal mine consisting of two main tunnels connected by various crosscuts (Figure 4.37). AMD occurs through one mine opening at a steady rate of about 5 gpm. Total mine voids were initially estimated to about 3900 cubic yards.

##### ***4.13.3 Geology and Hydrogeology***

The bedrock above the mine is sandstone and shale with thickness of about 100 feet. The bedrock below the mine consists of shale with occasional coal seams. The mine floor consists of a dense, dry, weathered shale and clay of low permeability.

Water-level data obtained from the boreholes show that the mine contains submerged and dry conditions. The upper tunnel appears to be essentially dry and the mine pool is present in the lower tunnel, generally at an elevation of about 2160 ft msl.

#### ***4.13.4 CCP Grout Mix***

The grout mixture used for the Frazee Mine project was about 60% FBC material from Morgantown Energy Associates Power Plant mixed with 20% FGD material and 20% Class F fly ash both from Mt. Storm Power Plant of Virginia Power Company. The median particle size of the FBC material was 42.3  $\mu\text{m}$  and 15  $\mu\text{m}$  for the Class F fly ash. The FGD showed some variation with the average particle size as 7.7  $\mu\text{m}$ . The FBC material contained about 5% free lime. The Atterberg tests were used to determine that the liquid limit and plastic limit for the fly ash were 29.3% and 27.1%, respectively. The FBC and FGD by-products were nonplastic. The chemical composition data of the grout admixtures based on x-ray fluorescence (XRF) analysis are presented in Table 4.27. The x-ray diffraction (XRD) analysis showed that calcium minerals were present in the FBC dominated by hannebachite, gypsum, anhydrite, and calcium oxide, with some quartz. The FGD material did not contain any free lime (CaO) and the calcium was primarily calcite, anhydrite, and hannebachite.

The grout mix was also tested by TCLP to obtain potential leaching characteristics of the mixture. The TCLP test results showed that the grout mixture was not a characteristic hazardous material. Arsenic and barium were found to leach at levels of 0.13 and 0.11 mg/L, respectively. The remaining six TCLP metals were not detected in the TCLP leachate.

#### ***4.13.5 Grout Injection***

CCP grout was injected in Frazee Mine from October 3, 1996, through November 7, 1996. Approximately 5600 cubic yards of CCPs were injected. Altogether 3800 tons of FBC material and 1200 tons of FGD material and Class Fly ash were utilized for the grout mixed. Mine water was pumped and used in mixing the grout.

A portable mixing plant was utilized to mix the grout and was pumped to the injection boreholes through steel pipes. Grout mixing required about 6 to 12 minutes for each 5 cubic yard batch and average injection rate was about 220 cubic yards for a 10-hour work day.

#### ***4.13.6 Pre- and Post-Injection Monitoring***

The preinjection water quality was typical of AMD quality water. The pH values ranged from 2.5 to 3.45 sulfate concentrations ranged from 80 to 1800 mg/L, TDS ranged from 160 to 2900 mg/L, total acidity ranged from 50 to 2400 g/L, and total iron concentrations ranged upwards of 200 to 300 mg/L.

Postinjection monitoring has been performed for water quality since 1996 to 2004. Robin Guynn of ERM, Inc., has kindly provided the summary tables and time-series plots for the L-2 seep location showing both the pre- and the post-injection measurements for calcium (Figure 4.38), iron (Figure 4.39), magnesium (Figure 4.40), potassium (Figure 4.41), sodium

(Figure 4.42), bromide (Figure 4.43), chloride (Figure 4.44), sulfate (Figure 4.45), aluminum (Figure 4.46), manganese (Figure 4.47), zinc (Figure 4.48), cobalt (Figure 4.49), copper (Figure 4.50), cadmium (Figure 4.51), nickel (Figure 4.52), total acidity (Figure 4.53), pH (Figure 4.54), flow rate (4.55), and TDS (Figure 4.56). Table 4.27 shows the average concentrations of the chemical constituents measured in L-2 seep during the preinjection period from January 1995 through September 1996 as well as for the post injection period from October 1998 through December 2004.

In addition, grout cores have been collected on a periodic basis from the Frazee Mine. Visual inspection and physical testing results indicate that the grout is in very good shape without evidence of in situ weathering. The unconfirmed compressive strength ranged from 560 to 1417 psi. The hydraulic conductivity of the cores ranged from  $10^{-8}$  cm/sec to  $10^{-6}$  cm/sec.

Overall, the water quality-monitoring results, presented in Table 4.27 and the time-series plots presented in Figures 4.38 through 4.56, show no significant increases in AMD-related parameters since the CCP grout was placed in the Frazee Mine.

#### ***4.13.7 Conclusion***

The Winding Ridge demonstration project at the Frazee Mine has shown that CCP grout mixture can be beneficially used for an abandoned underground coal mine to reduce acid formation as well to fill mine voids with a high-strength, low-permeability material that would control mine subsidence. The placement of the CCP grout appears to have not caused an unacceptable water quality impact either.

## **5.0 REFERENCES**

### ***Section 1.0***

American Coal Ash Association 2004. Coal Combustion product (CCP) Production and Use.

### ***Section 2.0***

Electric Power Research Institute 1987. Chemical Characterization of Fossil Fuel Combustion Wastes. Report No. EA-5321, Palo Alto, CA.

### ***Section 4.1.4***

Aqua Terra, 1997. [www.aquaterra.com](http://www.aquaterra.com)

Bicknell, B.R., J.C. Imhoff, J.L. Kittle Jr., A.S. Donigian, Jr. and R.C. Johanson. 1997. Hydrological Simulation Program -- FORTRAN, User's Manual for Version 11.

### ***Section 4.2***

Althouse, John. Coors Energy Co. to Weld County Commissioners. Personal Communication, 1986, November 14.

Doty and Associates, 1998. [www.dotyeng.com](http://www.dotyeng.com)

Walker, Byron. State of Colorado DNR to Colorado Dept of Health HMWMD. Personal Communication, 2000, October 30



### ***Section 4.4.3***

Hazen Research Inc., 1989 and 1991. [www.hazenus.com](http://www.hazenus.com)

### ***Section 4.3***

Personal Communications, 2001. Koehler, Karl. Trapper Mining Inc.

### ***Section 4.5***

Personal Communication, 1999. Wes Sprouse, Virginia Power Company.

### ***Section 4.7***

Branam, T.; Ennis, M.; Smith, R. 1999. Water-Quality Monitoring at an Abandoned Mine Land Reclamation Site Amended With Fly Ash and Fixated Scrubber Sludge. In Proceedings, 13th International Symposium On Use and Management of Coal Combustion Products (CCPs), EPRI Report TR-111829.

Olyphant, G.; Harper, D.; Branam, T. 1997. Hydrologic and Chemical Effects of Reclaiming A Refuse Deposit with Ash Fill and a Cap of Fixated Scrubber Sludge. Report From The Indiana Geological Survey Covering the Period Feb 1, 95 to Jan 31, 96.

### ***Section 4.8***

Fluid Placement of Fixated Scrubber Sludge in Abandoned Deep Mines to Abate Surface Subsidence and Reduce Acid Mine Drainage. EPRI Report TR-107053, November 1996.

### ***Section 4.10***

Schueck, J.; DiMatteo, M.; Scheetz, B.; Silsbee, M. 1996. Water Quality Improvements Resulting From FBC Ash Grouting of Buried Piles of Pyritic Materials on a Surface Coal Mine. Proceedings, American Society for Surface Mining and Reclamation

### ***Section 4.11.3***

Ash, S.H.; Doherty, R.E.; Miller, P.S.; Romischer, W.M.; Smith, J.D. 1951 Core drilling at shaft sites of proposed mine-water drainage tunnel: anthracite region of Pennsylvania Bureau of Mines, Washington, DC (USA) May 01.

Felegy, E.W.; Johnson, L.H.; Westfield, J. 1948 Acid Mine Water in the Anthracite Region of Pennsylvania - US, GPO

Growitz, D.J., Reed, L.A., and Beard, M.M. 1985 Reconnaissance of mine drainage in the coal fields of eastern Pennsylvania Water Resources Investigations Report 83-4274. pa.water.usgs.gov

Wood, C.R 1996 Water quality of large discharges from mines in the anthracite region of eastern Pennsylvania Water Resources Investigations Report 95-4243 - pa.water.usgs.gov

#### ***Section 4.11.5***

Becher, Albert E. 1991 *Groundwater resources in and near the anthracite basins of Schuylkill and adjacent counties, Pennsylvania* Water Resource Report Harrisburg. 1973, 1991 Pennsylvania Bureau of Topographic and Geologic Survey : Harrisburg, PA, United States

Loop, C.M., et al. 1999. Geochemistry of Acid Mine Waters in an Eastern Anthracite Strip Mine. Tailings and Mine Waste 199 © 1999 Balkema, Rotterdam, PP543-550 Proceedings of the Sixth International Conference

#### ***Section 4.12***

Canty, G.A.; Everett, J.W. 1999. An In Situ Remediation Method for Abandoned Underground Coal Mines Using Coal Combustion Products. Proceedings, 13th International Symposium on Use and Management of Coal Combustion Products. EPRI Report TR-111829-V3

# **APPENDIX A**

## **TABLES**

**Table 2.1 Summary of Total Concentrations of Selected Elements in Fly Ash, Bottom Ash, and FGD Sludge (from EPRI 1987)**

Element	Concentration (mg/kg solid)								
	Fly Ash (39 samples)			Bottom Ash (40 samples)			FGD Sludge (11 samples)		
	ND <sup>a</sup>	Mean	Range	ND <sup>a</sup>	Mean	Range	ND <sup>a</sup>	Mean	Range
Al	39	113,000	46,000–152,000	40	101,000	30,500–145,000	10	30,300	8400–73,000
As	39	156.2	7.7–1,385	34	7.6	<5–36.5	8	25.2	<5–53.1
Ba	39	1880	251–10,850	40	1565	150–9360	10	370	<25–2280
Ca	39	62,000	7400–223,000	40	52,000	2200–241,000	11	274,000	110,000–345,000
Cd	2	11.7	6.4–16.9	0	< 5	<5	0	< 5	<5
Cl	7	477	180–1190	8	712	<150–2630	9	2514	<150–8970
Cr	29	247.3	37–651	38	585	<40–4710	8	72.7	<40–168
Cu	39	185	44.6–1452	40	78.2	27.3–146	11	31.8	8.0–121
Fe	39	76,000	25,000–177,000	40	105,000	20,200–201,000	11	64,000	1300–138,000
K	39	14,300	3000–25,300	40	12,000	2600–24,000	11	1900	3700–17,000
Mg	39	11,800	1600–41,800	40	9700	2500–46,000	11	7200	600–17,800
Mn	39	357	44–1332	40	426	56–1940	11	138	37.3–312
Mo	36	43.6	7.1–236	36	14.4	2.8–443	8	12.2	<4.0–52.6
Na	39	9087	1300–62,500	40	6188	814–41,300	11	3817	200–16,500
Ni	39	141	22.8–353	39	216	<10–1,067	11	40.4	<5–145
P	24	3070	1100–10,340	19	1470	<500–4630	10	4271	<1000–5900
Pb	39	170.6	21.1–2120	38	46.7	4.6–843	10	29.2	<4–181
S	39	12,643	1300–64,400	40	7422	460–74,000	11	152,000	39,400–228,000
Sb	7	42.5	11–131	0	<10	<10	1	15.5	15.5
Se	30	14.0	5.5–46.9	10	4.1	<1.5–9.96	8	35.8	<2–162
Si	39	209,000	89,500–275,000	40	222,000	51,000–312,000	5	66,000	<500–170,000
Sn	18	43.6	7.9–56.4	24	28.2	<9–90.2	6	29.9	<10–50.5
Sr	39	1331	204–6,820	38	992	182 – 6,440	11	608	70.8–2990
Ti	39	6644	1310–10,100	40	5936	1,540 – 11,300	10	1,599	120–5050
U	13	18.7	11.1–30.4	16	11.9	<5 – 25.9	1	16.2	16.2
V	35	271.5	<95–652	30	176	<50 – 275	3	156	<50–261
Zn	39	449.2	27–2880	40	127	3.8 - 515	11	99.7	7.7–612

\* ND represents the number of measured values above the detection limit for a given element.

**Table 2.2. Ranges of Hydraulic Conductivity in Surface Mine Spoils (Hawkins, 2002)**

Geographic Area	Hydraulic Conductivity (M/A)
Western Pennsylvania	$4.2 \times 10^{-9}$ to $7.6 \times 10^{-2}$
Northern West Virginia	$9.5 \times 10^{-8}$ to $2.7 \times 10^{-4}$
Eastern Ohio	$5.4 \times 10^{-8}$ to $1.9 \times 10^{-5}$
Western Kentucky and Southern Illinois	$2.4 \times 10^{-5}$ to $4.1 \times 10^{-5}$
Western North Dakota	$2.9 \times 10^{-5}$ to $4.6 \times 10^{-5}$
Northern Great Plains	$8.0 \times 10^{-7}$
Wyoming	$1.9 \times 10^{-6}$ to $2.1 \times 10^{-4}$
Edmonton, Alberta	$1.5 \times 10^{-6}$

**Table 2.3 Chemical Analyses of Groundwater from Pre-mined Areas in the Denver Basin (from Kirkham and O'Leary, 1980)**

Sample No.	Location	pH	Dissolved Concentration (mg/L)													
			Alkalinity (as CaCO <sub>3</sub> )	Ca	Mg	K	Na	Cl	SO <sub>4</sub>	F	NO <sub>2</sub> + NO <sub>3</sub>	P	Si	Fe	Mn	TDS
DB-1	Watkins	7.7	230	230	95	4.4	380	140	1300	1.1	8.3	0.03	19	150	10	2440
DB-2		7.9	260	27	2.7	3.7	130	93	7.2	0.9	0.14	0.00	8.8	80	30	436
DB-3		7.8	160	92	15	5.3	39	50	140	0.6	6.3	0.07	29	20	3	495
DB-4		7.8	200	120	22	3.1	20	3.5	200	1.8	15	0.00	20	200	20	592
DB-5		8.0	180	86	16	3.7	43	33	140	0.5	7.2	0.03	24	10	3	486
AVG		7.84	206	111	30	4.0	122	64	357	0.98	7.4	0.03	20	92	13	890
DB-6	West Bijou Creek	7.6	88	97	8.2	6.9	87	14	430	0.8	0.14	0.00	11	1000	370	709
DB-7		8.4	240	5.6	0.6	1.6	160	8.6	130	1.7	0.59	0.07	9.7	80	9	465
DB-8		8.3	230	4.4	0.6	1.4	140	7.7	68	1.8	0.80	0.10	9.9	70	10	376
DB-9		7.7	170	99	13	5.6	110	4.3	370	0.5	2.6	0.00	19	670	120	736
DB-10		8.0	190	62	4.6	4.4	100	5.9	200	2.0	0.61	0.02	8.5	20	30	504
DB-11		8.2	230	13	1.2	2.4	180	7.1	200	1.1	0.49	0.03	9.9	60	20	555
AVG	8.03	191	47	4.7	3.7	130	7.9	233	1.3	0.87	0.04	11	317	93	558	
DB-12	Keenesburg	7.7	430	280	140	35	600	180	1700	4.7	27	0.01	17	10	300	3340
DB-13		8.1	540	3.0	0.8	2.1	300	110	5.7	4.1	0.39	0.05	11	60	10	781
DB-14		7.7	250	160	56	21	180	63	580	2.3	35	0.01	20	60	100	1390
DB-15		7.7	250	160	66	9.6	240	200	830	2.2	3.9	0.05	25	0.0	80	1800
DB-16		8.2	540	2.9	0.7	2.2	290	110	11	4.1	0.15	0.01	11	40	6	769
AVG		7.88	402	121	53	14	322	133	625	3.5	13	0.03	17	34	99	1616
DB-17	Matheson	6.1	35	67	15	3.2	16	4.8	210	0.7	3.4	0.03	41	2300	620	397
DB-18		7.2	99	27	5.5	3.4	18	2.1	29	0.5	0.13	0.01	29	70	30	175
DB-19		7.6	84	24	4.3	2.8	11	1.8	11	0.4	1.7	0.07	28	20	2	141
DB-20		7.6	100	24	5.0	3.0	18	1.4	14	0.4	0.69	0.06	25	10	1	154
AVG		7.12	80	36	7.5	3.1	16	2.5	66	0.5	1.5	0.04	31	600	163	217
State of Colorado <sup>1</sup> Groundwater Standard		6.5–8.5	–	–	–	–	–	250	250	2.0	10	–	–	0.3	0.05	–

<sup>1</sup> Human health/secondary drinking water standard or agricultural use standard, whichever is more stringent.

**Table 2.4 List of CCP Mine Placement Sites**

State		Mine Name	Type of Mine	CCP Types Placed
Arizona	1	Navajo Mine	Active and inactive, surface coal mine	Fly ash, bottom ash, fgd sludge
Colorado	2	Keenesburg Mine	Surface coal mine	Fly ash, bottom ash
	3	Trapper Mine	Active surface coal mine	FA, BA, SS
Illinois	4	Black Beauty, Riola Mine		
	5	Burning Star Mine		
	6	Cottonwood Mine No. 1		
	7	Forsythe Energy No. 5	Abandoned surface mine	FGD sludge, FA
	8	Freeman United Crown III		
	9	Freeman United, Fidelity No. 11		
	10	Freeman United, Orient No. 4		
	11	Harco Mine		
	12	Razorback No. 1		
	13	Creek Paum		
	14	No. 10 Randolph Prep		
	15	Razorback No. 11		
	16	Sahara, Mine No. 6		
	17	Silvercreek, Norris		
	18	Surefire, Majestic No. 14		
	19	Thunderbird Mine	Surface mine	FBC
	20	U.S.A. Coal, Mine No. 10		
Indiana	21	Arnold Willis City Mine	Abandoned underground coal mine	Scrubber sludge, fly ash
	22	Keywest Mine	Surface mine	FBC
	23	Midwestern Mine	Abandoned surface mine	Fixated scrubber sludge
	24	Center Pit	Surface mine	
	25	Little Sandy Mine	Sand and gravel mine	Fly Ash, FGD Sludge
	26	Prides Creek Mine	Active surface coal mine	Fly Ash/Bottom Ash
	27	Black Beauty, Viking	Active surface coal mine	
	28	Black Beauty, Miller Creek	Surface mine	FA,BA
	29	United Minerals, Deer Ridge	Surface mine	FA
	30	Black Beauty, Farmersberg		
Indiana	31	Black Beauty, Francisco Mine	Active Surface Coal Mine	
	32	Vigo, Cypruss Creek		
	33	Black Beauty, Somerville		
	34	Universal Mine	Surface pit	FA

Continued . . .

**Table 2.4 List of CCP Mine Placement Sites (continued)**

		Mine Name	Type of Mine	CCP Types Placed
Kentucky	35	Starfire Mining		
	36	Bluediamond		
	37	Buckhorn		
	38	Floyed County	Coal	FBC ash
Maryland	39	Mettiki Coal		
	40	Patriot Mining		
	41	Fraze Mine, Winding Ridge	Abandoned underground coal	Fly ash, FBC ash, FGD sludge
	42	Kempton Mine	Underground coal	
	43	BBSS Mine	Surface Sand and gravel quarry	Fly ash
	44	Rossville Mine	Surface clay	Fly ash
Ohio	45	Miller Mining, Bucks		
	46	Miller Mining,, Auburn		
	47	Painesville		
	48	Mead		
	49	Clayton		
	50	Milton		
	51	Washington		
	52	Roberts-Dawson		
	53	Broken Aro	Underground	FGD sludge
	54	Fleming Mine	Surface	FBC
Oklahoma	55	Georges Colliers		
	56	MIMHF, Inc.		
	57	Red Oak Mine	Abandoned Underground Coal Mine	FBC ash
Pennsylvania	58	Big Gorilla Pit	Surface	FBC
	59	Alden Mine	Surface	FBC
	60	Knickerbocker Pit	Surface	FBC
	61	McCloskey Site	Surface	FBC
	62	Abel Dreshman	Surface	FBC
	63	Wildwood	Surface	FBC
	64	Clinton County	Surface	FBC
	65	Centralia	Surface Coal Mine	Fly ash
	66	Morris Ridge	Surface Coal Mine	Stabilized ash
	67	Pine Hill	Inactive Coal Mine	FA, BA, mill rejects
	68	Rock Run	Inactive Coal Mine	FA, BA, mill rejects
	69	Zullinger Quarry	Abandoned Limestone quarry	Fly ash
	70	Harwick Mine	Underground	Fly ash
	71	Bognanni Mine	Surface	FBC, FA
72	Wheelabrator Mine	Surface	FBC	
73	Mckay Coal Mine	Surface	FBC	
74	Panther Creek Partners	Surface	FBC	
Texas	75	Monticello Winfield Mine	Lignite surface	Fly ash
	76	San Miguel Mine		FA, BA

Continued . . .



**Table 2.4 List of CCP Mine Placement Sites (continued)**

		Mine Name	Type of Mine	CCP Types Placed
	77	Big Brown Mine	Active Lignite Surface	Bottom ash
Washington	78	Centralia	Strip	BA, FA
West Virginia	79	Fairfax	Underground	FBC
	80	Omega Mine	Surface	FBC, FA
	81	Pierce	Surface	FA
	82	Mt. Storm	Active coal	FA, BA, mill rejects
	83	Long Ridge	Underground	FBC
Wyoming	84	Wyodak Mine	Active surface coal	FA, BA, SS
	85	Jim Bridger		
	86	Kemmerer Mine		
	87	Black Thunder		
	88	Arch Minerals		
Michigan	89	Sibley Quarry	Surface limestone	Fly ash
Missouri	90	Lafarge Sugar Creek		Fly ash
	91	Foster Mine		
	92	Tiger Mine		
Montana	93	Savage Mine	Surface lignite	FA, BA
New Mexico	94	San Juan Mine		
	95	Navaho		
North Dakota	96	Abby		
	97	Beulah		
	98	Buechler		
	99	Burlington		
	100	Center	Surface	FGD sludge, FA
	101	Falkirk		
	102	Freedom		
	103	Lehigh Road		
	104	Parshall		
	105	Scenic East		
	106	Wilton	Underground	Fly ash

**Table 3.1. Post-mining Water Quality Data for Several Pennsylvania Mines**

Mine Site	pH	Net				
		Alkalinity, mg/L	Fe, mg/L	Mn, mg/L	SO <sub>4</sub> , mg/L	Al, mg/L
A	3.2	-185	25	23	1434	N/A
B	5.6	6	0	0	<43	↓
C	7.6	382	5	5	744	
D	2.9	-814	51	29	981	
E	3.1	-361	52	31	432	
F	7.4	237	0	1	32	
Well 6	3.4	-1,140	120	NA*	4600	
Discharge	3.3	-380	48	N/A	2300	
Clinton	2.3	N/A	876	39.2	3477	256
County	2.5	N/A	747	48.1	2958	236

\* Not available.

**Table 4.1. Average Annual Ash Quantities Generated by Wyodak, Neil Simpson I, and Neil Simpson II Power Plants**

CCP Type	Generated Quantity of CCPs, tons/yr		
	Neil Simpson I	Neil Simpson II	Wyodak
Fly Ash	7665	–	–
Bottom Ash	2555	7280	38,325
Scrubber Ash	–	26,880	148,190

**Table 4.2. Summary of Ash-Filled Pits at Wyodak Mine**

Area No.	Year(s) of Ash		Compacted Liner
	Placement	Ash Type	
1	1978–1979	Fly ash	Yes
2	1980	Fly ash	No
2	1981	Fly ash	No
2	1982	Fly ash	No
3	1983	Bottom ash	Yes
3	1983	Fly ash	Yes
3	1984	Fly ash	Yes
3	1985–1987	Fly/scrubber ash	Yes
3	1988–1989	Scrubber ash	Yes
3	1990–1991	Scrubber ash	Yes
3	1992–1995	Scrubber/bottom ash	Yes
3	1995–1998	Scrubber/bottom ash	Yes
4	1998–2009	Scrubber/bottom ash	No

**Table 4.3. Results of 1983 Column Leaching Study for Wyodak (WY) Bottom Ash**

Analyte in Effluent	Effluent Concentration, mg/L unless otherwise noted		Difference, %	Wyoming Groundwater Standard <sup>1</sup>
	Overburden	Bottom Ash		
pH	8	8.2	2.5	6.5–8.5 (6.5-9.0)
TDS	3840	4790	24.7	5000 (500)
Al	<0.1	1	–	5.0 (–)
As	<0.005	< 0.005	0.0	0.2 (0.05)
B	0.07	6.97	9857	5.0 (0.75)
Ba	< 0.5	< 0.5	0.0	– (1.0)
Ca	473	634	34.0	–
Cd	<0.002	< 0.002	0.0	0.05 (0.01)
Cl	250	301	20.4	2000 (250)
Cr	0.02	0.03	50.0	0.05 (0.05)
Cu	0.01	0.02	100	0.5 (1.0)
F	0.96	0.39	–59.4	– (2.4)
Fe	<0.05	< 0.05	0.0	– (0.3)
Hg	<0.001	< 0.001	0.0	0.00005 (0.002)
K	46	45	–2.2	–
Mg	326	277	–15.0	–
Mn	0.13	< 0.02	–100	– (0.05)
Mo	<0.02	0.02	0.0	–
Na	248	413	66.5	–
NH <sub>3</sub> -N	1.53	0.46	–69.9	– (0.58)
Ni	0.06	0.04	–33.3	–
NO <sub>2</sub> + NO <sub>3</sub>	12.4	15.4	24.2	100 (–)
Pb	<0.02	< 0.02	0.0	0.1 (0.05)
Se	<0.005	< 0.005	0.0	0.05 (0.01)
SO <sub>4</sub>	2250	3060	36.0	3000 (250)
Zn	0.02	< 0.01	–100	25 (5.0)

<sup>1</sup> Class III standards for livestock watering and Class I standards for domestic use (in parentheses).

**Table 4.4. Batch Test Results from 1997–1998 on Wyodak Bottom and Scrubber Ash**

Analyte	Groundwater Concentration <sup>1</sup> , mg/L unless otherwise noted				Wyoming Groundwater Standard <sup>2</sup>
	Bottom Ash Test		Scrubber Ash Test		
	Preextraction	Postextraction	Preextraction	Postextraction	
pH (s.u.)	7.3	8.0	7.25	10.48	6.5–8.5 (6.5–9.0)
TDS	3220	3280	3285	3497	5000 (500)
Al	0.79	1.93	0	3.88	5.0 (–)
As	0	0.006	0	0.008	0.2 (0.05)
B	0.37	1.7	0.31	2.69	5.0 (0.75)
Ba	0	0	0	0.25	– (1.0)
Ca	321	279	347	483	–
Cd	0	0	0	0	0.05 (0.01)
Cl	127	119	160	208	2000 (250)
CO <sub>3</sub>	0	0	0	54.5	
Cr	0	0	0	0.25	0.05 (0.05)
Cu	0	0	0	0	0.5 (1.0)
F	0.37	0.22	0.15	3.15	– (2.4)
Fe	0	0	1.74	0.42	– (0.3)
HCO <sub>3</sub>	1120	905	1098	873	
Hg	0	0	0	0	0.00005 (0.002)
K	14.4	16.9	17.5	34.7	–
Mg	234	257	221	270	–
Mn	1.29	0.07	1.21	0.24	– (0.05)
Mo	0	0	0	0.12	–
Na	413	399	463	493	–
NH <sub>3</sub> -N	1.42	1.41	2.03	2.75	– (0.58)
Ni	0.01	0.02	0.01	0.03	–
NO <sub>2</sub> +NO <sub>3</sub>	0	0.09	0	1.48	100 (–)
Pb	0	0	0	0	0.1 (0.05)
Se	0	0.005	0	0.027	0.05 (0.01)
SO <sub>4</sub>	1560	1760	1538	2082	3000 (250)
Zn	0	0	0	0	25 (5.0)

<sup>1</sup> Post-extraction value represents the maximum concentrations in 3 to 10 sequential extractions with fresh groundwater.

<sup>2</sup> Class III standards for livestock watering and Class I standards for domestic use (in parentheses).

**Table 4.5. Groundwater Quality Data for Regulated Analytes in Selected Wells**

Analyte	Wyoming Groundwater Standard <sup>1</sup>	Groundwater Concentration, mg/L unless otherwise noted <sup>2</sup>											
		M-1A (1987–1999)		LF-5 (1990–1999)		M-5A (1984–1999)		M-12 (1977–1981)		M-17 (1977–1999)		M-22 (1981–1999)	
		Max	Mean	Max	Mean	Max	Mean	Max	Mean	Max	Mean	Max	Mean
pH (s.u.)	6.5–8.5	8.1	7.11	7.8	6.7	7.8	7.22	7.8	7.51	8.2	7.51	8.1	7.57
TDS	5000	2954	2403	<b>5468</b>	4831	4220	2558	2520	2520	2200	1781	842	759
Al	5.0	0.1	0.08	0.3	0.07	2.1	0.152	0.5	0.25	0.3	0.1	0.4	0.098
As	0.2	<0.005	<0.005	0.009	<0.005	<0.005	<0.005	<0.005	<0.005	<0.01	<0.005	<0.005	<0.005
B	5.0	0.21	0.09	0.42	0.29	0.31	0.098	<b>6.90</b>	3.49	0.5	0.212	0.22	0.092
Ba	–	0.5	0.36	0.25	0.27	0.5	0.40	0.5	0.5	0.5	0.43	0.9	0.513
Cd	0.05	0.003	0.002	0.003	0.0016	0.006	0.0017	0.03	0.01	0.03	0.0039	0.003	0.0017
Cl	2000	57.28	14.64	224.04	149.8	16.81	10.29	12	4.98	69.16	9.34	29.87	16.83
Cr	0.05	0.02	0.014	<b>0.1</b>	0.014	0.04	0.016	<b>0.1</b>	0.073	<b>1.0</b>	0.05	0.03	0.02
Cu	0.5	0.01	0.03	0.06	0.008	0.02	0.0082	0.01	0.027	0.06	0.012	0.05	0.0095
F	–	0.81	0.454	0.57	0.336	3.77	0.508	0.37	0.37	0.5	0.33	1.6	0.93
Fe	–	2.47	0.228	0.83	0.2	2.06	0.233	22.6	5.865	2.75	0.412	1.11	0.171
Hg <sup>3</sup>	0.00005	<b>0.002</b>	<0.001	<0.001	<0.001	<b>0.002</b>	<0.001	<0.001	<0.001	<b>0.002</b>	<0.001	<0.001	<0.001
Mn	–	1.57	0.56	2.41	1.52	0.21	0.111	0.37	0.257	0.19	0.107	0.04	0.018
NH <sub>3</sub>	–	3.07	0.81	1.86	0.82	10.42	3.12	2.54	2.54	11.86	3.86	3.47	1.67
NO <sub>2</sub> +NO <sub>3</sub>	100	2.42	0.347	0.89	0.121	4.35	0.26	2.8	1.01	4.1	0.68	0.35	0.0475
Pb	0.1	0.02	0.014	0.01	0.011	0.02	0.016	0.02	0.03	0.02	0.017	0.02	0.0165
Se	0.05	0.005	0.0035	0.0025	0.0027	0.005	0.0039	0.005	0.005	0.01	0.0044	0.005	0.004
SO <sub>4</sub>	3000	1427	1255	2930	2501	2543	1318	1510	1279	912	794	15	1.51
Zn	25	0.41	0.066	0.47	0.05	0.34	0.039	0.2	0.143	0.55	0.141	0.07	0.012

<sup>1</sup> Values represent Wyoming Class III livestock use standards.

<sup>2</sup> Values in boldface exceed Class III standards.

<sup>3</sup> The reported detection limit for Hg (0.001 mg/L) is higher than the current Class III standard (0.00005 mg/L).

**Table 4.6. Paste Extract Analysis of Fly Ash and Bottom Ash Samples Prior to Disposal at Keenesburg Mine (CO) (Hazen Research Inc., 1989)<sup>1</sup>**

Analyte	Units	Bottom Ash	Fly Ash
pH	s.u.	11	9.42
Electrical Conductivity	mS/cm	2650	11,900
Arsenic	mg/L	<0.01	0.13
Calcium	mg/L	579	494
Cadmium	mg/L	<0.001	0.008
Chromium	mg/L	0.02	0.17
Copper	mg/L	0.01	0.09
Iron	mg/L	0.04	0.11
Mercury	mg/L	<0.0001	<0.0001
Potassium	mg/L	44.1	89.3
Magnesium	mg/L	0.6	73.2
Manganese	mg/L	<0.01	0.02
Molybdenum	mg/L	0.99	13.3
Sodium	mg/L	260	4410
Nitrate	mg/L	1.39	1.31
Lead	mg/L	0.17	0.12
Selenium	mg/L	0.031	2.42
Sulfate	mg/L	1950	10,500
Zinc	mg/L	0.03	0.05

<sup>1</sup> Pastes prepared using 0.42 g H<sub>2</sub>O/1 g ash.

**Table 4.7. Results of Two Toxicity Characteristic Leaching Procedure Tests on Keenesburg Fly Ash and Bottom Ash Samples (Hazen Research Inc., 1991)**

Analyte	Units	January 1991		December 1991		EPA Limit
		Fly Ash	Bottom Ash	Fly Ash	Bottom Ash	
Silver	mg/L	<0.05	<0.05	<0.05	<0.05	5.0
Arsenic	mg/L	<0.01	<0.01	<0.05	<0.01	5.0
Barium	mg/L	1.6	<0.1	2.4	<0.1	100
Cadmium	mg/L	0.02	<0.01	<0.01	<0.01	1.0
Chromium	mg/L	<0.05	<0.05	<0.05	<0.05	5.0
Mercury	mg/L	<0.0001	<0.0001	<0.0001	<0.0001	0.2
Lead	mg/L	<0.1	<0.1	<0.3	<0.1	5.0
Selenium	mg/L	0.29	0.03	0.08	0.16	1.0
Final pH	s.u.	5.02	4.74	5.70	5.64	—

**Table 4.8. Historic Groundwater Concentrations (mg/L) of Selected Analytes at Keenesburg Mine (CO)**

Analyte	Standard, <sup>1</sup> mg/L	Well	Pre-Ash-Placement (1978–1986)		Post-Ash-Placement (1988–2000)	
			Max	Mean	Max	Mean
As	0.05 (0.1)	DH96	NA	NA	0.11	0.11
		DH122	NA	NA	0.11	0.11
Ba	2.0	AMW-1	NA	NA	0.03	0.03
		DH96	NA	NA	0.14	0.14
		FPW	NA	NA	0.05	0.05
Cl	250	SMW-2	950	815	920	766
Fe	0.3 (5.0)	DH96	0.464	0.464	NA	NA
		DH122	NA	NA	21	12.0
		FPW	1.15	0.69	NA	NA
Mn	0.05 (0.2)	SMW-2	2.7	2.25	1.1	1.015
		DH96	0.53	0.46	1.5	0.52
		DH122	0.96	0.74	1.2	0.71
		DH172	1.3	0.94	NA	NA
		FPW	0.14	0.10	0.33	0.16
		SMW-2	0.31	0.27	0.82	0.38
NO <sub>3</sub>	10.0	AMW-1	NA	NA	4.6	4.4
		DH96	9.7	6.4	NA	NA
		DH122	11.2	3.86	NA	NA
		FPW	9.8	4.7	NA	NA
Se	0.05	AMW-1	NA	NA	0.06	0.028
		DH122	NA	NA	0.05	0.05
		DH133	NA	NA	0.075	0.075
SO <sub>4</sub>	250	AMW-1	NA	NA	990	395
		AMW-2	NA	NA	4100	3567
		DH96	897	716	860	736
		DH122	591	515	690	578
		DH133	3300	3005	NA	NA
		FPW	514	364	280	265
		SMW-2	3500	3300	3800	3047
TDS	400 mg/L or 1.25× background level, whichever is least restrictive	AMW-1	NA	NA	1200	887
		AMW-2	NA	NA	7700	5833
		DH96	1750	1464	1400	1363
		DH122	2934	1818	1300	1175
		DH133	4710	4252	NA	NA
		FPW	720	601	610	610
		SMW-2	7300	6840	7300	6481

<sup>1</sup> State of Colorado basic standards for groundwater (values in parentheses represent standards for agricultural use).

**Table 4.9. Chemical analysis of Craig fly ash and bottom ash  
(Radian Corporation, 1991)**

Analyte	Concentration, mg/kg	
	Fly Ash	Bottom Ash
Aluminum	123,000	110,000
Arsenic	4.0	4.2
Barium	6700	5800
Boron	30	12
Cadmium	19	17
Calcium	65,000	63,000
Chlorine	0.0017	–
Chromium	81	57
Cobalt	30	22
Copper	69	40
Iron	37,000	44,000
Lead	42	16
Magnesium	15,700	13,000
Manganese	300	360
Mercury	0.02	0.02
Molybdenum	47	36
Nickel	54	36
Phosphorous	1900	2052
Potassium	9400	7800
Selenium	0.56	0.56
Silicon	250,000	285,000
Silver	6.9	4.7
Sodium	2400	2200
Strontium	2500	2400
Sulfur	1400	1800
Titanium	5500	5200
Vanadium	380	290
Zinc	170	96



**Table 4.10. Results of Batch Leaching Tests on Trapper Mine (CO) Fly Ash and Bottom Ash (Radian Corporation, 1991)**

Analyte	Units	Fly Ash RCRA Extraction <sup>1</sup>	Fly Ash DI Water Extraction <sup>2</sup>	Bottom Ash DI Water Extraction <sup>2</sup>	Groundwater Quality Standards <sup>3</sup>
pH	s.u.	–	11.4	8.6	6.5-8.5
Ag	mg/L	0.014	0.014	0.008	0.05
Al	mg/L	0.1	92	1.4	(5.0)
As	mg/L	<0.005	<0.005	<0.005	0.05 (0.1)
B	mg/L	12	42	0.55	(0.75)
Ba	mg/L	1.6	12	1.6	2.0
Cd	mg/L	<0.005	< 0.005	<0.005	0.005 (0.01)
Cl	mg/L	<1	<1	12	250
Cr	mg/L	0.025	0.18	0.015	0.1 (0.1)
Cu	mg/L	0.027	0.005	<0.005	1.0 (0.2)
Fe	mg/L	0.017	0.032	0.01	5.0 (0.3)
Hg	mg/L	<0.002	0.002	<0.002	0.002 (0.01)
Mn	mg/L	0.2	0.036	0.036	0.05 (0.2)
Mo	mg/L	0.12	0.48	0.04	–
Ni	mg/L	0.02	0.06	0.02	0.1 (0.2)
Pb	mg/L	<0.002	<0.002	<0.002	0.05 (0.1)
Se	mg/L	<0.002	<0.002	<0.002	0.05 (0.02)
SO <sub>4</sub>	mg/L	80	<3	190	250
V	mg/L	0.41	0.038	0.056	(0.1)
Zn	mg/L	0.09	0.01	0.01	5.0 (2.0)

<sup>1</sup> RCRA extraction performed with acetic acid buffer solution (pH ~ 5.0).

<sup>2</sup> DI water extraction performed with distilled water.

<sup>3</sup> Drinking water standards from Colorado “Basic Standards for Groundwater” (Regulation No. 41, effective March 2, 1999); values in parentheses represent standards for agricultural use.

**Table 4.11. Historic groundwater quality summary for Trapper Mine**

Analyte	Standard <sup>2</sup>	Analyte Concentrations, mg/L unless otherwise noted															
		Well GF6 (1982–2000)				Well GF7 (1987–2000)				Well GF11 (1988–2000)				Well GMP1 (1990–2000)			
		Max	Mean	NS	ND	Max	Mean	NS	ND	Max	Mean	NS	ND	Max	Mean	NS	ND
Al	(5.0)	0.37	0.026	42	34	0.13	0.01	45	39	<0.05	<0.05	22	22	0.25	0.02	34	27
As	0.05 (0.1)	0.034	0.0065	19	3	0.004	<0.001	15	13	0.002	<0.001	13	10	0.004	<0.001	11	8
B	(0.75)	0.24	0.12	45	3	0.3	0.22	45	0	0.19	0.13	22	0	0.36	0.24	34	0
Ba	2.0	0.42	0.11	45	7	0.3	0.046	45	0	0.2	0.067	22	0	0.23	0.12	34	0
Cd	0.005	<0.003	<0.003	20	20	<0.003	<0.003	16	16	0.02	<0.003	14	13	<0.003	<0.003	12	12
Cl	250	81	17.5	19	0	67	40.3	15	0	25	118.5	13	0	35	23.8	11	0
Cr	0.1	0.01	<0.001	42	40	<0.01	<0.01	44	44	0.01	<0.01	21	18	<0.01	<0.01	33	33
Fe	0.3 (5.0)	0.1	0.009	27	21	0.31	0.076	17	6	0.95	0.24	14	4	0.25	0.05	12	4
Mn	0.05	0.06	0.016	44	17	0.76	0.41	45	4	1.35	0.58	22	0	0.17	0.027	34	13
Mo	–	0.03	<0.01	44	42	0.09	<0.01	45	44	<0.05	<0.05	22	22	<0.05	<0.05	33	33
NH <sub>3</sub>	–	1.83	0.9	19	1	6.6	3.82	15	0	2.12	0.79	13	0	0.85	0.63	11	0
NO <sub>3</sub> +NO <sub>2</sub>	10.0 (100)	0.34	0.063	8	4	2.13	0.31	7	5	1.23	0.19	8	5	0.61	0.17	7	3
Pb	0.05 (0.1)	0.02	<0.02	19	18	0.06	<0.02	15	12	0.04	<0.02	14	12	<0.05	<0.05	11	11
pH (s.u.)	6.5 - 8.5	8.6	7.67	32	0	8.5	7.58	31	0	8.44	7.01	31	0	8.7	7.94	27	0
SO <sub>4</sub>	250	284	120	45	0	2840	1898	45	0	1090	569	22	0	873	194	34	0
TDS	1.25 × Background	980	740	42	0	4758	3390	25	0	2320	1581	39	0	1650	945	17	0

Continued . . .

<sup>1</sup> NS = total number of sampling events; ND = number of nondetect measurements.

<sup>2</sup> Colorado drinking water standards (agricultural use standards in parentheses).

A-15

**Table 4.11. Historic Groundwater Quality Summary for Trapper Mine (data from Trapper Mining, Inc.) (continued)**

		Analyte Concentration, mg/L unless otherwise noted															
		Well GD2 (1982–2000)				Well GD3 (1988–2000)				Well GF4 (1982–2000)				Well GF5 (1984–2000)			
Analyte	Standard <sup>2</sup>	Max	Mean	NS	ND	Max	Mean	NS	ND	Max	Mean	NS	ND	Max	Mean	NS	ND
Al	(5.0)	0.07	<0.05	42	40	2.1	0.10	22	20	2.1	0.10	60	39	1.01	0.04	53	44
As	0.05 (0.1)	0.002	<0.001	19	15	0.003	<0.001	13	10	0.003	<0.001	19	14	0.002	<0.001	17	13
B	(0.75)	0.74	0.19	44	0	0.23	0.17	22	0	0.23	0.17	62	1	0.47	0.35	54	0
Ba	2.0	0.3	0.09	45	7	0.22	0.07	22	0	0.22	0.07	64	7	0.68	0.27	53	2
Cd	0.005	<0.003	<0.003	20	20	0.005	<0.003	14	13	0.005	<0.003	21	20	0.005	<0.003	18	17
Cl	250	15	11.7	19	0	26	22.6	13	0	26	22.6	19	0	21	11.2	17	0
Cr	0.1	0.01	<0.004	44	43	0.04	<0.004	21	18	0.04	<0.004	60	57	0.01	<0.004	52	49
Fe	0.3 (5.0)	4.7	0.24	30	8	0.94	0.25	14	3	0.94	0.25	29	7	0.46	0.053	25	8
Mn	0.05	0.14	0.082	45	0	0.6	0.25	22	0	0.6	0.25	64	57	0.08	0.017	53	8
Mo	–	0.2	<0.05	43	40	<0.05	<0.05	21	21	<0.05	<0.05	62	58	<0.01	<0.01	52	52
NH <sub>3</sub>	–	4.1	1.7	19	0	7	1.35	13	0	7	1.35	19	0	3.59	2.85	17	1
NO <sub>3</sub> +NO <sub>2</sub>	10.0 (100)	0.03	0.004	7	6	0.9	0.2	7	4	0.48	0.11	7	3	3.69	0.53	7	4
Pb	0.05 (0.1)	0.06	<0.02	19	17	<0.05	<0.05	13	13	0.02	<0.02	19	18	<0.05	<0.05	17	17
pH (s.u.)	6.5 - 8.5	8.74	7.25	22	0	8.4	7.02	22	0	9.3	8.86	32	0	9.15	8.06	32	0
SO <sub>4</sub>	250	210	99.7	45	0	564	435	22	0	250	122	64	0	251	186	53	0
TDS	1.25 x background	900	793	31	0	1640	1325	28	0	1030	848	31	0	1300	1156	28	0

<sup>1</sup> NS = total number of sampling events; ND = number of nondetect measurements.

<sup>2</sup> Colorado drinking water standards (agricultural use standards in parentheses).

**Table 4.12. Summary of Annual Laboratory Leaching Studies from 1987 to 2000 for coal ash at Savage Mine (Holly Sugar) (Savage, MT)**

Analyte	Analyte Concentration, mg/L unless otherwise noted			Federal DWS <sup>1</sup>	Montana GQS
	Av.	Max.	Std. Dev.		
pH (s.u.)	8.37	9.49	0.68	6.5 – 8.5	–
As	0.005	0.018	0.0052	0.05	0.02
B	9.75	17.80	5.06	–	–
Ba	NM	NM	NM	2.0	2.0
Cd	0.002	0.02	0.0059	0.005	0.005
Cl	23.6	79	25.7	250	4.0
Cr	0.005	0.02	0.0064	0.1	0.1
Cu	0.007	0.02	0.0084	1.0	1.3
F	0.497	1.22	0.417	2.0	4.0
Fe	0.071	0.26	0.091	0.3	–
Hg	0.001	0.005	0.0016	0.002	0.002
Ni	0.01	0.02	0.0083	–	0.1
NO <sub>2</sub> + NO <sub>3</sub>	8.924	88.2	26.3	1.0	1.0
Pb	0.001	0.006	0.0018	0.015	0.015
Se	0.002	0.008	0.0025	0.05	0.05
SO <sub>4</sub>	2249	3824	751	250	–
Zn	0.039	0.238	0.0678	5.0	2.1

<sup>1</sup> Primary or secondary drinking water maximum contaminant level (MCL).

NM = not measured; DWS = drinking water standard; GQS = groundwater quality standard

**Table 4.13. Historic Maximum and Mean Concentrations of Trace Metals in Selected Wells at Savage Mine (MT)<sup>1</sup>**

Analyte	Montana Detection		Well 001		Well 106		Well 261		Well 263		Well 284		Well 286		Well 289		Well 290		Well 291	
	MCL (mg/L)	Limit (mg/L)	Max	Mean	Max	Mean	Max	Mean	Max	Mean	Max	Mean	Max	Mean	Max	Mean	Max	Mean	Max	Mean
As	0.02	0.002	0.002	0.0001	0.004	0.002	0.004	0.001	0.008	0.0013	ND	ND	0.006	0.0004	0.006	0.0024	0.035	0.016	0.29	0.20
B	–	0.1	0.64	0.090	0.72	0.532	0.54	0.36	0.54	0.36	0.58	0.38	0.76	0.59	0.25	0.12	0.59	0.43	0.87	0.68
Cd	0.005	0.01 <sup>1</sup>	0.01	0.0013	0.01	0.0014	0.013	0.0017	0.01	0.0010	0.01	0.0007	0.01	0.0007	0.01	0.001	0.01	0.0014	0.01	0.0017
Cr	0.1	0.05	ND	ND	ND	ND	ND	ND	ND	ND	ND	ND	ND	ND	ND	ND	ND	ND	ND	ND
Pb	0.015	0.002	0.027	0.0032	0.017	0.0046	0.017	0.0019	0.017	0.0028	0.004	0.001	0.007	0.001	0.016	0.0019	0.03	0.0032	0.027	0.0038
Ni	0.1	0.04	ND	ND	0.21	0.021	ND	ND	ND	ND	0.4	0.050	ND	ND	ND	ND	0.1	0.0071	0.09	0.012

<sup>1</sup> Nondetect readings were assigned a value of zero for evaluation of historic mean concentrations.

<sup>2</sup> Reported detection limit for Cd exceeds current Montana MCL.

**Table 4.14. Savage Mine**

	Federal Secondary MCLs	Max.	Min.	Downgraders	Upgraders
263	TDS (500 mg/L)	1156*	1156*	1430	1093
	SO <sub>4</sub> (250 mg/L)	320*	320*	438	380
284	TDS (500 mg/L)	578*	578*	1130	747
	SO <sub>4</sub> (250 mg/L)	226*	226*	320	192
286	TDS (500 mg/L)	650*	650*	1330	897
	SO <sub>4</sub> (250 mg/L)	321.1*	321.1*	541	290
289	TDS (500 mg/L)	1140	890	NA	NA
	SO <sub>4</sub> (250 mg/L)	430	304.6	NA	NA
290	TDS (500 mg/L)	1085*	1085*	1770	1235
	SO <sub>4</sub> (250 mg/L)	468*	468*	745	398
291	TDS (500 mg/L)	1611*	1611*	2550	2155
	SO <sub>4</sub> (250 mg/L)	798.9*	798.9*	1340	1093

\* Asterisk indicates that the reported value is based on analysis of a single groundwater sample prior to ash placement.

**Table 4.15. Annual Tonnage Deposited in the Universal Mine Pit**

Year	Coal Ash	Coal Gasification Slag
1989	270,364	0
1990	254,806	0
1991	0	0
1992	320,000	0
1993	0	0
1994	0	0
1995	75,194	0
1996	114,740	0
1997	95,387	0
1998	117,742	23,301
1999	54,368	14,113
2000	152,571	0
2001	151,335	0
Total Amount	\$1,607,507	37,414

**Table 4.16. Statistical Summary of Bulk Composition Data (mg/Kg) of Coal Ash Samples Placed in the Universal Mine Pit (Wabash River Station)**

Parameter	No. Of Samples	Median	Average	Maximum	Minimum
Aluminum	23	7150	7373	13,200	42
Iron	25	15,700	15,935	27,500	86
Potassium	23	1200	1271	2700	ND***
Magnesium	23	752	714	1280	ND
Sulfate	25	455	526	2000	55
Sodium	25	230	276	570	ND
Boron	25	223	241	455	ND
Calcium	4	5720	5755	6680	4900
Zinc	25	123	129	227	2.1
Barium	25	76	71	220	ND
Manganese	25	80	86	200	1.2
Arsenic	25	57	64	143	ND
Vanadium	23	42	45	71	ND
Nickel	25	40	40	77	ND
Chloride	25	24	41	270	ND
Lead	25	35	36	59	ND
Chromium	25	22	24	42	ND
Copper	25	21	21	41	ND
Fluoride	25	8	18	177	ND
Molybdenum	25	3.7	4.6	12	1.9
Selenium	25	4.1	4.6	9.8	ND
Cadmium	25	1.0	1.1	3.2	ND
Silver	25	ND	0.18	1.6	ND
Mercury	25	0.130	0.113	0.30	ND
Total Organic Carbon	25	52,300	58,357	153,000	5
pH*	22	9.0	9.1	10.6	7.5
Potential Acidity**	25	0.3	2.6	21.6	ND
Neutralization Potential**	25	17.1	19.8	48.6	7.5
Net Neutralization Potential**	25	15.5	17.6	48	ND

\* Unit for this parameter is s.u.

\*\* Unit for these parameters is T/1000T.

\*\*\* Nondetect.

**Table 4.17. Statistical Summary of Concentrations (mg/L) Measured in Coal Ash Leachates (Universal Mine Study – Wabash River Station Coal Ash)**

Parameters	18-hr Leachate			30-day Leachate	
	No. of Samples	Average	Median	Average	Median
Aluminum	23	3.43	2.9	2.73	2.6
Boron	25	2.65	2.3	3.39	3.1
Sulfate	25	135	31	56.8	47
Chloride	25	0.7	ND	1.34	1.1
Iron	25	0.67	ND	0.34	ND*
Magnesium	23	0.5	ND	0.44	ND
Potassium	23	0.84	ND	0.78	ND
Sodium	25	1.45	ND	1.59	ND
Arsenic	25	0.285	0.26	0.301	0.31
Fluoride	25	0.225	0.23	0.285	0.29
Vanadium	23	0.18	0.21	0.23	0.27
Molybdenum	25	0.12	0.09	0.13	0.11
pH (standard units)	24	10.05	10.05	9.63	9.66
Barium	25	2	0.04	0.078	ND
Cadmium	25	0.0009	ND	0.0005	ND
Chromium	25	0.01	ND	0.01	0.011
Copper	25	0.008	ND	0.002	ND
Lead	25	0.002	ND	0.006	ND
Manganese	25	0.022	ND	0.004	ND
Nickel	25	0.002	ND	0.003	ND
Selenium	25	0.067	0.058	0.102	0.085
Zinc	25	0.043	0.02	0.018	ND
Silver	25	ND	ND	0.001	ND
Mercury	25	ND	ND	ND	ND
Sulfide	25	0.133	ND	0.077	ND

\* Nondetect.



**Table 4.18. Summary Statistics for Measured Concentrations (mg/L) in MW-8 Leachate Water**

Parameter	No. Of Samples	Mean	Median	Minimum	Maximum
Alkalinity	17	276.2	220	120	530
Boron	17	44.2	46	ND*	56
Chloride	17	284.4	91	21	700
Sodium	17	190	120	ND	430
Sulfate	17	1847	1700	1400	3800
Total Organic Carbon	17	15.4	1.9	ND	110
Magnesium	17	6.6	6.9	ND	8.1
Molybdenum	17	1.7	1.6	0.96	2.3
Aluminum	15	0.38	0.44	ND	0.49
Arsenic	17	0.205	0.208	0.13	0.26
Sulfide	17	0.21	ND	3.4	ND
Barium	17	0.053	0.036	ND	0.35
Fluoride	17	0.007	ND	ND	0.12
Manganese	17	0.012	0.012	ND	0.023
Acidity	17	ND	ND	ND	0.0004
Cadmium	17	ND	ND	ND	ND
Chromium	17	ND	ND	ND	ND
Iron	17	ND	ND	ND	ND
Lead	17	ND	ND	ND	ND
Mercury	17	ND	ND	ND	ND
Selenium	17	ND	ND	ND	0.006
Silver	17	ND	ND	ND	ND
Zinc	17	ND	ND	ND	ND
pH (standard units)	17	8.96	9.2	9.5	6.9

\* Nondetect.

**Table 4.19. List of Water Quality Parameters Monitored at the Universal Site**

Acidity	Mercury
Alkalinity	Molybdenum
Aluminum	Nickel
Arsenic	ORP
Boron	Potassium
Cadmium	Selenium
Calcium	Silver
Chloride	Sodium
Chromium	Specific conductivity
Copper	Sulfate
Fluoride	Sulfide
Hardness	Temperature
Iron	TDS
Lead	TSS
Magnesium	TOC
Manganese	Zinc
	pH

**Table 4.20: Cheswick Power Station (Harwick Mine Complex, PA) Chemical and Leachate Analysis of Fly Ash**

Parameter	Total Constituent Analyses, mg/kg	EP Toxicity Leachate, mg/L	ASTM Water Leachate, mg/L
Aluminum	109,000	0.03	0.06
Antimony	<30	0.041	<0.005
Arsenic	<10	<0.005	0.033
Barium	158	0.07	0.08
Cadmium	<10	0.01	0.01
Chloride	–	0.8	8.0
Chromium (total)	148	<0.03	<0.03
Chromium (+6)	247	<0.03	<0.03
Copper	325	1.43	0.03
Iron	60,100	0.04	0.02
Lead	<10	0.01	0.05
Magnesium	5680	3.60	1.99
Mercury	<0.3	<0.0004	<0.0004
Molybdenum	19.7	0.006	0.038
Nickel	493	7.35	0.01
Selenium	2	0.023	0.020
Silver	19.7	0.01	0.01
Sulfate	2070	51	41
Sulfide by N <sub>2</sub> generations	<1	3	<3
Tin	10	<0.004	<0.004
Zinc	2436	0.11	0.01
pH	7.05	4.77*	7.21
Conductivity (µmhos/cm)	–	309	160
Total Suspended Solids	–	7.2	8.0
Chemical Oxygen Demand	–	110	<3
Corrosivity	No	–	–
Corrosive	7.0	–	–
pH	<1	<2	<2
Cyanide	>200	–	–
Flashpoint (°F)	0.6	–	–
Nitrate (as M)	–	<1.0	7.3
Oil & Grease`	<5	<0.005	<0.005
Phenols	–	237	134
Total Residue	2.54	–	–
% Volatile Residue	–	230	128
Total Dissolved Solids	6200	48.0	<1.0
Total Organic Carbon	<20	–	–
Total Organic Halogens	280	–	–
Total 1 Nitrogen	–	–	–

\* 12 mls acetic acid added.

**Table 4.21. Chemical Analysis Results for the Monarch Mine  
(Harwick Mine Complex, PA) Effluent, November 1973**

---

pH	6.0
Specific Conductance	4000 $\mu\text{mhos}/\text{cm}^2$
Total Acidity	<1 mg/L
Alkalinity	300 mg/L
Turbidity	200 JTU
Chloride	170 mg/L
Sulfate	1560 mg/L
Hardness	1400 mg/L
Calcium	184 mg/L
Magnesium	235 mg/L
Total Dissolved Solids	3854 mg/L
Total Iron	200 mg/L
Sodium	810 mg/L

---

**Table 4.22. Pre-and Post-Grouting Mean Concentrations of Mine Drainage Constituents for Wells Located in Discharge Plumes at the Clinton County, PA Site (Schuck et. al. 1996)**

**Monitoring Well FF62**

Condition	Lab, pH	TDS, mg/L	SO <sub>4</sub> , mg/L	Acid, mg/L	Fe		Al, mg/L	Mn, mg/L	Cd, µg/L	Cu, µg/L	Cr, µg/L	Ca, µg/L
					Tot, mg/L	Fe,+3, mg/L						
Pregrout	2.3	7970	3477	4088	876	737	256	39.2	83.6	806	221	58.1
Postgrout	2.5	5780	3110	2879	527	373	173	24.7	29.3	813	168	61.4

**Monitoring Well S80D**

Condition	Lab, pH	TDS, mg/L	SO <sub>4</sub> , mg/L	Acid, mg/L	Fe,	Fe,	Al, mg/L	Mn, mg/L	Cd, µg/L	Cu, µg/L	Cr, µg/L	Ca, µg/L
					Tot, mg/L	+3, mg/L						
Pregrout	2.4	9951	3500	5096	937	749	394	45.5	108.5	154.2	394	66.4
Postgrout	2.7	7222	3483	3230	530	254	282	32.4	24.9	771	232	58.7

**Monitoring Well W70**

Condition	Lab, pH	TDS, mg/L	SO <sub>4</sub> , mg/L	Acid, mg/L	Fe,	Fe,	Al, mg/L	Mn, mg/L	Cd, µg/L	Cu, µg/L	Cr, µg/L	Ca, µg/L
					Tot, mg/L	+3, mg/L						
Pregrout	2.6	9689	3695	4611	735	606	397	49.4	60.2	985	221	81.9
Postgrout	3.0	4795	3327	2348	268	185	180	21.8	17.3	635	156	56.3

**Monitoring Well V36**

Condition	Lab, pH	TDS, mg/L	SO <sub>4</sub> , mg/L	Acid, mg/L	Fe,	Fe,	Al, mg/L	Mn, mg/L	Cd, µg/L	Cu, µg/L	Cr, µg/L	Ca, µg/L
					Tot, mg/L	+3, mg/L						
Pregrout	2.7	6777	3568	3624	570	396	316	63.7	57.3	526	104	83.1
Postgrout	3.1	5330	3111	2351	380	263	212	33.8	21.6	689	149	71.9

**Table 4.23. Water Quality Data for Before Placement of Ash in the Big Gorilla Pit and after Placement of Ash in the Big Gorilla. Silverbrook Outflow Water Quality Data are also shown.**

Analyte	Big Gorilla 1993	Big Gorilla 1998	Silverbrook 1998
pH	3.2	11.4	4.3
Conductivity, $\mu$ mhos/cm	210	1273	443
Alkalinity, mg/L CaCO <sub>3</sub>	<1	172	6.2
Acidity mg/L	37.8	<1	78
Turbidity, NTU	0.24	1.6	<1
Dissolved Solids, mg/L	98	311	268
Chloride, mg/L	6	3	9
Sulfate, mg/L	59	369	193
Aluminum, mg/L	4.2	1.32	6.81
Arsenic, mg/L	<0.001	<0.004	<0.004
Barium, mg/L	<0.1	0.0013	0.028
Cadmium, mg/L	0.0007	<0.01	<0.01
Calcium, mg/L	3.95	195	27
Chromium, mg/L	<0.001	0.051	<0.05
Copper, mg/L	0.02	0.012	0.023
Iron, mg/L	0.4	<0.02	17.7
Lead, mg/L	0.001	<0.001	<0.001
Magnesium, mg/L	4.5	0.193	9.6
Manganese, mg/L	0.72	<0.01	1.64
Mercury, mg/L	<0.0002	0.0014	<0.001
Nickel, mg/L	<0.04	<0.05	0.091
Nitrogen, mg/L	<0.5	0.09	<0.04
Potassium, mg/L)	1	10.4	1.84
Selenium, mg/L	<0.002	<0.007	<0.007
Silica, mg/L	N/A	19.11	15.96
Sodium, mg/L	1.15	9.87	9.85
Zinc, mg/L	0.2	<0.01	0.295

NA Not available.

**Table 4.24. Average of Values Above Detection from Analyses Performed on NEPCO Fly and Bottom Ash for Module 25 Regulations from 1992–2002 (maximum allowable leachate concentration values provided for comparison)**

Parameter Name	Bulk Analysis, mg/Kg		Leachate Analysis, mg/L*		Max. Leachate Conc., mg/L
	Fly Ash	Bottom Ash	Fly Ash	Bottom Ash	
pH, s.u.	10.67	11.47			
Sulfate	4901	3073	440	169	2500
Aluminum	26,440	13,993	2.53	2.77	5
Antimony	2.24	LF	0.05	0.01	0.15
Arsenic	17.79	3.55	LF	LF	1.25
Barium	211	116	0.16	0.21	50
Boron	44.07	8.49	0.30	0.37	31.5
Cadmium	1.22	0.68	LD	LD	0.13
Chromium	27.25	11.49	0.09	LF	2.5
Cobalt	3.62	1.11	LF	LF	
Copper	28.13	8.18	0.09	0.07	32.5
Iron	8713	4399	0.14	0.24	7.5
Lead	29.99	12.17	LF	LF	1.25
Manganese	161.04	2672.65	0.20	0.21	1.25
Mercury	0.64	LF	LF	LF	0.05
Molybdenum	9.28	3.29	0.13	0.02	4.38
Nickel	11.75	5.08	LF	LF	2.5
Potassium	6737	4400	9.88	7.75	
Selenium	14.38	5.47	0.17	0.03	1
Silver	3.56	LF	LF	LF	
Zinc	18.96	9.78	0.18	0.26	125
Nitrate-N			1.27	2.92	
Chloride			15.75	54.67	2500
Sodium			10.73	6.14	
Total Organic Carbon			LF	2.11	
Acid Neutralizing Potential	847,400	1,258,625			

LD = always less than detection.

LF = less than 5 measurements above detection (of 22).

\*Leachate analyses were performed by TCLP before January 1995, and SPLP thereafter.

**Table 4.25. Average of Concentrations of Groundwater Samples from Wells Sampled Four times a Year on or Near the NEPCO Property**

Location	Well 1 5/89–2/91	Well 2 12/90–11/02	Well3 9/96–11/02	Well 4 12/01–11/02	Well 9 9/96–11/02
No. of samples	8	58	40	4	39
pH	4.30	5.04	4.30	3.75	3.7
Conductivity	89.13	68.88	249.28	528.25	455
Alkalinity	1.20	8.16	3.30		
Hot Acidity	37.56	47.79	47.49	114.95	147.1
Iron, T	3.77	0.60	1.74	18.22	0.6
Manganese, T	0.33	0.43	0.85	8.69	1.7
Sulfate, T	33.50	30.81	82.82	191.75	182.7
Chloride	0.95	1.89	2.26		6.6
Sodium	0.25	4.66	9.38	4.47	16
Dis. Solids	75.25	69.40	161.54	438	368.6
Sus. Solids	2.86	7.15	9.48	5.33	29.2
Nitrate N		1.49	0.07		0.2
Silica, T		7.38	10.26	28.61	57.7
Aluminum, T	0.66	0.45	2.65	10.09	18
Barium, T		0.03	0.03		
Calcium, T		6.26	20.65	32.03	18.8
Magnesium, T	2.70	3.79	5.84	14.23	8.9
Zinc, T	0.12	0.33	0.31	0.68	0.4
Potassium, T		1.68	1.84	2.34	3.9

All concentrations reported in mg/L except for conductivity ( $\mu\text{S}/\text{cm}$ ), turbidity (ntu), and pH (s.u.).  
T indicates total concentrations in the water samples.



**Table 4.26. Average Values for Chemical and Physical Characteristics of the Acid Mine Drainage from the Red Oak Mine Site**

Parameter	Concentration, mg/L
Aluminum	6
Calcium	63
Iron	200
Magnesium	42
Manganese	7
pH	4.3
Acidity (as CaCO <sub>3</sub> )	475

**Table 4.27. XRF Data for the Materials Used in Grout Admixtures**

Constituents, %	FBC By-Product	Class F Flyash	FGD Material	Quick Lime
K <sub>2</sub> O	1.6	2.4	0.2	None
MgO	2.3	1.1	0.67	1.5
Fe <sub>2</sub> O <sub>3</sub>	6.2	5.6	0.56	0.35
Al <sub>2</sub> O <sub>3</sub>	11.5	28.5	2.6	0.5
SiO <sub>3</sub>	12.3	0.59	47.1	0.04
SiO <sub>2</sub>	24.7	52.4	3.4	1.5
CaO	24.8	1.6	35.4	97.5

## **APPENDIX B**

### **FIGURES**

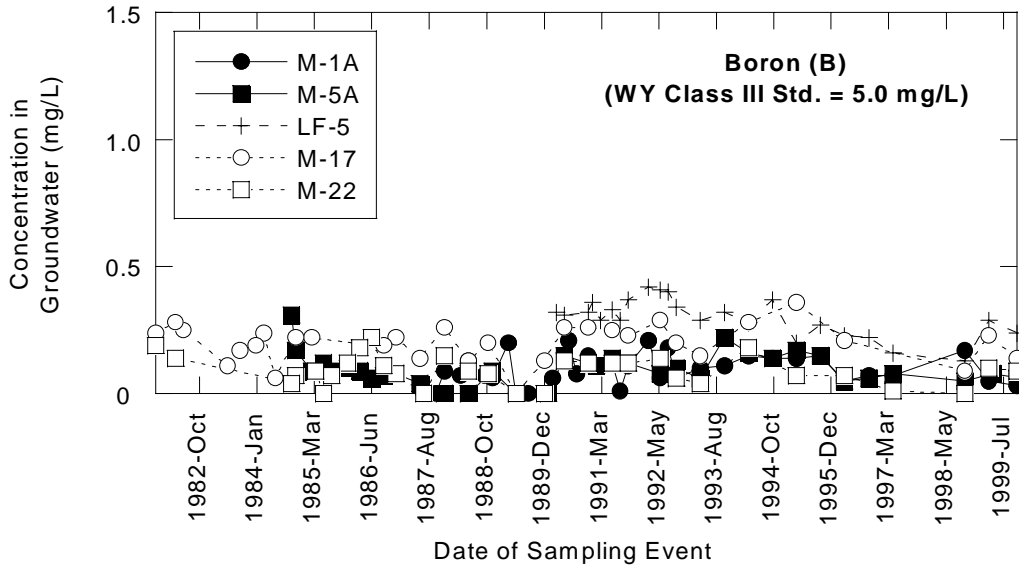


Figure 4.1. Historical trends of boron (B) in groundwater from selected wells at the Wyodak Mine.

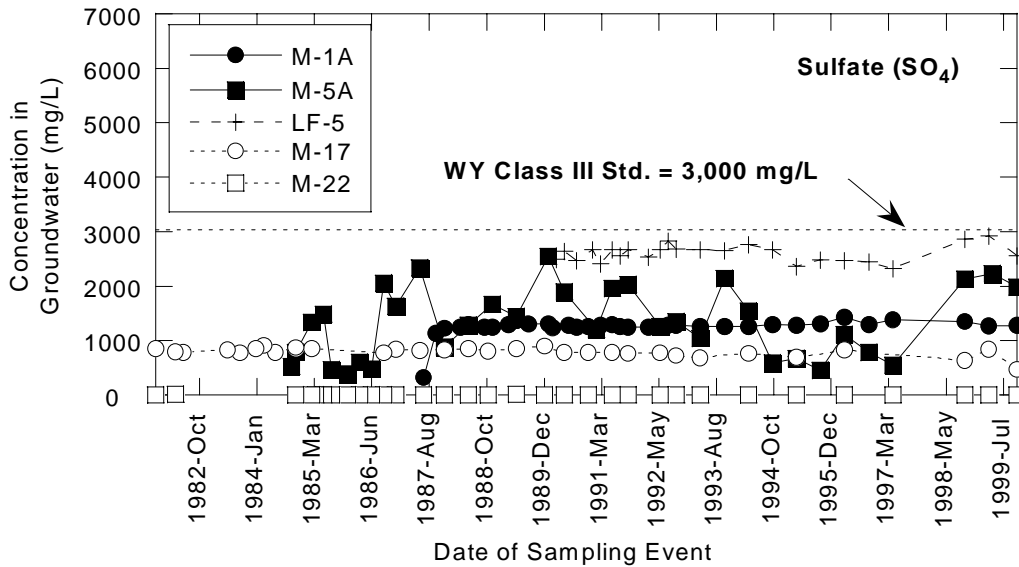


Figure 4.2. Historical trends of sulfate (SO<sub>4</sub>) in groundwater from selected wells at Wyodak Mine.

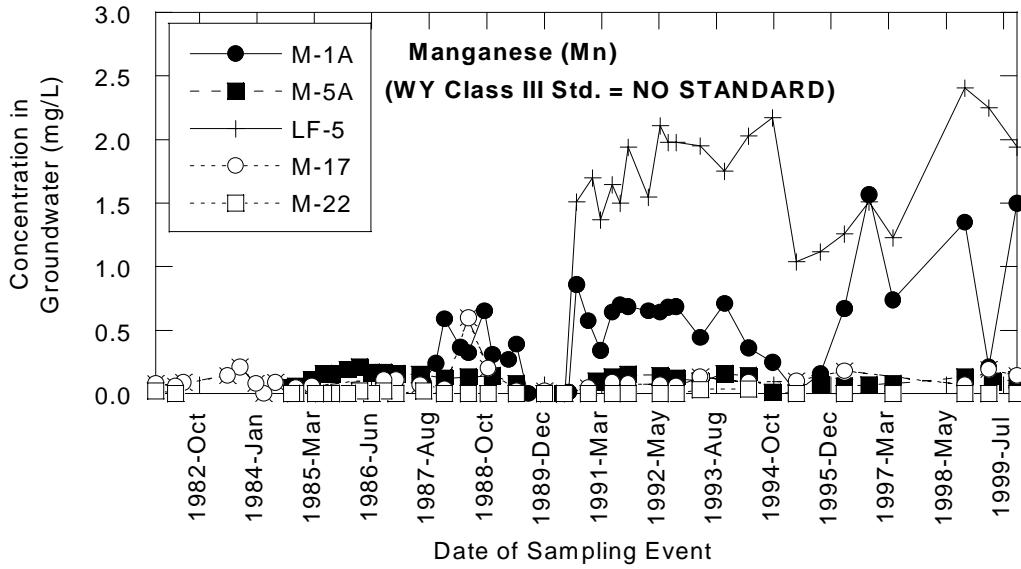


Figure 4.3. Historical trends of manganese (Mn) in groundwater from selected wells at Wyodak Mine.

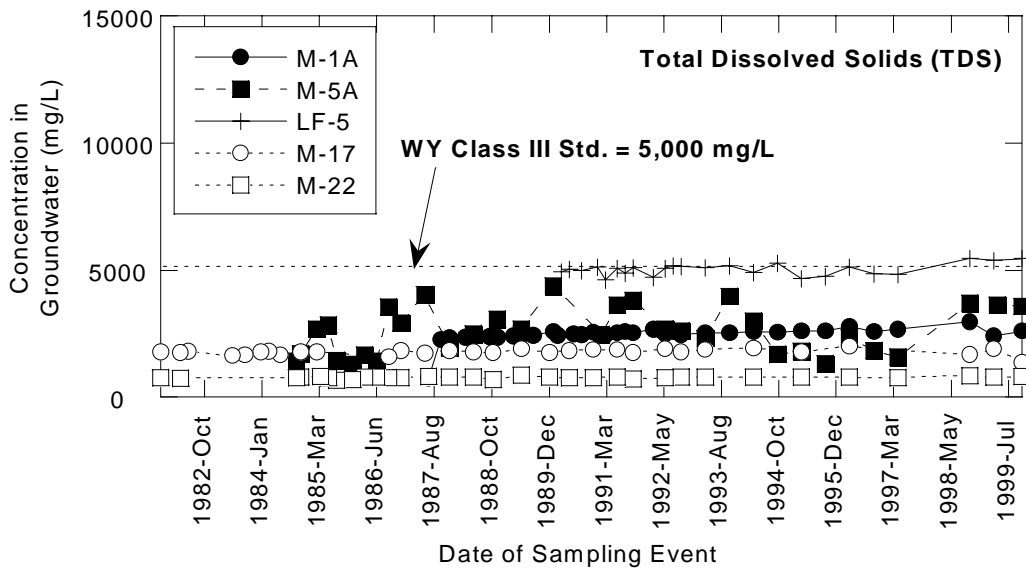


Figure 4.4. Historical trends of total dissolved solids (TDS) in groundwater from selected wells at Wyodak Mine.

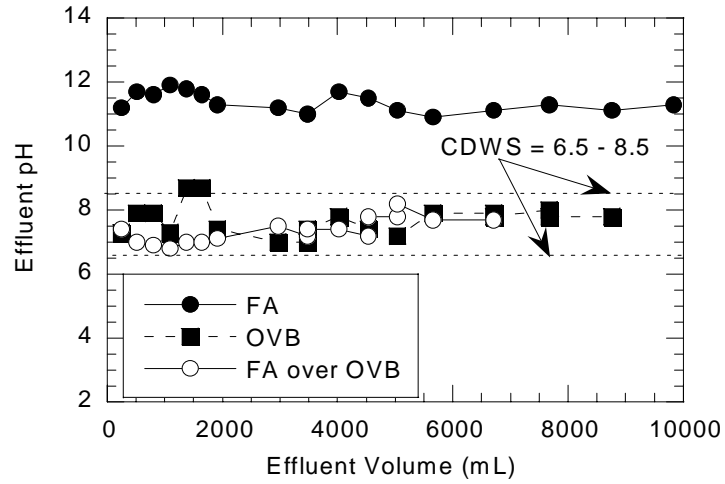


Figure 4.5

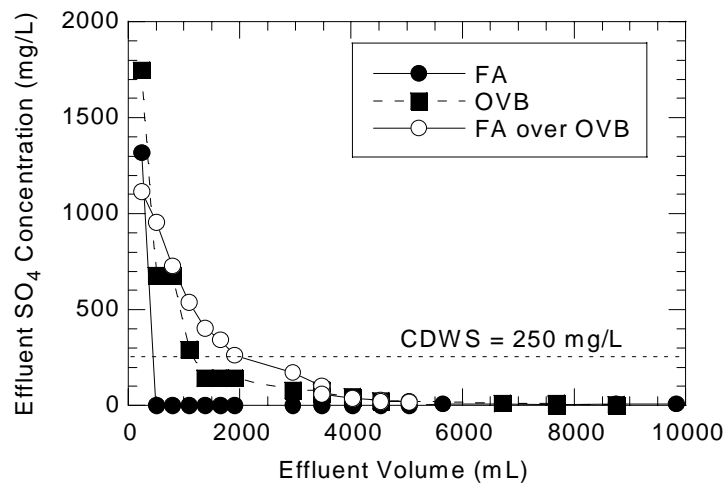


Figure 4.6. Effluent levels of pH SO<sub>4</sub>, Al, and Ba measured in Trapper Mine (CO) column leaching study (FA = fly ash, OVB = overburden, CDWS = Colorado drinking water standard).

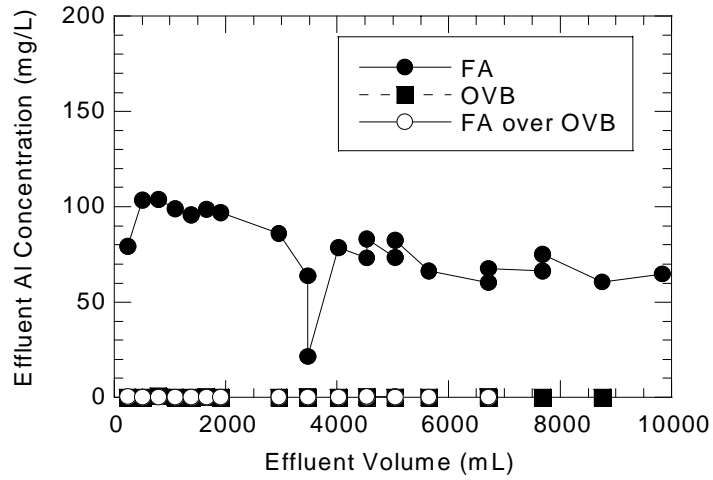


Figure 4.7. Effluent levels of B, Cr, Mn, and V measured in Trapper Mine (CO) column leaching study (FA = fly ash, OVB = overburden, GWS = Colorado groundwater standard).

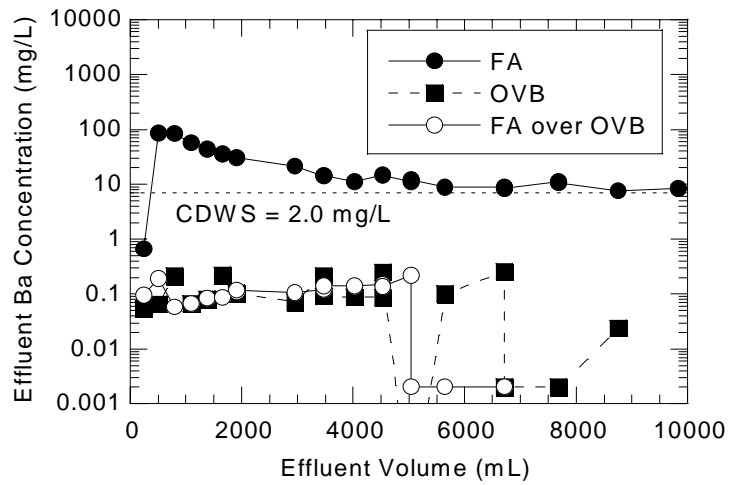


Figure 4.8

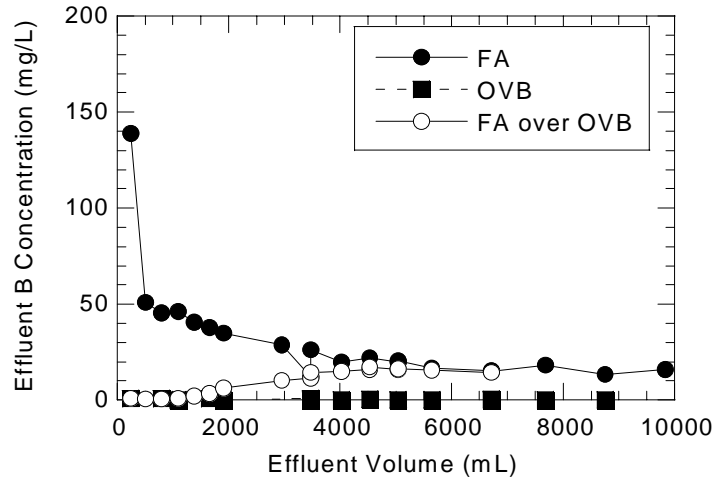


Figure 4.9

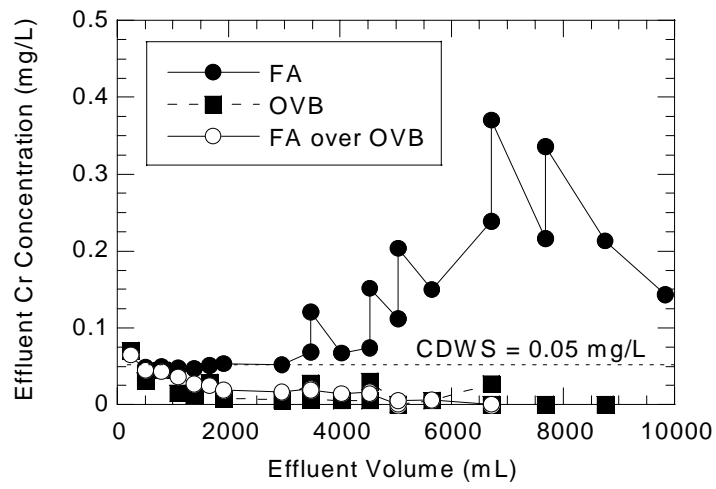


Figure 4.10



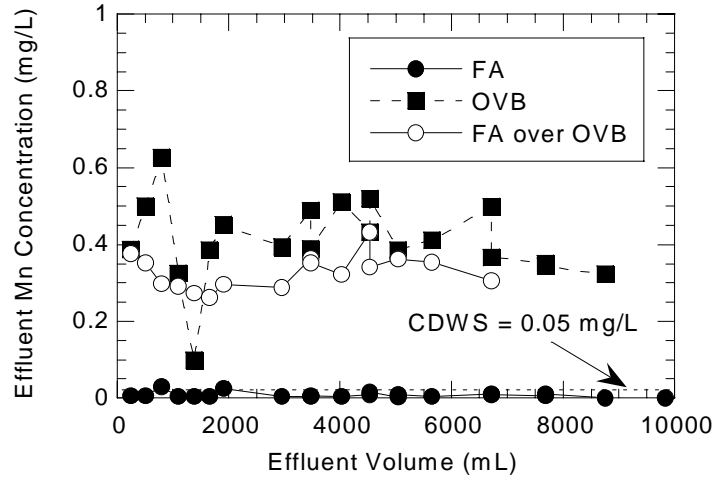


Figure 4.11

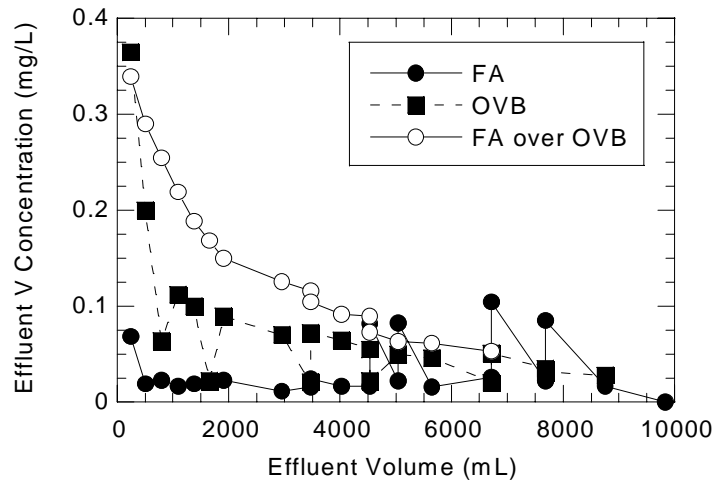


Figure 4.12

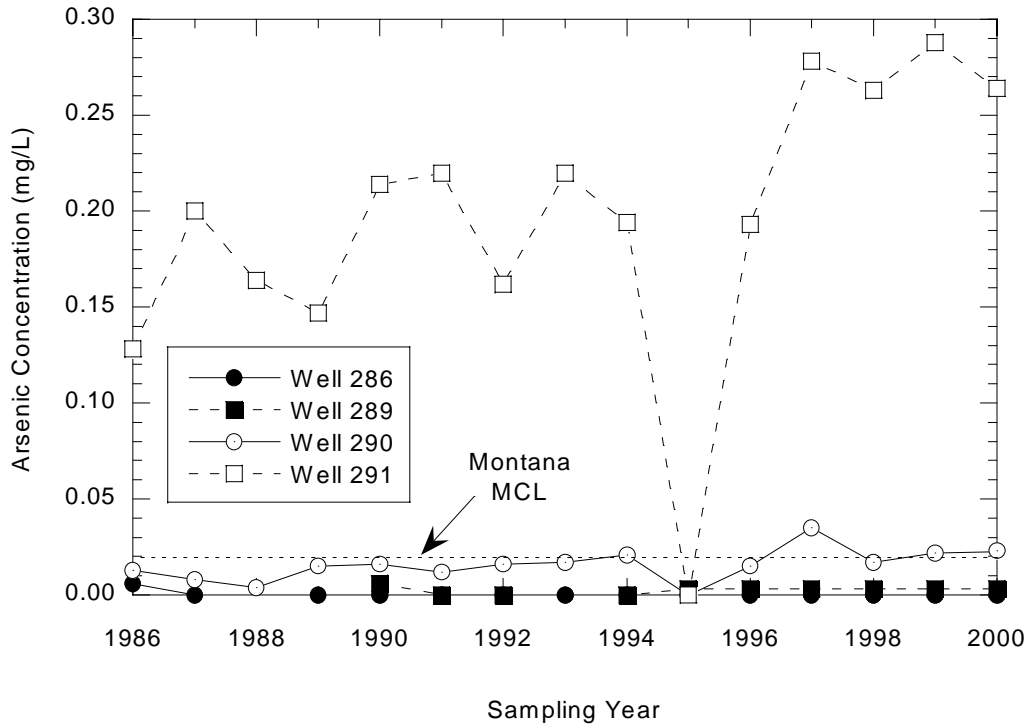


Figure 4.13 Historic arsenic (As) concentrations in groundwater monitoring wells at Savage Mine (MT).

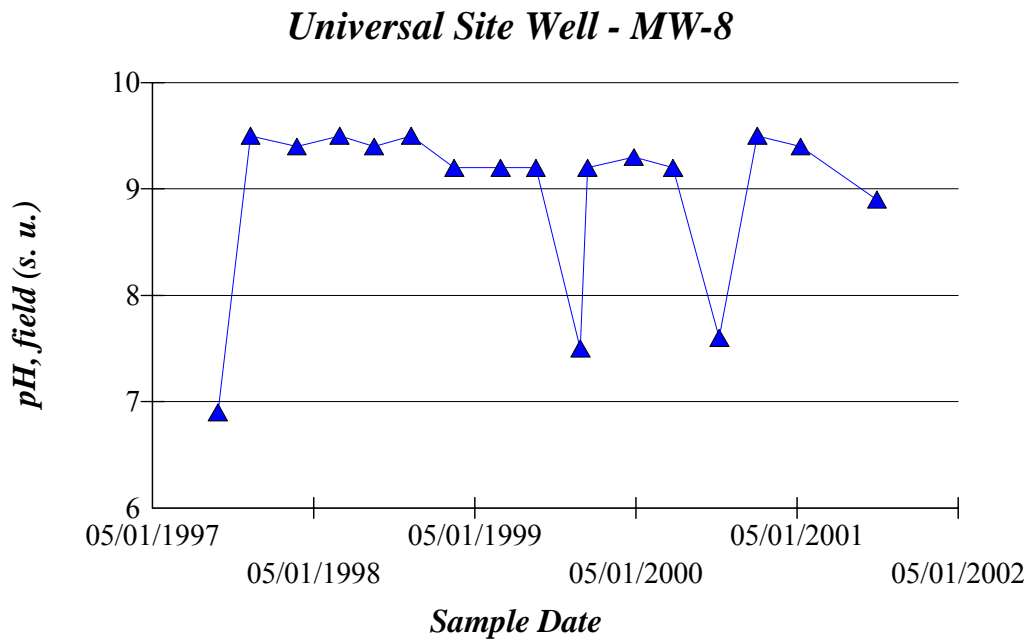


Figure 4.14 Time-series plot of measured pH in field leachate samples.

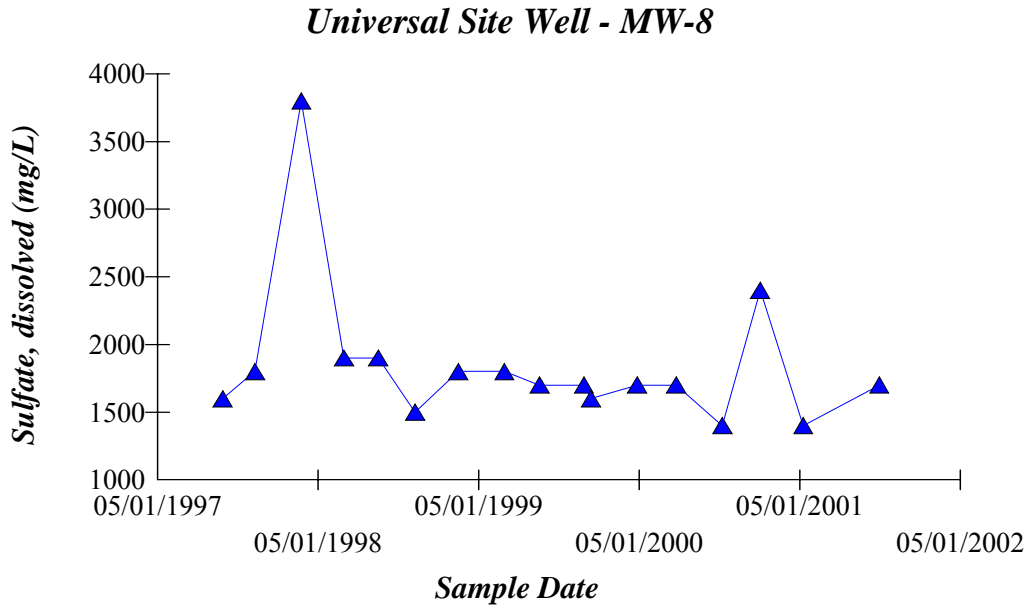


Figure 4.15. Time-series plot of measured sulfate concentrations in field leachate samples.

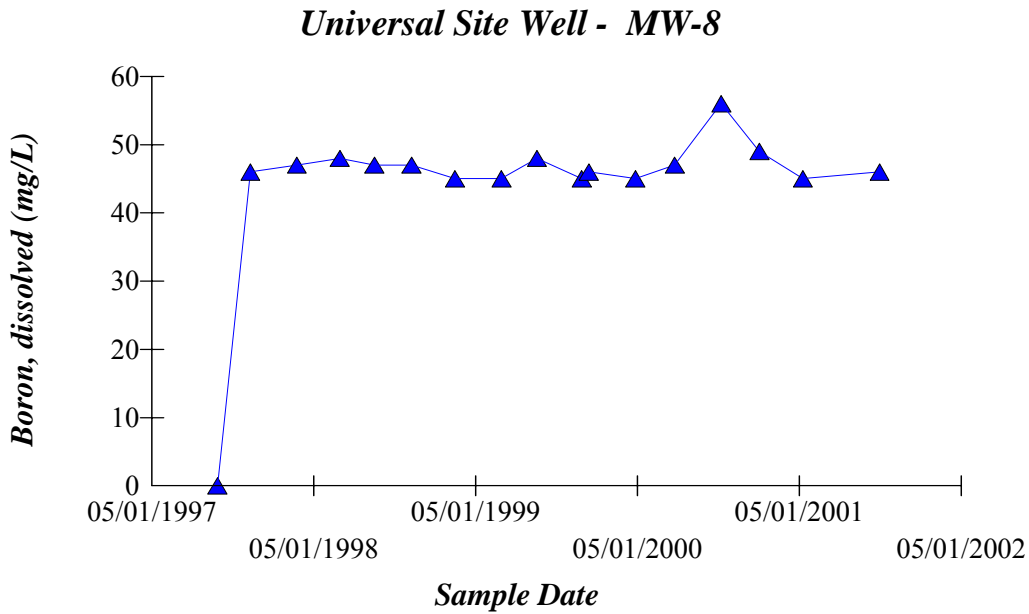


Figure 4.16. Time-series plot of measured boron concentrations in field leachate samples.

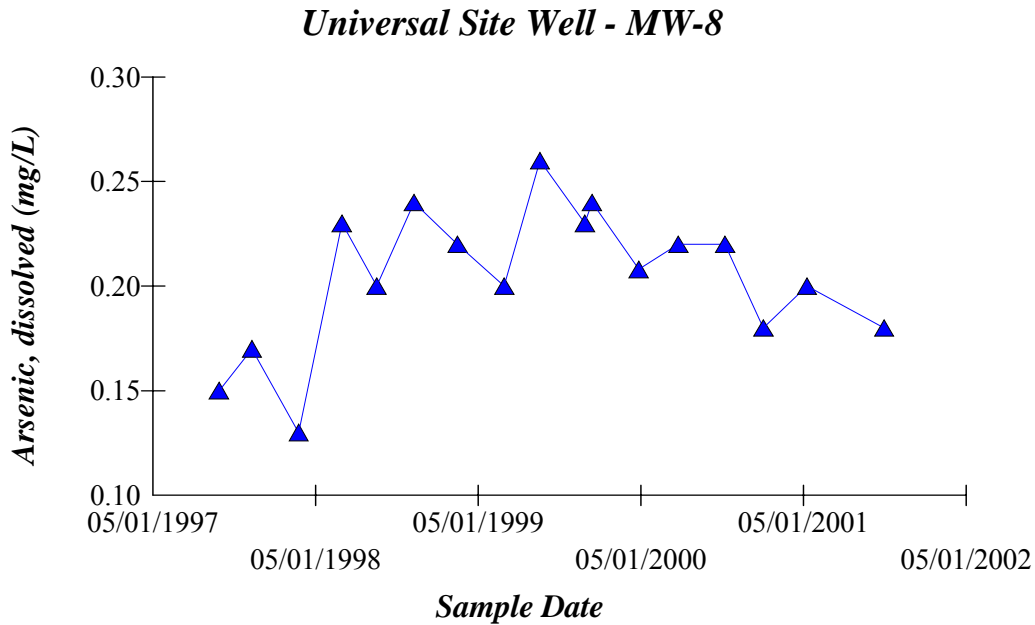


Figure 4.17. Time-series plot of arsenic concentrations in field leachate samples.

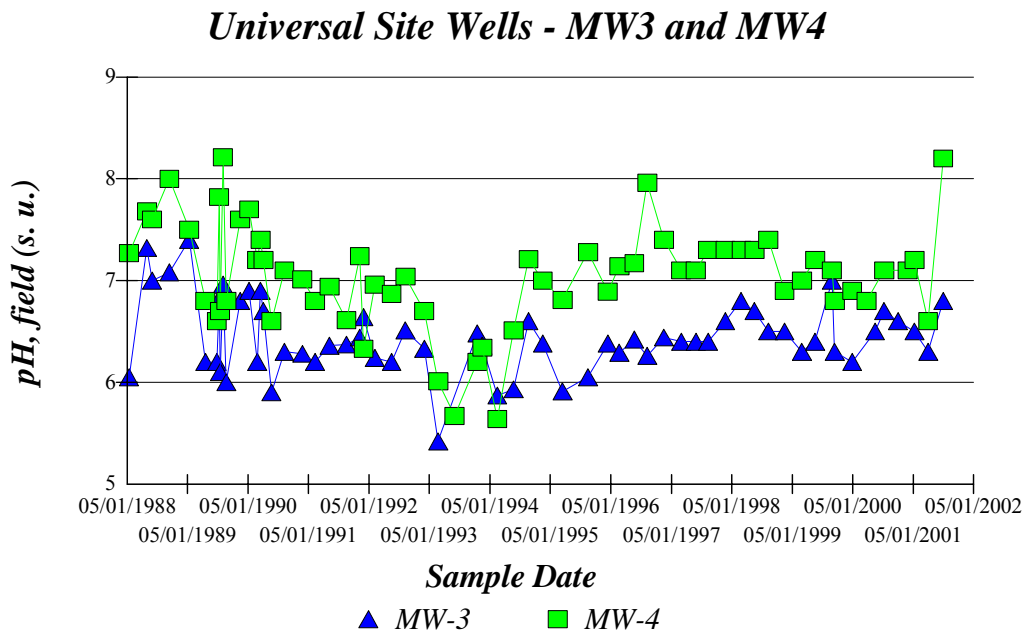


Figure 4.18. Time-series plot showing pH measured in groundwater samples.

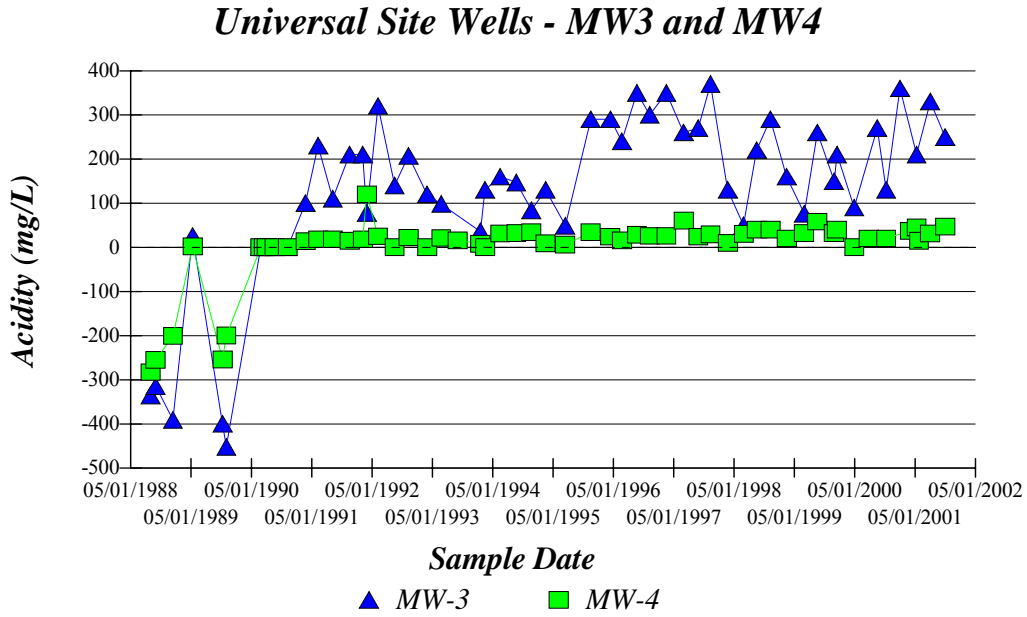


Figure 4.19. Time-series plot of acidity measured in groundwater samples.

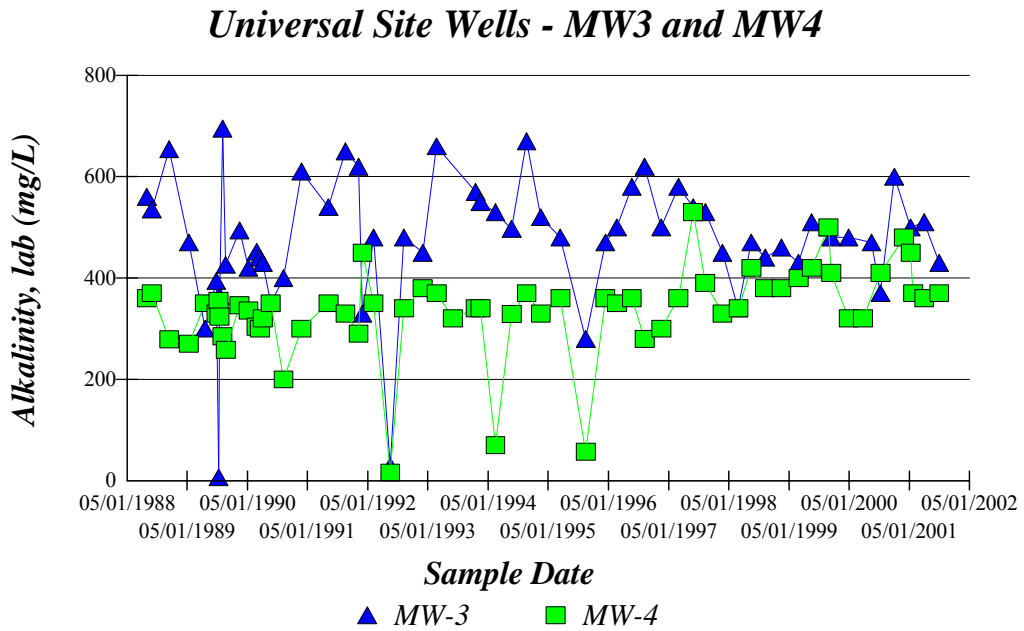


Figure 4.20. Time-series plot of alkalinity measured in groundwater samples.

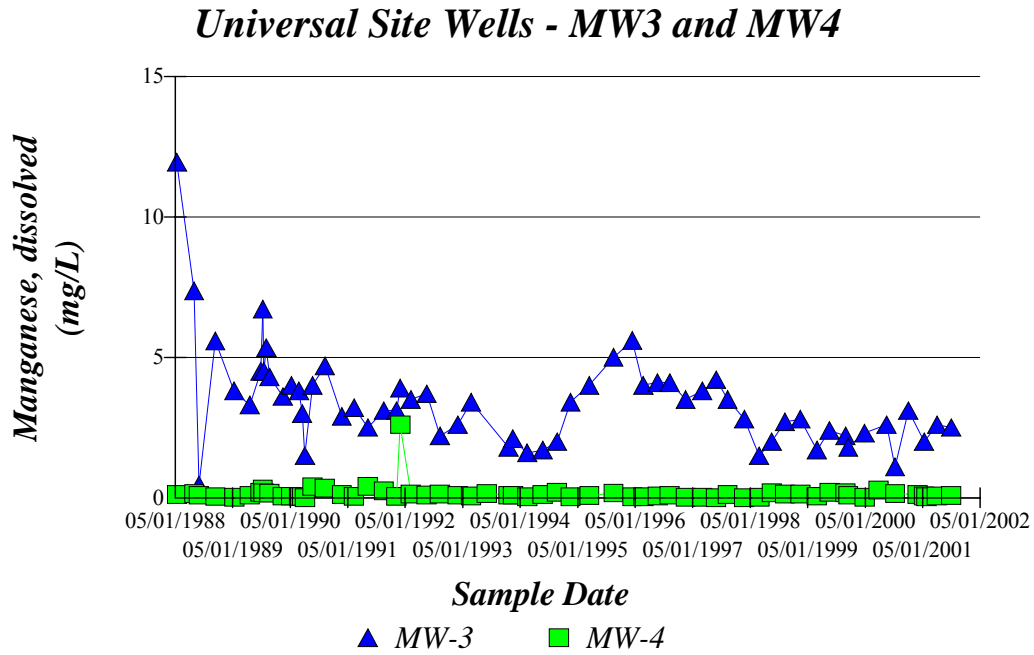


Figure 4.21. Time-series plot of manganese measured in groundwater Samples

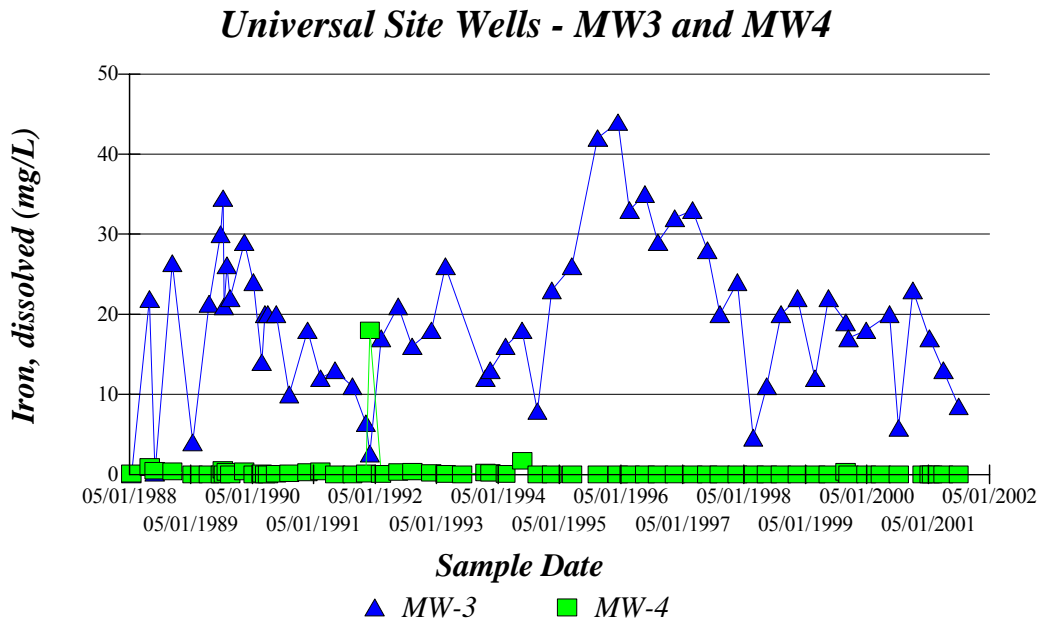


Figure 4.22. Time-series plot of iron measured in groundwater samples.

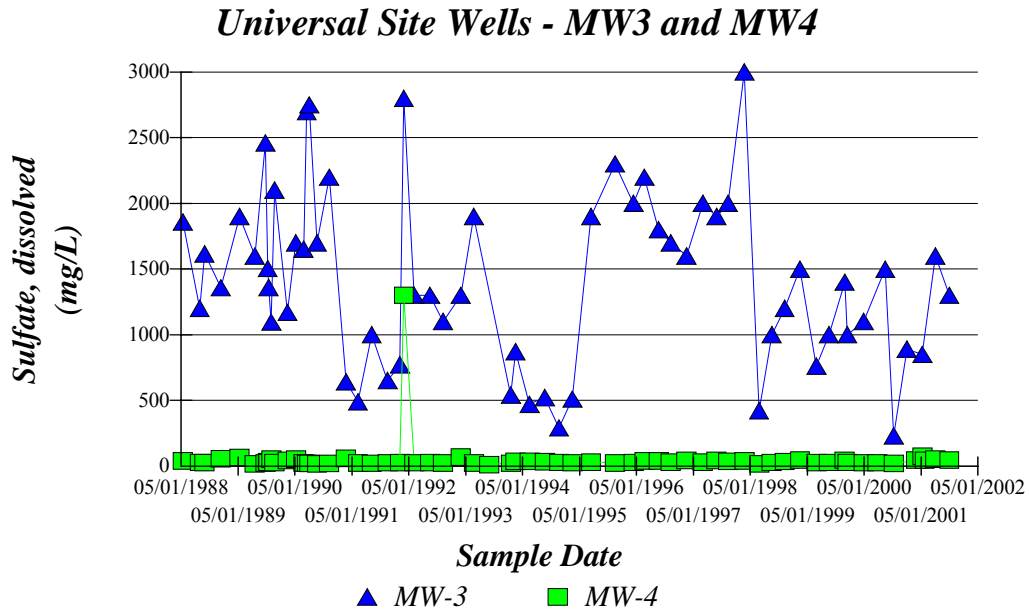


Figure 4.23. Time-series plot of sulfate measured in groundwater samples.

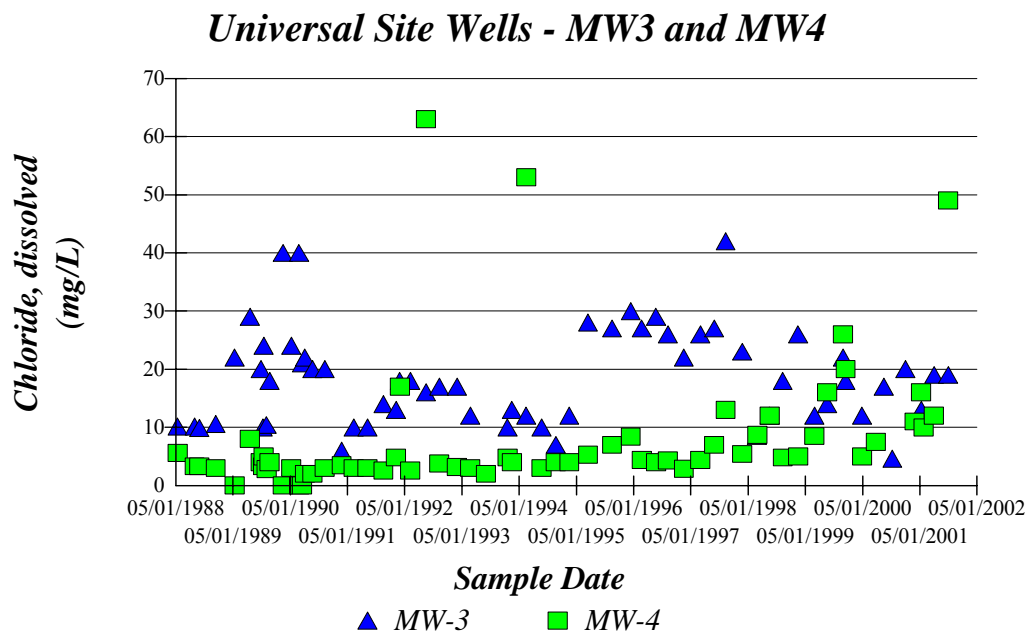


Figure 4.24. Time-series plot of chloride measured in groundwater samples.

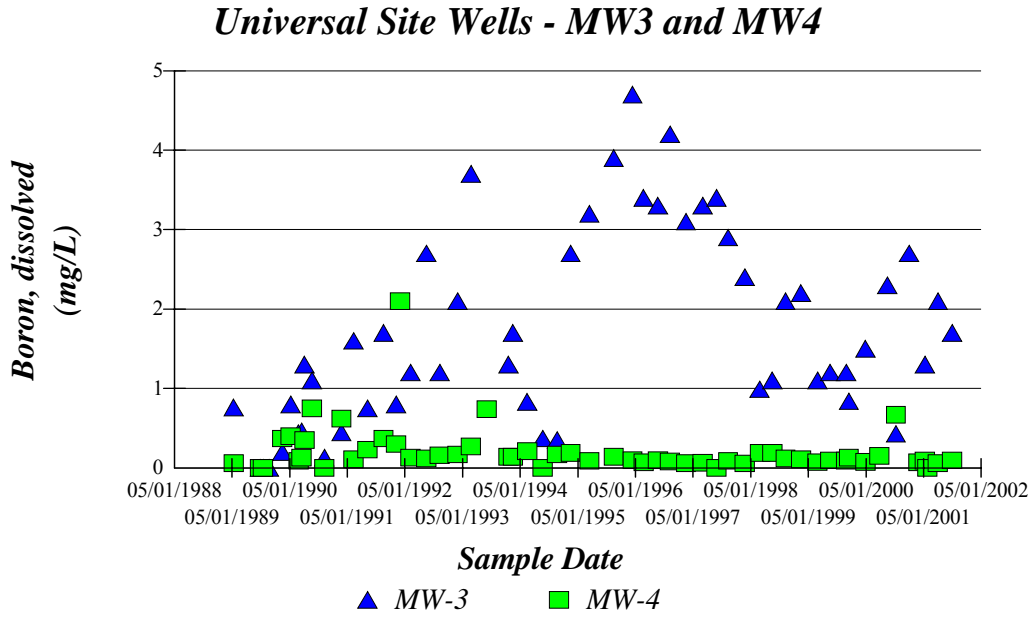


Figure 4.25. Time-series plot of boron measured in groundwater samples.

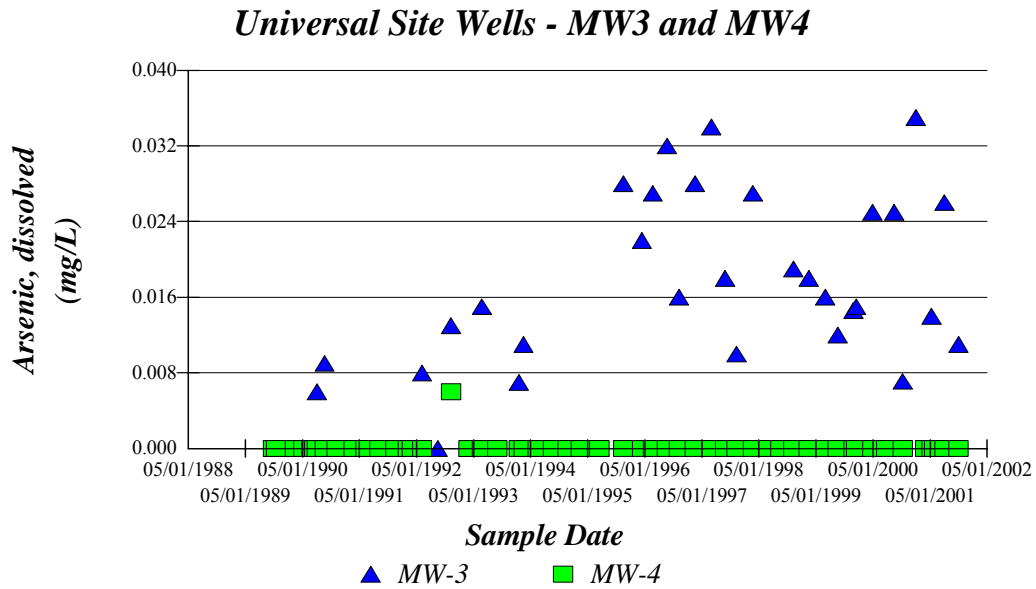


Figure 4.26. Time-series plot of arsenic measured in groundwater samples.



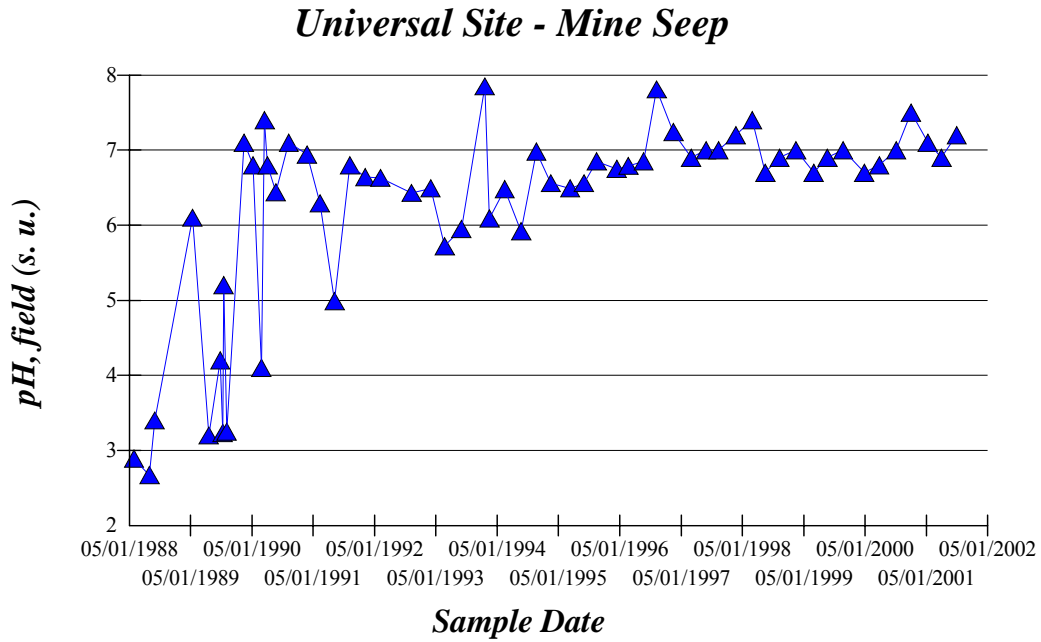


Figure 4.27. Time-series plot of pH measured in mine-seep water samples.

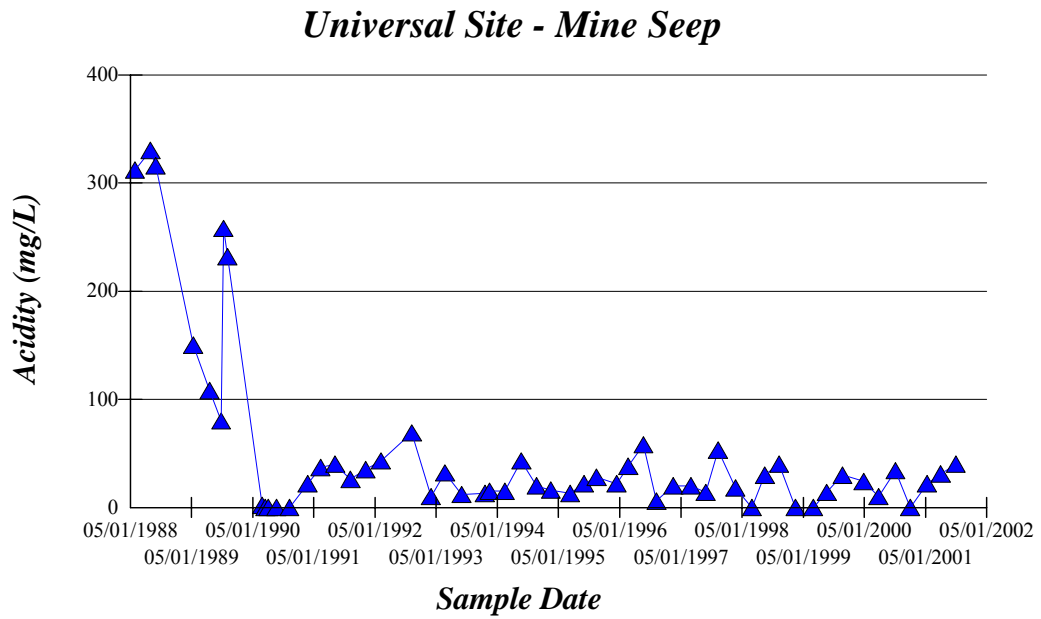


Figure 4.28. Time-series plot of acidity measured in mine-seep water samples.

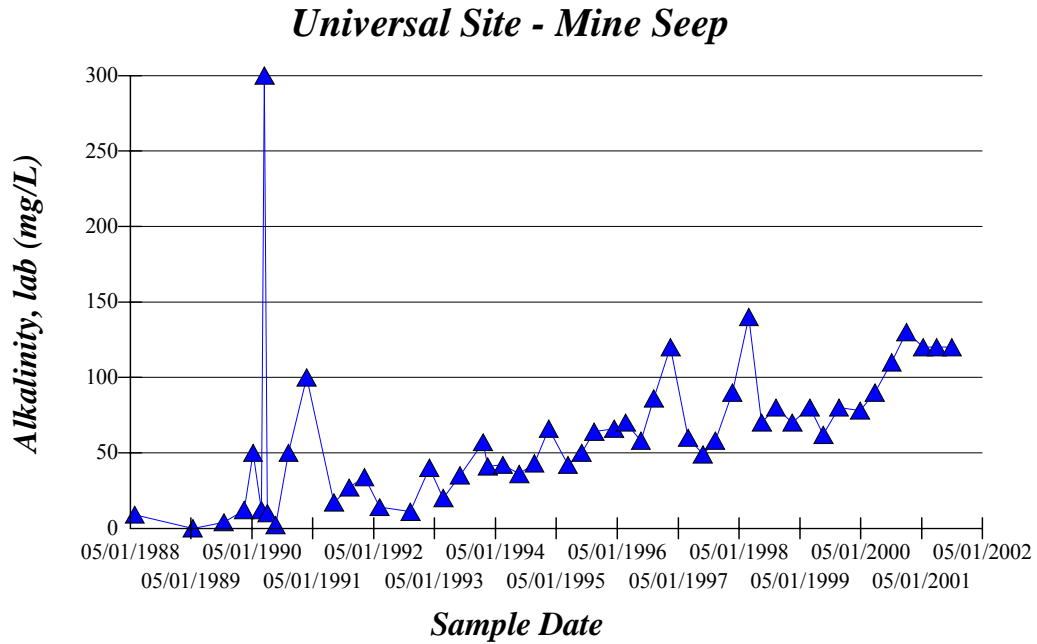


Figure 4.29. Time-series plot of alkalinity measured in mine-seep water samples.

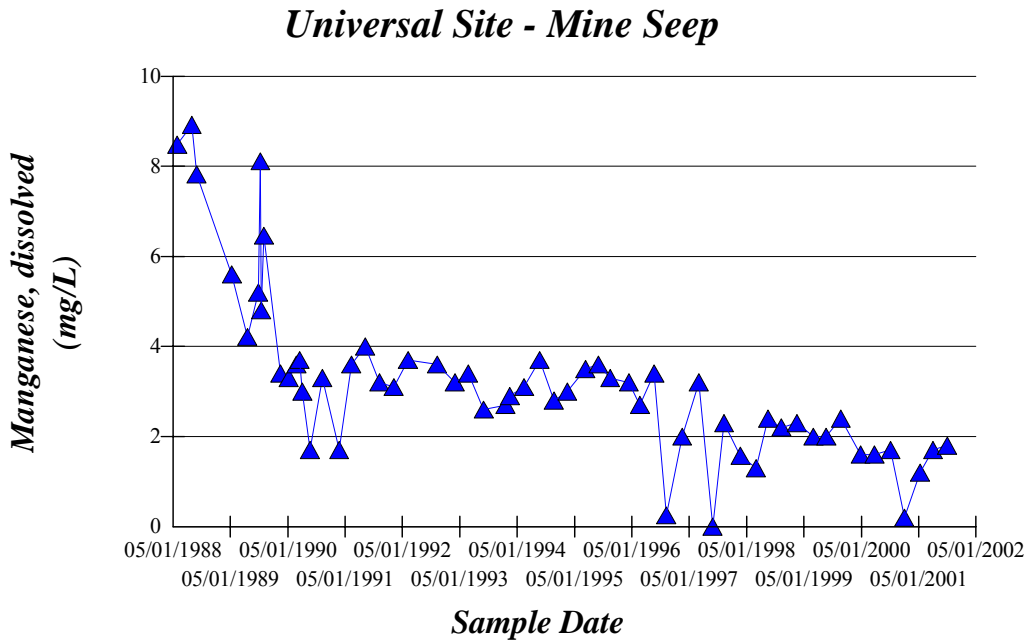


Figure 4.30. Time-series plot of manganese measured in mine-seep water samples.

*Universal Site - Mine Seep*

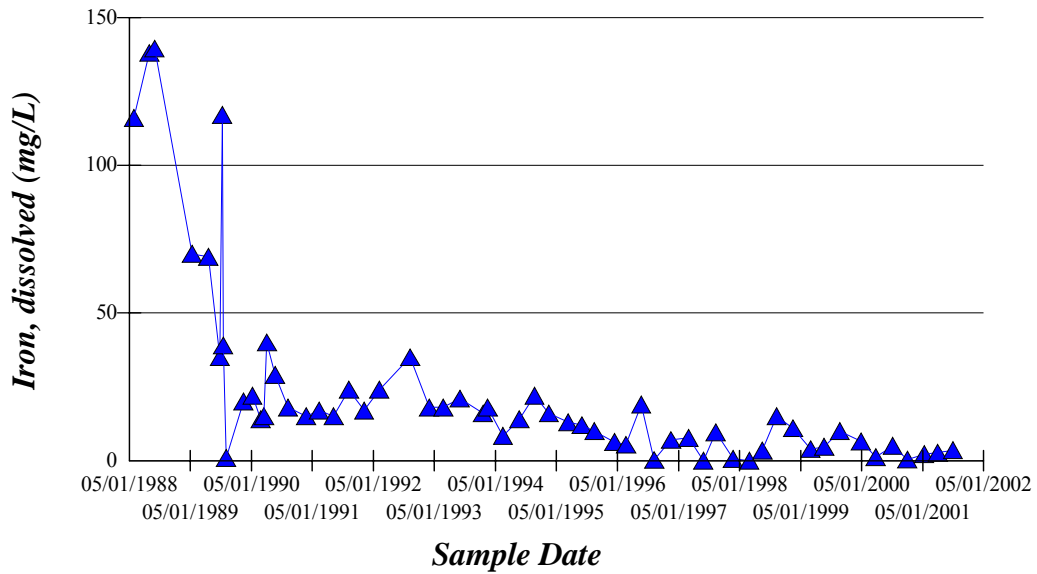


Figure 4.31. Time-series plot of iron measured in mine-seep water samples.

*Universal Site - Mine Seep*

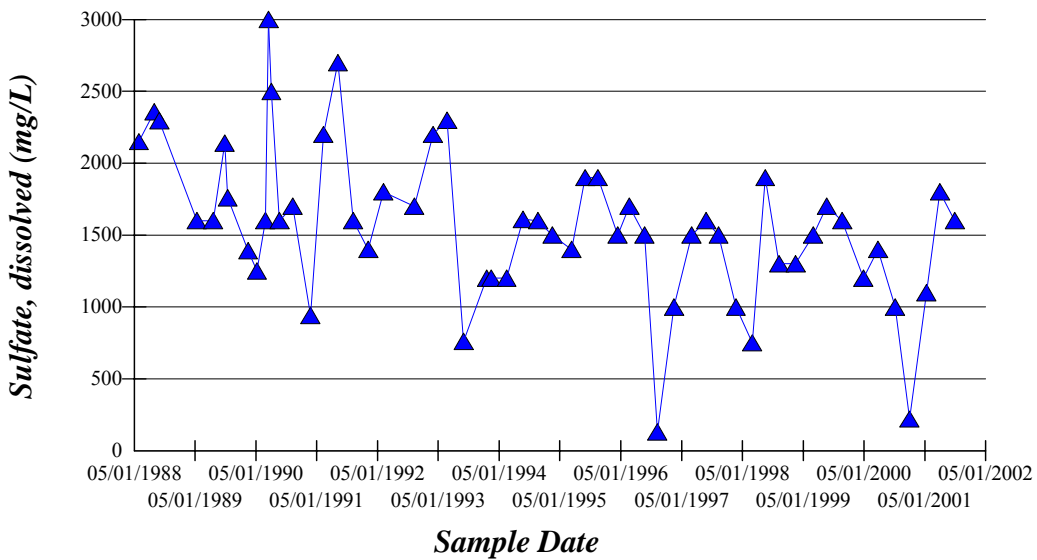


Figure 4.32. Time-series plot of sulfate measured in mine-seep water samples.

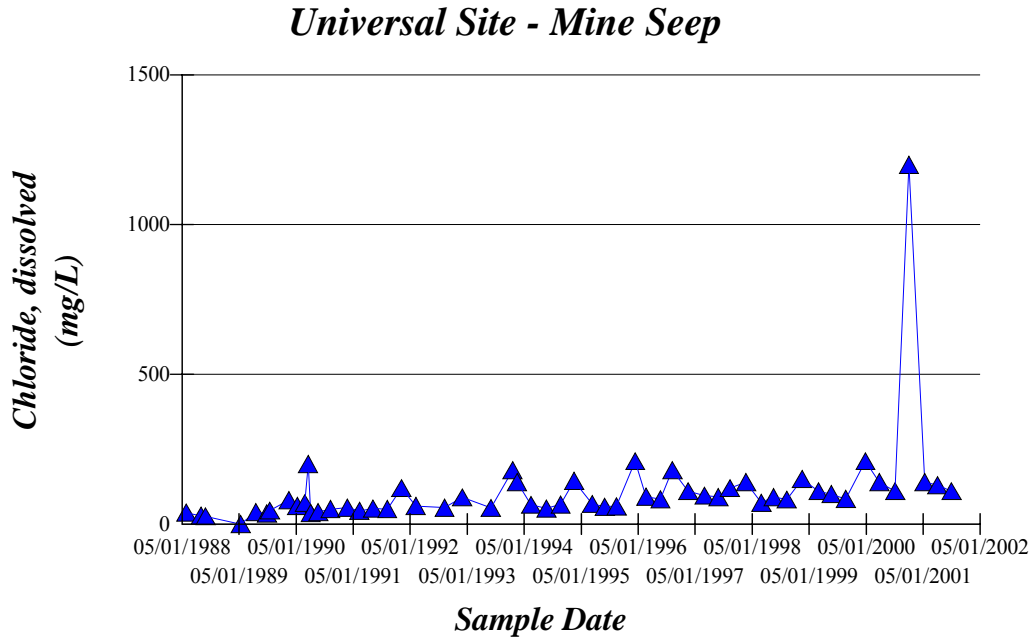


Figure 4.33. Time-series plot of chloride measured in mine-seep water samples.

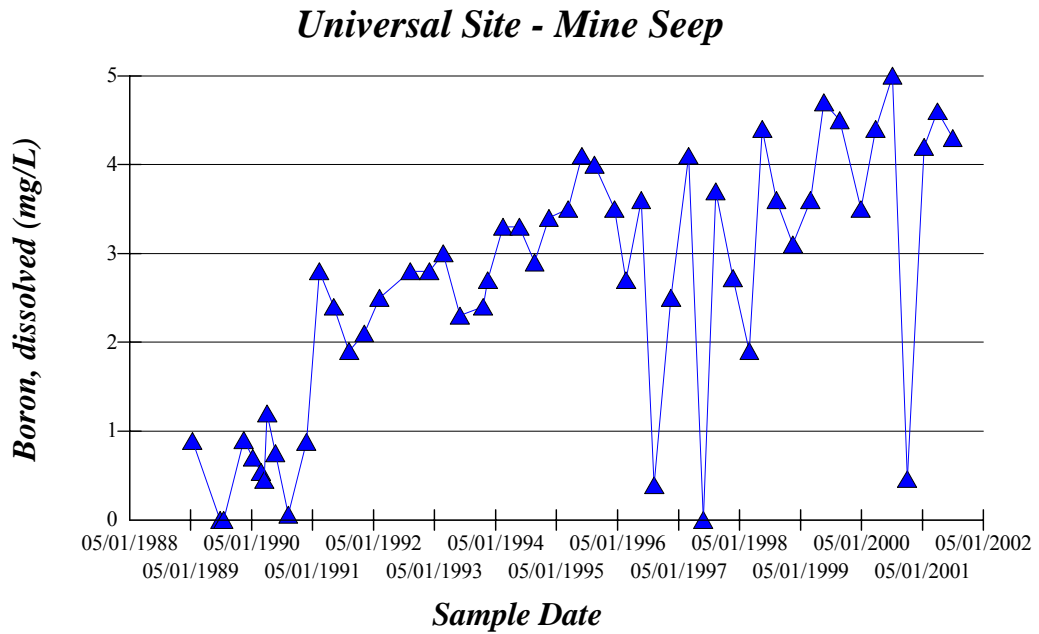


Figure 4.34. Time-series plot of boron measured in mine-seep water samples.

Figure 4.35. Alkalinity and pH values versus time for the mine discharge for 1-year postinjection.

Figure 4.36. Concentration of iron, aluminum, manganese, and pH versus time for the mine discharge for 1-year postinjection.

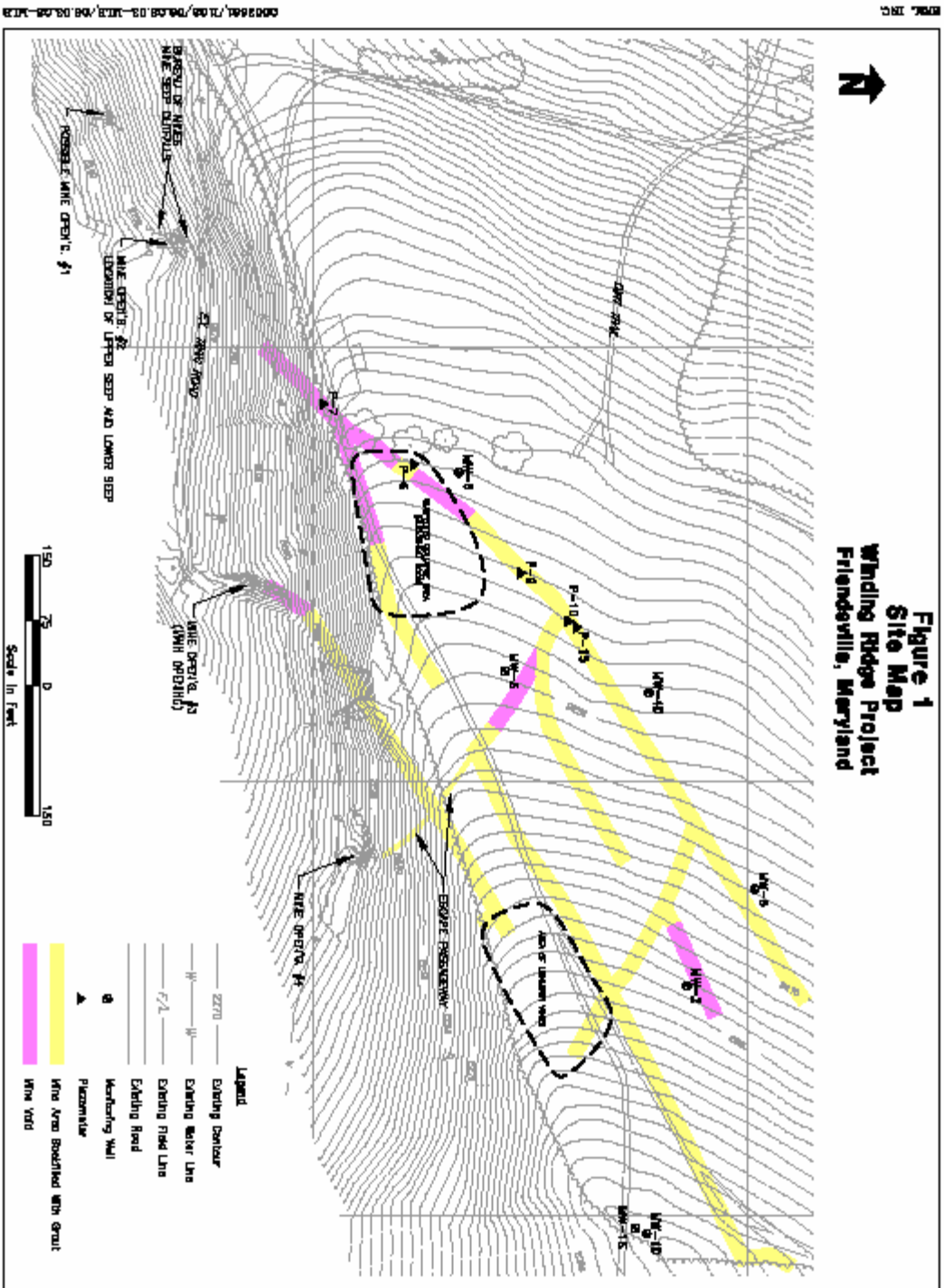


Figure 4.37

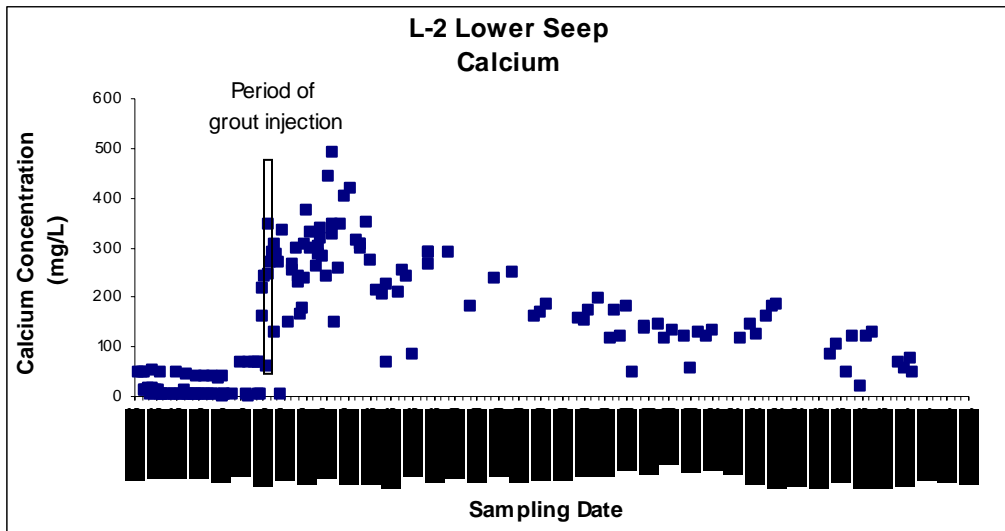


Figure 4.38. Time-series plot for measured calcium concentrations.

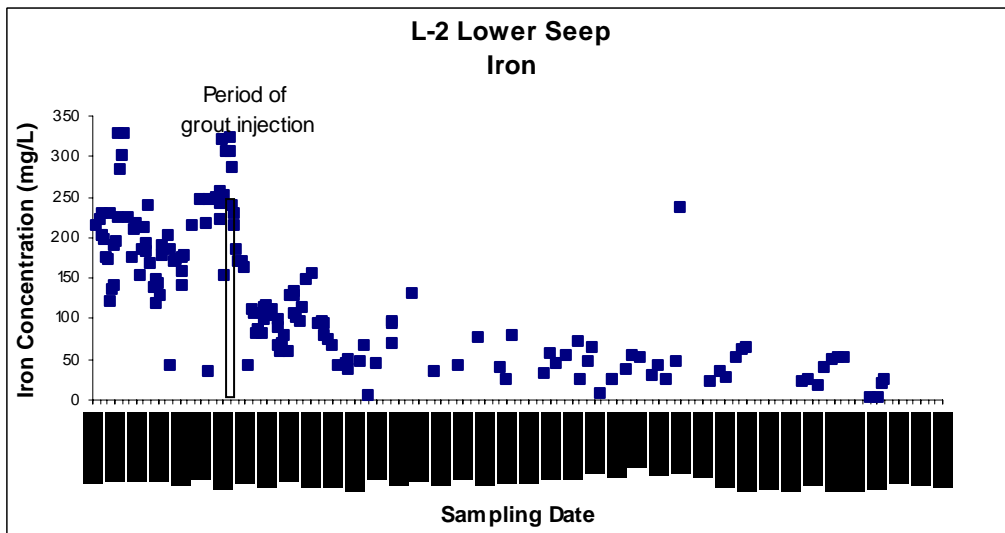


Figure 4.39

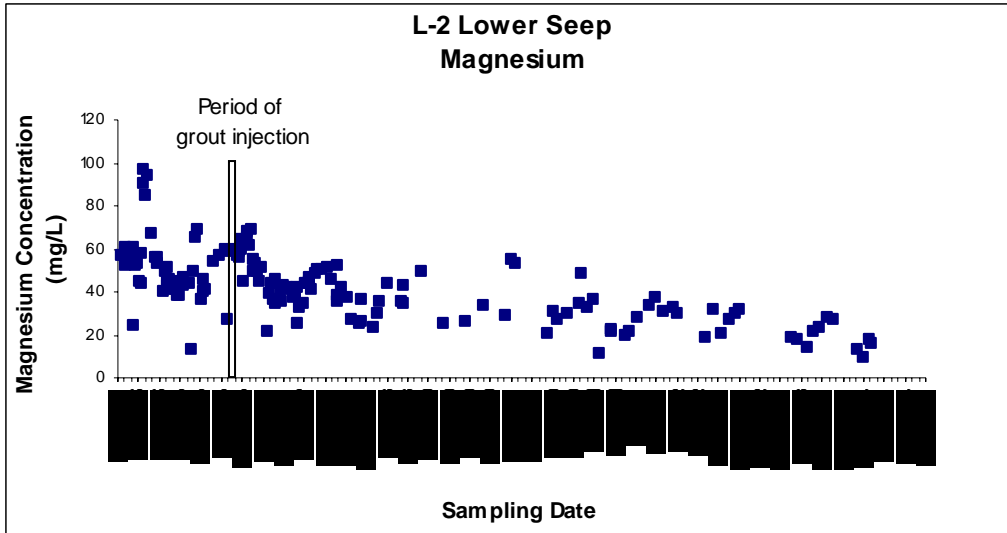


Figure 4.40

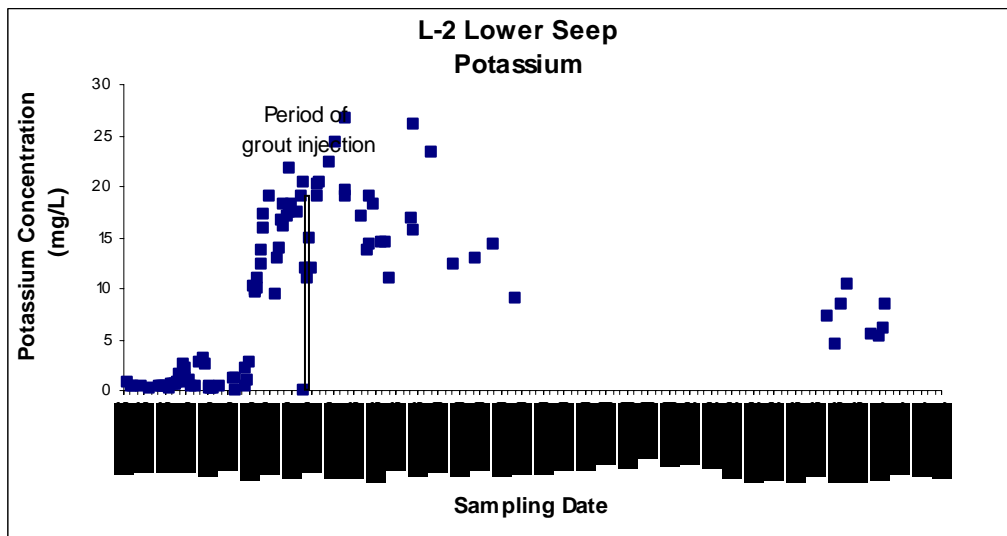


Figure 4.41



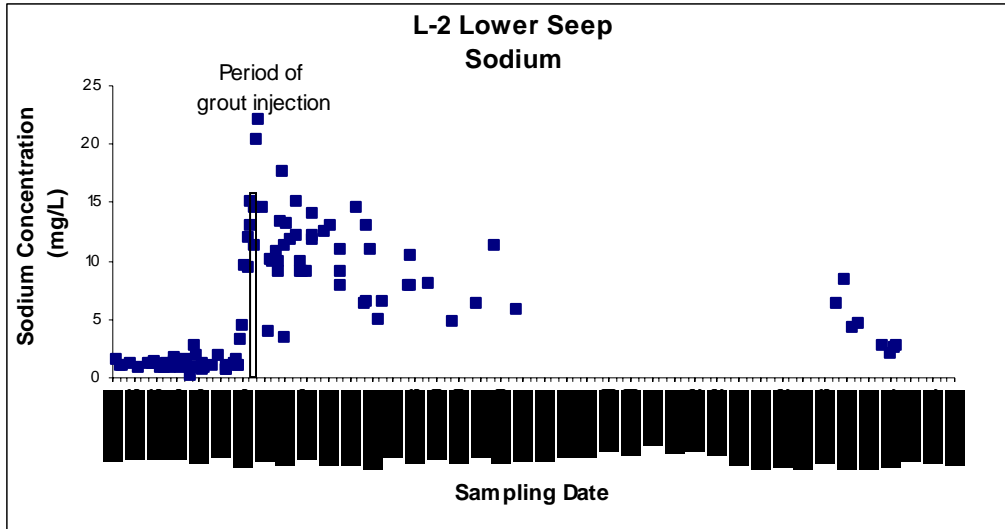


Figure 4.42

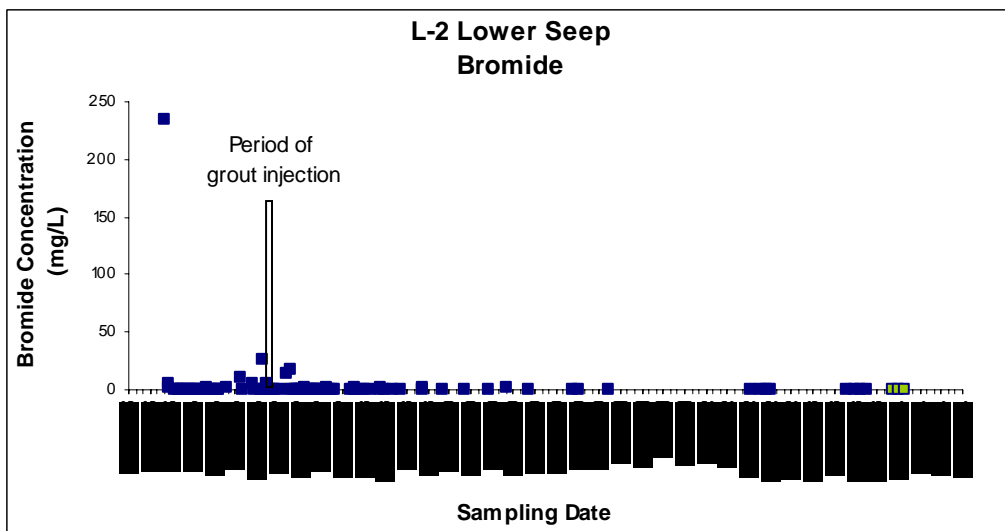


Figure 4.43

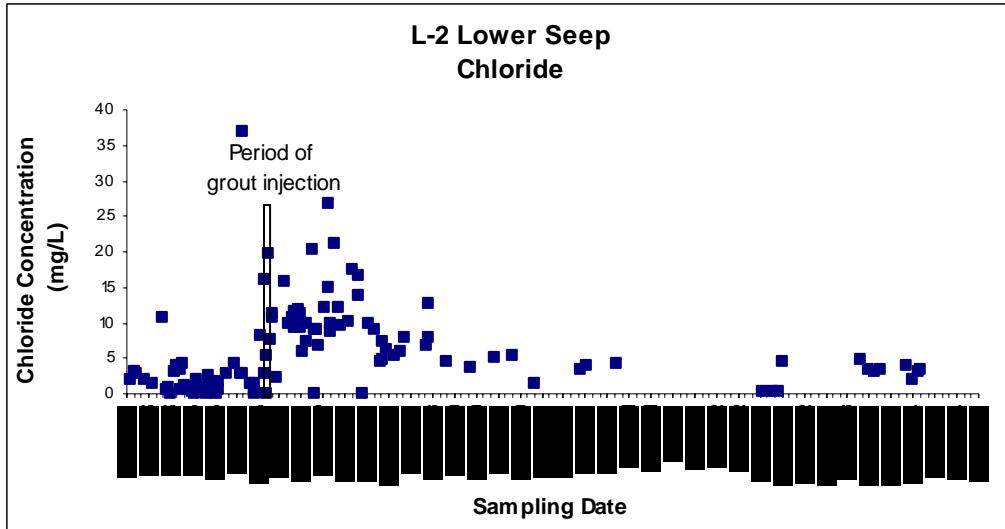


Figure 4.44

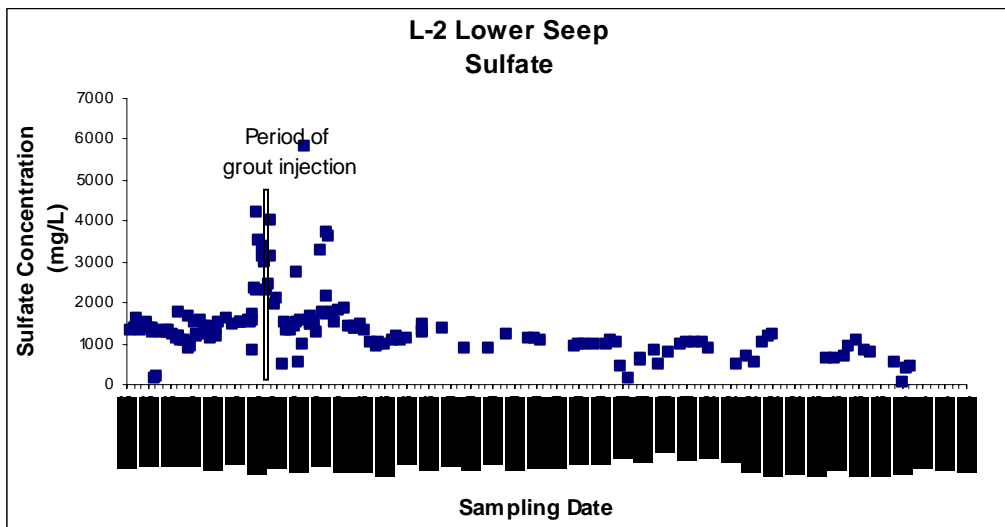


Figure 4.45

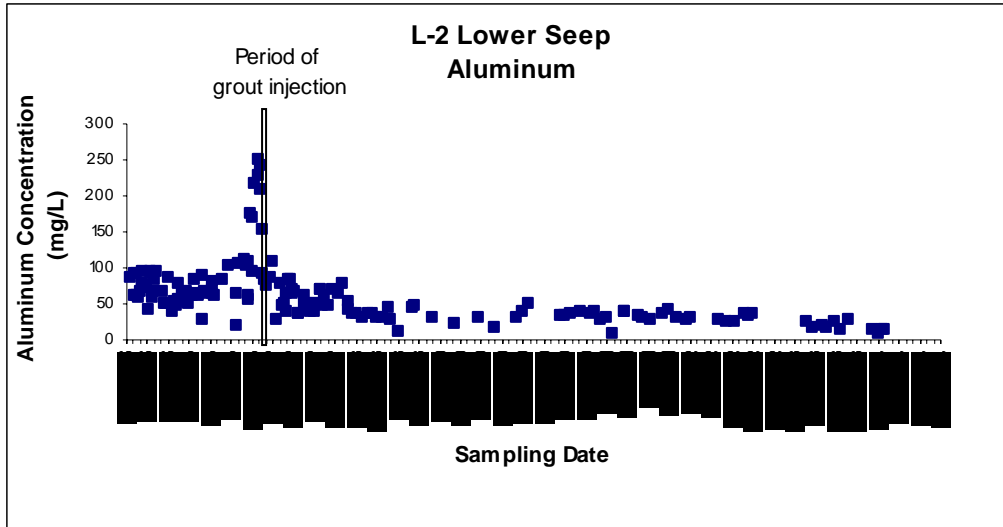


Figure 4.46

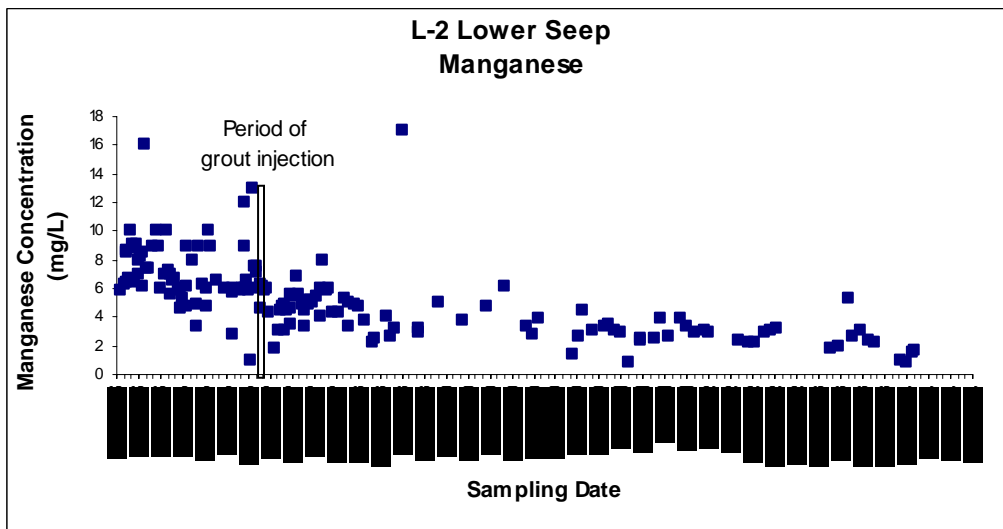


Figure 4.47

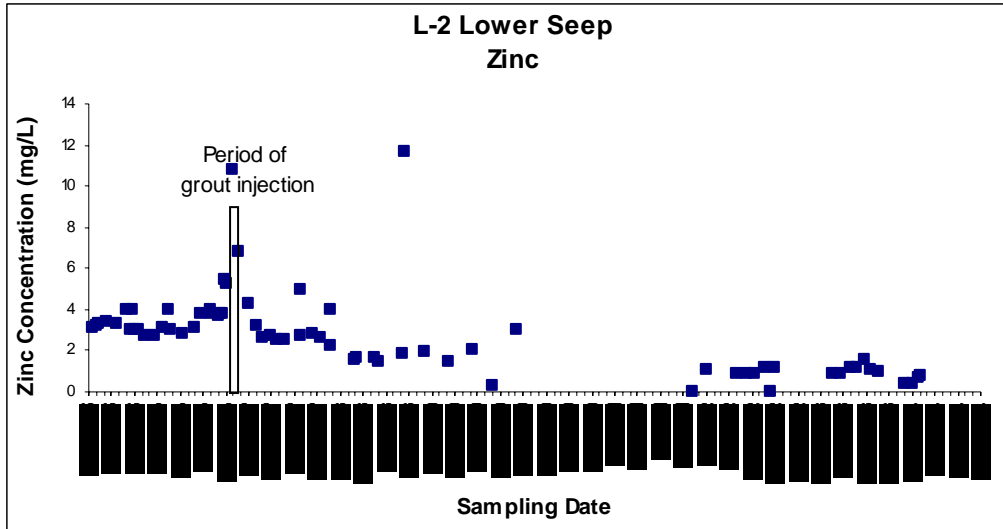


Figure 4.48

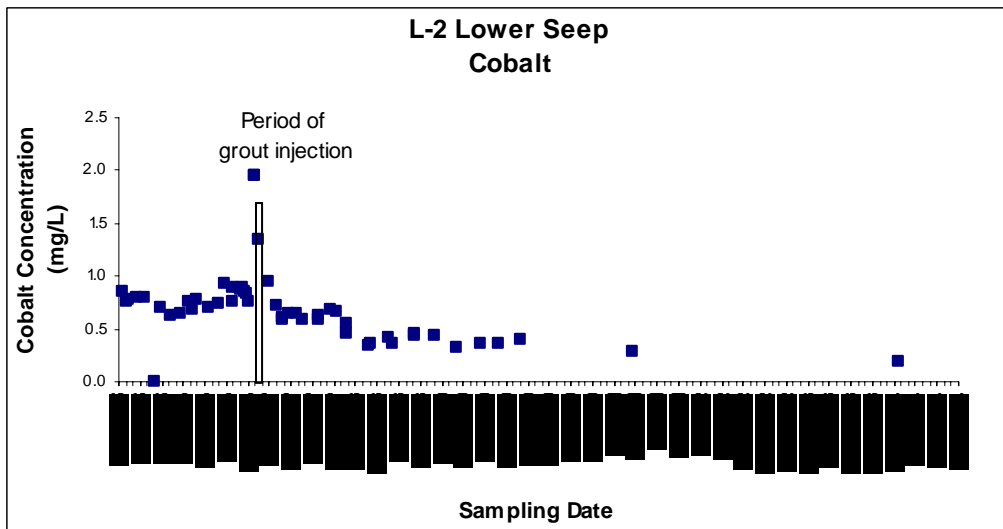


Figure 4.49

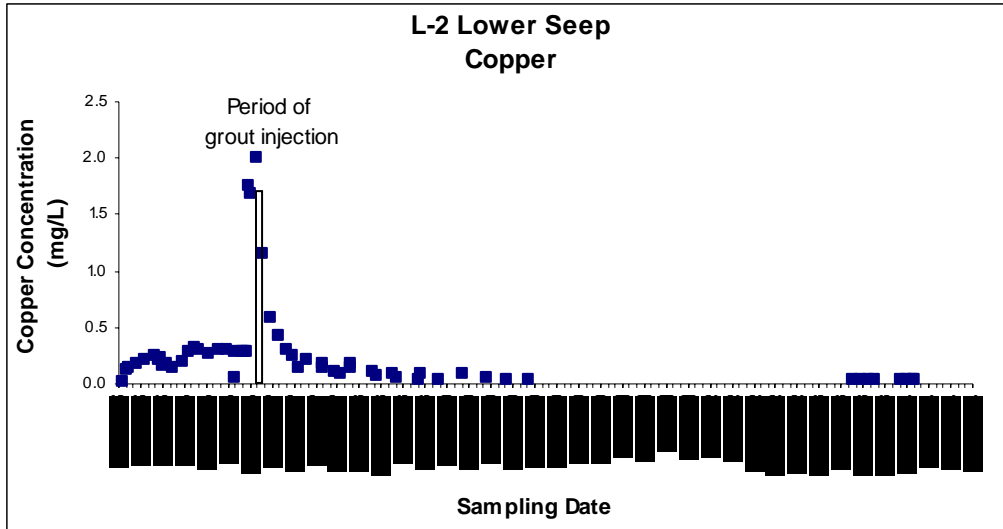


Figure 4.50

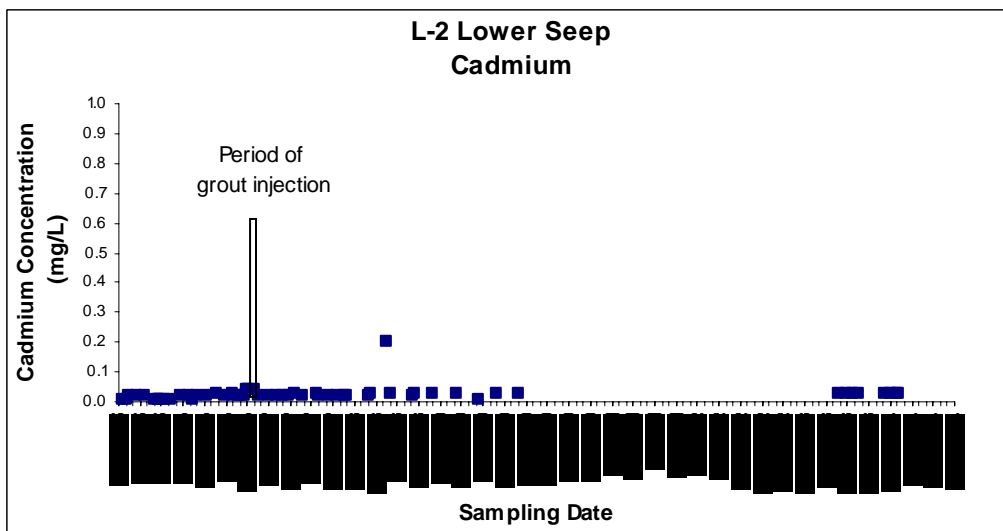


Figure 4.51

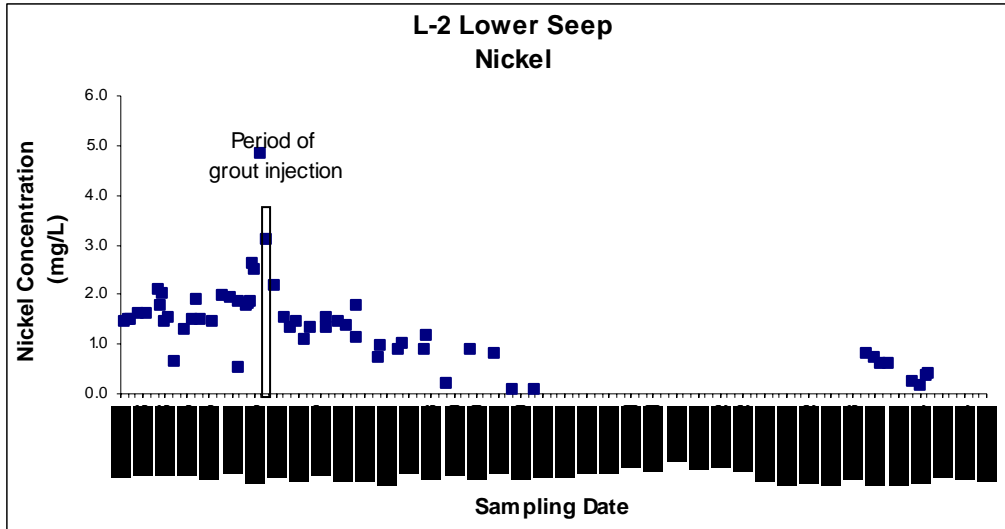


Figure 4.52

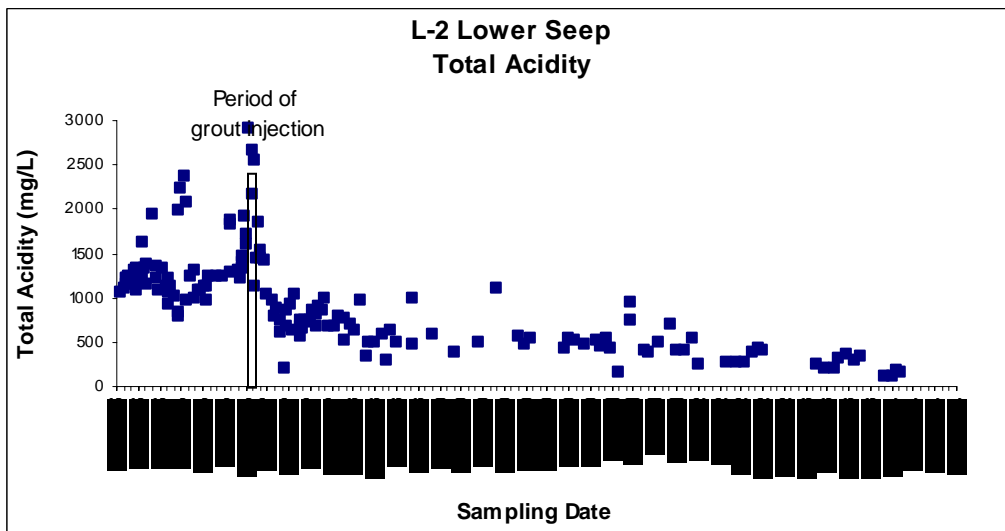


Figure 4.53

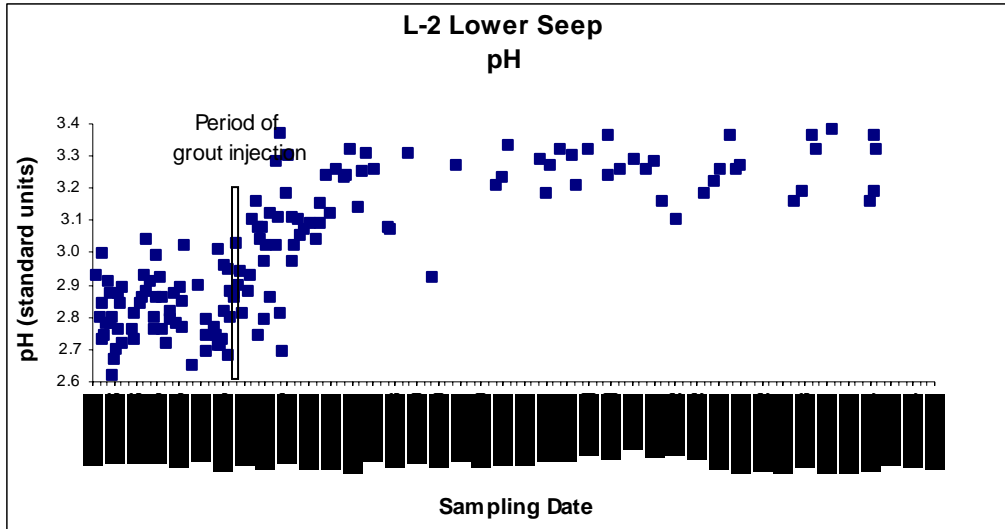


Figure 4.54

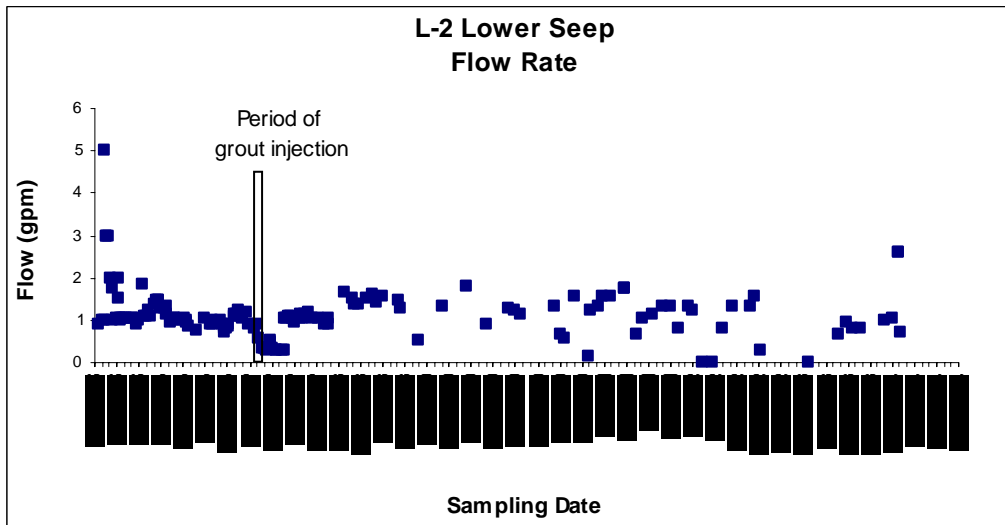


Figure 4.55

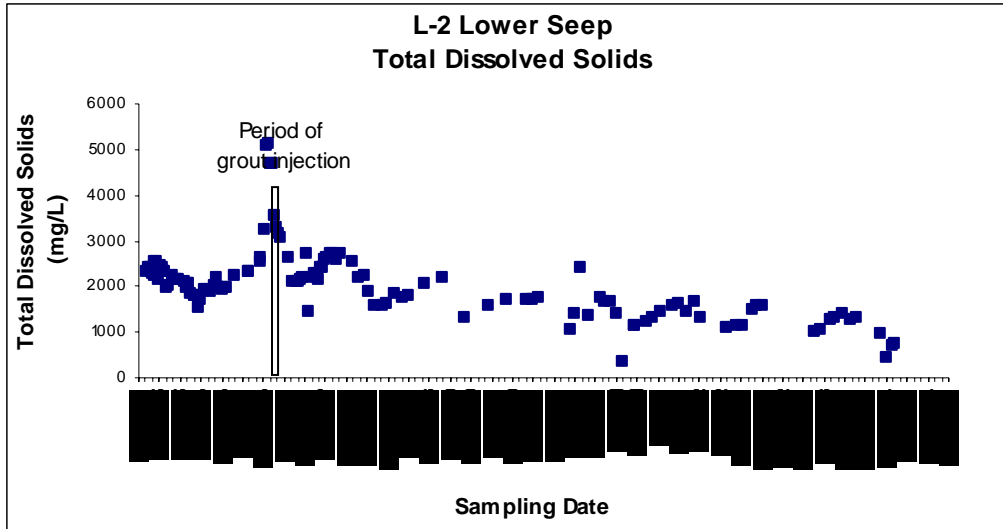


Figure 4.56